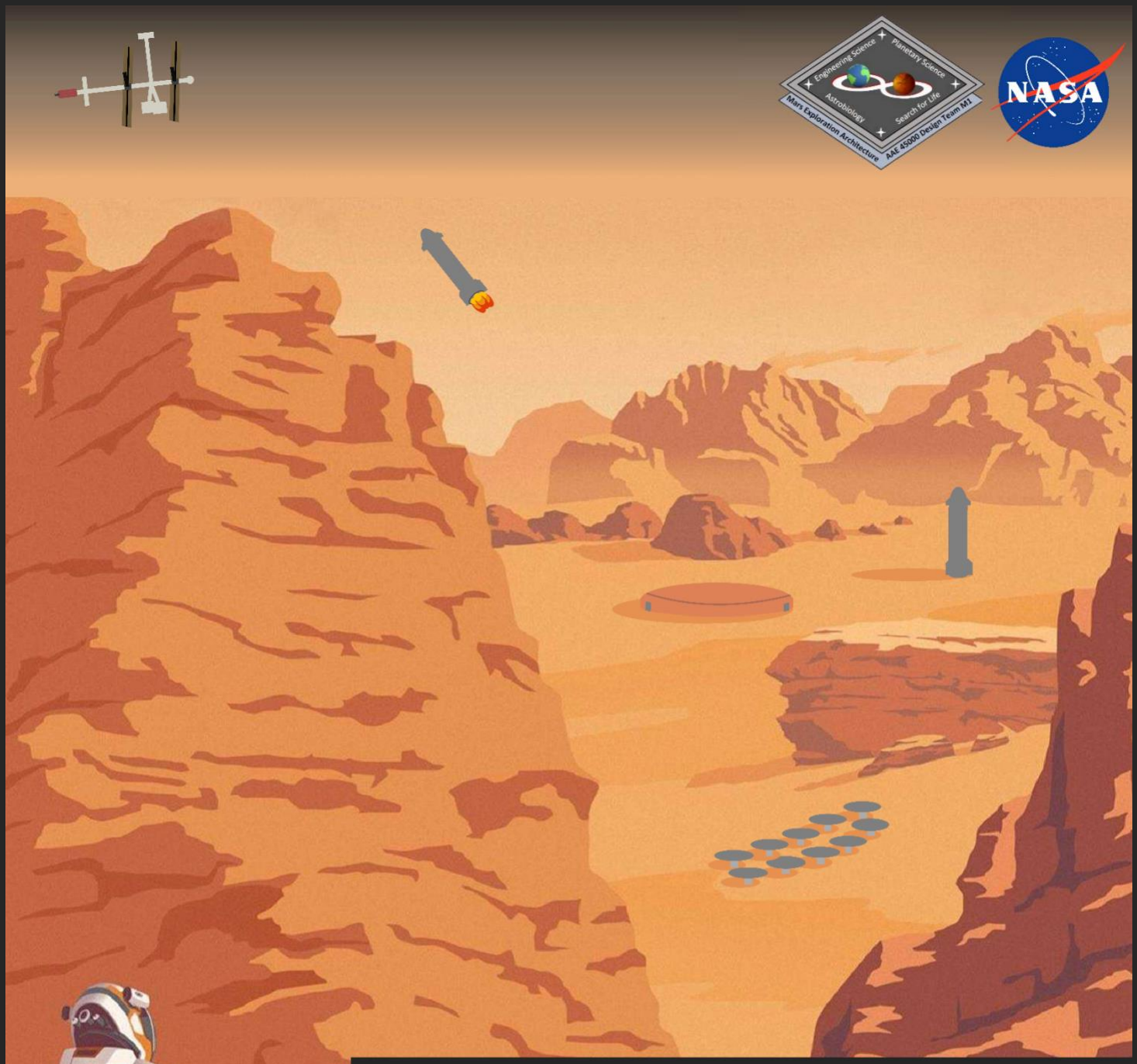

M.A.R.S.T.E.A.M. O.N.E.

Martian Advanced Research Society for Technologically Equipped Adaptation and Migration to Orbiting and Non-terrestrial Environments

Mission: Human Exploration of Mars

Leadership: Brian Wodetzki (PM), Luke Harpring (SE)

Engineers: Nathan Berry, Andrew Darmody, Ryan Horvath, Matt Kelley, Zachary Kessler, Austin Koeblitz, Mark Paral, Chris Manilla, Luke Miller, Tim Osifchin, Veronica Rankowicz, Vishnu Vijay

1: Acronyms and Abbreviations *6*

2: Introduction (Brian Wodetzki) *8*

3: Mission Summary (Brian Wodetzki) *9*

3.1 General Architecture **9**

3.2 Space Transit Vehicle **10**

3.3 Mars Operations **11**

3.4 Telemetry **12**

3.5 Mission Outline (Ryan Horvath) **13**

4: Science Mission and Objectives *16*

4.1 Objective Definition (Ryan Horvath) **16**

4.2 Science Objective Prioritization (Zachary Kessler and Mark Paral) **17**

5: Transportation Systems *19*

5.1 Cycler Orbit (Veronica Rankowicz) **19**

5.1.1 Assumptions (Veronica Rankowicz) 19

5.1.2 Lambert's Theorem (Veronica Rankowicz) 20

5.1.3 Trajectory Results (Veronica Rankowicz) 21

5.1.4 Incorporating Ephemeris Model for Full Mission (Veronica Rankowicz) 23

5.2 Cycler Radiation Analysis (Luke Miller) **25**

5.2.1 Familiarization with the Radiation Problem (Luke Miller) 25

5.2.3 Radiation Shielding Approach (Luke Miller) 28

5.2.4 NASA OLTARIS and Radiation Study Methodology (Luke Miller) 29

5.2.5 Radiation Study for the Cycler (Luke Miller) 30

5.3 Life Support System for the Cycler (Luke Miller and Matt Kelley) **34**

5.3.1 Cycler Life Support Demands 34

5.4 Artificial Gravity Investigation and Implementation (Tim Osifchin) **35**

5.4.1 Microgravity Environment (Tim Osifchin) 35

5.4.2 Rotational Artificial Gravity (Tim Osifchin) 37

5.4.3 Implementation of Artificial Gravity (Tim Osifchin) 46

5.4.4 Artificial Gravity System Bearings & Motor Analysis (Nathan Berry) 48

5.4.5 Sizing Fuel Requirements for AGM Start and Stop (Vishnu Vijay) 51

5.5 Cycler ADCS (Vishnu Vijay) **52**

5.5.1 Determining Cycler ADCS Power and Mass Budget 52

5.5.2 Cycler Operational Modes 53

5.6 Cycler Propulsion **53**

5.6.1 Boost of Cycler to S1L1 Orbit (Chris Manilla and Mark Paral) 53

5.6.2 Orbital Correction Propulsion (Zachary Kessler) 54

5.7 Power & Thermal Analyses **56**

5.7.1 Cycler Power Analysis (Chris Manilla) 56

5.7.2 Cycler Thermal Analysis (Nathan Berry) 59

5.8 Cycler Construction (Tim Osifchin) 62

5.8.1 Components of the Cycler (Tim Osifchin) 62

5.8.2 Construction Process (Tim Osifchin) 64

5.9 Interplanetary Trajectory, EDL, and ΔV Budget (Chris Manilla) 66

5.9.1 Crewed Missions (Chris Manilla and Mark Paral) 67

5.9.2 Supply Missions (Chris Manilla) 68

6: Surface Operations 70

6.1 Pre-Supply 70

6.1.1 Design (Mark Paral and Austin Koeblitz) 70

6.2 Habitat 71

6.2.1 Design (Tim Osifchin) 71

6.2.2 Construction (Tim Osifchin) 73

6.2.3 Landing Location Considerations (Mark Paral) 74

6.2.4 Landing Location Evaluations (Mark Paral) 76

6.2.3 Landing Location Selection (Mark Paral) 79

6.3 Surface Operations Radiation Analysis (Luke Miller) 80

6.3.1 Radiation Study for Habitat and Surface Operations (Luke Miller) 80

6.3.2 Final Considerations on Radiation (Luke Miller) 84

6.4 Life Support System for Habitat (Matt Kelley and Nathan Berry) 86

6.4.1 Greenhouse Sizing (Matt Kelley) 87

6.4.2 Life Support System Sizing (Matt Kelley) 88

6.5 In-Situ Resource Utilization (Austin Koeblitz) 88

6.5.1 Motivation (Austin Koeblitz) 88

6.5.2 Goals (Austin Koeblitz) 89

6.5.3 Systems – High Level (Austin Koeblitz) 89

6.5.4 Systems – Low Level (Austin Koeblitz) 89

6.5.5 Conclusion and Sizing (Austin Koeblitz) 97

6.6 Habitat Power and Thermal Analysis (Austin Koeblitz and Nathan Berry) 98

6.6.1 Habitat Power Analysis (Austin Koeblitz) 98

6.6.2 Habitat Thermal Analysis (Nathan Berry) 101

6.7 Ascent Operations (Zachary Kessler) 104

6.7.1 Propellant Storage 104

6.7.2 Ascent from Martian Surface 105

6.8 Crew Time (Vishnu Vijay and Zachary Kessler) 105

7: Telemetry, Tracking, & Command 109

7.1 Point Design Selection (Nathan Berry) 109

7.2 New Ka-Band/Optical DSN Network (Nathan Berry) 110

7.3 Data Volume & Rates (Andrew Darmody) 111

7.4 Satellite Constellation (Andrew Darmody) 111

7.4.1 Satellite Operational Modes (Vishnu Vijay) 112
7.5 Mass and Power Budget (Andrew Darmody) 113
7.5.1 New ADCS System (Vishnu Vijay) 113
7.5.2 Preliminary Sizing for New Satellite Solar Panels (Nathan Berry) 114
7.6 Antenna Sizing and Link Budget Results (Nathan Berry) 114
7.7 Satellite Deployment Strategy (Andrew Darmody, Chris Manilla) 116
7.8 Conjunction Mitigation Strategy (Andrew Darmody) 117
7.9 Satellite Orbit Tracking (Chris Manilla) 118
7.10 EVA Communication (Andrew Darmody) 119
7.11 Mission Control (Nathan Berry) 119
8: Cost Estimation (Ryan Horvath) 121
9: Risks and Mitigation (Luke Harpring) 125
9.1 Mission Segments 127
9.2 Spaceflight Risk 127
9.2.1 Risk Assessment and Mitigation Strategies 127
9.3 Mars Surface Risk and Mitigation 131
9.3.1 Risk Assessment and Mitigation Strategies 132
9.4 Limitations of Analyses 136
10: Methodology (Luke Harpring and Brian Wodetzki) 138
10.1 Initial Design Definition (Luke Harpring) 138
10.2 Design Refinement (Brian Wodetzki) 140
10.2.1 Trade Study 140
10.2.2 Science Mission Selection 141
10.3 Design Validation (Brian Wodetzki) 142
11: Future Work (Brian Wodetzki and Everyone) 143
11.1 Habitat Downsizing (Luke Miller) 143
11.2 Detailed Risk Analysis (Luke Harpring) 144
11.3 Combined Fuel Production and Fuel Storage Systems (Brian Wodetzki) 145
11.4 Future Work on Cycler ADCS (Vishnu Vijay) 145
12: Appendix 146
12.1 System Requirements 146
12.2 Link Budget Equations & Results (Nathan Berry) 152
12.3 Starship Accounting (Mark Paral) 156

12.4 Linear Acceleration (Tim Osifchin) 160

References*..... *162

1: ACRONYMS AND ABBREVIATIONS

ADCS	Attitude Determination and Control System
ALARA	As Low as Reasonably Achievable
ARMS	Autonomous Repair and Maintenance System
BHA	Bottom Hole Assembly
BOL	Beginning of Life
CER	Cost Estimation Relationship
CT	Coiled Tubing
ECLSS	Environmental Control and Life Support System
EDL	Entry Descent and Landing
EOL	End of Life
EVA	ExtraVehicular Activity
GCR	Galactic Cosmic Rays
GNC	Guidance, Navigation, and Controls
HEPA	High Efficiency Particulate Air
IOC	Initial Operating Capacity
ISRU	In-Situ Resource Utilization
ISS	International Space Station
KRUSTY	Kilopower Reactor using Stirling TechnologY
LEO	Low Earth Orbit
LMO	Low Mars Orbit
MARS TEAM ONE	Mars Advanced Research Society for Technologically Equipped Adaption and Migration to Orbiting Non-terrestrial Environments
MIT	Massachusetts Institute of Technology
MOXIE	Mars Oxygen In-Situ Resource Utilization Experiment
MRO	Mars Reconnaissance Orbiter
NASA	National Aeronautics and Space Administration
NNSA	National Nuclear Security Administration
OLTARIS	On-Line Tool for the Assessment of Radiation in Space
RASSOR	Regolith Advanced Surface Systems Operations Robot

SHARAD	Shallow Radar
SMAD	Space Mission Analysis and Design
SOXE	Solid Oxide Electrolysis Unit
SPE	Solar Particle Event
STOUR	Satellite Tour Design Program
TRL	Technology Readiness Level
MSL	Master Systems List

2: INTRODUCTION (BRIAN WODETZKI)

Purdue University's Spring 2023 senior design students were posed with the task of creating a reference architecture for a manned mission to Mars. A list of major mission requirements was provided to define the intended outcomes of the mission. These requirements are stated as follows. The crewed mission needs to have humans on the Martian surface for seven years. For the duration of the mission, a crew of 4 needs to be on the surface of the planet. This mission needed to have astronauts on the surface of Mars at the earliest 2035 and at the latest 2040. The crew needs to return between 2040 and 2050. A minimum of five science objectives need to be pursued throughout the duration of the mission. Three novel technologies need to have been demonstrated through this mission. The mission is limited to a single pre-supply mission, and a maximum resupply payload of 5,000 kg to the surface of Mars.

Figure 1: Artist's Rendition of Martian Society [1]

These core requirements lay a foundation for a flagship mission that will prove that humans can stay on Mars for an extended period. These requirements also guide the mission towards a well-scoped, lean design with firm dates and limited supplies. MARS TEAM ONE was the group of students who took on the challenge to design a mission that satisfied these basic requirements and several much more stringent self-imposed requirements.

MARS TEAM ONE was composed of a diverse array of 14 seniors in Purdue University's School of Aeronautics and Astronautics' Class of 2023. This team included a Project Manager, Systems Engineer, Propulsion sub-team, Telemetry sub-team, Space Environment sub-team, Mission Design sub-team, Structures sub-team, Attitude and Controls sub-team, and a Cost and Schedule Estimation sub-team.

MARS TEAM ONE approached these requirements with the intention not only to prove this mission was possible, but also to prove that this mission to Mars is a worthwhile endeavor due to the limitless science potential and that it should not be the last manned Mars missions. The team's vision involved laying the groundwork for future, more advanced missions to the Red Planet that not only provide scientific advancement, but also aim at turning it into a habitable location for future generations. To realize this vision, the team looked towards designing each component of the mission with the goal of making future missions to Mars a more regular occurrence.

The strategy and implementation of this mission should not be taken to be seen as a completed mission, but instead one that lays the groundwork for a deeper analysis. The goal of this architecture is to both prove the feasibility of this specific mission structure, and to act as a compiled resource for a cohesive mission design concept that outlines how to best put life on the surface of Mars.

3: MISSION SUMMARY (BRIAN WODETZKI)

The mission architecture proposed in this document was tailored to meet, and exceed, the set of core requirements posed for the project. These core requirements are shown in Table 1.

Table 1: Core Project Requirements

Core Project Requirements
The system shall support a mission duration of 7 years.
The system shall support a continuous crew of at least 4 throughout the entire mission.
The system shall accomplish at least 5 scientific objectives during its mission.
The mission shall include the usage of at least 3 novel technologies.
A TRL of 6+ shall be the baseline for all system components unless a citation is provided on the prospect of the lower TRL technology.
The system shall deploy no more than 2 years' worth of logistics and spares prior to the start of the crewed mission.
The system shall require no more than 5,000 kg of consumable cargo from Earth every two years after the crewed mission begins.
The first crew shall land between 2035 and 2040, and the last crew shall return between 2040 and 2050.
The system architecture shall include launch, in-space transportation, Mars entry-descent-landing, surface habitation and operations, and any other additional logistics support required from Earth to sustain the crew and their systems.

3.1 General Architecture (Brian Wodetzki)

Manned missions to Mars are not only prohibitive due to cost and political factors, but also due to the health risk to the astronauts undergoing this mission. Due to this high health risk, this mission architecture assumes the use of two separate crews that will divide up the 7-year mission time. The two-crew strategy will limit the amount of radiation exposure that a single crew will receive on the surface of Mars. Without this implementation, the mission would require excessive radiation shielding mass to be sent to Mars to protect the astronauts. The radiation budget and effects are further discussed in future sections of this architecture.

To complete the mission objectives, this architecture chose SpaceX's Starship to be the primary launch vehicle of both cargo and crewed missions. This decision was made due to the projected low cost of Starship launches, the high payload capacity, and the reusability of the vehicle. Furthermore, Starship is reported to have the highest payload and mass and volume to both LEO and Mars of any available launch vehicle. Starships are also touted to be purpose built for a Mars mission. This points to SpaceX designing the vehicle for this type of mission structure and making

it capable of both landing on the surface of Mars and ascending from the surface. With these capabilities in mind, Starship was chosen and will operate as the primary vehicle for all ascent and EDL operations, both crewed and uncrewed, for this mission.

3.2 Space Transit Vehicle

This architecture baselined two space transit vehicles, called the Cyclers. One that will shuttle astronauts from Earth to Mars and one from Mars to Earth. The driving factors of the design of this vehicle were to keep the crew as healthy as possible throughout the flight and to increase reusability of the system. The transit vehicle was designed to improve the health of the astronauts by addressing two main and mitigatable risks of spaceflight. These are the effects of microgravity and the effects of radiation on the human body. Furthermore, the reusability aspect was addressed through placing the transit vehicles in a cycler trajectory that allows for constant transportation between Earth and Mars with little control input.

For long-duration space inhabitation, microgravity is a major risk to astronauts as it causes many astronauts to lose consciousness, have vision loss, and loss of strength due to muscle atrophy and loss of bone density [2]. Research suggested that it would be unacceptable to send a crew to a Martian environment after a long spaceflight with no mitigation in place to operate at a high level in the stressful environment. If the health effects were not mitigated, finishing building, and setting up a habitat in a high stress environment would be very difficult for astronauts to complete if they were weak from a long transit. As a result, in this architecture, microgravity is mitigated by designing an artificial gravity system on the Cycler space station.

Furthermore, space's high radiation environment poses the possibility of causing irreparable harm to an astronaut's health eventually resulting in cancer or death if a high dose of radiation is received. To keep the astronauts safe, it is imperative to keep the radiation dosage below NASA's lifetime limit. It is also important to note that this architecture utilized the "As Low as Reasonably Achievable" motto when it comes to radiation. To reach these goals, the architecture outlines the radiation shielding sent to the Cycler station to reduce dosage, along with baselining a trajectory with a short transfer time between the two planets.

From the requirements set by microgravity and radiation mitigation, the size of the Cycler space station would be prohibitively massive to be repeatedly actively boosted between the two planets. Additionally, from the requirements set by radiation mitigation, the Cycler must have a short transit time. This is achieved through utilizing two separate trajectories, the S1L1 inbound and S1L1 outbound cycler. These trajectories cycle quickly between Mars and Earth, and Earth and Mars respectively, jointly satisfy both major requirements as the crew can take the fast leg of the cycler to and from Mars to limit the radiation exposure. The results from the trajectory analysis, shown in section 5.1, show providing on average a 158-day inbound transit time and an average 160-day outbound transit time [3]. The S1L1 cycler exhibits ballistic trajectory characteristics which means that once an object is on this trajectory, theoretically, there is no delta-V required to maintain its trajectory. As a result, the Cycler will be boosted once, and continuously transit between Earth and Mars, without the need for repeated boosting.

In summary, the architecture baselined the use of two space transit vehicles, one in the outbound cycler trajectory, that transits astronauts between Earth and Mars, as well as the inbound cycler trajectory that transits astronauts from Mars to Earth. These two transit vehicles are each equipped with thick radiation shielding and an artificial gravity system that keeps the crew in peak physical and mental condition throughout the two space transits required for the mission.

3.3 Mars Operations

The proposed mission architecture involves a pre-supply mission that will travel to Mars, deploy satellites for a new communication network, and scout landing locations for a suitable spot for the habitat. The scouting mission will consist of two rovers that will explore two different locations, Erebus Montes as well as Acheron Fossae, the latter being the primary intended landing location. Once the landing location has been well-scouted and chosen, a secondary pre-supply mission will be launched carrying the habitat, along with all equipment necessary to build the habitat and support astronauts on the surface. The systems required to sustain human habitation is outlined in the Master Systems List (MSL) in Table 2.

Table 2: Master Systems List

Master Systems List	
System	**Payload (kg)**
2x Landing Location Scout Rover	2,050
4x New Mars Relay Network Satellites	7,944
Habitat Structure	1,056,338
Water Management	1,540
Waste Processing	208
Thermal Control	1,000
Greenhouse Materials	24,000
Life Support Systems	2,730
18 KRUSTYs	27,000
22 RASSORs with Support Equipment	1,750
Propellant Conditioning Equipment	7,000
Water Production Equipment	10,000
Science Payloads	6,100
2x Space Exploration Vehicles	6,000
Total:	1,153,660

While on Mars, astronauts will reside in a modular habitat buried in regolith. Modularity of the habitat was chosen primarily for risk mitigation. In case of a breach of one module of the habitat,

the other modules will be able to be sealed off and remain unaffected. This additionally provides the option of baselining a large habitat, that is made up of relatively small habitat modules. Having a large interior volume gives the crew plenty of living space, as well as space for experiments and a greenhouse. Regolith is a readily available in-situ resource on the surface of Mars and can act as an effective radiation shield. The use of regolith as a radiation shield reduces the mass of the habitat devoted to radiation shielding.

To assemble the habitat, wheels and a drivetrain will be pre-assembled on each deployed module so they can be remotely driven and assembled. Additionally, a fleet of RASSOR 2.0 vehicles will be sent on the pre-supply mission to collect regolith on Mars and dump it on the habitat to shield it from the environment. On the surface of Mars, the crew will receive water using two methods. First, by harvesting regolith with the RASSORs and baking it to extract the water. This will again utilize the RASSOR fleet to harvest the regolith. Second, water is collected using the Redwater Well, a system that will burrow deep into the surface and melt ice to retrieve water. As the crew requires oxygen within the habitat, the architecture baselined MOXIE to generate oxygen. These systems work by gathering CO_2 from the atmosphere and converting it to O_2 using electrolysis. The crew will receive power from nuclear reactors on the surface.

Acheron Fossae has multiple interesting science opportunities that astronauts will need to leave the habitat to research. The crew will routinely conduct extravehicular activities (EVAs) to reach these locations. These EVAs will involve the use of a crew transport system that will provide the crew with transportation and shelter outside the habitat. The astronauts will also use spacesuits in all EVAs to protect themselves from the harsh Martian environment.

3.4 Telemetry

The telemetry system for this mission was designed to provide necessary communications to and from Mars. To complete this goal, a new Mars Relay Network was designed to replace the current, aging Mars Relay Network. This new relay network will utilize four identical satellites that will be in a 3500 km altitude orbit around Mars. These satellites will enable constant communication between the astronauts on the surface of Mars and mission control on Earth. During solar conjunction, the telemetry relay system utilizes the Cycler space stations as an additional relay point between the Earth and Mars to keep communications. To ensure that there is adequate bandwidth for the astronauts, the communications network will be a hybrid optical/radio network. To receive these signals on Earth at DSN locations, a NASA JPL novel 34-m hybrid radio frequency and optical communication antenna will be utilized to receive all signals from Mars. These antennas also allow for the portion of the DSN to be purely devoted to the manned mission instead of competing for antenna time with other deep space missions.

3.5 Mission Outline (Ryan Horvath)

Figure 2 represents the schedule for the entire planned mission to Mars. The first part of the schedule starts with the conceptual design and proposal which will be completed with the creation of this report.

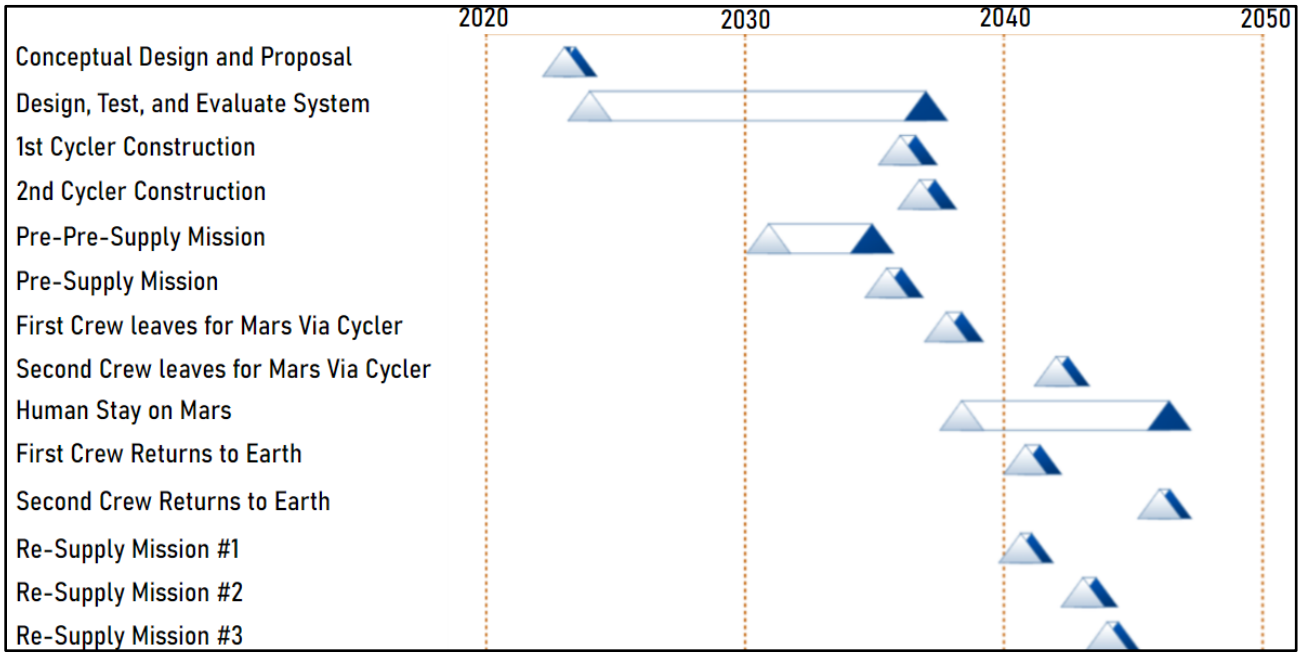

Figure 2: Mission Schedule

Next is the design, test, and evaluation of the system. Theoretically, the span of this segment can start immediately after the completion of this report. This would include the Mars Cyclers, the Martian Habitat, Starship launch vehicles, ground control, and any other equipment necessary throughout the lifetime of the mission. This phase would end at the eventual planned launch of the cyclers on October 13th, 2037.

The construction of both Cyclers would occur within a 1.5-year span before the initial launch. The cyclers will be constructed consecutively instead of simultaneously for increased precision and focus to ensure each is constructed flawlessly. Additionally, constructing one first allows for addressing any potential unforeseen assembly issues before investing in construction of the second Cycler.

The pre-pre-supply mission includes two different tasks. The first is the direct transfer of two rovers, each one going to one of the top two landing locations. These rovers will confirm that the landing location chosen for the mission is satisfactory and if not, then the second most viable option can be considered. If neither is suitable, the mission will be delayed until a proper landing location is confirmed. The launch of these rovers would occur in 2031, with the eventual completion of survey in 2033. The second task in this is the launch of the satellites used in the

New Mars Relay Network that would be sent out on April 17th, 2033. It would then arrive later that year on October 26th, 2033, setting up the new network.

With the confirmation of the landing location, the second pre-supply mission would occur with a launch on June 26th, 2035. This payload would include all instrumentation necessary to complete the scientific objectives, the entirety of the Martian Habitat, RASSORs, KRUSTYs, and all other necessary supplies discussed in the pre-supply section of the report.

Following the successful pre-supply launch and landing on Mars, the Martian Habitat structure will be set up remotely for the eventual arrival of crew after their launch. The first crew leaves for Mars via the Outbound Cycler on October 13th, 2037. They will then be in transit for 216 days, eventually arriving and landing on the surface on May 18th, 2038, initiating the human stay on Mars.

During the first crew stay the first re-supply mission will occur then. The direct transfer starts when it leaves Earth on August 26th, 2040. It would arrive on Mars about 260 days later, on May 13th, 2041.

The first crew would then end their stay on November 5th, 2041. They would take the Inbound Cycler home for 177 days and arrive back on Earth on May 1st, 2042.

While the first crew is returning home, the second crew will begin their ride to Mars on the Outbound Cycler on January 1st, 2042. The second crew will arrive on Mars 160 days later, on June 17th, 2042. Comparing this date to that of when the first crew leaves Mars, there is a noticeable 7–8-month gap between crews on Mars. This is perfectly allowable for this mission and fits in requirements as this decision was made for the ultimate benefit of the crew and the habitat and science systems can still run autonomously when a crew is not present.

The second crew will have two re-supply missions occur during their stay on Mars. The first during their stay, and second overall, would launch on September 1st, 2042. It would eventually arrive around May 19th, 2043, which is almost a year into their stay. The final re-supply mission would then begin on January 10th, 2044. This final supply will arrive on August 13th, 2044, setting up crew 2 to last for the rest of the operation.

The final segment of this mission occurs with the departure of crew 2 from Mars to return to Earth. The Inbound Cycler will be boarded by the crew on January 7th, 2046. After 218 days, the mission will be complete with the return of the second crew on August 13th, 2046. The entire mission summary is encapsulated in Figure 3.

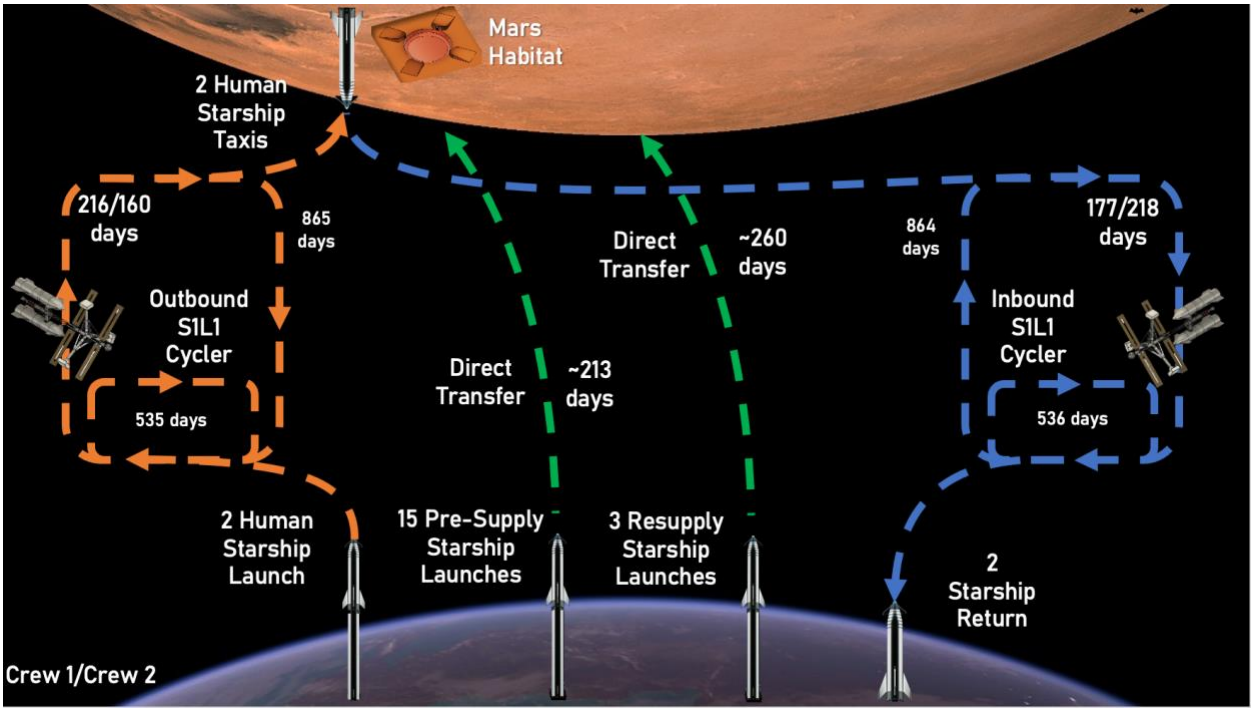

Figure 3: Mission Bat Chart

4: SCIENCE MISSION AND OBJECTIVES

4.1 Objective Definition (Ryan Horvath)

Five major scientific objectives were chosen for the mission: Effects on Humans in Space, Search for Life, Search for Water, ISRU for Materials, and ISRU for Fuel Production.

Starting with the effects on humans in space, it can be broken down into two factors of human health, physical and mental, during the crew's stay on Mars. Due to the physical isolation from the people on Earth, measuring the psychological impact of this on the crew will be important to make sure they are mentally sound. Their psychological well-being will be measured through use of behavioral data. Analyzing the difference in physical health from before and after prolonged periods of time would provide the scientific results desired to determine the effects on humans on Mars. These comparisons can be measured with various tests like the tandem walk test, recovery from fall tests, sensorimotor tests.

The next science objective is the search for life. The main objective of this is to determine if there are any biosignatures currently on Mars. To determine this the crew would need to locate proof of fossils through geomicrobiology, discover isotope patterns, or discover organic molecules. This work would continue the research that has already been conducted by Mars rovers.

The third major science objective is the search for water on Mars. This theme can also be split up into two objectives, one is the confirmation of water on Mars and the second is to determine if it is possible to make the water consumable for human use. To make this objective more reasonable to the crew, guaranteeing the landing location is within an area theorized to have water within a reasonable distance to it is important. Once water is confirmed and possessed by the crew then the next objective can begin. To see if the Martian water is even consumable for humans would be the goal. Gaining proper analysis of it the water is safe to drink or if it could be made safe to drink can possibly reduce the amount of water needed during re-supply missions.

The fourth science objective is the use of ISRU for materials during the stay on Mars. This specifically entails determining if the Martian regolith can be used viably for synthesizing construction material. Being able to continuously collect, process, and test various concrete samples will result in the success of this objective.

Lastly, the ISRU for fuel production will determine the viability of synthesizing propellants on the Mars surface using its resources processed by microorganisms. By testing the resulting I_{sp} and production rate of the fuel made on the surface, it can be determined if this is a worthwhile endeavor for any future Mars operations.

These scientific themes can be represented in the following science traceability matrix:

Table 3: Science Traceability Matrix

Science Theme:	Science Objectives:		Measurements:	Instruments:	Mission Requirements and Constraints:
Effect on Humans in Space	HUM1	Analyze the Psychological impacts of space isolation on the astronauts	Behavioral Data	Crew Health Care System (CHeCS) Data Collection Tool (DCT)	[SO-HUM-1.0] The system shall have the capability to send results from CHeCS back to Earth for a psychologist to analyze.
	HUM2	Analyze the impacts of living on Mars and in Space for prolonged periods of time	Comparison of samples before and during mission, Tandem walk tests, recovery from fall tests, sensorimotor tests, etc.	Tools capable of gathering samples of their health from astronauts like x-rays, ultrasounds, swabs, blood pressure monitor, heart rate monitor, etc. Cameras to record various tests to send back	[SO-HUM-2.0] The system shall be capable of analyzing the physiological effects on the crew from prolonged habitation on the Maartian surface. [TEL-1.0] The system shall return science data within two weeks of acquisition.
Search for Life	LIF1	Determine if there are any biosignatures currently on Mars	Proof of fossils through geomicrobiology, discovery of isotope patterns, or discovery of organic molecules	Drilling equipment to gather soil samples, electron microscope for Geomicrobiology, isotope-ratio mass spectrometer to measure isotope patterns, mass spectrometer. Mars ground transport vehicle	[SO-LIF-1.0] The system shall collect Martian soil and gas samples from diverse locations on the surface of Mars. [LIF-2.0] The system shall be able to analyze samples on the Martian surface or otherwise be able to return select samples back to Earth.
Search for Water	WAT1	Confirm the existence of water beneath or within Martian regolith	Collection of Water	Drilling equipment to either collect Martian Regolith or dig past it to reach potential underground lakes and containers able to hold the samples collected	[WAT-1.0] The system shall be at a landing site chosen within areas previously noted to potentially have water within from satellite information.
	WAT2	Determine if it is possible to make it usable by humans	pH of water and no existance of harmful contaminates within them	Salinity tester, PH testers, secchi disk, and other tools capable of testing safety of water	[WAT-2.0] The system shall include the ability to analyze Martian water composition and potability.
ISRU for Materials	MAT1	Determine the viability of synthesizing construction materials from Martian regolith.	Compressive strength of Martian concrete with natural variance in composition	Concrete cube/cylinder test stand, regolith collection rovers, concrete fabricator	[SO-MAT-1.0] The system shall enable the collection of regolith, processing of concrete, and testing of numerous concrete samples.
ISRU for Fuel production	FUE1	Determine the viability of synthesizing propellants utilizing Martian resources processed by mircoorganisms.	Isp and production rate of fuel produced	Reactors for chemical processing, bacteria culture environment, propellant storage tanks, propellant temperature/pressure instruments	[SO-FUE-1.0] The system shall enable production of 2,3-butanediol through photosynthesis of cyanobacteria, breakdown of bacteria into sugars by enzymes, and breakdown of sugars by E.coli to produce rocket propellant.

4.2 Science Objective Prioritization (Zachary Kessler)

The most important science objective when astronauts arrive on Mars is Regolith Extraction. This mission will be started before the astronauts arrive, as the RASSOR rovers can work autonomously. The base, once covered with regolith, will provide exceptional radiation protection. Water can also be extracted from the regolith, so starting early on with the RASSORs can guarantee usable water quickly once the astronauts arrive. Lastly, regolith will also be needed for growing plants. As the mission progresses, the need for regolith will decrease and this objective will move down the priority list.

The next science objective is the Search for Water. As the astronauts arrive to Mars with water, finding water is not an instant need. However, as astronauts need to have a constant source of water produced on Mars, either from regolith or ice extraction, this is a critical science objective to address early. Due to its mass, astronauts cannot rely solely on resupply missions to supply sufficient water. Thus, it is mission critical to find water on Mars. Water is required for astronaut consumption, hygiene, and the greenhouse.

Growing plants will be the next critical science objective. While sending food is more mass efficient than sending water, growing and testing how food is grown on Mars is also mission

critical. The astronauts will need to grow food for the seven years they are present on Mars to sustain themselves. This is also very important to explore how plants grow in different soils, especially Mars, where there is interest in setting up permanent settlements in the future.

Space effects on humans is a mission critical science objective that will be running from the time the astronauts reach the Cycler to the time they set foot back on Earth. There will be constant monitoring of behavioral, physical, and psychological effects of the astronauts. This is mission critical, as if the effects of the first crew are too drastic, the decision to abort the launch of the second crew and bring the first home earlier could be made. This is also very important as data for how future missions can be pursued with humans.

The last two science missions have the lowest priority as neither are mission critical. The search for life is something that has always been a question on Mars but would not put the mission in jeopardy. Lastly, bio-propellant production has the lowest priority, as this is a test of the system that hopefully can produce propellant in a very easy manner. This propellant is not going to be used for anything other than tests and scientific data, which will be sent back to Earth for evaluation. The collected data will be critical to future human missions but not for the seven-year mission.

5: TRANSPORTATION SYSTEMS

5.1 Cycler Orbit (Veronica Rankowicz)

The ballistic S1L1 cycler orbit repeatedly encounters Earth and Mars and does not require any ΔV maneuvers to achieve this orbit due to its ballistic nature. This orbit repeats itself every two Earth-Mars synodic periods, so approximately every 4 2/7 years, where it has a flyby order of Earth-Mars-Earth-Earth [4]. This orbit can be broken down further into two types: the inbound cycler and the outbound cycler. The inbound cycler prioritizes minimizing the time of flight from Mars to Earth while the outbound cycler prioritizes minimizing the time of flight from Earth to Mars. As a result, two cycler vehicles will be used, one in the inbound trajectory and one in the outbound trajectory to minimize flight time for the astronauts in both directions of travel (Earth to Mars and Mars to Earth). Both cyclers begin operation at similar times and will be in operation by their respective Earth-1 encounter dates where they will have been boosted into their S1L1 orbits.

5.1.1 Assumptions (Veronica Rankowicz)

To generate potential mission itineraries for both the inbound and outbound cycler for a thirty-year time frame, simplifying assumptions were made to determine the key parameters of this trajectory. A circular-coplanar model was used for Earth and Mars' orbits as this allows for a simple solution to be found that gives us a better understanding of the problem at hand, which given more time enables the development of a more realistic model as simplifying assumptions begin to be eliminated. The Cycler is also assumed to lie on the ecliptic plane along with Earth and Mars, where the ecliptic plane is the plane on which the Earth orbits with respect to the Sun. It was also assumed that Mars encounters do not alter the Cycler's trajectory and that Mars' gravitational effects can therefore be neglected. However, Earth's gravitational effects cannot be neglected so it does provide gravity assists and it is assumed that these occur instantaneously. To determine this orbit, it was assumed that the Earth-Mars synodic period is 2 1/7 years.

Due to the nature of this trajectory, the Cycler repeats its trajectory every 30 years, so the trajectory parameters determined by Dr. McConaghy can be adjusted by increments of 30 years to have data that aligns with the time frame of the mission. The precise dates of the encounters are given such that an encounter is defined as the closest approach altitude from the planet the cycler is passing by. Additionally, the closest approach altitudes, V∞ values, and time of flight (TOF) values between encounters are provided by Dr. McConaghy [4]. The values are outlined in Table 4 and Table 5 below.

Table 4: Outbound Cycler Itinerary Parameters [4]

Encounter	Date	V_∞ (km/s)	Closest Approach Altitude (km)	TOF (days)
Earth-1	10/13/2037	5.19	21400	N/A
Mars-2	5/18/2038	2.98	11200	216
Earth-3	7/15/2040	7.02	24800	790
Earth-4	1/8/2042	7.02	37400	542
Mars-5	6/17/2042	5.89	9800	160
Earth-6	10/10/2044	5.31	25500	846
Earth-7	3/29/2046	5.31	35200	535

Table 5: Inbound Cycler Itinerary Parameters [4]

Encounter	Date	V_∞ (km/s)	Closest Approach Altitude (km)	TOF (days)
Earth-1	8/7/2039	6.24	19100	N/A
Mars-2	11/5/2041	4.78	6800	820
Earth-3	5/1/2042	7.06	29800	177
Earth-4	10/25/2043	7.06	24800	542
Mars-5	1/7/2046	2.75	9900	805
Earth-6	8/13/2046	4.15	13600	218
Earth-7	1/25/2048	4.15	22500	530

5.1.2 Lambert's Theorem (Veronica Rankowicz)

In order to determine what the trajectory will look like, NASA's SPICE database [5] was utilized to obtain precise positions of the Earth and Mars with respect to the Sun at the previously listed encounter dates in Table 4 and Table 5. As SPICE provides ephemeris models, a python library called *Spiceypy* was used to extract the planetary position data for both Earth and Mars at the encounter dates in the ecliptic plane with respect to the sun at any given time within the time frame of the selected ephemeris model [6]. These positions were then used to calculate the transfer angle between the initial position and final position (first encounter location to the second encounter location) using the space triangle to solve Lambert's problem. The transfer angle is then used to determine which type of elliptic orbit (1A, 1B, 2A, or 2B) will be used where a transfer angle less than 180 degrees indicates a type 1 orbit and a transfer angle greater than 180 degrees indicates a type 2 orbit.

To determine whether the orbit type is A or B, the TOF of the minimum energy transfer between the initial and final position must be calculated, known as TOF_{min}:

$$TOF_{min} = \sqrt{\frac{{a_{min}}^3}{\mu}}[(\alpha_0 - sin\alpha_0) - (\beta_0 - sin\beta_0)]$$

where

$$a_{min} = \frac{s}{2}, \alpha_0 = 2sin^{-1}\sqrt{\frac{s}{2a_{min}}},$$

and

$$\beta_0 = 2sin^{-1}\sqrt{\frac{s-c}{2a_{min}}}.$$

When the given TOF in Table 4 or Table 5 is smaller than TOF_{min}, this indicates a type A orbit where a TOF greater than TOF_{min} indicates a type B orbit.

Knowing the type of orbit (1A, 1B, 2A, or 2B), the semimajor axis (a) can now be computed using an iterative process to solve Lambert's Equation, which can be modified for each type of orbit:

$$\sqrt{\frac{\mu}{a^3}} \cdot TOF = \begin{cases} (\alpha_0 - sin\alpha_0) - (\beta_0 - sin\beta_0) & \text{Type 1A} \\ (2\pi - \alpha_0 - sin(2\pi - \alpha_0)) - (\beta_0 - sin\beta_0) & \text{Type 1B} \\ (\alpha_0 - sin\alpha_0) - (-\beta_0 - sin(-\beta_0)) & \text{Type 2A} \\ (2\pi - \alpha_0 - sin(2\pi - \alpha_0)) - (-\beta_0 - sin(-\beta_0)) & \text{Type 2B} \end{cases}$$

Having calculated the value of the semimajor axis, the semilatus rectum (p) of the orbit can now be calculated:

$$p = \frac{4a(s-r_1)(s-r_2)sin^2\left(\frac{\alpha_0 \pm \beta_0}{2}\right)}{c^2}$$

where the maximum p value must be found for type 1A and 2B orbits, and the minimum p value must be found for type 1B and 2A orbits. By knowing the values of both the semimajor axis and semi-latus rectum, it is possible to determine any other orbital parameters desired including the eccentricity of the orbit.

5.1.3 Trajectory Results (Veronica Rankowicz)

A multi-revolution Lambert solver was designed to produce the orbital parameters needed to plot the S1L1 orbit of both cyclers. The cycler's orbit for both the inbound and outbound cycler are broken up into legs, where each leg refers to the path taken from one planetary encounter to the next.

The outbound cycler's purpose is to transport the crew from Earth encounter points to Mars encounter points (minimize TOF during this), so as a result the cycler vehicle completes only about 0.5 revolutions of the elliptical orbit between the Earth-1 and Mars-2 encounter points. However, the cycler completes approximately 1.5 revolutions on the elliptical orbit from Mars-2 to Earth-3 and again approximately 1.5 revolutions on the new elliptical orbit from Earth-3 to Earth-4 where at the Earth-4 flyby the cycler of the outbound cycler then repeats itself. The Earth-3 to Earth-4 leg occurs because two synodic periods have not yet elapsed. This is seen in Figure 4 below.

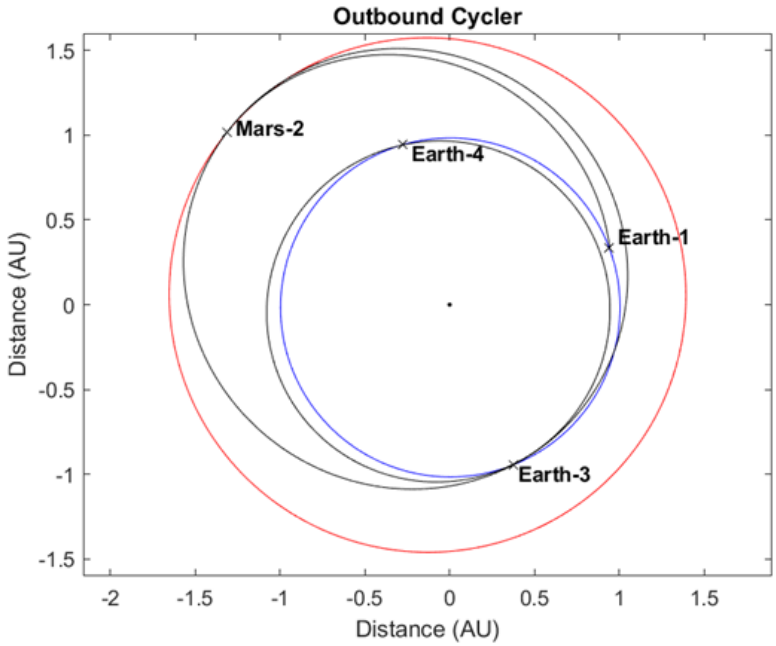

Figure 4: One Cycle of S1L1 Outbound Cycler Trajectory in Circular-Coplanar Model

For the inbound cycler, as its goal is to reduce the TOF from Mars to Earth encounters, the cycler vehicle completes approximately 1.5 revolutions on the elliptical orbit from Earth-1 to Mars-2, where it then encounters the Earth at Earth-3 in under half a revolution. However, since two full synodic periods have not yet occurred, the cycler vehicle travels on the Earth-3 to Earth-4 elliptical orbit for approximately 1.5 revolutions where at the Earth-4 flyby the cycle then repeats itself. As the inbound cycler's purpose is to return astronauts back to Earth from Mars, crew 1 will board the inbound cycler at Mars-2 and depart at Earth-3. Meanwhile, crew 2 will board the inbound cycler at Mars-5 and depart at Earth-6. This is seen in Figure 5 below.

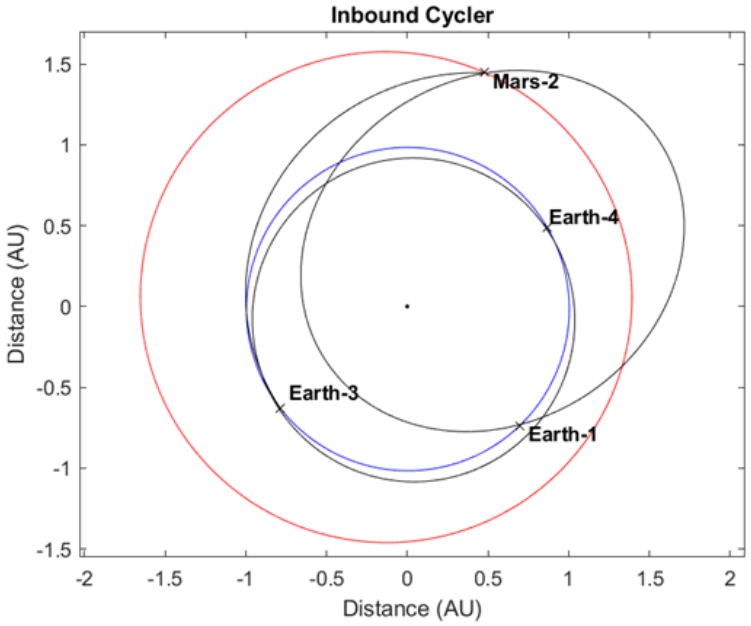

Figure 5: One Cycle of S1L1 inbound Cycler Orbit in Circular-Coplanar Model

5.1.4 Incorporating Ephemeris Model for Full Mission (Veronica Rankowicz)

By incorporating ephemeris data, the relative positions of Earth and Mars no longer repeat precisely so in reality this trajectory is nearly ballistic but will require minimal ΔV capabilities to correct the Cyclers' trajectories. This will be accomplished using either the two Starship vehicles docked to the cycler or a backup cycler propulsion system when there are no Starships present on the cyclers.

Examining the plot for the outbound cycler trajectory for the duration of the mission, it is very clear that it is favorable for astronaut transport from Earth to Mars where for the mission, Crew 1 will spend 216 days onboard the outbound cycler (Earth-1 to Mars-2), and Crew 2 will spend 177 days onboard the outbound cycler (Earth-4 to Mars-5). This is illustrated in Figure 6 where the encounter points are marked on the plot.

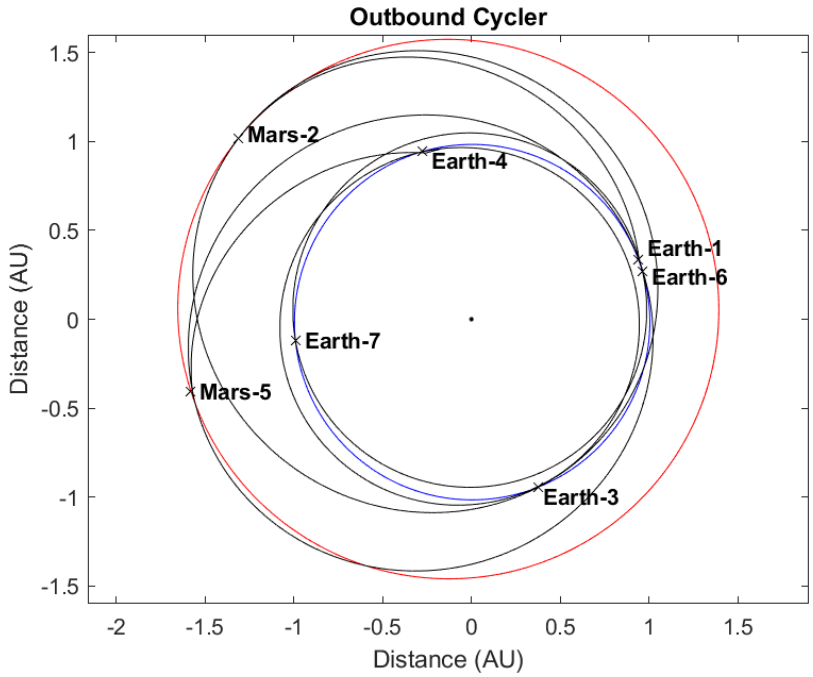

Figure 6: Outbound Cycler Trajectory for Entire Mission in Circular-Coplanar Model

Examining the plot for the inbound cycler for the duration of the mission, it is very clear that it is favorable for astronaut transport from Mars back to Earth, where Crew 1 will spend 160 days onboard the inbound cycler (Mars-2 to Earth-3). Meanwhile, Crew 2 will spend 218 days onboard the inbound cycler (Mars-5 to Earth-6). This is illustrated in Figure 7 where the encounter points are marked on the plot.

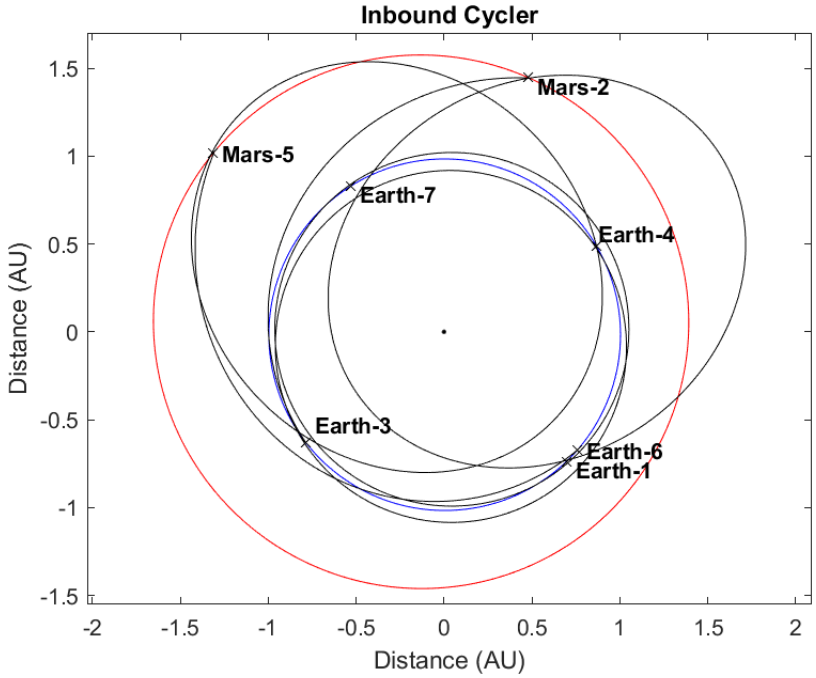

Figure 7: Inbound Cycler Trajectory for Entire Mission in Circular-Coplanar Model

In total, Crew 1 will spend a combined 393 total days onboard both cyclers and Crew 2 will spend a combined 378 total days onboard both cyclers, making their total flight times onboard the cyclers very similar. Crew 1 will also be onboard the outbound cycler as it is being boosted into its S1L1 orbit to the Earth-1 encounter point. Crew 2 will rendezvous with the cycler at the Earth-4 encounter point. Neither crew will be onboard the inbound cycler as it is being boosted to its S1L1 orbit at its Earth-1 encounter point.

It is also important to note that although the legs of the cycler going from one Earth encounter to another Earth encounter appear to be very near to the Earth, the cyclers are actually millions of kilometers away from the Earth. Even at the closest approach points, the cyclers are anywhere between 13,600 km to 37,400 km away from the Earth which is close enough for the flyby maneuvers to provide a gravity assist however at the speeds that the cyclers are flying by the Earth at, their speeds and distances away from the Earth are large enough to ensure that the cyclers do not capture into the Earth's orbit but instead remain in a heliocentric orbit (orbit around the Sun).

5.2 Cycler Radiation Analysis (Luke Miller)

Exposure to radiation is ubiquitous in any space mission. Therefore, radiation considerations were investigated for both the transit to Mars, and the surface stay. The following section will introduce the radiation problem along with highlights of how radiation was analyzed for the mission. A discussion on the findings for managing radiation during the transit to Mars will also be included in the following section. Discussion regarding radiation exposure during surface operations can be found alongside other surface stay considerations on page 80. Here total mission radiation totals will be presented as well.

5.2.1 Familiarization with the Radiation Problem (Luke Miller)

Potentially the most daunting hazard of a human mission to Mars is the space radiation environment. Here a short summary of the relevant concepts of space radiation is presented to provide unfamiliar readers with a sense of orientation. In brief the natural radiation environment can be summarized as follows:

- **Solar Particle Events (SPEs):** In the context of Solar Particle Events, the solar particles of principle interest are protons that are ejected from the sun in a solar flare or accelerated by a coronal mass ejection [7]. After emission from the sun these protons propagate outward into the solar system. When a large number of protons are emitted in a short time period, it is referred to as a Solar Particle Event. The frequency of SPEs is directly related to the 11-year sunspot cycle where SPEs are more frequent at the "solar maximum" and less frequent at the "solar minimum" [8]. In general, while SPEs can occur several times a day in a solar maximum, the events are typically not strong enough to be of significant concern [7]. SPEs are of low enough energy that their effect can be effectively mitigated with shielding [9]. However, they are extremely intense and there is a lack of capability in forecasting the timing and severity of SPEs [9]. This means that in free space, an unprotected or under protected astronaut could receive a fatal dose of radiation within

minutes to hours [9]. Solar Particle Events vary in the proton flux, energy spectra, and duration of each event. Typically, the sum of the solar particle events that happened in October of 1989 is used as a reference value when discussing SPEs. These particular events had a proton flux of 40,000 pfu (proton flux units) greater than 10 MeV [10]. This makes the Oct. 1989 events some of the largest SPEs measured, and thus a good reference [10].

- **Trapped Radiation:** Trapped radiation refers to the protons and electrons trapped in the magnetic field of celestial bodies. In a mission to Mars the primary trapped radiation concern is the Van Allen belts which are formed by Earth's magnetosphere. Here the energies of the trapped particles are similar to the energies of particles from SPEs. With the current proposed mission, the time spent passing through regions with considerable amounts of trapped radiation will be negligible compared to the whole mission. Additionally, typical SPE shielding is adequate for shielding from trapped particles [8]. Therefore, trapped radiation was not a driver of radiation mitigation strategies in this mission concept.
- **Galactic Cosmic Radiation (GCR):** The third form of radiation of concern in GCR. GCR represents the omnipresent background radiation in space. GCR originates from beyond the solar system and is composed mainly of protons and heavier ions with very high energies [9]. At such high energies these particles can move through meters of material unimpeded [9]. This makes shielding against GCR infeasible without using meters of material. The intensity of GCR also follows the solar cycle [9]. At solar maximum GCR is least intense, and at solar minimum GCR is most intense [9]. From solar minimum to solar maximum GCR intensity varies by nearly a factor of two [9]. While GCR is far more energetic than SPEs and always is present, it is also less intense than the typical SPE [9]. This means that while GCR is challenging to shield against, the dose rates are low. However, in a long duration mission, the accumulation of GCR exposure is one of the largest radiation concerns.

In the ensuing discussion of radiation, the SI unit of Sievert (Sv) will be used. It is important to understand that a Sievert is not measuring the exposure to radiation. Instead, the Sievert measures stochastic health consequences caused by radiation exposure. For context, a single chest x-ray clocks in at 0.1 mSv [11]. It is critical for mission planners to understand the role radiation plays on multiple timescales. In the perspective of shorter timescales (minutes to hours), radiation is discussed as acute radiation dosages. Large acute dosages can result in massive cell death that can lead to symptoms of radiation sickness and potentially rapid death of the astronaut [9]. In a mission to Mars, the most likely source of a large acute radiation dose is SPEs because of their very high intensity [9]. This is why it is of paramount importance to properly shield the crew from SPEs. The other timescale that should be kept in perspective is the dose received over the duration of the mission and the rest of a crew member's life. These dosages are referred to as chronic dosages and represent the accumulation of radiation exposure over a long time. High chronic radiation dosages can have long term health effects. Chiefly among them is a heightened chance of developing cancer due to the damage that radiation inflicts on the reproductive processes of cells [9]. These concerns are a main driver of the requirements formulated to reduce radiation exposure in a mission. In the context of chronic radiation exposure, the combined effects of SPE and GCR exposure must be

considered, however, the persistence of GCR tends to dominate the total exposure over the duration of a mission to Mars [9].

Another key aspect of the radiation environment is secondary radiation. This is a phenomenon where the original high energy radiation particle collides with the shielding material and causes fragmentation of the nuclei of shielding material [9]. This means that in addition to the original radiation, additional radiation is produced from the fragmentation of the shielding nuclei, creating the potential for elevated radiation levels above what would have been measured with no shielding [9]. Physically, this is shown in a diagram in Figure 8.

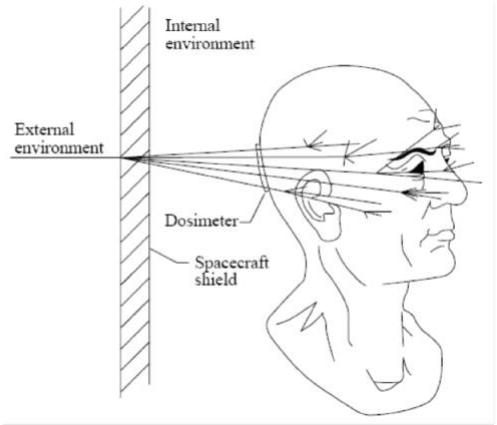

Figure 8: Secondary Radiation [9]

A plot which shows how secondary radiation can change the total dosage due to GCR is shown in Figure 9 below. From Figure 9 it is evident that as the depth of the shielding material increases (in this case the material is Aluminum) there is an initial decrease in dose. This corresponds to a regime where lower energy GCR is shielded by a thin layer of aluminum. However, as the aluminum thickness is increased, the dosage begins to rise against intuition. This demonstrates the importance of understanding secondary radiation. It is in this regime where the shielding material is thick enough to generate many secondary particles, but it is too thin to effectively stop them. The result is a shield that causes more harm than good. Finally, a depth of shielding material is reached that results in a substantial decrease in dosage. It is at this point where the material is thick enough to contain its own secondary radiation and effective shield from GCR. However, by this point the shield has become quite thick, making it infeasible to be placed on a spacecraft due to mass constraints. Different materials respond differently to radiation and some produce more secondary radiation than others. This will be discussed further in material selection for the radiation shielding.

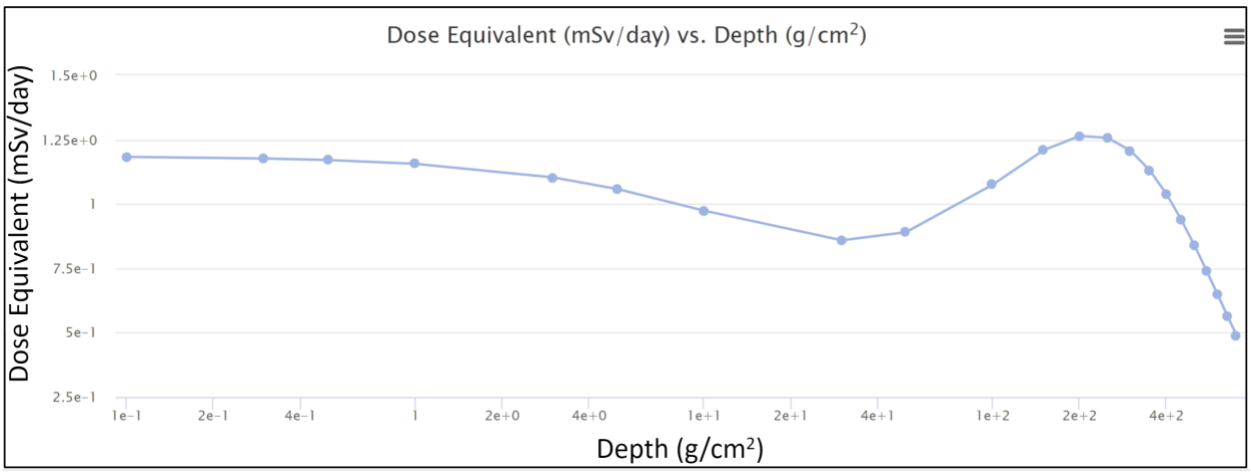

Figure 9: Impact of Secondary Radiation on Aluminum: Log-x Scale4.2.2 NASA Radiation Standards (Luke Miller)

For crewed missions, NASA has standards with respect to the radiation dosages that astronauts may receive. Key NASA standards are presented in Figure 10below.

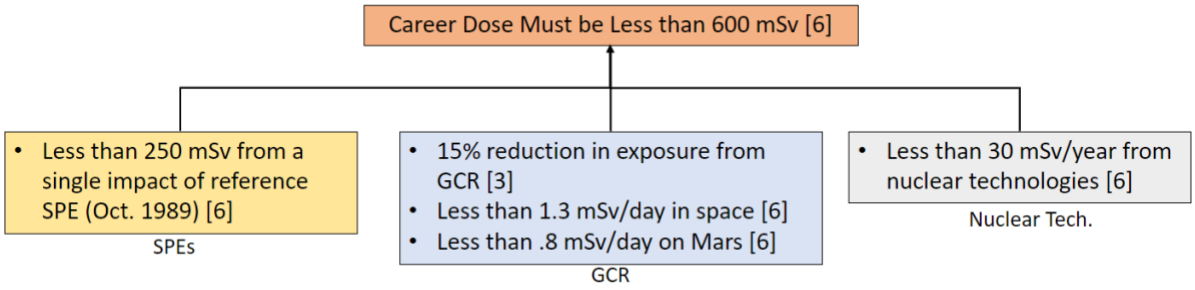

Figure 10: NASA Radiation Standards

Figure 10 shows that in an astronaut's career, the total cumulative radiation dose is not to surpass 600 mSv [12]. For the present mission concept, the major potential radiation sources are SPEs, GCR, and nuclear technologies. For SPEs, NASA requirements state that a crew should be protected in a manner that sufficiently reduces the dosage from the October 1989 SPE to below 250 mSv [12]. This requirement is in place so that acute radiation doses are managed, and crew members do not suffer from radiation sickness [12]. NASA also requires that shielding reduces GCR exposure by 15% which on average equates to about 1.3 mSv/day in free space and 0.8 mSv/day on the surface of Mars [12]. Another guideline of importance to the mission being discussed is limiting radiation exposure due to nuclear technologies to less than 30 mSv/year [12]. Finally, NASA sets an "as low as reasonably achievable" (ALARA) principle that must be observed [12]. According to this principle radiation exposure should be minimized wherever possible.

5.2.3 Radiation Shielding Approach (Luke Miller)

Radiation shielding represents a central tradeoff in the planning of a space mission. In order to mitigate risk due to radiation exposure, shielding mass must be included as payload. However, the

large amount of mass needed to effectively shield crew members from radiation can quickly become a prohibitively expensive payload from the perspective of a propulsion system. Therefore, it is necessary to balance acceptable risk due to radiation exposure with acceptable launch cost due to shielding mass. The approach taken in this architecture is to accept larger dosages from GCR on the Cycler where there is a large cost to adding mass for shielding. This is allowable because of the relatively short amount of time spent on the Cycler. However, considerations must be taken to minimize secondary radiation during this mission phase. To better protect from SPEs a "storm shelter" using the water already onboard the Cycler is proposed. While on the Martian surface the approach is to use in situ resources to aggressively shield from GCR. This is an advantageous approach because it reduces the amount of mass that must be launched from Earth, while preventing GCR dosages from accumulating to unacceptable levels during the long stay on Mars.

5.2.4 NASA OLTARIS and Radiation Study Methodology (Luke Miller)

The tool used for the presented radiation studies is the NASA On-Line Tool for the Assessment of Radiation in Space (OLTARIS). OLTARIS is based on the HZETRN (High Charge and Energy Transport) space radiation transport code [13]. In summary, OLTARIS uses transport algorithms to propagate particles from an ambient space environment through shielding materials and tissue [13]. OLTARIS has capabilities to analyze trapped radiation, SPEs, and GCR. It has functionality for analysis of radiation on the Martian surface as well as free space, both of which are of particular use for the mission profile being considered. For more information on OLTARIS, including its limitations, readers are referred to the OLTARIS User Guide (source [13]) and its associated documents.

An overview of the approach taken in the radiation study is presented below.

1. Treat geometries of the habitat and Cycler as spheres with the same "average thickness" as the real geometry. This can be achieved by approximating the Cycler gravity modules as rectangular prisms and the Martian habitat as cylinders. A 2D visualization of this is shown in Figure 11.

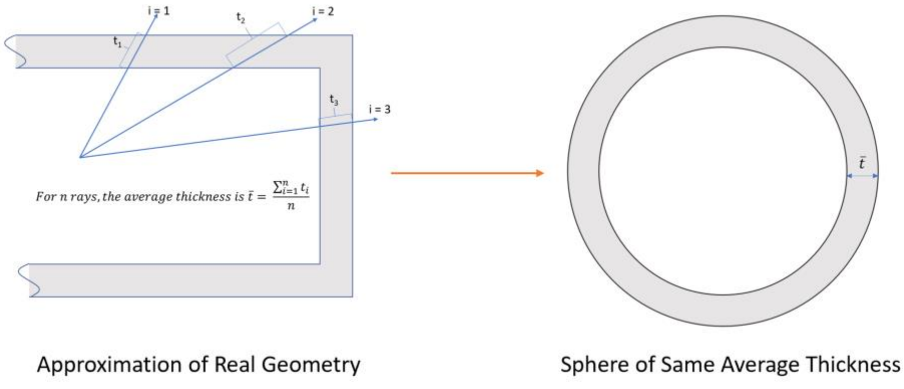

Figure 11: Approximate Geometry for Radiation Studies

Approximating real geometry as spheres of uniform thickness is a large assumption made in this analysis. However, this assumption is fairly regular in preliminary radiation analysis [14]. Without this assumption analysis of full 3D effects becomes computationally expensive and complicated raytracing routines would need to be implemented. As a design is rapidly iterated upon, the simplified approach is preferred to get rough estimates of radiation exposure, but later in the design cycle it would be necessary to do full radiation modeling of complex geometries. To verify that the simplified approach is reasonable, the team used NASA to provide real 3D geometries of ISS modules to compare the full 3D analysis to the spherical approximation. This analysis was done for a free space GCR environment. The results are shown in Table 6.

Table 6: Assessing Spherical Geometry Assumption with ISS Modules

	US Lab	Service Module	Node 1	Cupola
Effective Dose - 3D Geometry (mSv/day)	1.068	1.017	1.049	1.044
Effective Dose - Spherical Approximation (mSv/day)	1.171	1.037	1.050	1.141
%Difference	8.8%	1.9%	0.1%	8.5%

Table 6 shows that simplified approach of approximating the geometry as a sphere quite reasonable. However, it is important to understand that this is still just an assumption, and as parameters of the problem are changed this assumption may break down. This makes full 3D radiation simulations important for future work.

2. Run OLTARIS for different shield configurations to determine the optimal shield thickness and composition. In this stage the proper radiation environment had to be specified. For the Cycler phases of the mission the inputs in Table 7 were used.

Table 7: OLTARIS Inputs for Cycler

Category	Selection
Environment	Free Space 1AU
GCR Model	Badhwar-O'Neill 2020
Dose Target	Tissue
Dose Weighting Factors	ICRP 60
Anatomical Model	Computerized Anatomical Male

3. Translate the average thickness of the spherical approximation back into true thickness of the geometry.

5.2.5 Radiation Study for the Cycler (Luke Miller)

Materials Considered:

The performance of any radiation shield is highly dependent on the materials being used. For the Cycler the team considered several options including bismuth trioxide, aluminum, polyethylene, phenolic novalac, and water amongst others. While phenolic novalac and bismuth trioxide have

been shown to be effective shielding materials, the assessment of the team is that they are not mature enough to be considered as primary shielding materials in this mission architecture [15][16]. Of the remaining materials the team sought out materials that are proven effective at shielding from radiation, that have relatively low densities and high hydrogen content. High hydrogen content is desirable because hydrogen is more effective in shielding GCR while producing less secondary radiation than other elements [17]. This leads to the selection of water and polyethylene for radiation shielding purposes. Amongst these, polyethylene is preferred. This is because polyethylene is a more effective shield, less dense, and easier to work with than having a liquid water shield. Figure 12 demonstrates how polyethylene is a more effective shielding material.

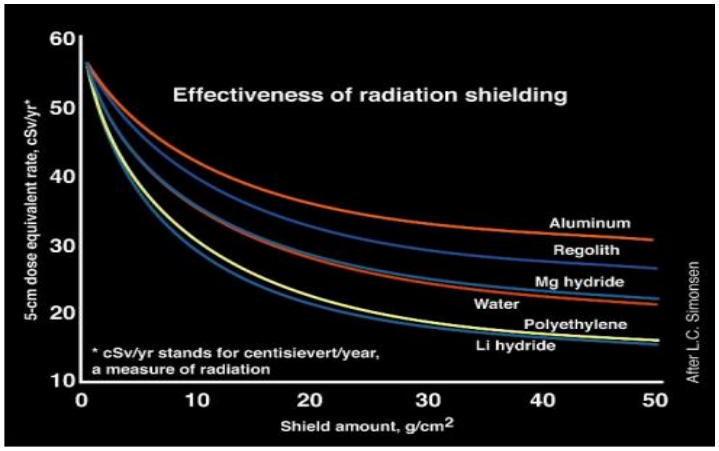

Figure 12: Effectiveness of Radiation Shielding for Different Materials [8]

However, the team also seeks to leverage the water that must be onboard the Cycler for life support needs. Therefore, while polyethylene will be the primary shielding material, water will also be used for added shielding for a SPE storm shelter to satisfy ALARA obligations. Additionally, there is a necessity to use aluminum for structural purposes. This affects the radiation response of the spacecraft and is incorporated into radiation analysis.

GCR Results:

The goal of the shielding on the Cycler is to be at a thickness that can block lower energy particles without generating secondary radiation at a rate that is detrimental to the overall radiation dosage (see Figure 9). 5cm of aluminum is accounted for in this analysis based on structural needs. This configuration has structural aluminum on the outside of the vehicle backed by polyethylene. Figure 13 shows that the GCR dosage while on the Cycler is minimized at 15cm for both crews. Selecting this value for the Cycler design results in an expected GCR radiation dosage of 284 mSv for Crew 1 and 253 mSv for Crew 2 while on the Cycler.

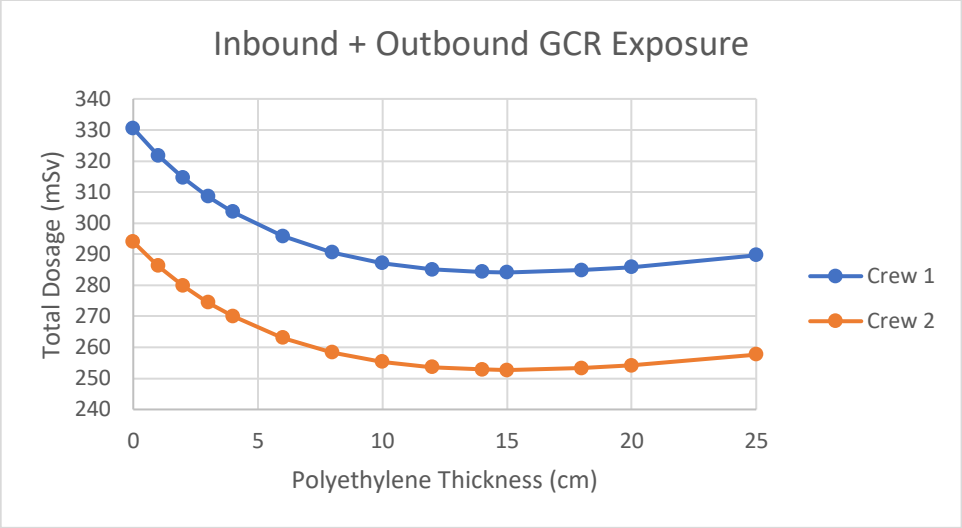

Figure 13: Expected Cycler GCR Dosages

A noteworthy driver of the results in Figure 13 is how the timing of the transit to Mars aligns with the solar Sunspot Cycle. While the Sunspot Cycle is about 11 years long, this is variable, making it difficult to project what solar activity will look like during the mission [9]. The results shown in Figure 13 assume that the Sunspot Cycle will follow an exact 11-year period so that the radiation environment can be extrapolated to the time of the proposed mission. This represents the best estimate of the environment that the crews will see. However, to set bounds for the best case and worst case GCR exposure historical data from the 2001 Solar Minimum and 2010 Solar Maximum was used. This is shown in Figure 14 for the Crew 1 mission profile. The Crew 2 profile would show nearly identical results. It is worth noting again that GCR exposure is lowest during solar maxima, and highest during solar minima.

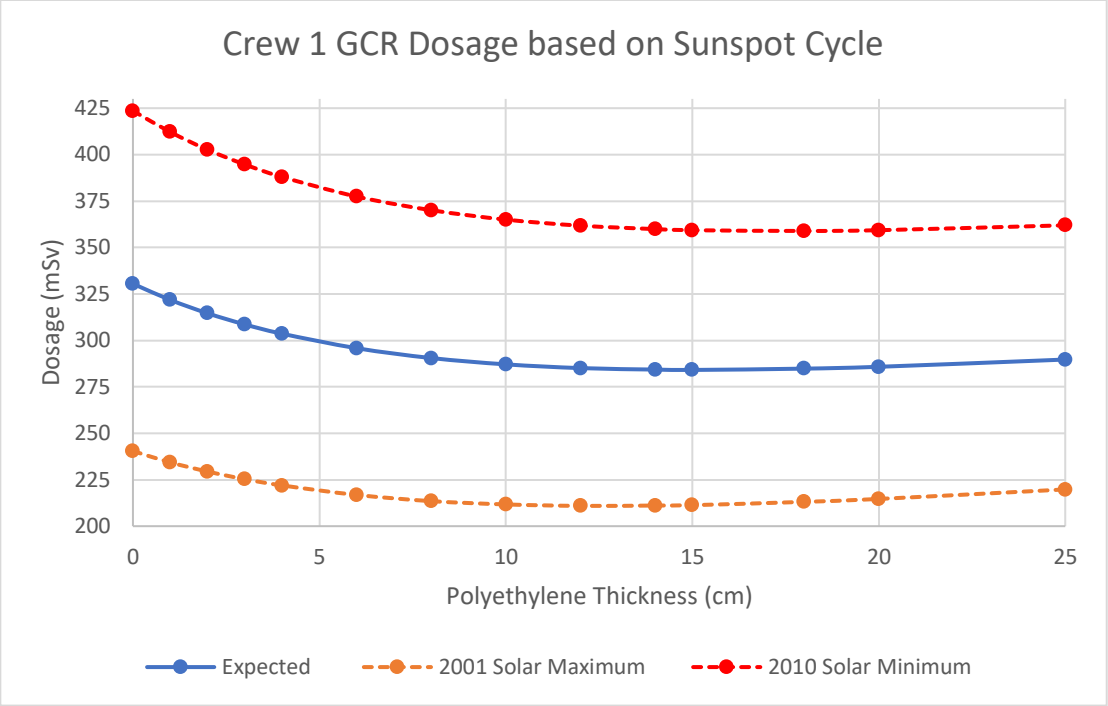

Figure 14: GCR Dosage for Different Times in Sunspot Cycle

SPE Results:

The next analysis seeks to quantify what impact SPEs would have on the Cycler leg of the mission. In this study the goal is to examine the effectiveness of the proposed storm shelter at shielding from the reference SPE (Oct. 1989 event). The planned shelter is to have the same thickness of aluminum and polyethylene as the rest of the cycler with an additional 10cm of onboard water when full. Using 3800kg of onboard water a 3.2m spherical shelter can be achieved with this water thickness. This shelter is planned to be in the Remote Command Module; however, this is still an open question in the Cycler design. A representative cross section is shown in Figure 15.

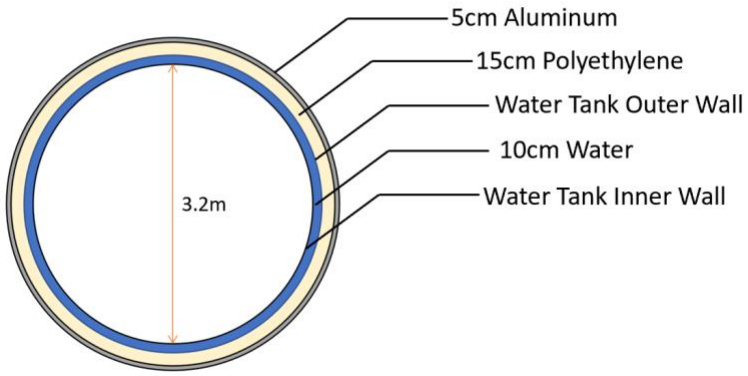

Figure 15: Representative Radiation Storm Shelter

The performance of the SPE is characterized in Table 8. Here it is shown that with no shielding at all the dosage received would be an astonishing 26210 mSv. However, with only the base Cycler shielding the dosage is greatly reduced to 53.3 mSv, well below NASA standards. This is improved to 35.9 mSv with a full storm shelter, however as water supplies are depleted the shelter's effectiveness is depleted. By the time the shelter is down to 1cm of water it can only add an added 0.8 mSv of protection. However, it is emphasized that even with no extra water the crew is protected well beyond NASA's standards for SPEs.

Table 8: Dosages from Sum of October 1989 SPEs

	NASA Standard	No Shielding	5cm Al + 15cm Polyethylene	+ 1cm Water	+ 10cm Water
Effective Dose (mSv)	250	26210	53.3	52.5	35.9

It is farcical to try to exactly predict the exact SPE dose a crew would receive on a mission years in advance (much like trying to forecast the weather on Earth over a decade ahead of time). However, for this mission it is reasonable to set aside a conservative estimate that while on the Cycler the crews will receive up to 75 mSv from SPEs. It should be noted that this is a "doomsday" type estimate. This estimate comes from the desire to be prepared for an event like the reference SPE with a factor of safety of 1.4. The reference SPE has been described as a once in a century event and it is unlikely that this mission would encounter anything as strong as that [8]. However, during times of solar activity smaller SPEs can occur several times a week [9]. Up to 95% of SPEs pose very little risk beyond ALARA considerations though [8]. These smaller SPEs are anticipated to deliver doses well under 1 mSv per event. Therefore, the team assesses 75 mSv as the best conservative estimate of the SPE dosage while on the cycler.

5.3 Life Support System for the Cycler (Luke Miller and Matt Kelley)

5.3.1 Cycler Life Support Demands

Ensuring the survival and health of the astronauts is an absolutely essential aspect, and similarly one of the greatest challenges, of manned spaceflight. Human spaceflight missions have to be designed to meet the basic metabolic needs of humans in the barren environment of space. Life support systems were originally designed using completely consumables, with no regeneration or recycling, as mission durations were short enough that consumables were more mass and power efficient. Long-term missions, like the International Space Station, currently utilize reclamation techniques that allow for the re-use of consumables such as water and oxygen.

Of vital importance to the proposed mission is the life support infrastructure. Here the high-level demands of the life support infrastructure in the Cycler will be summarily outlined. Beginning with food requirements, astronauts onboard the ISS consume about 0.71 kg of food per astronaut per meal [18]. An additional 0.12 kg/meal of packaging is required for this food [18]. This results in a daily food need of 9.96 kg/day for the proposed mission. For the Cycler leg of the mission all food will be sent from Earth with the astronauts. The second leg of the life support

system is the water requirement. Once again, ISS consumption values shall be taken to estimate values needed for a mission to Mars. Onboard the ISS, 3 gallons of water are used per astronaut per day for consumption and hygiene needs [19]. This equates to 11.4 kg of water per astronaut per day. However, the ISS has a reclamation rate that is conservatively estimated at 70% [20]. The team believes that this value is reasonably achievable for the life support system on the Cycler. Therefore, while 11.4 kg of water is used by each astronaut each day, only 3.4 kg of water leaves the system per astronaut per day, resulting in a much lower total water need for the mission. The last leg of the life support infrastructure considered is the oxygen (O2) needs of the astronauts. The ISS uses electrolysis to produce O2 from water [22]. While oxygen consumption can be highly variable, an average value of 0.84 kg of O2 needed per person per day is a reasonable estimator [21]. Using the chemical equation for electrolysis in Figure 16 below the water needed to produce the requisite O2 is 0.95 kg of H2O per astronaut per day.

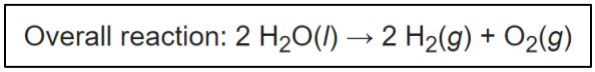

Figure 16: Hydrolysis Chemical Equation

It should be noted that this electrolysis process will draw 1.4 kW of power [23]. The total mass of water and food demanded for each transit leg to and from Mars is given in Table 9.

Table 9: Consumable Masses for Nominal Cycler Legs

Mission Leg	Food Mass (kg)	Water Mass (kg)
Crew 1 Outbound (216 days)	2152	3760
Crew 1 Inbound (209 days)	2080	3640
Crew 2 Outbound (218 days)	2171	3797
Crew 2 Inbound (160 days)	1593	2786

5.4 Artificial Gravity Investigation and Implementation (Tim Osifchin)

5.4.1 Microgravity Environment (Tim Osifchin)

Over the past million years, humans have been continually adapting and evolving. The environments being adapted to all have their slight differences, like temperature and atmospheric pressure, but in terms of a universe of different environments, the variations of Earth environments in mute. When compared to environmental conditions the universe has to offer, humans have evolved to survive in a singular environment with specific temperature, pressure, humidity, atmospheric composition, and gravity field. Adapting to new environments takes time even if they are relatively similar in the grand scheme of things. The environment present in a spacecraft orbiting the Earth is one such environment that in most aspects is entirely like Earth. However, there is one key difference that is of extreme importance – microgravity. While astronauts on the International Space Station (ISS) are still within the Earth's sphere of influence and therefore experience a gravity pull from Earth, they do not feel this gravity force because they are in a continuous freefall. The only reason the entire ISS does not fall to Earth is because it is balanced by its velocity which if un-acted upon would result in escape from the Earth's sphere of influence.

For humankind to travel far beyond the Earth, not just for a quick round-trip but mass colonization, humans will need to learn how to survive in both microgravity and low-gravity environments. The first step is of course understanding what exactly happens to the human body in these environments.

Effects of Microgravity:

Thanks to all the experiments done aboard the ISS, the effects of microgravity are well understood. In short, microgravity is not a friendly environment to be in and causes all manner of health problems. The three most significant challenges to adapting to this type of environment are deteriorating skeletal structures, muscle and soft tissue damage, and disruption of fluid flow within the body.

Studies aboard the ISS have shown that bone loss occurs at a rate of 1% to 1.5% per month in a microgravity environment. Nearly all this bone loss is localized to load bearing skeletal regions, such as the legs. Even this small loss of bone mass can lead to a significantly higher chance of bone fractures. In addition to this increased chance of fracture, any fracture that does occur in microgravity is significantly more difficult to recover from [24].

Losing bone mass does not mean that this mass is simply leaving the body. It is all making its way to soft tissues. Calcification of soft tissues is not pretty and terrible for the functionality of soft tissues. The body can only do so much to fight this calcification. What ends up happening is that astronauts will continually battle kidney stones as the body attempts to expel calcium from soft tissues [24]. Muscles face additional deterioration like the skeletal structure. No longer having to fight against Earth gravity will result in loss of muscles mass, especially in the legs [25]. Even with some mitigation strategies, astronauts who return from extended stays aboard the ISS have extreme difficulty standing on their own. Adaptation back to Earth gravity can range from a few weeks to a whole year depending on the astronaut and how long they were in microgravity [26]. However, one positive aspect of this is that many negative effects of microgravity are reversible with time.

The last major challenge in adapting to microgravity is the loss of fluid pressure that disrupts blood flow. On Earth, gravity creates a pressure difference across the human body. Blood in the legs is at a significantly higher pressure than blood in the head. This is natural and why it feels extremely uncomfortable to hang upside down. In this orientation the pressure difference is reversed. In microgravity, there is no pressure difference at all so the feeling would be in between the normal pressure gradient and the upside-down pressure gradient. The most notable effects of this loss in pressure difference are bulging eyes [25]. On Earth the pressure behind the eyes is rather small because a relatively small amount of fluid is above the eyes in the brain. In Microgravity the pressure in the entire body is equalized so the eyes have significantly more pressure and feet feel significantly less pressure. This increase in pressure behind the eyes causes them to bulge and deform. Sight is an extremely important sense and bulging eyes will impact that. Vision loss is not that uncommon for astronauts living in microgravity for extended periods of time [24]. Pressure also affects the heart. While the heart is typically working against the pressure gradient in the body,

in microgravity there is no gradient to work against. Like the rest of the muscles in the body, prolonged stays in microgravity will weaken the heart [25].

Current and Future Mitigation Strategies:

Numerous different methods are being used aboard the ISS to mitigate the negative effects of microgravity, but only so much can be done. Bone loss and calcification of soft tissue are usually mitigated with medication. This medication is not 100% effective so bone will still occur at a decreased rate, kidney stones may be produced less often, and the astronaut will be dealing with side effects to the drug. It is far from a perfect solution, but it has allowed astronauts to stay in microgravity than before implementation of medication. Continuous exercise is another key aspect of the microgravity effect mitigation strategy aboard the ISS. Putting the body under loads like those experienced on Earth counteracts both bone and muscle deterioration.

Blood pressure loss is significantly more difficult to deal with. While bones and muscles simply need to be under a load to correct for microgravity, a force field is needed to correct for loss of blood pressure. The gravity field on Earth is what gives every single particle in blood weight, which in turn generates pressure. Simply running on a treadmill with elastic bands pulling the astronaut downward does not generate a force field. As mentioned earlier, medication has allowed the length of stay in microgravity to increase. However, this is only up to a point because the lack of a mitigation strategy for blood pressure loss is the limiting factor. Various research groups are looking to develop technologies that generate some pressure gradient in the body, but none have done enough to push microgravity exposure beyond 6 months.

Looking to the future of space travel, it may no longer be viable to simply treat the symptoms of microgravity. A new strategy of dealing with microgravity environments could be to eliminate the microgravity altogether. Spacecraft that can generate a force field which impacts the human body in a manner like gravity would be one way to treat the cause instead of dealing with the results when it comes to microgravity. However, there is a reason why this technology is still only theoretical. The viability of any method to generate such a force field has proven less than ideal. Nonetheless it is important to continually push the boundaries of knowledge and redefine the impossible as reality. The next section will focus on artificial gravity generation and its viability on a manned mission to the red planet.

Until anti-matter and gravity generators become more than just science fiction, there are only two methods that could generate artificial gravity on a space station or spacecraft. The first utilizes linear acceleration and the second involves rotation. While no spacecraft has been built with the capability of generating artificial gravity, they have been theorized in various media. Linear acceleration proved to be infeasible. This proof can be found in the appendix. Rotational Artificial gravity, on the other hand, is feasible to an extent. The minimum system size that makes this type of artificial gravity feasible is outlined in the next section.

5.4.2 Rotational Artificial Gravity (Tim Osifchin)

The concept for rotational artificial gravity has been around for several decades now. In short, an astronaut at the outer edge of a rotating spacecraft would experience a constant centripetal

acceleration from the floor that keeps them at the same radial distance from the axis of rotation. The inertial force they are feeling, centrifugal force, is the artificial gravity force. While linear acceleration is indistinguishable from true gravity, centrifugal force is not. Astronauts in a rotating spacecraft will also have to deal with Coriolis forces that result in further deviation from true gravity. Even though there are differences between what an astronaut will feel in true gravity versus a rotating spacecraft, these differences are reduced at extremely large spacecraft radii and extremely slow spin rates. As such the first proposed rotational artificial gravity space stations to be proposed were enormous.

$$\bar{a}_{cent} = -\bar{\omega}_0 \, x \, (\bar{\omega}_0 \, x \, \bar{r})$$

Equation 1: Centripetal Acceleration

American physicist Gerard O'Neill was among the first to propose a design of a rotational artificial gravity space station. His design became known as an O'Neill Cylinder. Exactly as the name implies these space stations would be cylinders. The length and diameter of the space station were proposed to be twenty miles and four miles, respectively [27]. These dimensions give an extremely large livable area. Having the primary length scale of this livable area be parallel to the axis of rotation eliminates Coriolis effects in this direction (cylinder length, as opposed to the circumference). As shown in the equation below, Coriolis acceleration is a cross product between the angular velocity of the spacecraft and the velocity of the individual within the rotating frame of reference.

$$\bar{a}_{corr} = -2(\bar{v} \, x \, \bar{\omega}_0)$$

Equation 2: Coriolis Acceleration

With the above definition in mind, it makes sense that if the angular velocity and the individual's velocity within the rotating frame are parallel, the individual will experience no Coriolis effects. In an O'Neill cylinder, inhabitant activities will primarily involve moving parallel to the axis of rotation and therefore their overall exposure to Coriolis effects is decreased. However, the primary downside of having one incredibly long cylinder rotating about its axis of symmetry is unstable. The transverse moment of inertia for a cylinder of this size will be larger than its axial moment of inertia. This relation between the two results in instability of spin about the axis of symmetry. The way O'Neill decided to combat this instability was to cut the cylinder in half lengthwise and spin the two halves in opposite directions [27]. While the inhabitants can no longer walk the entire length of the space station, they will also not experience sudden rapid flipping of the spacecraft about a transverse axis.

The second type of rotational artificial gravity space station is called a Stanford Torus, named after the students at Stanford University who developed this design. Originally these structures were envisioned to have diameters of about one mile [28]. As a result of the torus shape, the two key considerations discussed for the O'Neill cylinder are flipped for the Stanford Torus. The torus will have a significantly greater axial moment of inertia than the transverse moment of inertia. This means that a spinning Stanford Torus is very stable. The sacrifice that was made for this stability was changing the primary length scale of the livable area. Now movement in the primary length scale (circumference) does result in Coriolis effects because it is not parallel to the axis of rotation.

Even a spacecraft of the scale of a Stanford Torus, let alone an O'Neill Cylinder, is certainly outside the scope of a mission to Mars. Nonetheless, these structures highlight the two different approaches one can take to sizing a rotating spacecraft. While engine performance limited the application of linear acceleration, mass is going to be the limiting factor for a rotating spacecraft. A Stanford Torus and an O'Neill Cylinder of the same mass will have very different dimensions with the Stanford Torus having a significantly larger radius, and the O'Neill Cylinder having a much larger axial length. Since rotational artificial gravity best approximates true gravity at larger spacecraft radii, the Stanford Torus is a more appropriate choice for small scale spacecraft design. Before moving forward with the spacecraft design, a more in-depth feasibility analysis is required. The primary purpose of such an analysis would be to determine the minimum spacecraft radius, and therefore spacecraft mass, that makes rotational artificial gravity feasible. This analysis begins with the experienced gravity force.

Experienced Gravity Force:

The entire reason for generating artificial gravity is to have a specified gravity force that the crew can survive in. This experienced gravity force is the first parameter in sizing the radius and spin rate of the spacecraft. These two quantities are linked simply by the equation for centripetal acceleration. The other key piece of information to get values for radius and spin rate is going to be the bounds on the experienced gravity force. Earth gravity of 1.0g or 9.81m/^2 is an easy choice for the upper limit. While humans can adapt to higher g forces, there is no reason to put astronauts in that situation. For the same spacecraft, simply lowering the rpm can bring us from above 1.0g to exactly 1.0g, and, as will be discussed in more detail later, the spin rate should be as low as possible.

$$a_{cent} = \frac{v^2}{r} = \frac{(\omega * r)^2}{r} = r * \omega^2 \quad \rightarrow \quad r = \frac{a_{cent}}{\omega^2} = \frac{const.}{\omega^2}$$

Equation 3: Centripetal Acceleration Solved for Radius.

In terms of the lower bound there are two likely candidates – Lunar and Martian gravity. The Moon's gravity is around one sixth of Earth's [29]. While this is certainly better than a microgravity environment, it is not clear exactly by how much better given that all the data available on this is from the Apollo program. While cumbersome spacesuits can be blamed for a large portion of the difficulty astronauts had traversing the surface of the moon, the low gravity itself is not blameless. However, some research does suggest that Lunar gravity is the absolute minimum needed for an astronaut to maintain balance and sense of direction [30]. For these reasons Lunar gravity will be considered but only if all other options prove infeasible.

Martian gravity is the ideal choice for sizing an artificial gravity spacecraft that is meant to deliver astronauts to Mars and back. The red planet has about 38% the gravity of Earth, which has seen no human experimentation whatsoever [29]. Despite this, it is reasonable to assume that astronauts will fare better on Mars than the Moon due to a smaller deviation from Earth gravity. An additional benefit of setting Martian gravity as the lower bound is that the significant experimentation on the survivability of the Martian environment can be determined before the rotating spacecraft even leaves low Earth orbit.

Now that the bounds are set for gravity force, the comfort zone of all possible spacecraft radii and spin rates has been narrowed down slightly. To best visualize this comfort zone, spacecraft radii and spin rates can be placed on a log scale plot. The centripetal acceleration equation is quite simple, but it is non-linear. Moving to a log scale plot turns the relation between radius and angular velocity (spin rate) into a linear relation as shown in Figure 17. As stated earlier, Lunar gravity is certainly not an ideal operating point, but keeping it in mind and plotting it provides more insight on what extremes might need to be reached so that artificial gravity becomes feasible.

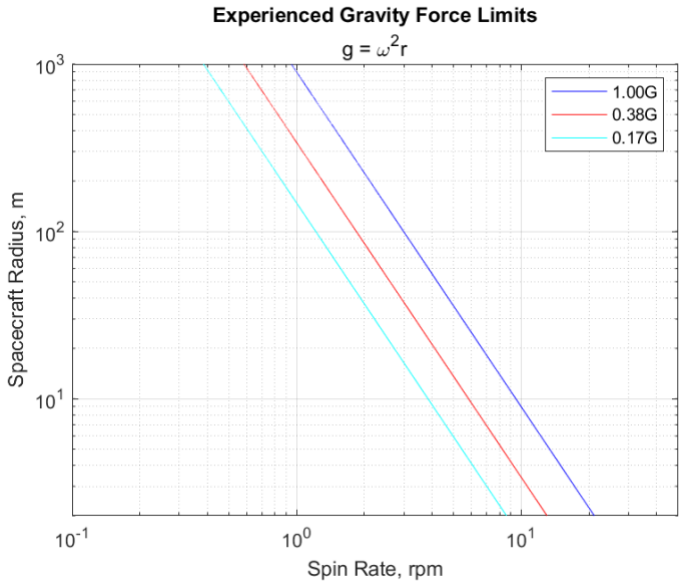

Figure 17: Experienced Gravity Force Limits

Tidal Acceleration:

For a given spin rate, the spacecraft radius will set the experienced gravity force. However, this gravity force technically exists only at the radius specified. When the height of the crew member standing in a rotating spacecraft is comparable in size to the average spacecraft radius, the crew member will experience different gravity forces across their body. The entire body is rotating at a constant rate, but the head is closer to the axis of rotation than the feet. This difference in gravity force from head to toe is known as tidal acceleration. Building spacecraft with diameters on the order of miles like the Stanford Torus and O'Neill Cylinder, tidal acceleration does still exist but can be neglected given that most people are shorter than 6ft. This exact height (or 1.83m) is what will be used to judge the tidal acceleration experienced by crew members of the rotating spacecraft.

There are no lower limits for this problem as the ideal case would be exactly zero difference in the felt gravity force across the human body. A lower limit is established by picking a percentage deviation from the average gravity force. The development of the equation used for determining tidal acceleration is shown below.

$$\Delta a_{12} = a_2 - a_1 = \omega^2(r_2 - r_1) = h\omega^2$$

Equation 4: Change in Centripetal Acceleration

$$a_{avg} = \frac{a_2 + a_1}{2} = \frac{\omega^2}{2}(r_2 + r_1) = \left(r_2 - \frac{h}{2}\right)\omega^2$$

Equation 5: Average Centripetal Acceleration

$$T = \frac{\Delta a_{12}}{a_{avg}} = \frac{h\omega^2}{\left(r_2 - \frac{h}{2}\right)\omega^2} = \frac{h}{\left(r_2 - \frac{h}{2}\right)} \quad \rightarrow \quad r_2 = \frac{h}{T}\left(1 + \frac{T}{2}\right) = K_{TA} = const.$$

Equation 6: Tidal Acceleration Solved for Radius.

As can be seen in the final equation, the result of setting a limit on tidal acceleration is a constant radius independent of angular velocity. Now all that is needed to complete this analysis is an acceptable value for tidal acceleration. This acceptable limit is not precisely known despite all the rotational artificial gravity research NASA conducted in the 1970s. A best guess starting point would be an order of magnitude less than the gravity force, or 10% of the centripetal acceleration. Having this number in mind, a minimum spacecraft radius can be added to the log plot from the gravity force analysis. The new plot is shown in Figure 18. A value of 7% tidal acceleration can also be placed on the figure to get more insight on exactly how the selected limit influences minimum spacecraft radius. The value of 7% is not a new limit, or upper limit, but instead another point of reference.

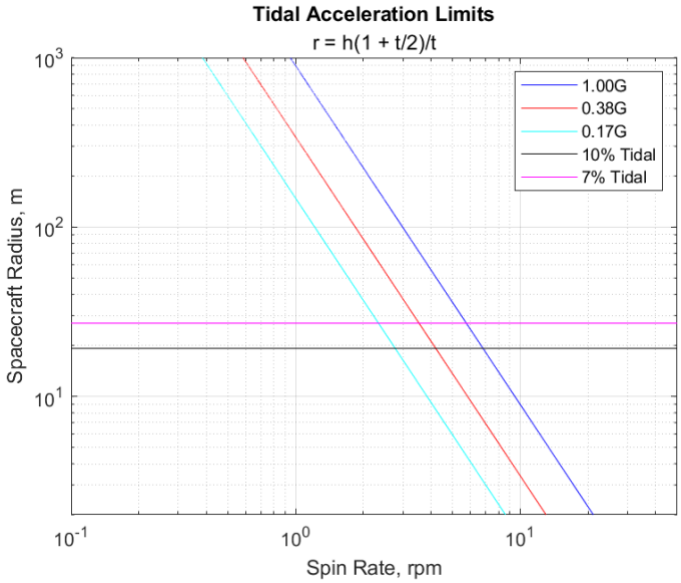

Figure 18: Tidal Acceleration Limits

Vertical Coriolis:

The crew will be moving around while conducting all manner of experiments aboard the spacecraft so that the 6-month transit to Mars is not wasted time. This brings us to the first of two motion related Coriolis effects. The first is called the Vertical Coriolis. While the motion resulting in this effect is tangential, the change in gravity force is radial, or from the perspective of the astronauts, vertical. Consider a member of the crew walking along the direction of the spacecraft's spin. This astronaut has effectively changed their spin rate in inertial space. Walking in a retrograde fashion

with respect to the artificial gravity ring will lower their inertial spin rate, and therefore decreases the gravity they feel. Walking in a prograde fashion accomplishes the exact opposite with a perceived increase in the gravity force. This relation between walking speed and change in the gravity force can be summarized in the following equations.

$$C = \frac{\Delta a}{a_0} = \frac{a - a_0}{a_0} = \frac{\frac{v^2}{r} - \frac{v_0^2}{r}}{\frac{v_0^2}{r}} = \frac{(v_w + v_0)^2 - v_0^2}{v_0^2} = \left(\frac{v_w}{v_0}\right)^2 + 2\left(\frac{v_w}{v_0}\right) = (V^*)^2 + 2(V^*)$$

Equation 7: Vertical Coriolis Definition

$$V^* = -1 \pm \sqrt{1 + C} \quad \rightarrow \quad \omega_0 = \frac{v_0}{r} = \frac{v_0}{r}\left(\frac{v_w}{v_w}\right) = \frac{v_w}{rV^*} = \frac{v_w}{r\left(-1 \pm \sqrt{1 + C}\right)}$$

Equation 8: Nondimensional Velocity Definition

$$\omega_0 = \frac{v_w}{r\left(\sqrt{1 + C} - 1\right)} \quad \rightarrow \quad r = \frac{v_w}{\omega_0\left(\sqrt{1 + C} - 1\right)} = \frac{K_{VC}}{\omega_0} = \frac{const.}{\omega_0}$$

Equation 9: Vertical Coriolis Relation Solved for Radius.

Again, with the spacecraft radius related to the spin rate and a constant, the vertical Coriolis effect can easily be added to the rotational artificial gravity sizing plot. This constant value is calculated with the walking speed and an acceptable change in gravity force. The walking speed is somewhat arbitrary. No astronaut will need to sprint along the artificial gravity ring to maintain fitness, like what is shown in the movie, *Space Odyssey: 2001*. They will have treadmills to stay fit. For these reasons a relatively slow speed of 1.2 m/s or 2.7 mph was selected. Research by Nesti et al places a change in gravity force of 5% as imperceptible [31]. In terms of a maximum for human comfort, centrifuge experiments have suggested that a 25% tidal acceleration becomes uncomfortable [32]. These two values will find their way onto the plot that is shown in Figure 19. The comfort zone is above 25% Vertical Coriolis. Adding a plot line for 5% Vertical Coriolis begins to show exactly how big the spacecraft must be for it to approximate true gravity.

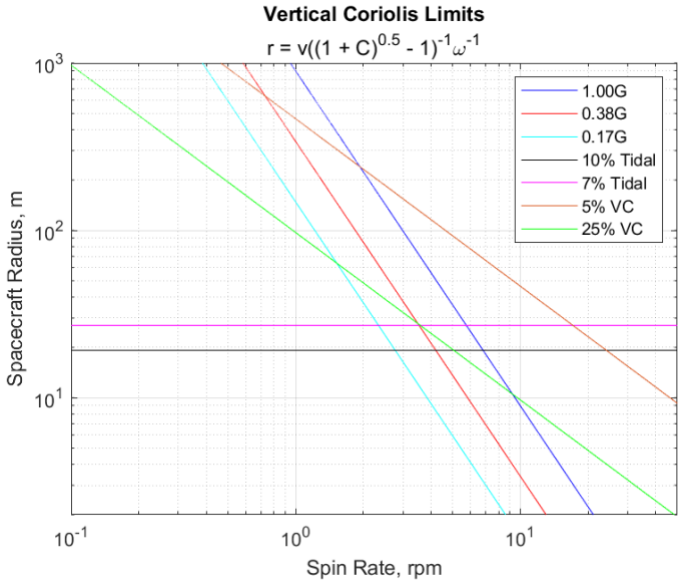

Figure 19: Vertical Coriolis Limits

Radial Tipping:

Movement in the tangential direction resulted in a radial gravity deviation so it is only natural that movement in the radial direction results in a tangential gravity deviation. The Coriolis effect caused by radial motion is known as Radial Tipping. The "tipping" part of the name comes from how an astronaut would perceive this type of change in gravity. When an astronaut moves closer or further from the axis of rotation, it will feel as though the walls of the vehicle around them are tipping over or tilting. In the rotating reference frame, the astronaut could be climbing up a perfectly vertical ladder from the main ring to the central hub of the rotating spacecraft. However, because of their motion, they will perceive the ladder at an incline. The magnitude of the incline will depend on how fast they are climbing or descending on the ladder, and the direction of the incline will depend on how the ladder is oriented relative to the spin direction.

Due to the nature of this type of Coriolis force it is impossible to avoid it entirely unless there is no central hub for the spacecraft. Near the central hub, the radius drops to nothing, but the spin rate is still at full speed to maintain a specific gravity force at the ring. Picking out an acceptable combination of radius and spin rate will for Radial Tipping is not simply a consideration of the actual spacecraft radius. What is more important is that the Radial Tipping effect is diminished for as much of the range of spacecraft radii as possible. For example, if the spacecraft is sized for a radius of 40 meters and a spin of 4 rpm, as much of the 40-meter range as possible, at the given spin rate, should fall under acceptable limits for Radial Tipping. The difficulties associated with Radial Tipping are often why rotational spacecraft are typically designed to either avoid extensive use of its central hub or contain an elevator to bring crew safely between the hub and outer ring.

Just like with the Vertical Coriolis, the velocity of is critical importance. When an astronaut stands up from a seated or laying down position, they will experience a Radial Tipping Coriolis. However, the change in radius of this motion is essentially negligible when considering the limitations that are already being placed on the spacecraft. The primary concern for Radial Tipping is the

climbing/descending speed. A value of 0.5 m/s (1.1 mph, 1.6 ft/s) was chosen for the Radial Tipping calculations. This is significantly slower than the walking velocity partially because the astronauts will likely find it extremely difficult to climb any faster except very near the outer edge of the spacecraft. As stated earlier, Radial Tipping cannot be eliminated so there cannot be a true limit, instead two reference points will be taken into consideration – 30% and 8% (typical wheelchair ramps have slopes of 8%) [33].

Additional considerations include the orientation of the ladder which will change the direction of the perceived incline. Orientation essentially makes the difference between hanging from monkey bars or crawling above them, and one of these is significantly easier than the other. Therefore, orientation of the ladder is of prime importance for allowing astronauts to handle more than the chosen 30% limit/reference.

Before the climbing speed and Radial Tipping limit can be placed in the plot, the relation between radius and spin rate that produce the limit must be determined. The derivation of the relation is shown below.

$$R = \frac{a_{corr}}{a_{cent}} = \frac{-2(\bar{v}\ x\ \bar{\omega}_0)}{-\bar{\omega}_0 x\ (\bar{\omega}_0\ x\ \bar{r})} = \frac{2v}{\omega_0 r}$$

Equation 10: Radial Tipping Definition

$$R = \frac{2v}{\omega_0 r} \quad \rightarrow \quad r = \frac{2v_{climb}}{\omega_0 R} = \frac{K_{RT}}{\omega_0} = \frac{const.}{\omega_0}$$

Equation 11: Radial Tipping Relation Solved for Radius.

Utilizing the above equations, the Radial Tipping limit and reference (8%) can be plotted in the artificial gravity sizing figure. To avoid overcrowding the plot, reference conditions for the Vertical Coriolis (5%), Tidal Acceleration (7%), and Gravity Force (Lunar gravity) will be removed. Figure 20 is this updated artificial gravity sizing plot.

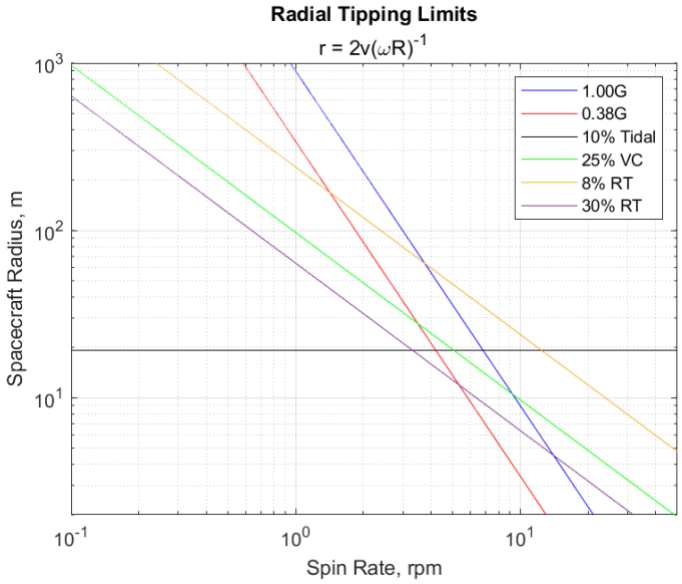

Figure 20: Radial Tipping Limits

Canal Sickness:

The final consideration when sizing a rotational spacecraft is the risk of motion sickness, or Canal Sickness. While no studies have been conducted on rotational spacecraft because none exist, NASA has done extensive research in adaptation to rotating environments on Earth. Various different types of studies were conducted that resulted in the acceptable limits of the previous analyses. The experimental setup for Canal Sickness testing simply involved placing a circular room on a turntable and placing test subjects in the room for multiple days at a time. Since Canal Sickness is almost entirely based on spin rate, therefore simply varying this parameter for the rotating room allowed NASA to determine acceptable spin rates for future rotational spacecraft [34]. An image of the slowly rotating room, with some of the experiments that happened inside the room, is shown in Figure 21, below.

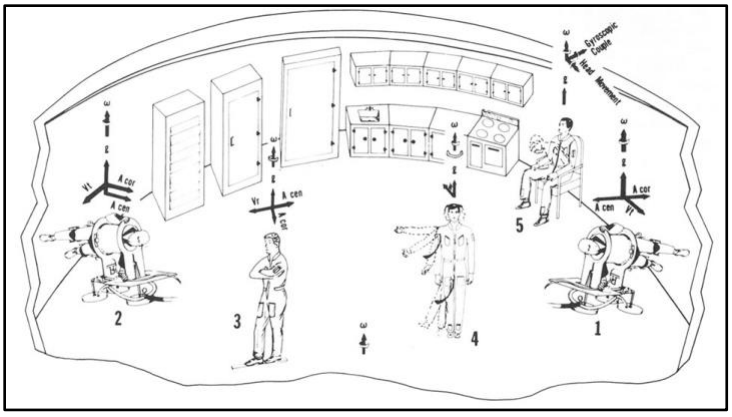

Figure 21: NASA Slowly Rotating Room Diagram

The slowly rotating room experiment revealed that the average person could adapt to almost 3.82 rpm within a day and experiencing only mild symptoms. Spin rates of 5.44 rpm were highly

stressful for the subjects but adaptation to the environment was still possible in just over a day. The highest spin rate tested was 10 rpm and this was significantly more stressful and very few subjects were able to adapt to the environment even after two days. On the other end of the spectrum, spin rates below 2.5 rpm only resulted in mild symptoms with quick adaptation to the environment [34]. These experiments have a limit to the applicability for rotating spacecraft. The primary distinction that might allow for higher spin rates is the orientation of the crew within the rotating frame. Research by Nesti et al suggested that humans have a higher sensitivity to horizontal acceleration than vertical [31]. This means that, due to their orientation, subjects in the slowly rotating room were in a harsher environment than what would be experienced by the same subject in a rotational spacecraft. Due to these differences an upper limit of 6 rpm will be taken as the comfort limit for Canal Sickness. Having settled on a value, the artificial gravity sizing plot has reached its final state. Figure 22 shows how a Canal Sickness limit impacts the comfort zone.

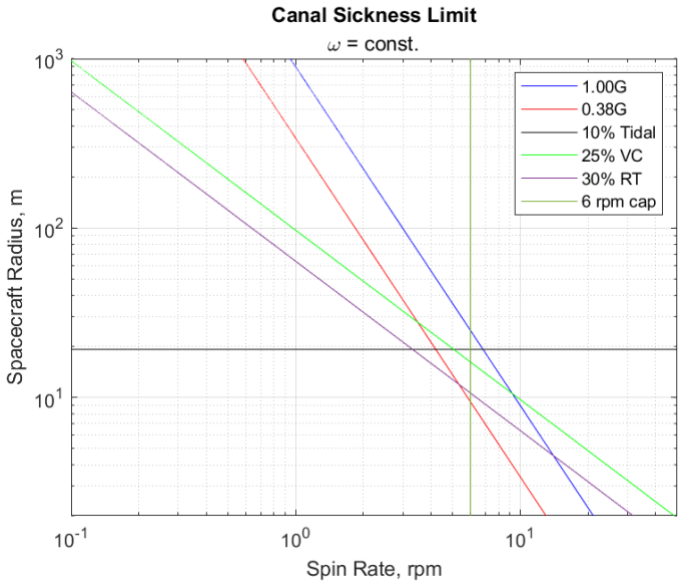

Figure 22: Canal Sickness Limit

5.4.3 Implementation of Artificial Gravity (Tim Osifchin)

Now that all the necessary relations are shown on the rotational artificial gravity sizing plot, feasible operating points can be selected. Since it is extremely desirable to be able to operate at both Earth and Martian gravity, operating points should lie on the 1.00G and 0.38G lines while remaining above the Vertical Coriolis limit and to the left of the Canal Sickness limit. These two operating points must also be for the same spacecraft radius. This limitation is set because switching between the operating points by changing the radius is significantly more difficult than varying the spin rate. Considering all these limitations, the final radius will be 30 meters and its two spin rates will be 3.36 rpm and 5.45 rpm for Martian and Earth Gravity, respectively. While Tidal Acceleration is an important parameter, it is not one of the major limiting factors. A final plot containing these operating points is shown in Figure 23.

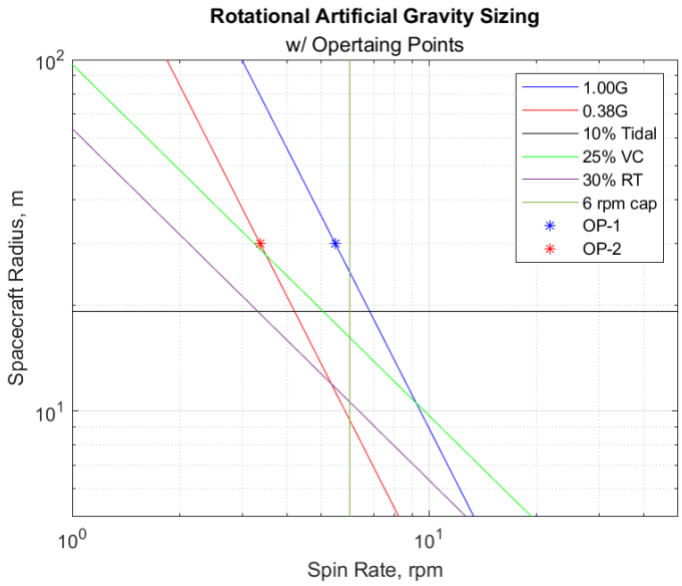

Figure 23: Final Rotational Artificial Gravity Sizing Plot

The final parameter that has yet to be considered in this sizing is Radial Tipping. As mentioned earlier, determination of acceptable limits is quite difficult. At the spin rates of the two operating points, the Radial Tipping allowance is exceeded at different radii. For the slower spin, this radius is 18.4 meters, and for the faster spin, this radius is 11.7 meters. Since the faster spin rate corresponds to Earth gravity, it is the primary operating point. Exceeding the 30% Radial Tipping in only 40% of the travel from ring edge to hub center is about as good as can be expected. If the ladders are oriented in such a way as to approach a crawl instead of climbing an overhanging rock wall, the astronauts should have little difficulty traversing the spacecraft. Another important note is that the Radial Tipping tolerance is a percentage of the gravity force at a particular radius. With a reduction in gravity force as the astronaut climbs from the ring edge to the hub center, even large Radial Tipping percentages will be manageable.

With feasible operating points determined, a general design of the spacecraft that employs rotational artificial gravity can begin. Feasibility from this point onward is going to be entirely based on mass. The mass of the ISS is on the order of 420 metric tons [35]. A good starting estimate for the mass of the rotational artificial gravity spacecraft will be twice the ISS mass at 840 metric tons. To get to even this approximate mass, the spacecraft will likely have to be trimmed down significantly. While a Stanford Torus will typically have livable area in a full circumference, to meet the mass requirement of the relatively miniscule spacecraft, a full circumference is infeasible. Sacrificing this aspect of the Stanford Torus design is that much of a sacrifice because only four crew members will be living aboard the spacecraft at one time. The actual livable volume needed for one crew member to be comfortable is 25 cubic meters [36]. Accounting for all the volume of facilities and storage equipment that the astronauts need, this minimum per person can be tripled to 75 cubic meters. Since the artificial gravity ring is being broken up into sections or pods, additional volume for contingencies should be considered. An extra volume of 100 cubic meters (total, not per crew member) will be added to satisfy the contingency strategy of simply moving

out of uninhabitable pods in favor of the remaining pods. Four crew brings the final estimate for livable volume of the entire artificial gravity ring to 400 cubic meters.

The floor radius will be set as the 30-meter radius from the operating point analysis. To have a ceiling of 2.4 meters, this places the artificial gravity ring between 30 meters and 27.6 meters in radius. Spheres are the strongest pressure vessel shapes. Therefore, the pods of the artificial gravity ring will be sized so that their length and width are quite similar (cube instead of long thin rectangular prisms). To obtain the 400 cubic meter volume, the side lengths of each pod should be around 7.5 meters for three pods, 6.5 meters for four pods, or 9 meters for two pods.

Two main considerations go into determination of the number of pods in the artificial gravity ring. The first is crew comfort. Constantly having to traverse the structure from one pod to the next is certainly not ideal. Therefore, two or three pods will be preferred for crew comfort. The second consideration is risk mitigation. Having only two pods means that if there is a problem with one of the pods, half the artificial gravity ring would become a useless counterweight until repairs can be made. This decrease in livable volume was accounted for, but attempts should still be made to mitigate the risk of significantly dropping livable volume. Therefore, more pods are better able to deal with unforeseen circumstances. Splitting the difference between the two aspects, with a slight favoring to less pods, leads to the choice of three. The slight favoring toward fewer pods is for the sake of decreasing mass as much as possible. More pods would require additional spokes connecting them to the central hub.

This concludes the sizing of the rotational artificial gravity sizing. An image of this module on the spacecraft can be seen in Figure 24. While the general sizing has been completed, the design is far from complete. Component level design and stress simulations are required to fully define the structure that astronauts would be living in for the duration of their trip to Mars.

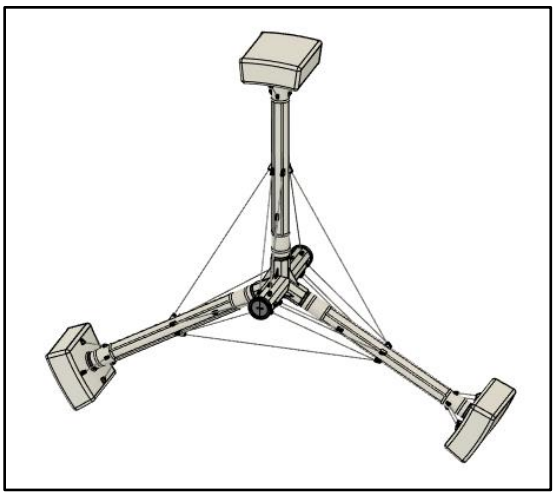

Figure 24: Final Artificial Gravity Module [37]

5.4.4 Artificial Gravity System Bearings & Motor Analysis (Nathan Berry)

As this artificial gravity system is a novel technology, further analysis of how the spin of the artificial gravity system will be maintained was a focus point to validate the feasibility of the

design. To gain a reference of spinning artificial gravity modules in space, the proposed ISS Centrifuge Rotor (CR) design was investigated. This system was developed by the Japan Aerospace Exploration Agency (JAXA) to develop an artificial gravity rotor on the ISS to prove the technology in a space environment but was never launched due to delays and issues within the Space Shuttle program [38].

The first area of analysis conducted was on how to enable the artificial gravity wheel to spin. Through investigating the Centrifuge Rotor at a component level, it was determined that using both spin motor and rotor shaft bearings, an electric motor can be used to maintain the spin of a rotating structure in space. Furthermore, slip rings can be utilized to transmit power and electrical signals in the static cycler modules to the rotating artificial gravity wheel. The component breakdown of how the bearings and slip ring assembly will be constructed on the cycler can be seen in Figure 25.

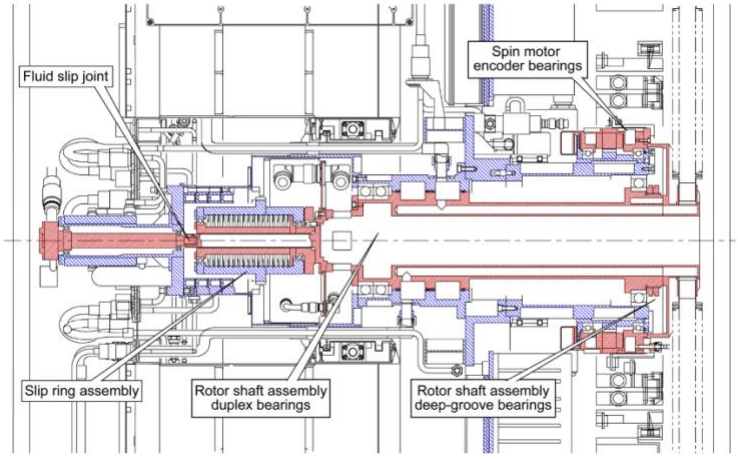

Figure 25: ISS Centrifuge Rotor Slip Ring & Bearing Assembly [39]

The second major analysis was defining an estimated power draw of an electric motor to counteract friction within these bearings. The analysis utilized the friction due to the angular contact and deep groove bearings within the CR as a reference for the friction within the Cycler's AGM bearing assembly. The analysis was conducted using numbers presented in the Analysis of Space System Centrifuge Rotor Bearing System presented in Reference [39]. This analysis presented the radial loads experienced by the 19.050 mm bore diameter bearings for the 1875 kg CR centrifuge. As the Cycler's Artificial Gravity Module has a mass of 458.153 metric tons, the radial forces presented in the previously mentioned analysis were scaled linearly to account for this mass. The resulting radial force on both the angular contact and deep groove bearings are presented in the following table.

Table 10: Centrifuge Bearing Radial Loads

System	Radial Load on Angular Contact Bearings [N]	Radial Load on Deep Groove Bearings [N]
ISS Centrifugal Rotor	270,000	120,000
Cycler Artificial Gravity Module	65,974,032	29,321,792

Additionally, the friction factor was researched and considered for both types of ball bearings. Typical friction factors are summarized in the table below.

Table 11: Typical Friction Factors for Bearings [40]

Friction Factor for Angular Contact Bearings	Friction Factor for Radial Load Bearings
$\mu = 0.0015$	$\mu = 0.0013$

Utilizing these factors, the torque resulting from the friction for both types of 19.050 mm bore diameter bearings were computed and summed together. The equation utilized for this is shown below where M is the resulting friction torque, μ is the friction factor, RL is radial load, and d is the diameter of the bearings.

Equation 12: Friction Torque from Bearings [40]

$$M = \mu * RL * \frac{d}{2}$$

The resulting friction forces are summarized in the table below.

Table 12: Bearing Friction Torque Results

Bearing Type	Friction Torque for Angular Contact Bearings	Friction Factor for Radial Load Bearings	Total Friction Torque
Friction Torque [N*m]	816.92	418.94	1235.86

Finally, the force and the 5.46 rpm required to maintain 1g of gravity were considered to size the power requirement of the motor. This was completed through utilizing the following equation where P is power, M is torque, and n is spin-rate in rounds per minute.

Equation 13: Electric Motor Power for Set Torque and Spin Rate [41]

$$P = \frac{M * n}{9.549}$$

The results are shown in the table below. An additional 30% margin was added to account for other losses such as motor inefficiencies, electrical losses, and other frictions in the system.

Table 13: Bearing Friction Torque Results

	Power Required to Counteract Bearing Friction	Power Required to Counteract Bearing Friction + 30% Margin
Electric Motor Power [kW]	0.71	0.92

This analysis was performed to gain a rough order of magnitude estimate to initially size control systems, power systems, and gain a better understanding of future analyses required in this area. Future work would require a deeper analysis into the true forces on a rotating system while in zero-gravity conditions and test the system in a laboratory environment to gain insight into true friction torques experienced in the system. Additionally, an exploration into larger, stronger bearings will be required to properly account for the large increase in mass that the AGM presents over JAXA's CR.

5.4.5 Sizing Fuel Requirements for AGM Start and Stop (Vishnu Vijay)

Due to the large mass of the AGM, the spin-up and spin-down of the module was deemed too large a task for electric motors alone. Instead, chemical engines will be used for this task. It is assumed that Aerojet Rocketdyne R-40B engines will be used for this task. One engine will be placed on each pod of the AGM. To arrive at a value for the fuel required for one spin-up or spin-down maneuver, it was assumed that the whole vehicle is being spun up or spun down. This means the moment of inertia for the whole vehicle is used rather than that of the AGM alone. Rotational kinematics were used to arrive at the following equation for the approximate time to accomplish the maneuver:

$$t = \frac{\Delta\omega I_x}{nFr\delta_t}$$

where $\Delta\omega$ is the difference in angular speed between the AGM's nominal operations and stop, I_x is the moment of inertia, n is the number of engines being used, F is the maximum thrust of one engine, r is the distance from the center of rotation that the engine is being placed, and δ_t is the throttle level of the engine.

It is assumed that the thrust and mass flowrate of the engine is linearly related to its throttle level. The following equation is derived from this assumption:

$$m_{fuel} = n\dot{m}\delta_t t$$

where $\dot{m}$ is the mass flowrate of the engine at maximum thrust. Substituting the equation for t derived above gives:

$$m_{fuel} = \frac{\dot{m}\Delta\omega I_x}{Fr}$$

Using this equation, the R-40B maximum mass flowrate and thrust of $\dot{m} = 1.4$ kg/s and $F = 4{,}000$ N, respectively [42], the cycler's maximum change of spin rate $\Delta\omega = 0.10472$ rad/s, the cycler's moment of inertia about its axial direction $I_r = 2.446\text{e}8$ kg-m^2, and the distance from the engines to the AGM's rotation axis $r = 30$ m, the fuel required for a single spin-up or spin-down maneuver was determined to be:

$$m_{fuel} \approx 299 \text{ kg}$$

To allow for redundancy and the ability to spin-up and spin-down the AGM multiple times per cycle for routine maintenance, the AGM fuel tanks were sized for a little more than 4 times this amount. That is,

$$m_{AGM,fuel} = 1200 \text{ kg}$$

5.5 Cycler ADCS (Vishnu Vijay)

5.5.1 Determining Cycler ADCS Power and Mass Budget

The cycler vehicle attitude determination and control systems were sized to determine a sufficient maximum value for mass and power required. Due to requirements of the DSOC system, the attitude determination instruments are required to have high precision to support the pointing accuracy of optical communication. Each cycler vehicle will have 4 Jena-Optronik star tracker sensors [43], 4 Honeywell Miniature Inertial Reference Units (MIMUs) [44], and 16 Adcole coarse sun sensors [45]. These are based on the Psyche mission that tested Deep-Space Optical Communications and scaled for redundancy. The total power draw of these instruments is 120 W. The mass of these instruments is 30 kg.

The control systems are approximately sized; accurate sizing of control systems the vehicle must be done in the future. The feasibility of using control moment gyroscopes (CMGs) for attitude control is in question due to the potential risk it would face to a manned crew mission should a CMG fail. Additionally, due to the dynamic nature of the cycler vehicle's design, determining a specific number of attitude reaction thrusters is infeasible. Thus, the potential power and mass from using reaction wheels alone and thrusters alone for a main attitude control system were considered and the maximum of these values is used for consideration.

First, the case that the ISS CMGs are the sole attitude control system on the vehicle was considered. Each of the four CMGs on the ISS takes about 200 W [46] and has a mass of 100 kg [47]. Scaling these values linearly for the cycler vehicle, which has a mass twice as large as the ISS, the power and mass budget would be 1600 W and 800 kg, respectively.

The Space Transportation System's (STS) Orbital Maneuvering System's Aerojet Rocketdyne R-40 was considered for the case of reaction thrusters being used for attitude control. The STS was 100 metric tons and used 38 thrusters [48]. Scaled up for the cycler vehicle's mass, approximately 350 thrusters will be used, resulting in a mass of 3,700 kg and power of 24.5 kW. From [48], a 100 metric ton S1L1 cycler with 38 R-40 thrusters would need 1,000 kg of propellants. With a cycler vehicle of mass 9 times that amount would require 9,000 kg.

Thus, the approximate maximum power and mass a cycler ADCS could require should be 24.5 kW and 13,000 kg.

5.5.2 Cycler Operational Modes

The cycler vehicle's operational modes are summarized below:

Table 14: Cycler Operational Modes

MODE	Explanation
Acquisition	System initialization after launch or on system reset
Orbital Insertion	Large ΔV maneuver to enter the ballistic cycler trajectory
Nominal Human Transit	Normal Operations with humans onboard
Nominal Autonomous	Normal Operations without humans onboard
AGM Spin-up	Spinning-up the AGM (nominal / routine)
AGM Spin-down	Spinning-down the AGM (nominal / routine)
AGM Emergency Stop	Quickly spin-down the AGM due to emergency
Main Engine Orbital Boost	Use cycler vehicle main engines for course corrections
Starship Orbital Boost	Use Starship engines for course corrections
Slew	Reorienting system when required
Safe	Lower power usage in case of fault detection

The modes in Table 14 were inspired by the SMAD, with additions to account for the cycler's mission. The inclusion of two nominal modes is one such addition. The cycler vehicle will be in the *nominal human transit* mode if it is transporting humans. Similarly, the vehicle will be in the *nominal autonomous* mode if it is not transporting humans, but still in the cycler trajectory. The operational modes associated with the AGM are required for routine maintenance and emergencies. Two orbital boosting modes are proposed to account for the case where the attached Starship(s) have sufficient fuel for an orbital boost.

5.6 Cycler Propulsion

5.6.1 Boost of Cycler to S1L1 Orbit (Chris Manilla and Mark Paral)

Once the cycler station is constructed in LEO, it must be boosted into the S1L1 trajectory. The values for ΔV are from Rogers et al. and were derived using STOUR. Analytical ephemerides are used for the location of the planets along with patched conics to find valid trajectories which include gravity assist. All maneuvers were derived under the assumption that an impulsive ΔV would be used. From this analysis, the ΔV required to reach the S1L1 trajectory from LEO is 3.796 km/s [52]. This value does not account for potential savings from V_∞ leveraging. With that in mind,

this ΔV is a maximum expected value for the maneuver and could be lowered with the addition of V_∞ to the simulation. Using this maximum expected value, calculations on the boosting of the cycler were performed in appendix 12.3. The boosting of the cycler will require the use of two starships each with 967.65 metric tons of propellant. This would require a maximum of 13 Starship launches to sufficiently fuel the two boosting Starships in orbit.

5.6.2 Orbital Correction Propulsion (Zachary Kessler)

The cycler will have propulsion capabilities if a small correction burn is needed for the cycler to remain in the S1L1 orbit. The main propulsion system aboard the cycler will be the SpaceX Starships that will be docked with the cycler. This is the method of initially boosting the cycler into the S1L1 trajectory from the LEO orbit in which the cycler is constructed. Due to the docking points being off axis on the cycler design, this method of propulsive corrections would only be feasible when two Starships are docked with the cycler at the same time, being able to provide perfect forward thrust.

To alleviate this issue with two Starships not always being present or able to perform a correction burn, a hypergolic engine will be present on the symmetric axis of the cycler. This engine is the Aerojet LR87-11, which uses a propellant of Dinitrogen Tetroxide (N_2O_4) and Aerozine-50. Aerozine-50 is a 50:50 blend by weight of hydrazine and unsymmetric dimethylhydrazine (UDMH). The LR87-11 was the propulsion system used for the first stage of the Titan II rocket and provides 1218.80 kN of thrust [49], which provides enough thrust to perform any emergency orbit correction burns when Starship is not present to able to perform such maneuvers. The engine assembly can be seen below in Figure 26.

The maximum velocity for orbital corrections of 300 m/s was determined from a range of potential correction velocity values, 0.15 – 0.25 km/s. To ensure that the cycler has enough propellant to perform all orbital corrections, the maximum value in the range of possible values was chosen to size the propellant tanks, including a 20% margin in case of emergency, totaling a 0.3 km/s correction ability. Using Equation 14 with this 300 m/s, a constant g value of 9.81 m/s^2, and I_{sp} = 302 s [49] for the LR87-11 engine, the mass ratio was determined. This value depicts the ratio of the final mass of the spacecraft, after the propellant is used, and the initial mass of the spacecraft, including the propellant mass. This value was then used in Equation 15, along with a structural mass fraction of $\lambda = 0.9$, which is a standard estimate. This equation gave the total mass of propellant for the orbital correction. Using the oxidizer to fuel ratio of 1.91, [49] the relative masses of both the fuel and oxidizer were determined. To size the propellant tanks, the volume of the fuel, Aerozine-50, and the oxidizer, N_2O_4, were determined from the propellant masses calculated and the density of the liquids. From this analysis, the orbital correction engine will require 58,580.59 kg of N_2O_4, which requires 40.40 m^3 of volume for the oxidizer, as well as 30670.44 kg of Aerozine-50, which requires 33.97 m^3 of fuel [50].

$$MR = e^{\frac{\Delta V}{g * I_{sp}}}$$

Equation 14: Ideal Rocket Equation

$$m_{prop} = m_{payload}\left(\frac{MR-1}{MR-\left(\frac{MR-1}{\lambda}\right)}\right)$$

Equation 15:Propellant Mass Equation

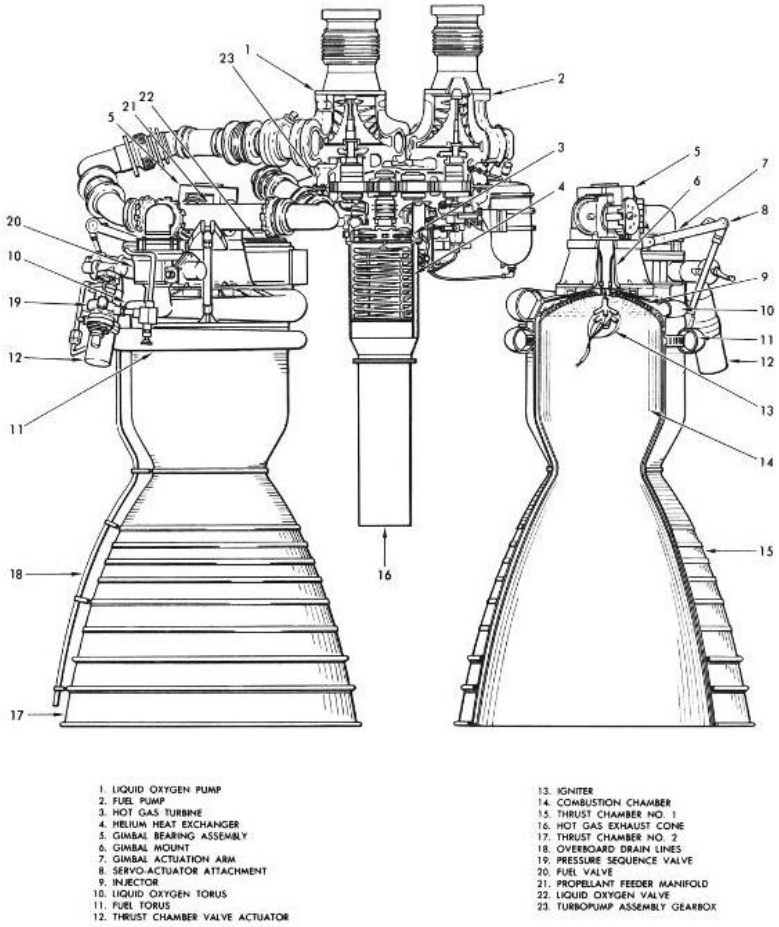

Figure 26: LR87-11 Engine Assembly [51]

5.7 Power & Thermal Analyses

5.7.1 Cycler Power Analysis (Chris Manilla)

The cycler vehicle must supply sufficient power to support a crew of four for up to 220 days nominally and 1082 days in contingency situations. Power needs were categorized by system as seen in Table 15, with more specific breakdowns in Table 16 through Table 20. The values in Table 16, Table 17, and Table 18 were derived from [23] and scaled for the needs of the mission. Table 19 was similarly derived from [53] and Table 20 from [46]. Crew systems include food storage and preparation, hygiene, and medical facilities. ECLSS covers the oxygen and water needs for the crew. The ARMS is a set of robotic arms that are used to maintain the facilities. The GNC system is of note due to its higher power draw relative to other systems. This high draw is largely due to the significant mass of the cycler spacecraft and the inclusion of an artificial gravity module. The module requires its own dedicated thrusters for spin up and spin down maneuvers to reach the desired rotation rate. When the module is spinning, electric motors are to be used to maintain the spin rate. Due to the relatively low surface area for friction to act on, the team assumed that the power used for the Space Shuttle rocket engines to spin up and spin down could be used for the motors maintaining the rotation since only one would be in operation at any given time. Using a direct energy transfer efficiency of 80%, the total power that the cycler system must generate is 75.79 kW.

Table 15: Power Requirements for Cycler Vehicle

System	Power (kW)
Crew Systems	16.69
ECLSS (Life Support)	4.52
Thermal Control	8.78
Autonomous Repair and Maintenance	4.83
Guidance, Navigation, and Control System	25.82
Subtotal	60.64
Total (80% Efficiency)	75.79

Table 16: Crew Systems Power Requirements [23]

Crew Systems	
Resource	Power (kW)
Microwave Oven	0.9
Dishwasher	1.2
Toilets	0.09
Showers	1
Vacuums	0.4
Washer/Dryer	4
Trash compactor/Air lock	0.85
Personal Stowage	2.8

Freezers	1.4
Fixtures, gloveboxes, etc.	1
Test and Photography equipment	1.4
Medical Suite	1.5
Exercise Equipment	0.15
Total	16.69

Table 17: Thermal Control Power Requirements [23]

Thermal Control	
Component	Power (kW)
Pumps with Accumulator	5.18
Heat Pumps	3.60
Total	8.78

Table 18: ECLSS Power Requirements [23]

ECLSS (Environmental Control and Life Support System)	
Component	Power (kW)
4-Bed molecular sieve	1.2
Trace Contaminant control system	0.2
Oxygen-generation assembly	1.4
Multifiltration	0.16
Vapor compression distillation	0.12
Supercritical water oxidation	1.44
Total	4.52

Table 19: ARMS Power Requirements [53]

ARMS (Autonomous Repair and Maintenance System)	
System	Power (kW)
SSRMS	2
SPDM	2
MBS	0.83
Total	4.83

Table 20: Guidance, Navigation, and Control Power Requirements [46]

Guidance, Navigation, Control System	
Component	Power (kW)
Inertial Measurement Unit	0.02
Sun Sensor	0.002
Star Tracker	0.02

6 R-40/Electric Motors	0.91
350 R-40 reaction control thrusters	23.94
Total	25.82

Power sizing for the cycler vehicle was performed for the use of solar panels for power generation. The Cycler does not eclipse at any point during the inbound or outbound trajectory and has a maximum distance from the Sun of 1.56 AU [48]. The constant line of sight between the spacecraft and the Sun limits the need for batteries for energy storage and 1.56 AU is well within the distance solar power is considered effective for, considering the Juno mission using solar power around Jupiter (5.2 AU). To find the necessary area and mass of solar panels needed to meet the cycler power needs, Equation 16-Equation 20 and the values from Table 21 were used. Using a power input density of 508 W/m^2 and an efficiency of 30%, the expected output density of the solar array is found. This density is then adjusted for BOL and EOL and is scaled to still be capable of peak power needs at EOL. For this Mars mission, the lifespan of the array is planned to be ten years, which covers the entire mission from cycler launch until the second crew lands safely back on Earth.

Equation 16: Solar Array Power Output Density [46]

$$P_o = P_{i_{mission}} * n$$

Equation 17: Power Density at Beginning of Life [46]

$$P_{d_{BOL}} = P_o * I_d$$

Equation 18: Power Density at End of Life [46]

$$P_{d_{EOL}} = P_{d_{BOL}} * L_d$$

Equation 19: Lifetime Degradation [46]

$$L_d = (1 - D)^L$$

Equation 20: Area of Solar Panels Required [46]

$$Area\ Required = \frac{P_{req}}{P_{d_{EOL}}}$$

Table 21: Values used in Power Sizing [46]

Variable	Value
Energy Conversion Efficiency (n)	30%
Annual Degradation (D)	2.5%
End of Life (L)	10 Years
Mean Solar Irradiance at 1 AU (P_i)	1367 W/m^2
Mean Solar Irradiance at 1.56 AU ($P_{i_{mission}}$)	508 W/m^2
Inherent Degradation of Solar Cells (I_d)	0.72

Mass per Area	2.06 kg/m^2

The final power density allows for an estimate of the area of solar panels needed to provide peak power at EOL. The expected mass of the array was calculated using a mass per area of 2.06 kg/m^2. An additional margin of 30% was added to the solar array mass to account for the mass of the structure and deployment [48]. The final area of 889 m^2 and mass of 2382 kg are shown in Table 22. The area of the solar array is equal to roughly one-third the ISS array, showing the scale of the system to be reasonable for constructing in space.

Table 22: Solar Array Sizing

Array Sizing	
Area of Solar Array (m^2)	889.75
Mass of Solar Array with 30% Margin (kg)	2382.76

5.7.2 Cycler Thermal Analysis (Nathan Berry)

As the Cyclers will be carrying astronauts to and from Mars, it is critical to analyze the thermal properties of the spacecraft. The cycler thermal analysis was taken at two critical points within the mission structure. These points are when the cycler is in near proximity to Earth as this is when the structure is the hottest and when the cycler is out past Mars in the furthest point of the trajectory as this is when the spacecraft is the coldest. The following analysis details the thermal control volume of the cycler and the thermal systems required to cool the spacecraft to habitable temperatures.

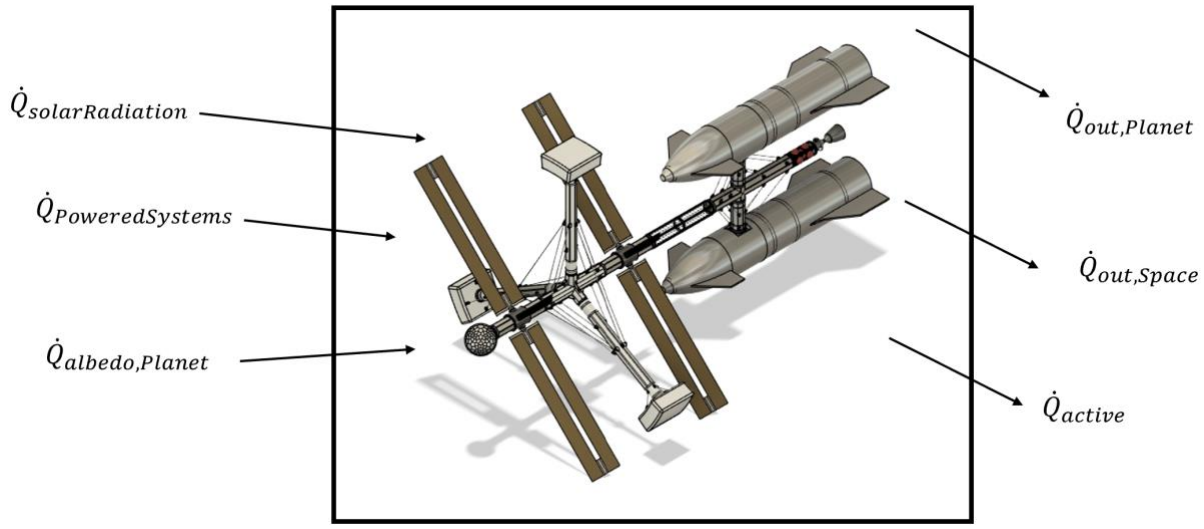

Figure 27: Cycler Thermal Control Volume

To better control the thermal properties of the Cycler, a thermal blanket made of "Beta Cloth Cover" was incorporated into the design [54]. The ISS utilizes the same beta cloth thermal blanket to not only maintain a consistent temperature, but also to further protect from micrometeoroid

impacts. It is worth noting that while it has beneficial thermal qualities, this thin layer provides little to no effect against all primary sources of radiation except UV radiation, so it was deemed to be negligible in the analysis presented in section 4.2.5 [55]. The absorptivity and emissivity of the beta cloth are also summarized in the table of thermal properties below.

Table 23: Cycler Thermal Properties

Metric	Near Earth Value	Furthest Trajectory Point	Sources [Earth]/[Mars]
Absorptivity, α	0.38	0.38	[56]/[56]
Emissivity, ε	0.85	0.85	[56]/[56]
Frontal Area, $A_{sc,F}$	1459 m^2	1459 m^2	System Design
Total Surface Area, $A_{sc,tot}$	2917 m^2	2917 m^2	System Design
View Factor Planet, $F_{sc,planet}$	0.47	$3 * 10^{-6}$	[57]
View Factor Space, $F_{sc_{space}}$	0.53	~1.00	[57]
Spacecraft Temperature, T_{sc}	293 K	293 K	Room Temperature
Planet Temperature, T_{planet}	290 K	210 K	[58]/[58]
Temperature in Space, T_{space}	4 K	4 K	[59]/[59]
Distance From Sun	1 AU	1.56 AU	[48]

The view factors for the planet and space can be computed using the following equations where R_{planet} is the radius of the nearest planet in km and d_{planet} is the distance to the planet from the spacecraft in km.

Equation 21: View Factor of Planet [57]

$$F_{sc,planet} = \sin^2\left(\operatorname{atan}\left(\frac{R_{planet}}{d_{planet}}\right) / 2\right)$$

Equation 22: View Factor of Space [57]

$$F_{sc,space} = 1 - F_{sc,planet}$$

Furthermore, viewing the control volume in Figure 27, the following thermal balance can be formulated.

Equation 23: Cycler Thermal Balance Equation

$$\dot{Q}_{solarRadiation} + \dot{Q}_{poweredSystems} + \dot{Q}_{albedo,planet} = \dot{Q}_{out,planet} + \dot{Q}_{out,space} + \dot{Q}_{active}$$

The individual terms in this balance can be computed using the following equations. It is worth noting that as this is an iterative process, the maximum power input was calculated utilizing the max power input of all non-thermal systems plus the assumption that the thermal control system required 4.90 kW.

Equation 24: Cycler Powered System Thermal Equation [57]

$$\dot{Q}_{poweredSystems} = P_{input,max}$$

Equation 25: Cycler Solar Radiation Thermal Input [57]

$$\dot{Q}_{solarRadiation} = \alpha * A_{sc,F} * \left(\frac{1}{AU^2}\right) * 1367\frac{W}{m^2}$$

Equation 26: Nearest Planet Albedo Thermal Equation [57]

$$\dot{Q}_{albedo,\,Planet} = \alpha * A_{sc,tot} * F_{sc,planet} * 410\frac{W}{m^2}$$

Equation 27: Thermal Transfer to Nearest Planet from Spacecraft [57]

$$\dot{Q}_{out,Planet} = \varepsilon * A_{sc,tot} * F_{sc_{planet}} * \sigma * (T_{sc}^4 - T_{planet}^4)$$

Equation 28: Thermal Transfer to Space from Spacecraft [57]

$$\dot{Q}_{out,\,space} = \varepsilon * A_{sc,tot} * F_{sc_{space}} * \sigma * (T_{sc}^4 - T_{space}^4)$$

The σ value in the above equation is the Boltzmann Constant. The results are shown in the table below where all positive values represent heat entering the system and negative is out of system.

Table 24: Cycler Thermal Analysis Results

	Near Earth	Furthest Trajectory Point
$\dot{Q}_{poweredSystems}$ [kW]	+70.33	+70.33
$\dot{Q}_{solarRadiation}$ [kW]	+757.89	+311.43
$\dot{Q}_{albedo,Planet}$ [kW]	+213.60	+0.001
$\dot{Q}_{out,Planet}$ [kW]	-19.64	-0.002
$\dot{Q}_{out,Space}$ [kW]	-549.14	-1036.11
$\dot{Q}_{active}$ [kW]	-473.04	+654.35

With the need to dissipate 473.04 kW while near Earth, two major design considerations were analyzed. The first was the size of the radiators required to dissipate this heat. Through an analysis of the ISS's 14-radiator array, each radiator weighing 997.9 kg and a 10.68 m^2 area, it was found that the ISS dissipates 224 kW of thermal heat [60]. Scaling this system to account for the increased thermal load of the new vehicle, the Cycler requires 30 of the ISS radiators which have a potential of dissipating 480 kW and have a total mass of 29,937 kg.

The second consideration was how much power was needed to run the thermal system and utilize these radiator arrays. According to Ref. [23], it requires roughly 0.36 kW of power to dissipate 25 kW of heat with a heat pump and 0.575 kW of power to dissipate 25 kW with pumps with accumulators in typical space vehicle thermal control systems. As it would take 19 heat pumps with 25 kW dissipation capabilities to meet the Cycler's needs, splitting the pumps half with and half without accumulators as was done in the aforementioned textbook, it shows that the Cycler would need 8.775 kW to operate onboard heat pumps to dissipate the heat.

At the furthest point in the trajectory, the Cycler is in deep space and requires additional an additional 654.35 kW heat to be provided into the system to maintain the internal 20°C temperature. However, in a nominal mission, the cycler could be lowered in temperature to approximately -30°C which is well above the lower limit of space electronic operating temperatures (-65°C) [61]. In this case, the Cycler will have to dissipate 108.43 kW of heat which is well in the capabilities of the thermal dissipation system. However, in the case that the crew was unable to depart from the Cycler and land on Mars and is instead riding it around to return to Earth, this heat could be provided through utilizing a mixture of heaters and emergency RTGs or funneling combustion gasses from burning excess fuel to heat the astronaut cabin. Furthermore, heating limited submodules to sustain the crew would require a much lower power requirement than heating the entire spacecraft to the desired temperature. This analysis has been considered and would be a primary focus of future thermal analysis to validate this mission contingency.

5.8 Cycler Construction (Tim Osifchin)

5.8.1 Components of the Cycler (Tim Osifchin)

The Cycler spacecraft can be divided into three main sections – power generation, artificial gravity, and propulsion/docking. The power generation section consists of three modules. These modules are the two Solar/Radiator Arrays (SRA), and the Remote Command Module (RCM). SRA modules function exactly as their name would suggest, they produce energy from the mass roll-out solar panel arrays and reject excess heat via radiators. While the RCM does not produce any power, it is included in the power generation section because it is responsible for controlling the distribution of power for the Cycler and being a central hub for managing all the systems and processes that occur on the Cycler. An image of this section is showcased in Figure 28. The base of the artificial gravity module is included in the image even though it is not part of this section because power generation is on both sides of the artificial gravity module.

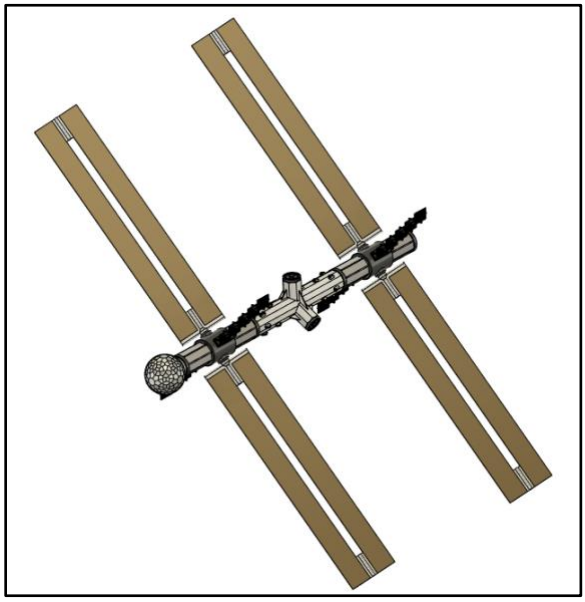

Figure 28: Cycler Model - Power Generation Section [37]

The second section is the artificial gravity module (AGM) consisting of a base, three struts and three pods. This module is sized to produce anywhere between 0.38g and 1.0g of artificial gravity. The crew will primarily live and work in this section. Figure 24, from the artificial gravity investigation, depicts this section of the Cycler.

The last section – propulsion and docking – is at the rear of the Cycler and consists of the Twin Starship Dock (TSD) and the Hypergolic Propulsion System (HPS). The crew should only ever be present in this section during arrival/departure and to perform maintenance on the section. An image of this section is provided in Figure 29, shown below.

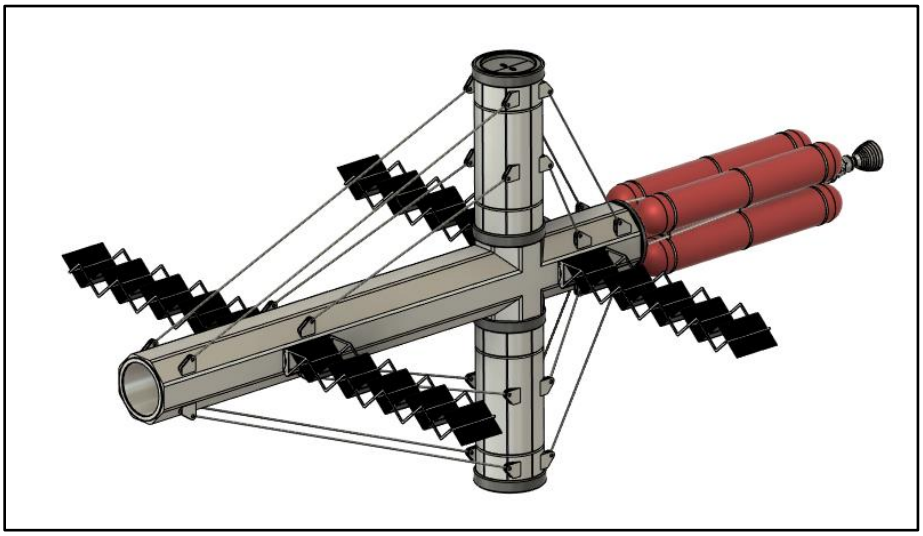

Figure 29: Cycler Model - Propulsion and Docking Section [37]

One of the primary considerations for construction of this nearly 900 metric ton spacecraft is how the mass is distributed between the modules. This mass can be simply derived from the 3D model of the vehicle. Volume is another factor in determining how modules will be delivered to low Earth orbit for assembly. This too can be derived from the 3D model; however, it is important to consider that the packing of these components into launch vehicles will not be perfect. To best judge the packaged volume of each module, the overall dimensions will be used instead of the volume that actual mass is contributing to. For example, a cylindrical section, although hollow, will be considered a solid volume for packaging. Table 25, shown below, is a summary of the masses, volume resulting from mass, and packaged volume of each module.

Table 25: Cycler Component Mass and Volume Breakdown

Module	Mass (mt)	Volume (m^3)	Pkg Volume (m^3)	Quantity (1)
SRA	87.902	70.432	145.404	2
RCM	27.104	20.965	54.362	1
TSD	131.018	86.639	232.733	1
HPS	10.656	70.430	88.040	1
AGM-Base	80.530	49.612	131.623	1
AGM-Strut	57.263	38.322	89.806	3
AGM-Pod	68.612	69.042	138.084	3

HPS-Fuel	78.568	66.800	66.800	1

5.8.2 Construction Process (Tim Osifchin)

Requirements:

Power is required to construct the Cycler and as such power generation systems must be among the first to be delivered to LEO. The RCM is a critical piece of early construction work because it will house all the communications equipment required to manage the construction process. Since astronauts are quite prohibitively expensive to be used for Cycler construction, the assembly process will heavily rely on autonomous docking and remote robotic assembly. This further emphasizes the need for modules of the power generation section to be delivered to LEO first.

Once power generation is established the more complicated assembly and testing can begin. Therefore, components or systems that will need to be tested rigorously for extended periods of time must be the next to be delivered to LEO. One such system is the Artificial Gravity Module. The lowest priority when it comes to cycler assembly is the HPS. Its primary purpose is to keep the Cycler in its ballistic trajectory when the trajectory begins to degrade. Starships docked at the TSD will provide primary high thrust propulsion whenever possible. With all these requirements in mind, a launch schedule can be produced that which modules launch on the same vehicle and in what order the vehicles launch.

Starship Loading:

Due to its high payload mass capacity, the Starship was selected to launch Cycler components to LEO for assembly. Starship Superheavy is designed to deliver 150 metric tons to LEO or 100 metric tons to geosynchronous orbit [62]. Its user manual also includes a dimensioned drawing of the cargo space. The volume that these dimensions produce is approximately 685 cubic meters. These two numbers represent the limit on Starship loading. To minimize the number of Starship launches required to get the entire Cycler to LEO, the limits should be approached closely. Table 26, shown below, is the final breakdown of Cycler components into Starships. The top row of this table contains the mass and volume limits for Starship. A total of seven launches will be able to get the Cycler and one crew to LEO. As can be seen in the table, mass is the limiting factor for all launches. Even utilizing the overestimates on packaged volume of each module, the cargo space is more than twice as big as what is needed. Placing modules within the cargo space will certainly not be as easy as adding volumes so it is good to have a significant amount of extra room for the case when the modules don't compact nicely. What can also be seen in the table is the order of when modules are delivered to LEO. This order generally follows the requirements put in place to allow the mass spacecraft to be assembled quickly.

Table 26: Cycler Construction Starship Launches

Launch	Modules	Mass (mt)	Volume (m^3)
0	-	150	685
1	SRA-1 / RCM	115.006	199.766

2	AGM-B / AGM-S1	137.793	221.429
3	SRA-2 / AGM-S2	145.165	235.210
4	AGM-S3 / AGM-P1 / HPS	136.531	315.930
5	AGM-P2 / AGM-P3	137.224	276.168
6	TSD	131.018	232.733
7	Crew / HPS-F	~130	~500

Construction Phases:

Scheduling launches and detailing what happens between the launches is the final step in determining the construction process. Similarly, to how the Cycler itself can be divided into three sections, the construction process can be divided into three phases. Each phase will serve as a checkpoint that ensures operations are running smoothly before attempting to overcome overwhelming difficulties. The first phase can be summarized as laying the groundwork for a functioning Cycler. The second phase will bring major systems to a fully operational status. The third and final phase completes the physical construction and leads into full scale testing. To construct the second cycler, there will be three additional phases identical to the first three. Construction of the two Cyclers is done consecutively to be able to learn from constructing the first and apply it to construction of the second. This will also allow one Cycler to be completed sooner and be subjected to significantly more testing and maintenance checks before departing for Mars.

Starship launches 1 to 3 will be part of the first phase. The first launch delivering the RCM and SRA-1 will form the base of the Cycler that other modules will be autonomously docked with. The other two large modules delivered in this phase are the AGM-B and SRA-2. Also included in this phase is an equivalent mass of one strut for the AGM. The use of strut mass and volume was simply an accounting strategy. What will be delivered in this phase is one third of each strut. This way the AGM is balanced, and testing of the rotation system can be tested. Once it is confirmed that the AGM can spin-up and spin-down without issue, the next phase can begin. This transition to the second phase is estimated to be two months after the first Starship launch.

The second phase begins with Starship launches 4 and 5 in rapid succession. Systems delivered to LEO in this phase will complete the AGM. Due to the complexity of the AGM, assembly will require both Canadarms and autonomous docking. The Canadarms are robots consisting of an articulating arm with grippers at both ends. Arms are remotely controlled and used to pull two modules in line with each other so they may be joined. Canadarms also have the capability of traversing the exterior of spacecraft by climbing gripper over gripper [63]. To adequately test the completed AGM, up to two months will be allocated for this construction phase. The HPS is also delivered in this phase but, since the TSD has yet to arrive in LEO, it cannot be moved into the final position. Instead, the HPS will simply be temporarily tethered to the Cycler.

Phase three involves two launches but not in rapid succession. The first will deliver the TSD to LEO and allow for completion of the physical structure. Once it is confirmed that the TSD is

secured to the rest of the cycler, a crew configured Starship will be able to dock there. At this point, and no sooner, the first crew to inhabit the Cycler arrive. With the extra mass capacity of Starship, enough Dinitrogen Tetroxide and Aerozine-50 to fill the tanks of the HPS will also be sent with the crew. Crew missions are already acceleration limited to keep the crew alive, so it makes sense to have hypergolic propellants on this launch and experiencing lower accelerations. As a precaution, an abort system will need to be specially developed for a launch such as this, so that the crew can get far enough away from the hypergolic propellants in unforeseen circumstances. To get adequate data on human adaptation to rotational artificial gravity, phase three will be allocated three months, instead of two like the others.

After seven months and seven Starship launches the first Cycler is complete and fully operational. The crew returns to Earth aboard the Starship they arrived on, and construction of the second Cycler can begin. Having gone through the process of constructing a complete Cycler already, an estimated time savings of two months is anticipated for phases 4, 5 and 6. These construction phases are identical as phases 1, 2, and 3 but for the second Cycler. Figure 30, shown below, is of the final Cycler model (version 4). Dark gray discs are airlocks where modules dock with each other. The support cables of the TSD and AGM will make use of the Canada Arms being sent to aid with construction.

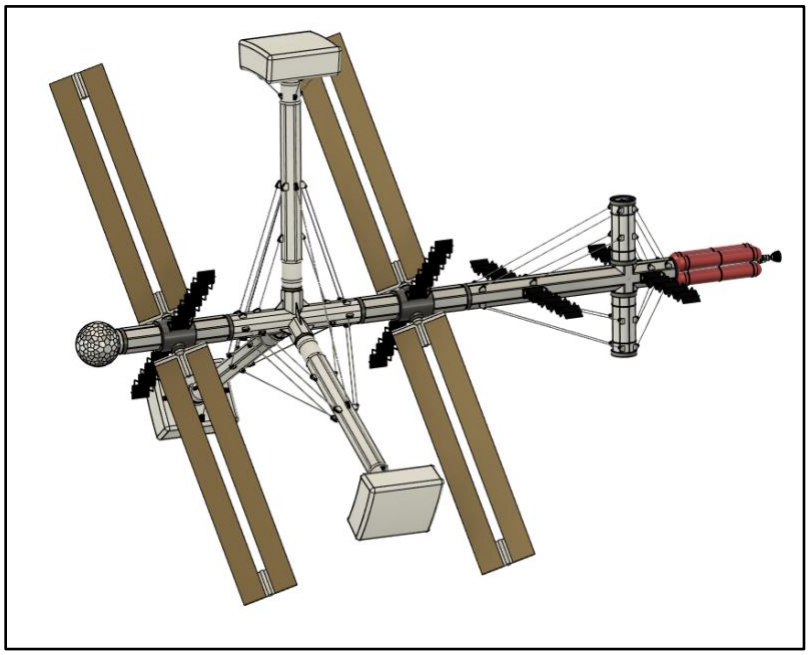

Figure 30: Final Cycler Model [37]

5.9 Interplanetary Trajectory, EDL, and ΔV Budget (Chris Manilla)

The ΔV budget for both the Crewed and Supply mission profiles were derived using data from [64] and [52]. Additional calculations were needed to find the expected ΔV for the S1L1 to LMO leg of the journey. For the approximation of the LEO to S1L1 and S1L1 to LMO, a Hohmann transfer

was used for simplicity, where μ is the standard gravitational constant of Mars ($\mu = 42828.37$ km/s).

Equation 29: Hohmann Transfer ΔV

$$\Delta V = \sqrt{\frac{\mu}{r_1}}\left(\sqrt{\frac{2r_2}{r_1 + r_2}} - 1\right)$$

The radii were then approximated using the average closest approaches for each leg listed in **Error! Reference source not found.**. This gives the expected ΔV needed of 1.18 km/s. The ΔV from LMO to Mars Surface was derived by estimating that 10% of the maximum expected entry velocity of the Starship, or 10% of 7.5 km/s, would be needed for safe landing after considering atmospheric assistance. An additional safety factor of up to 20% in the interest of crew safety and contingency.

Table 27: Radii for LMO and S1L1 Orbits [48]

LMO to S1L1	
$r_1\ (km)$	$r_2\ (km)$
1000	10500

The S1L1 Cycler trajectory is not as ΔV efficient as a comparable direct transfer, but the travel times are consistently faster for the S1L1 trajectory, with average transit times over 14 revolutions of the S1L1 being 158 days for the outbound trajectory and 160 days for the inbound trajectory [48]. Times in space for comparable ΔV direct transfers range from 190 days to 240 days [65]. For this reason, the Cycler is used primarily for crewed missions to minimize time in space for the crew.

5.9.1 Crewed Missions (Chris Manilla and Mark Paral)

Earth Ascent

The first crew will be on board the outbound cycler during its initial boost into the S1L1 orbit. Following this unique ascent method, subsequent crews (crew 2) will lift off in a crewed Starship, along with the Super Heavy booster, and achieve a parking orbit in LEO. The spacecraft will then refuel at an orbiting fuel depot and continue the mission. The mission profiles then diverge between the crewed and supply missions. For the crewed missions, the Starship will rendezvous with the outbound cycler station, where the crew will stay until they reach Mars. Rendezvous with the cycler from LEO will require 3.79 km/s of ΔV. Calculations for the propellant required can be viewed in appendix 12.3. In total, 905.3110 metric tons of propellant will be required to rendezvous with the cycler and land on Mars. This will take a maximum of 7 Starship refueling propellant launches. Additionally, 13 metric tons of food and water will be sent with the astronauts on their taxi Starship which has been accounted for.

Mars EDL

Once the station is at its closest Mars approach, the Starship will detach and perform a maneuver to reach LMO. Once in descent to the surface, atmospheric effects along with retro propulsion will be used to safely land the crew on the Martian surface. More propulsion will be needed to land than in the Earth condition due to the less dense atmosphere of Mars [66]. The ΔV for the Earth to Mars trip can be seen in **Error! Reference source not found.**.

Table 28: Earth to Mars (km/s) [64] [52]

Earth Surface to LEO	LEO to S1L1	S1L1 to LMO	LMO to Mars Surface
9.4	3.79	1.18	0.75 - 1.50 (Atmospheric)

Mars Ascent

On the return trip from Mars to Earth, the ascent process is as follows. The Starship will lift off from Acheron Fossae up to a LMO to prepare for rendezvous with the inbound cycler station. Rendezvous will require a ΔV of 1.18 km/s. The required propellant calculations can be viewed in appendix 12.3. In all, the Starship will require 198.60 metric tons of propellant to complete its mission back to Earth. This propellant will be initially sent with the crew and stored on Mars for the duration of their stay.

Table 29: Mars to Earth (km/s) [64] [52]

Mars Surface to LMO	LMO to S1L1	S1L1 to LEO	LEO to Earth Surface
4.10	1.18	3.79	0.25 (Atmospheric)

Earth EDL

The Starship will detach from the cycler station at the closest Earth approach and enter LEO to prepare for EDL. Once in LEO, the Starship will slow its speed to exit orbit and begin descent. During descent, the spacecraft will be oriented to perform a "bellyflop" to maximize use atmospheric effects and retro propulsion to safely touchdown near the surface [66]. The ΔV budget for the Mars to Earth trip is listed in Table 29.

5.9.2 Supply Missions (Chris Manilla)

As in the Crewed mission, the Supply Starship will lift off from the Earth with the aid of the Super Heavy Booster and refuel at an orbital refueling station in LEO. Supply missions will use a direct transfer trajectory, ΔV for the pre-supply mission along with the three planned resupply missions are listed in Table 30. Since travel time is less of a concern for supply missions than crewed missions, the supply mission trajectories were chosen to minimize ΔV. The supply missions will fly every two years to meet the requirements stated for the mission, arriving in 2040, 2042, and 2044. As stated for crewed missions, the ΔV for LMO to Mars Surface is 10% to 20% the maximum expected entry velocity of 7.5 km/s. Propellant sizing calculations can be found in appendix 12.3. In total, 432.791 metric tons of propellant would be needed to complete the direct transfer with a maximum of 3 Starship refueling launches.

Table 30: LEO to Mars Direct (km/s) [64, 67]

Earth Surface to LEO	Pre-supply	Resupply 1 (Aug-26-2040)	Resupply 2 (Sep-01-2042)	Resupply 3 (Jan-10-2044)	LMO to Mars Surface
9.40	4.33	4.35	5.17	5.46	0.75 - 1.50

6: SURFACE OPERATIONS

6.1 Pre-Supply

6.1.1 Design (Mark Paral and Austin Koeblitz)

The total pre-supply mission is outlined in Table 31. It is broken up into two sub-missions denoted as the pre-pre-supply and the pre-supply. The pre-pre-supply mission is distinct from the rest of the pre-supply mission as the items in the pre-pre-supply mission are required for the nominal operation of the pre-supply mission.

The pre-pre-supply mission itself can be broken up into two distinct launches. The first is the launching of the landing location scout rovers. For the purposes of sizing this mission, the scout rovers were estimated to be 1025 kg each, approximately the size of the 2020 Perseverance Rover [68]. These scout rovers will act as the mission's first "boots on the ground." Before any additional hardware is committed, it will be necessary to confirm the presence of expected resources (primarily water-ice) at the landing location, as well as determine that the location is suitable for human landing vehicles (level smooth terrain). The team baselined two scout rovers for these purposes. One will scout the selected landing site of Acheron Fossae while the other will scout Erebus Montes as a backup landing location. These rovers will be sent on a single Starship and arrive in late 2031. The team determined that the rovers will be given until 2033 to make a final determination on the feasibility of the landing location(s).

The second pre-pre-supply launch will consist of the New Mars Relay Network (NMRL), which is comprised of four satellites which will orbit above the selected landing site. This will arrive in late 2033 on a single Starship and be deployed at the proper inclination above the landing site. The NMRL's operation will be necessary for mission control back on Earth to monitor the autonomous deployment of pre-supply systems.

The pre-supply mission will be launched in 2035 and arrive in 2036. It will consist of thirteen Starships containing the habitat structure, water, waste, thermal, life support, propellant conditioning, and mining systems as well as materials for the greenhouse, the KRUSTY reactors, science payloads, and two space exploration vehicles (SEVs). After arriving in 2036, the equipment will begin to communicate with mission control through the NMRL and autonomous deployment will begin. First, the KRUSTY reactors will be deployed, and powered on as necessary, to create enough power for the other systems to operate. Following this, the RASSORs will begin mining operations, working to clear the habitat installation pit and install gently sloped ramps such that habitat modules can later position themselves. This process will begin with the habitat modules driving themselves down into the pit and autonomously aligning. Then, the habitat modules will self-level and dock themselves to each other. Life support and other vital systems will then begin to come online while the RASSORs begin to use the cleared regolith to cover the habitat in a 3 m radiation shield. These operations will continue into 2038 when the first astronaut crew arrives.

Payload Item	Mass (kg)	Launch	Arrival	ΔV (km/s)	Starship(s)
2x Landing Location Scout Rover	2,050	Dec 21, 2030	Oct 5, 2031	4.7	1
4x New Mars Relay Network Satellites	7,944	Apr 17, 2033	Oct 26, 2033	4.62	1
Habitat Structure	1,056,338	Jun 26, 2035	Jan 20, 2036	4.31	11
Water Management	1,540	-	-	-	-
Waste Processing	208	-	-	-	-
Thermal Control	1,000	-	-	-	-
Greenhouse Materials	24,000	-	-	-	-
Life Support Systems	2,730	-	-	-	-
18 KRUSTYs	27,000	-	-	-	-
22 RASSORs with Support Equipment	1,750	-	-	-	-
Propellant Conditioning Equipment	7,000	-	-	-	-
Water Production Equipment	10,000	-	-	-	-
Science Payloads	6,100	Jun 26, 2035	Jan 20, 2036	4.31	1*
2x Space Exploration Vehicles	6,000	Jun 26, 2035	Jan 20, 2036	4.31	1

Table 31: Total Pre-Supply Mission

6.2 Habitat

6.2.1 Design (Tim Osifchin)

Many different designs have been proposed for the initial habitation of the red planet. Each makes use of the resources of the planet to significantly trim down the amount of mass being shipped from Earth to Mars. When looking at various potential layouts some of the key factors of interest are as follows: access to the surface, ease of interior traversals, storage capacity, construction automation potential, and crew standard of living. For habitats that make extensive use of Martian resources, the amount of the resource that needs to be extracted is another consideration to be made.

As a team, each of the above considerations were weighed against each other and used to validate certain habitat layouts. The most weighted considerations were access to the surface, ease of interior traversal, consequence of single section loss, and required excavation mass. The layouts chosen for the analysis ranged from rings to pyramids to underground tunnels. Upon completion of the analysis, a ring with central hub layout was selected for the habitat. This design involves exactly what it sounds like, a center module with an array of modules surrounding it. Astronauts can very easily access the surface from the outer ring modules. Due to all the connections/corridors between modules, multiple paths can be taken to get from one module to another. This effectively

decreases the consequence of losing a single module. Having modules dedicated to specific tasks will also provide the crew with a higher standard of living. Changing environments can be very beneficial to the crew's mental well-being.

Sizing the habitat was the next step in the design process. The final habitat design consisted of nine almost identical modules. Each module had an 8-meter outer diameter and an inner ceiling height of 2.3 meters. The diameter was selected so that the modules could fit with Starship. The latest Starship user manual set the maximum diameter of the cargo section at 8 meters, so that is exactly what the modules will be set to. The inner diameter of the modules is set by the outer diameter and the wall thickness. Wall thicknesses will be discussed in the radiation analysis of Section 6.3. The inner ceiling height was set to 2.3 meters for the sake of the crew. They will be spending a large amount of time working in the habitat and so it is important they do not feel cramped or claustrophobic. Figure 31, shown below, is of the final habitat design and sized as stated above.

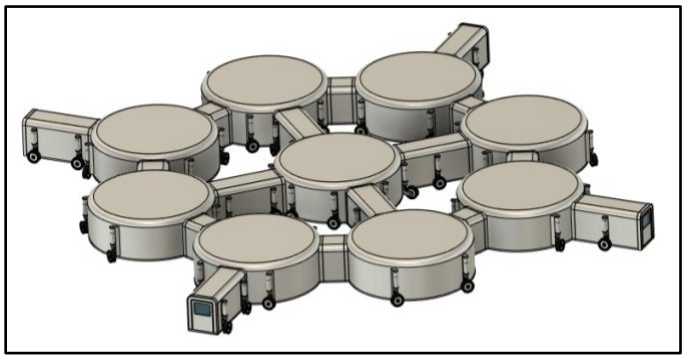

Figure 31: Habitat CAD - Modules Only [69]

As will be shown in Section 6.3 it is infeasible to bring everything needed for adequate radiation shielding from Earth. Therefore, Martian regolith will be used to complement the shielding provided by the modules themselves. To decrease the amount of regolith needed to be excavated, the habitat will be partially buried. Figure 32 and Figure 33 depict the uncovered and covered final habitat models.

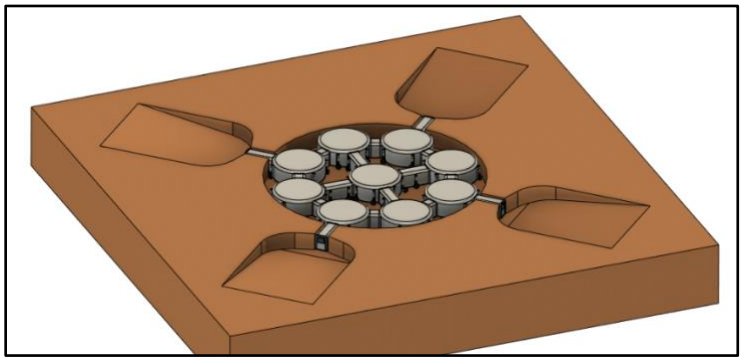

Figure 32: Uncovered Habitat Model [69]

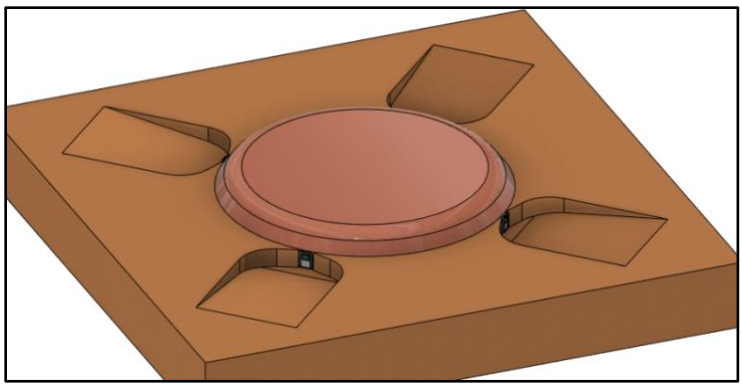

Figure 33: Covered Habitat Model [69]

6.2.2 Construction (Tim Osifchin)

The potential for automated construction was one of the more important considerations made for the habitat design, and, as can be seen in Figure 31, each module has wheels for this exact purpose. When excavation equipment and the habitat modules arrive on Mars, the construction of the habitat begins right away. By the time the crew arrives, they should arrive at a completed habitat that is ready for move-in.

As with the Cycler construction, the habitat construction process can be divided into three phases. The first will involve excavation. A 34-meter diameter area needs to be dug to a depth of 2.70 meters with ramps around its perimeter so that modules may be brought down into the excavated area. Excavation will be completed autonomously with RASSOR systems (see section 6.5.4). At the end of the excavation phase, the area the habitat site will look like what is shown in Figure 34.

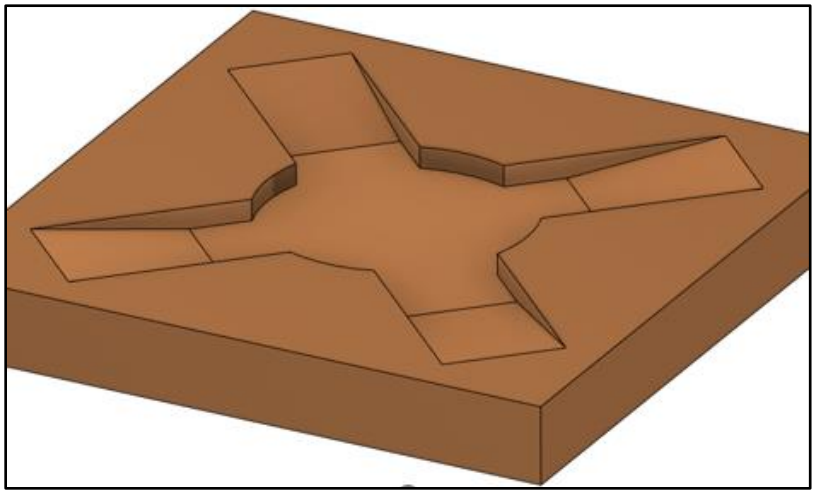

Figure 34: Final Excavated Volume [69]

The second step in constructing the habitat will involve placing and connecting modules in the excavation site. Modules will be lowered to the ground with Starship's built in crane. Upon touching down on the surface, the modules will unfold themselves with actuators. Being 8 meters

in diameter, to fit inside Starship, the walls simply need to fold in on themselves. The floors and ceilings of each module can be one fully assembled piece. Once the module has unfolded itself, the motorized wheels at its base will move it into position. The modules of the habitat will simply be docked with each other autonomously, just like Cycler modules are docked to each other when it is being assembled. The first module to position itself in the excavation site is the center module. The four corridors around the center module are next. The outer 8 modules and their attached corridors then arrange themselves around the central hub. Once all the modules are in place and securely docked with one another, this phase of construction is complete.

The final phase of habitat construction involves covering the habitat in regolith. Since this phase will remove access to the outside of the habitat, a significant amount of pressure testing must be done in the previous phase. Confirmation that the habitat is sealed can then lead to using RASSOR to cover the habitat with all the regolith that was excavated in phase 1. Overall, the process of constructing the habitat will take approximately 360 sols. This gives the RASSORS 170 sols to excavate the site. Assembly of the habitat is given 10 sols. Covering the habitat with the RASSORS is expected to take slightly longer than the excavation at 180 sols.

6.2.3 Landing Location Considerations (Mark Paral)

An aspect of preeminent importance to any Mars mission is the landing location. The location will be a driver of many habitat and science objective specifications of the larger mission, and for this reason an optimal site must be selected accounting for several vital evaluation criteria. The considerations required include weather/dust, elevation, terrain, temperature, water prevalence, prior mission history, geology, energy harvesting potential, communication concerns, launch/descent assist, and radiation protection. These considerations were combined and simplified to perform an accurate analysis of potential landing sites with available information. The breakdowns of these considerations will now be described in further detail.

Water is a necessary part of any mission to Mars. With a limited resupply potential of 5000 kg every two years, astronauts cannot rely on water from Earth to sustain themselves. For this reason, a location must be selected that offers a high potential of water extraction.

Elevation is another important aspect, as a lower elevation indicates a thicker atmosphere which is beneficial for multiple reasons. A thicker atmosphere provides additional atmospheric drag when descending in a launch vehicle as well as providing vital radiation protection to the astronauts. Because of these, a low elevation is most desirable for the landing location.

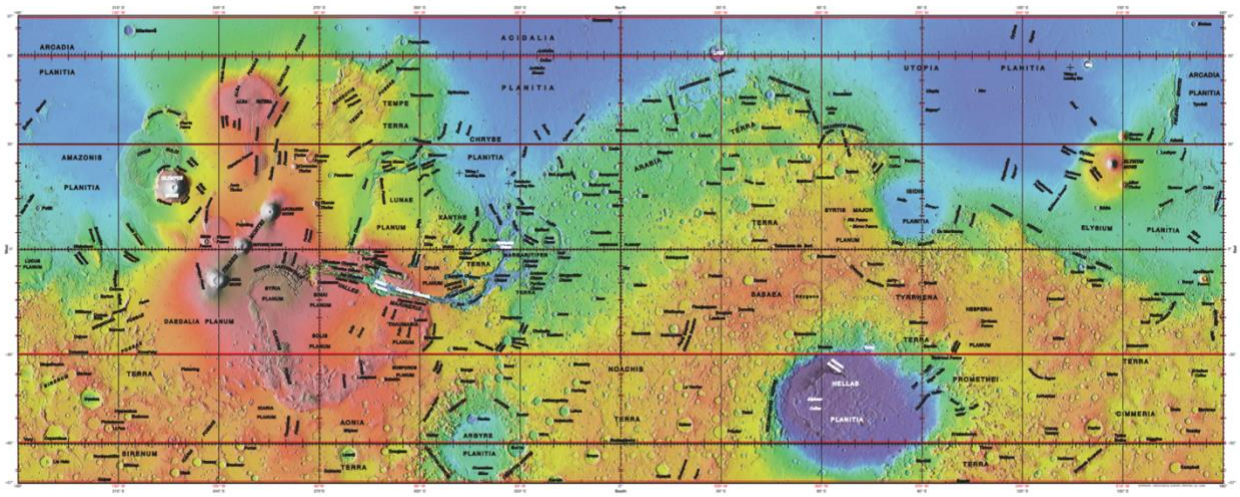

Figure 35: Martian Elevation Map [70]

Terrain considerations must be evaluated to ensure that the landing location is level and smooth. These terrain characteristics are necessary for safe landing as sloped or rocky terrain could result in a landing failure [71].

Latitude is important as an indicator of the expected temperature as well as the launch assistance potential. Closer to the equator results in a larger launch assist and a higher average temperature, which consequentially means less power to maintain a livable temperature in the habitat [71]. This relationship is visualized in Figure 36. For these reasons, latitudes closest to the Martian equator will be preferable.

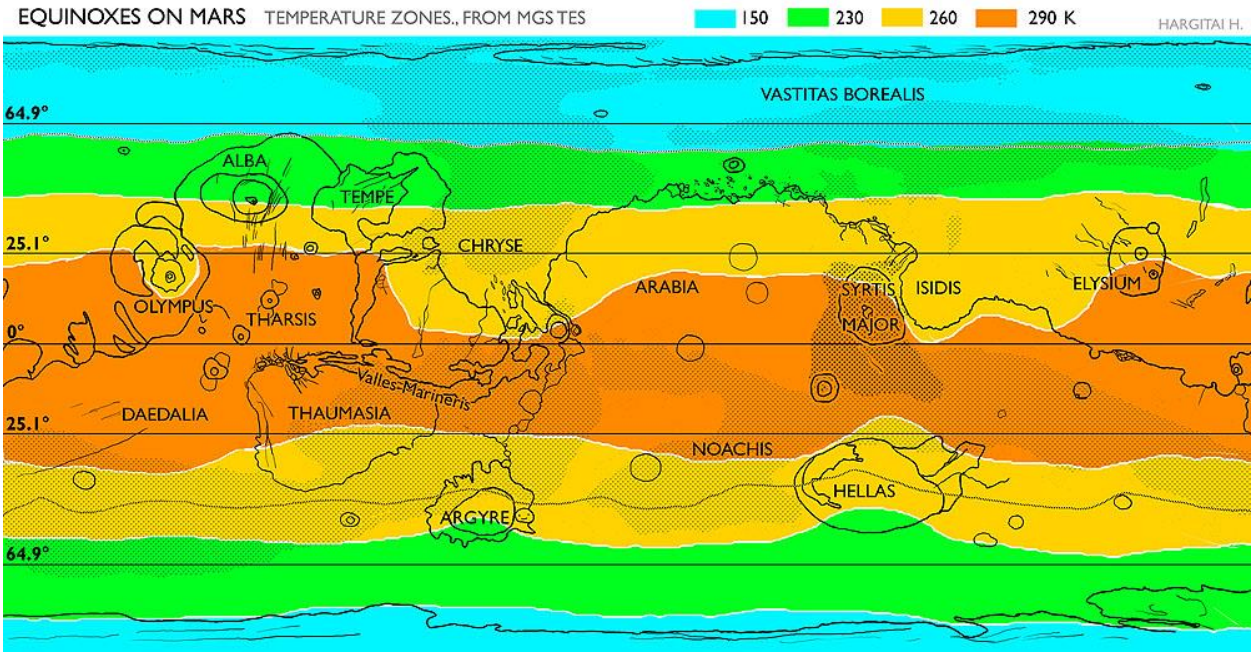

Figure 36: Mars Temperature Ranges [169]

The weather and dust considerations impact Earth based mission controls' ability to communicate with the astronauts as well as energy harvesting in the form of solar power. Dust storms are not atypical on Mars, and these events, while not physically dangerous, do act to interfere with the communications and any potential solar power the design would be harnessing. Additionally, there is a risk of static electric arcing with the electrical equipment causing electromagnetic interference [72]. Previous analysis has determined that dust storms have the potential to cause 3 dB of attenuation to Ka band communications (a maximum of 3.4 dB when including tropospheric attenuation) and significant attenuation to optical bands [73]. For these reasons, avoiding areas of frequent dust storms would be desired.

When considering previous mission history, Michael Meyer, a lead scientist for the Mars Exploration Program at NASA, may put it best with "You feel like you know the place already, and then when you get there it's different. It's always a great surprise" [74]. Surprises are not welcome when human astronauts are involved, and a physical scouting mission of selected landing locations would be necessary before any physical hardware commitments are made. Importantly, if a previous mission has visited the landing site this requirement may already be satisfied.

Geology works to facilitate the understanding of Martian history and additionally aids in the understanding of Earth. Different geological phenomena are therefore of great interest to the mission.

A final consideration was regolith quality, which was not deemed to be concerning. This is because the regolith of Mars is largely homogeneous due to global dust storms. This has been verified by previous Martian landers including Spirit, Viking, and Curiosity [75].

6.2.4 Landing Location Evaluations (Mark Paral)

Evaluation of literature candidates left the team with 16 potential landing locations of interest on Mars. These include Hellas Basin, Valles Marineris, Elysium Planitia, Jezero Crater, Olympus Mons, Southwest Melas Basin, Holden Crater, Eberswalde Crater, Mawrth Vallis, Nili Fossae, Hebrus Valles, Gale Crater, Gusev Crater, Acheron Fossae, Deuteronilus Mensae, and Erebes Montes.

The team was able to quickly eliminate Elysium Planitia [76, 77, 78], Jezero Crater [79], Holden Crater [80, 81, 82], Eberswalde Crater [80, 83, 82], and Mawrth Vallis [80, 82] due to a lack of water potential. Olympus Mons [84], Nili Fossae [85, 86], and Gusev Crater [87, 88] were eliminated based on high elevations. Finally, Deuteronilus Mensae [89] was eliminated due to rocky, uneven terrain. This left seven finalist locations which will be detailed below.

Hellas Basin is located 42 degrees south of the Martian equator and has the lowest known elevation on Mars at 8.2 km below the datum. There is evidence to suggest the presence of water-ice glaciers beneath the surface as well as prior volcanism, tectonism, and lava tubes. Due to its elevation, it is frequently the origin location for dust storms including global dust storms [90, 91].

Valles Marineris is an extensive canyon on Mars located 14 degrees north of the Martian equator with an elevation of 5.5 km below the datum. Being a canyon, rich evidence of Mars's geological history (tectonics, landslides, volcanism, erosion, etc.) are detailed on the walls of Valles

Marineris. Additionally, it has been theorized that some water-ice may be located at the base of the canyon. The weather in this region is also quite interesting as it includes reoccurring fog phenomena as well as high winds along the outer walls [92, 93, 94, 95, 96, 97].

Southwest Melas Basin is located at 15.52 degrees south of the Martian equator with an elevation of 3.668 km below the datum. The location is theorized to have been host to an ancient lake at one point in Mars's history. While not likely to have water-ice at the Basin, there are polyhydrated sulfates which have the potential to be processed into usable water for Mars missions. However, new technologies would need to be expressly developed for this purpose. Finally, the terrain at Southwest Melas Basin is relatively even with less than 10-degree slopes making it an idea location for landing a vehicle [96].

Hebrus Valles is located 20.05 degrees north of the Martian equator and 4 km below the datum. The Valles is home to caverns, troughs, pits, and craters, although with slopes of less than 1-degree inclines and boulders no larger than 1 meter. It is thought to have previously held an ocean as well as plentiful sediment deposits. If life once existed on Mars, it is a probable location for fossils. There is also evidence of water-ice at the location [98, 99].

Gale Crater is located 4.5 degrees south of the Martian equator and 4.4 km below the datum. It is believed to have been the location of an ancient lake despite the surrounding mountainous region. It has been previously explored by the curiosity rover and data on the area is plentiful. There is no evidence of water-ice; however, opals, from which water could be extracted, have been discovered by the Curiosity rover. As with polyhydrated sulfates, more advanced harvesting technologies would be required to fully realize this potential [100, 101, 102].

Acheron Fossae is located 39.8 degrees north of the Martian equator and 3.1 km below the datum. The location is believed to contain tectonic and volcanism elements, as well as prior water flows and glacial activity. This likely resulted in subglacial liquid water flow which would be a probable location for biosignatures. There is also extensive evidence to suggest that there is currently abundant subsurface water-ice at the Fossae. Finally, current elevation maps of the region suggest that the terrain is smooth enough to land on [103, 104].

Erebus Montes is located 39 degrees north of the Martian equator and 4 km below the datum. It is believed to be home to lava tubes, caves, and volcanism. Additionally, the location appears to be a large (but filled) impact crater which is likely the result of glacial activity. As with Acheron Fossae, there is extensive evidence to suggest the presence of water-ice. This includes a recent meteor impact which exposed some of this water-ice to NASA's orbital imaging. It is believed to be smooth enough to land at [103, 89, 104].

Taking this information into consideration, the locations were evaluated in Table 32 using the important characteristics outlined previously. The characteristics were weighted against one another to scale between 0 and 1. Note that negative numbers indicate an undesirable effect. Following this, a first order algorithm was created using the weights seen in Table 33. After the weighting and summation analysis, the final numerical results were reported in Table 34 with higher numbers indicating better suitability.

Landing Location	Weather/ Dust	Elevation	Terrain	Water	Previous Missions	Geology	Latitude
Hellas Basin	-1.00	1.00	0.00	0.25	0.00	0.80	-1.00
Valles Marineris	-0.50	0.67	0.25	0.25	0.00	0.80	-0.33
SW Melas Basin	-0.50	0.45	1.00	0.00	0.00	0.80	-0.37
Hebrus Valles	0.00	0.49	1.00	0.25	0.00	0.50	-0.48
Gale Crater	0.00	0.54	1.00	0.00	1.00	0.00	-0.11
Acheron Fossae	0.00	0.38	1.00	1.00	0.00	1.00	-0.95
Erebus Montes	0.00	0.49	1.00	1.00	0.00	0.80	-0.93

Table 32: First Order Algorithm Values

Category	Weight
Weather/ Dust	3
Elevation	9
Terrain	7
Water	10
Previous Missions	3
Geology	7
Latitude	8

Table 33: First Order Algorithm Weights

Landing Location	Weighted Score
Hellas Basin	6.10
Valles Marineris	11.72
SW Melas Basin	12.17
Hebrus Valles	13.57
Gale Crater	13.97
Acheron Fossae	19.82

Erebus Montes	19.56

Table 34: First Order Algorithm Results

6.2.3 Landing Location Selection (Mark Paral)

From these results, the landing location selected is Acheron Fossae (Figure 37). This is due to its abundant subsurface water-ice, geological interest (tectonic rifting, volcanism, water erosion, slope lineae, etc.), low elevations, and potential for biosignatures. Additionally, Acheron Fossae has abundant loose regolith which will prove beneficial during the construction of a suitable Martian habitat [103, 104, 105, 106].

Erebus Montes was a close runner up, and for this reason the team will use this location as a possible backup site should the scouting of Acheron Fossae expose undesirable or mission endangering characteristics.

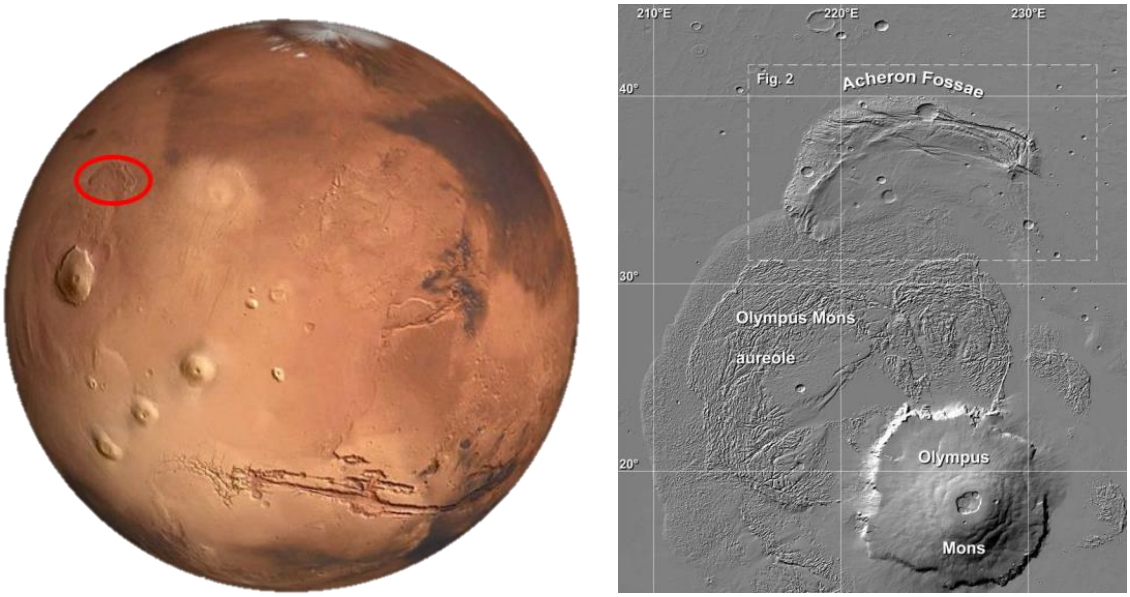

Figure 37: Landing Location Maps (Left [170], Right [105])

A potential landing location in Acheron Fossae is proposed in Figure 38. Indicated are multiple locations of interest near the actual landing location. SROI-1 denotes areas of tectonics, erosion, biosignatures, and subsurface ice. SROI-2 indicates potential past subglacial liquid water, and biosignatures. SROI-3 denotes subsurface ice. SROI-4 indicates unique crater deposits and subsurface ice. Finally, ROI-1/2 denotes locations of excess water ice [103].

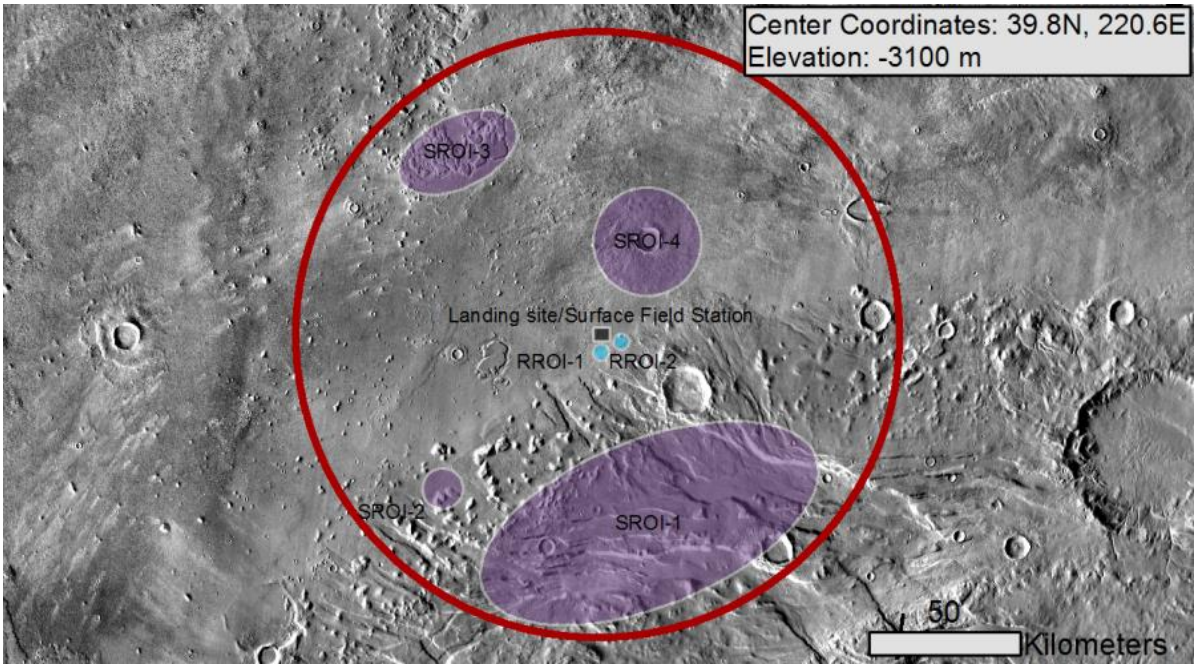

Figure 38: Landing Location [103]

6.3 Surface Operations Radiation Analysis (Luke Miller)

6.3.1 Radiation Study for Habitat and Surface Operations (Luke Miller)

A majority of the mission time will be spent on the surface of Mars. Here the crew benefits from both the protection of the Martian atmosphere (albeit thin) and the planet beneath their feet providing hemispherical protection from radiation. However, the radiation environment on the Martian surface is still inhospitable. This is especially true for long-stay missions such as the current proposal. While on the Mars surface there is the possibility of using in situ resources to aggressively shield without needing to increase payload mass sent to Mars. The goal of this study is to fully leverage this so radiation dosages can be limited within the habitat. This allows for a bolstered scientific return of the mission by permitting more time for the crew to explore beyond the walls of the habitat.

Materials Considered:

Material considerations for the habitat were largely the same as for the Cycler, except with the added option of being able to use Martian regolith and water collected on Mars. With the objective of aggressively shielding from deep penetrating GCR there is no other option but to create a very thick and massive shield. This necessitates the use of in situ materials. While water performs better in regard to shielding, Martian regolith is the preferred option over collected water for the habitat due to the following reasons:

1. Storing regolith is simple, water would require potentially complex tanks and thermal control.

2. Using regolith creates less risk because it is not contingent upon the extra complexities of removing water from regolith or drilling for water.
3. Using regolith lowers the consequence of being able to obtain less water than expected. If water is used for shielding and water production needs cannot be met, then all water production would need to be directed away from radiation shielding to life support. This is a scenario that needs to be avoided.

Habitat GCR Results

The following objectives were identified prior to sizing the habitat shield:

1. Radiation dose accumulated inside the habitat must be kept below 110mSv for the duration of the mission for each crew.
2. Regolith thickness should be kept below 3 meters due to structural and regolith collection constraints.
3. Mass sent from Earth to shield should be limited.

The initial approach was to use strictly Martian Regolith and 10cm of structural aluminum to create the radiation shield. However, as shown in the dotted lines in Figure 39 the diminishing returns of adding more regolith resulted in a design that violates the less than 3m regolith objective. Thus, 20cm of polyethylene was added to bring the regolith thickness down. The cost of this is payload mass. The design with the additional polyethylene is shown by the solid lines in Figure 39. Figure 39 shows the upper bound of GCR radiation that could be received in blue, and the lower bound in orange for both missions. These upper and lower bounds correspond to if the entire mission was exposed to the GCR levels at solar minimum and maximum respectively. In reality the dosage would fall between these bounds. Figure 39 is shown for Crew 2's Mars stay because it is longer at 1300 days compared to the 1267 day stay of Crew 1.

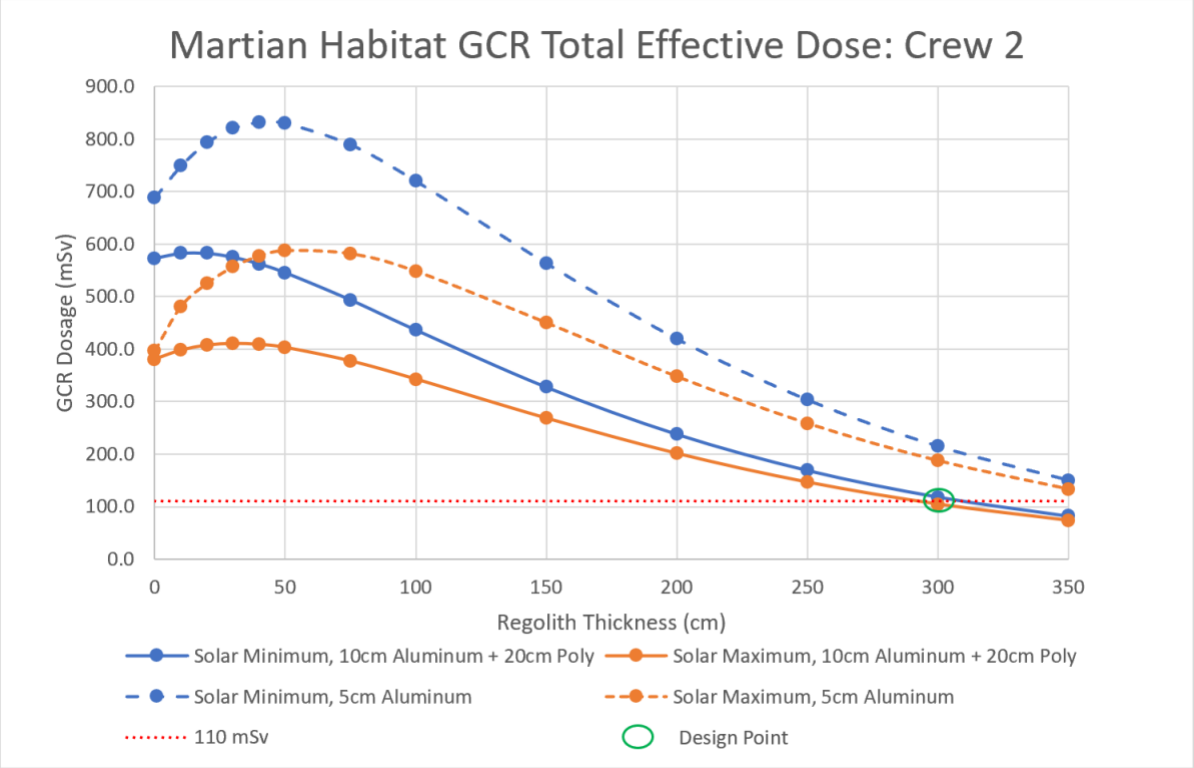

Figure 39: Crew 2 GCR Dosage while in Habitat

Ultimately, the design will be a 20cm polyethylene backing of a 10cm aluminum structure covered in 3m of Martian regolith. This is shown by the green circle in Figure 39. To approximate the dosage received an average of the solar maximum value and the solar minimum value was taken. The resulting dosage is 108 mSv for Crew 1 and 111 mSv for Crew 2.

SPEs While on Mars Surface

As introduced earlier, the protons from SPEs are less capable of penetrating material. For this reason, the SPE threat while on Mars surface is greatly reduced by the Martian atmosphere. This is corroborated by the RAD unit on the Curiosity Rover. Figure 40 contains data from the RAD unit which shows that by the time SPEs reach the surface of Mars they are only 2-3 times stronger than the background GCR radiation [107].

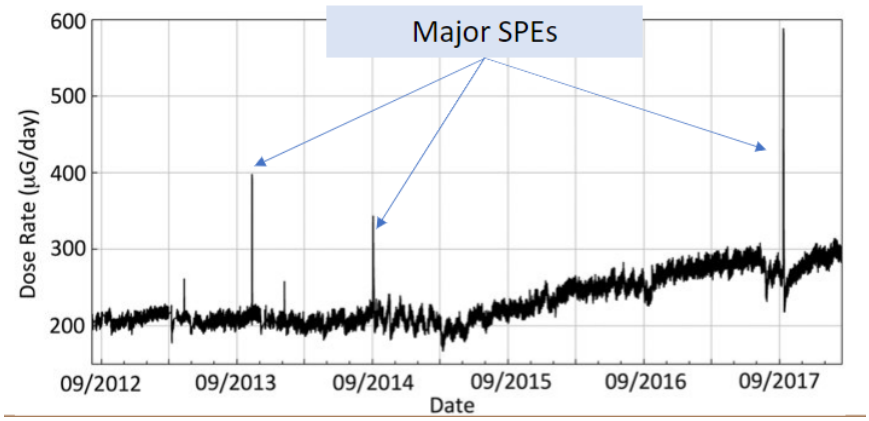

Figure 40: Radiation Exposure from Curiosity's RAD Unit

In fact, while in the habitat, even the largest SPEs pose very little threat due to their inability to penetrate the thick regolith. However, while beyond the habitat these large SPEs can be disruptive. The reference SPE would impose a 41.8 mSv dosage onto an unprotected astronaut (however this would be distributed across the length of the SPE, typically hours to days, allowing them to seek shelter). Fortunately, while beyond the habitat the astronauts would always be near the Space Exploration vehicle which would provide significant shielding against SPEs in case of an emergency [108].

Radiation Budget and Mission Radiation Summary

The culmination of this radiation study is to ensure that the crew does not exceed the 600 mSv NASA requirement. From the previous analyses a radiation budget can be constructed. This budget determines how much time an astronaut can spend completing science objectives beyond the habitat. The budget for Crew 1 is given in Table 35 and Crew 2 is given in Table 36.

Table 35: Crew 1 Radiation Budget

Crew 1	
Mission Leg	Dose (mSv)
GCR while on Cycler	284
GCR while in Habitat	108
SPE while on Cycler	75
SPE while in Habitat	0
Available for Mars Exploration	133
Total:	600

Table 36: Crew 2 Radiation Budget

Crew 2	
Mission Leg	Dose (mSv)
GCR while on Cycler	253
GCR while in Habitat	111
SPE while on Cycler	75
SPE while in Habitat	0
Available for Mars Exploration	161
Total:	600

A reasonable average dose rate at the Martian surface is 0.7 mSv/day [153]. Using this value leads to the ability to go beyond the habitat for 3.6 hours/day for each crew member in Crew 1. Similarly, it results in 4.3 hours/day for crew 2. Finally, a comparison was made between a cycler trajectory and a direct trajectory. Both trajectories assume the exact same radiation shielding and time on Mars as the Crew 2 mission. The only difference is the transit time of the Cycler vs. the direct transfer. For the direct transfer a typical direct transfer time of 235 days was used. This analysis demonstrates the benefits of the Cycler which allows for 1.7 hours/day per astronaut beyond the habitat. This will allow for a significant increase in science return. These results are summarized in Table 37.

Table 37: Time Allowed for Exploration Beyond the Habitat

Mission Profile	Time allowed for Beyond Habitat Activity (hours/day)
Crew 1 - Cylcer	3.6
Crew 2 - Cycler	4.3
Crew 2 - Direct	2.6

6.3.2 Final Considerations on Radiation (Luke Miller)

To conclude this discussion on radiation there are a few more salient points that must be mentioned. Firstly, all previous discussions have been based around radiation protection for humans. However, electronics are also sensitive to radiation. For this reason, when doing a deeper component level design, it is imperative to mission success that all critical electronics are sufficiently radiation hardened and have appropriate redundancies. Another important technology to consider in the radiation discussion is the nuclear technology being used. It is vital to make sure that the KRUSTY units are well shielded. Beyond improving the KRUSTY design radiation exposure can be limited by creating a large standoff distance between where crew members typically operate near the habitat and where the KRUSTY units are located. Additionally, a regolith berm could be constructed around the KRUSTY units if additional shielding is required. In light of these facts, the team approximated the exposure to nuclear technologies to be negligible compared to other radiation sources.

It is also paramount that the numbers presented above are taken as mere estimates. Forecasting radiation dosages is challenging and a subject of active research. Along with the limitations of

OLTARIS, the presented radiation analysis was completed as a preliminary estimate for a design that is rapidly changing. Radiation dosages can be sensitive to the 3D geometry of the structures, which could not be analyzed at this stage. Active dosimetry will be used in the actual completion of this mission. Here, astronauts could wear a dosimeter at all times and monitor their total dosage received throughout the mission. Adaptive scheduling of science objectives beyond the habitat gives the mission planners a way to limit radiation exposure if limits are being approached. Additionally, real time SPE forecasting is planned on being used to inform day to day operations. This type of forecasting can predict SPEs on the order of minutes to hours before they occur [154]. This provides the opportunity for the crew to take appropriate sheltering actions. Dependence on this capability is another reason why the communication system needs to have no blackout time. It is important to understand what impact a 600 mSv mission will have on the astronauts. The upshot is that the risk of lifetime mortality for the astronauts would increase by 3% [8]. This is shown in Figure 41. Beyond this there are a lot of uncertainties in terms of the biological risks of radiation exposure [9]. For this reason, a 2008 report from the National Research Council adamantly called for further research into the effects of radiation exposure prior to a crewed mission to Mars [9]. This emphasizes that this mission architecture will require a large research budget to help prepare for the challenge of the space radiation environment.

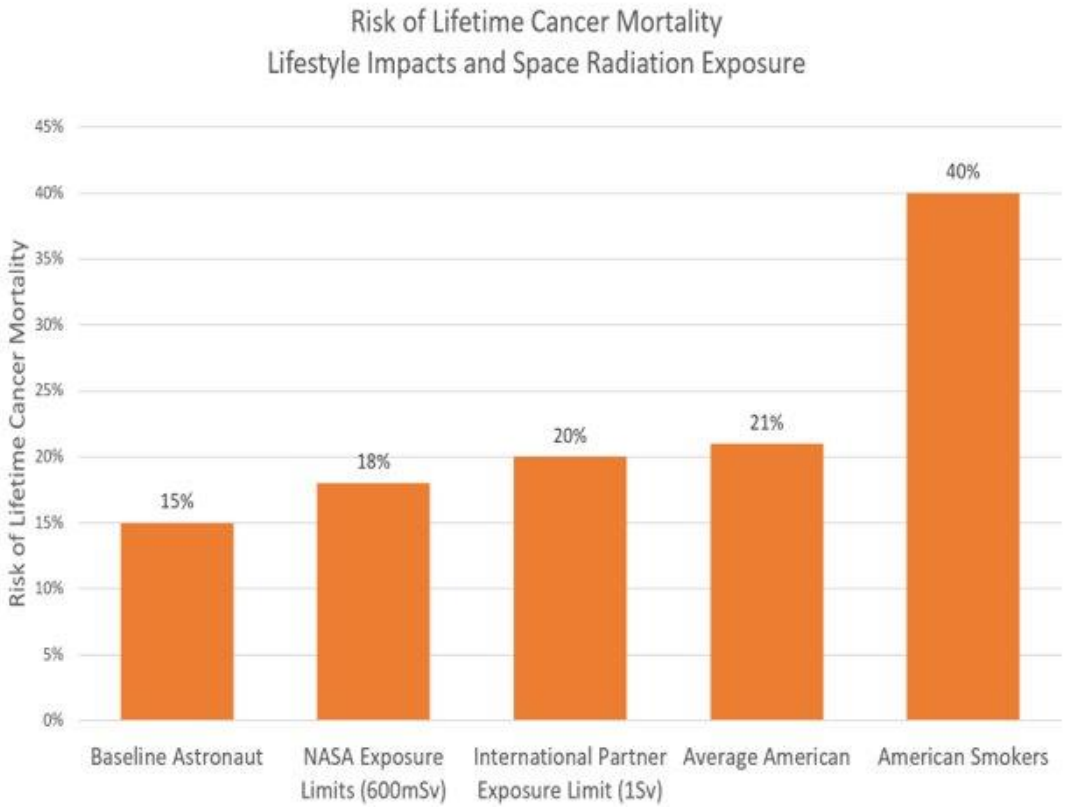

Figure 41: Risk of Lifetime Cancer Mortality Considering Radiation Exposure

6.4 Life Support System for Habitat (Matt Kelley and Nathan Berry)

The life support system analysis on the custom habitat addresses three major areas required to maintain astronaut life. These include oxygen production for breathing, water consumption for drinking and hygiene, and food requirements for the astronauts.

The given food requirements for the astronauts and mass values are based on the per-day food consumption values utilized for our cycler mass sizing. The greenhouse we will be incorporating in our habitat will help mitigate some of the risk and help supplement our food source.

The first system analyzed was the atmospheric systems required to obtain necessary oxygen levels in the air of the habitat. This is a mission critical analysis as the astronauts need a certain oxygen content within the air to survive. However, through metabolic processes, leakage from the habitat, airlock losses, other small losses, the oxygen levels in the habitat decrease every day. To replace these losses, oxygen will be produced using the MOXIE system. The requirements for O2 production are provided in Table 38. These requirements come from the Mars One Habitat Conceptual Design. Using reclamation rates given in the paper we determined the amount of oxygen that needs to be produced in order to mitigate the losses.

Table 38: O_2 Production [156]

	O2		
	Source	**Amount (kg/person/day)**	**Amount (4 crew)**
Losses	Crew Metabolism	0.9	3.6
	Leakage	-	1
	Airlock	-	0.75
	Misc. Losses		0.535
	Daily Production (kg/day)		**5.885**

A single MOXIE system can produce 2.4 kilograms of oxygen per day and requires 300 Watts of power [157]. Therefore, to obtain our daily oxygen production needs, three MOXIE systems and a total power draw of 0.9 kW will be required to produce our required oxygen needs with an excess margin of 22.3%.

The water consumption rate in Table 39 was determined using the data values given in the paper. The sizing of our water system was then based on this daily water need in order to mitigate these losses. This water need incorporates the adjusted recycling rates of the Mars One ELCSS architecture while taking into consideration the oxygen production needed from water. While our sizing for MOXIE and other things doesn't consider the production of oxygen from water electrolysis, it is included for the sake of analysis. This analysis is an upper bound of the required water.

Table 39: Water Consumption [156]

	Water					
	Source	**Amount (kg/person/day)**	**Amount (4 crew)**	**Recycle Rate**	**Recycled Amount**	**Amount Lost**
Losses	Drinking Water	2.59	10.36	0.75	7.77	2.59
	Food Rehydration	1.03	4.12	0.75	3.09	1.03
	Hygiene	7.8	31.2	0.98	30.576	0.624
	O2 Metabolic		4.04	0.75	3.034	1.01
	O2 Losses		2.57	0	0	2.57
	Misc. Losses		5.23			
	Total		57.52			**7.8227**

Table 40: ECLSS Mass and Power

Mars 1 ECLSS		
Component	**Mass (kg)**	**Power (kW)**
Atmosphere	2730	4.8
Water	1540	2.2
Wet Waste	208	3
Thermal	1085	0.5
Total	4478	10.5

The values shown in Table used in our mass and power sizing calculations were from the Mars One habitat concept. Note that the thermal system mass given in the concept was used in these calculations, but it would not be necessary as we have sized our own thermal system.

6.4.1 Greenhouse Sizing (Matt Kelley)

Table 41: Greenhouse Data

	Units	**Values**
Area	m^2	136.00
Power, LED Lighting	kW	72.60
Thermal	kW	99.18
Food Produce	kg/day	2.49
O2 Produce	kg/day	2.66
CO2 Consume	kg/day	3.52
Greenhouse Mass	kg	16488

The values for the greenhouse design given in Table 41 were obtained from a design for a lunar greenhouse module [158] that would utilize hydroponics for plant growth. The necessary food to supplement the astronaut's diet over the duration of their stay on the Martian surface required a greenhouse area of 136 square meters.

Given the required plant growth, the power and thermal loads were determined, and our power and thermal systems were sized accordingly. The primary power requirement comes from the necessary power to the LED lighting system to simulate light for plant growth. The additional thermal load comes from auxiliary support systems to support the greenhouse. This power and thermal requirement are upper bounds that occur at the peak operating times and are not constantly operating. The oxygen production and carbon dioxide consumption were noted and not necessary for the design and operation of the habitat life support system as these production values fluctuate with the operational cycle of the greenhouse.

6.4.2 Life Support System Sizing (Matt Kelley)

Table 42: Atmospheric Conditioning Equipment

Atmosphere Management		
Component	**Mass (kg)**	**Power (kW)**
Pressure Control	91	0.1
Air Revitalization	1914	4.7
Gas Storage	644	0
Fire Detection & Atmosphere Recovery	80	0
Total	2729	4.8

The atmosphere management system from the Mars One Habitat Conceptual Design [156] addresses the ability of the habitat to manage the pressure for human comfort, recirculate air and purify it, the ability to store the gases, and how to mitigate the fire emergencies. The atmosphere management system utilized in the paper was sized for 4 astronauts and addresses the needs to produce and manage nitrogen and trace gases in the habitat. These systems incorporate technologies used on the cycler while adding in components that utilize the Martian atmosphere. Given the requirements in the paper the atmosphere management system was sized and included in the mass and power loads. Note that the values given for this atmospheric system utilize were sized without considering the production from MOXIE. However, the power consumption of their system is on the same order of magnitude as the MOXIE that we intend on using.

6.5 In-Situ Resource Utilization (Austin Koeblitz)

6.5.1 Motivation (Austin Koeblitz)

With current technology, a mission to Mars cannot be made economically viable without the use of in-situ resource utilization. This simple fact is the result of what is often termed "the tyranny of

the rocket equation". In short, landing more supplies and equipment on Mars would require more out of the existing launch vehicles. For such a mission as the one currently being described, that ask would exceed their physical capabilities. The only options then, are to either rapidly increase the number of vehicles that are sent to Mars, which would result in exponential increases in both cost and logistical complexity, or to invest heavily in systems which utilize the surrounding environment to generate the resources needed "on planet". The difference between these two methods is quite clearly the difference between travelling to Mars and dreaming that it is possible.

6.5.2 Goals (Austin Koeblitz)

Deciding to invest in ISRU technologies is a critical step in bringing the mission into reality. However, it also creates a lot of questions. What goals should be prioritized? Which endeavors will result in the greatest scientific payoff? Which will result in the greatest economic payoff?

These questions are partially answered by the science objectives laid out earlier, but they are further qualified by the following goals:

1. Water is one of the most expensive commodities to be brought from Earth. Within the suite of ISRU technologies, there is to be a method by which liquid water can be collected on the surface of Mars for use by humans, crops, and science experiments, reducing reliance on shipments.

2. The habitat, the construction of which has previously been described, is to have its radiation shielding augmented using a 3-meter-deep regolith cover. This requires an installation process enabled by the use of ISRU technology.

3. Precious O_2, brought from Earth and recycled, is to be supplemented by extraction from the Mars atmosphere. This supplementation is to be made possible by ISRU technology and will replace losses and facilitate scientific research.

4. Surface power is to be reliable, redundant, efficient, and compatible with the ISRU systems. While it need not strictly be considered ISRU technology itself, the power system should possess many of the same characteristics as ISRU technology: being self-contained and significantly expanding the capabilities of the astronauts.

6.5.3 Systems – High Level (Austin Koeblitz)

With these goals in place, several ISRU technologies have been selected and analyzed which meet and exceed their intended functions. These technologies are the Honeybee Redwater, the Swamp Works RASSOR 2.0, the NASA/MIT MOXIE, and the NASA/NNSA KRUSTY. Combined, these technologies can address every goal set in the previous section. Additionally, they facilitate exploration beyond the initial expectations due to their potential for application on large scales.

6.5.4 Systems – Low Level (Austin Koeblitz)

Redwater:

The first ISRU technology necessary for this mission is Honeybee Robotics' Redwater [158]. Redwater makes use of two known technologies, coiled tube drilling and Rodriguez wells, to enable the extraction of liquid water from subsurface ice. This system is currently TRL 4/5 with testing scheduled to push it to TRL 6 [158].

During the mission, Redwater will operate as described by Honeybee. Before summarizing that operation, however, it is important to understand the challenges that Redwater must overcome. The Mars Reconnaissance Orbiter (MRO) used a device called SHARAD (shallow subsurface radar) to map up to 15 meters beneath the ground. This revealed that there are many regions within which glaciers are covered by several meters of rocky overburden, a layer of regolith and rocks that must be cleared before access is possible. This overburden is thought to have prevented the glaciers from vaporizing due to Mars' low pressures and temperatures [159]. These mark the two greatest obstacles for the system. First, the ice must be reached, which may require drilling through up to 20 meters of rocky overburden. Then, the ice must be protected during the extraction process, as well as after extraction has ceased.

With these obstacles in mind, Redwater's operations can now be summarized. First, Redwater consists of four major systems: "the bottom hole assembly (BHA), the coiled tubing (CT), the CT injector assembly, and the CT drum assembly" [158]. The BHA consists of subsystems like the heated auger, the heated fluid transfer line assembly, the packer assembly, and subsequent systems. It is supplied with power, gas (CO_2 or N_2), and commands via the CT, which bundles the power, signal, pneumatic, and hydraulic lines around a cable heater within the 2.54 cm outer diameter tube (1.651 mm thickness). Because it is the link between the BHA and the surface, the CT must run down the length of the borehole. This necessitates the CT injector assembly, which utilizes two "drive/preload rollers responsible for gripping and pushing the coiled tube downward and generating required weight-on-bit forces for drilling" [158]. The CT injector assembly spools the CT off the CT drum assembly, a passive system that is also capable of passing CT from the rotating drum to a stationary bulkhead [158].

Figure 42. BHA Subassemblies [158]

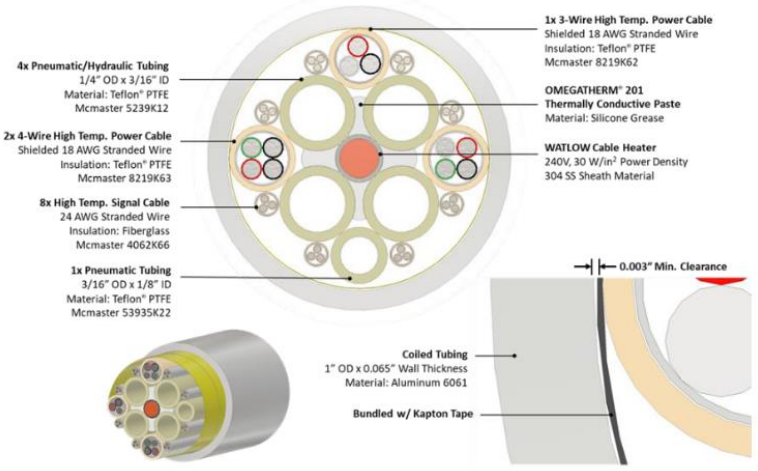

Figure 43. CT Bundle Breakdown [158]

The major systems described above work in conjunction to drill to depths of up to 35 meters [158]. The BHA drills the borehole using downward force supplied by the CT injector and transmitted by the CT. As material is loosened, compressed gas (CO_2 or N_2) is released to clear it. This process continues until the BHA reaches a depth of about 3 meters into subsurface ice. At that point, the packer inflates to seal off the hole and compressed gas is pumped in to achieve a pressure high enough to permit the existence of liquid water. Then, the auger is heated to a set point that is maintained and monitored by thermocouples. Rotating at a rate of 120 rpm to generate convective waves, the auger melts the surrounding ice and begins to function as a Rodriguez well. A portion of the melted ice is pumped to the surface for use by the crew, while the remainder is heated and used to continue melting surrounding ice [158].

This system is estimated to be capable of producing just under 6 kg of water per hour while requiring just under 3 kW of power [158]. As a result, it is not expected that this system will need to operate continuously for the duration of the mission. Water stores will be kept near capacity (with emergency reserves as backup), but recycling initiatives are expected to do a large portion of the work. Rather, the water generated by this system will be used to replace losses, conduct scientific research, and enable future endeavors towards large-scale fuel production.

A final note for this system is that it is fit for mobile applications. Honeybee has generated a concept that depicts the Redwater system mounted on a rover that would be capable of storing large amounts of extracted water and the compressed gas needed to reach it.

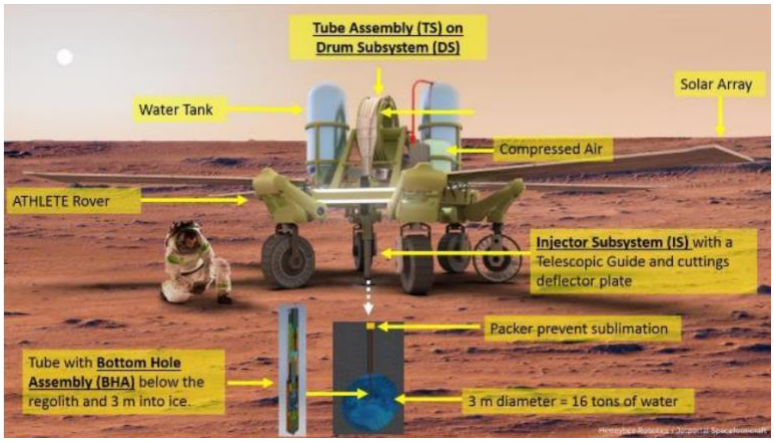

Figure 44. Mobile Redwater Concept

RASSOR:

The next ISRU technology to be included in this mission is Swamp Works' RASSOR, a lightweight (66 kilogram) device that utilizes "counteracting excavation forces on two opposing digging implements" to mine regolith without a resulting horizontal reaction force [160]. This will enable the collection and use of regolith on a large scale, facilitating its use in radiation shielding, water extraction, infrastructure build up, and science missions. This system is currently represented by RASSOR 2.0, which is TRL 4, but RASSOR 3.0, which is under development, will take the technology to TRL 5 [160].

RASSOR will be deployed during the pre-supply mission(s) stage and will operate fully within the scope of its design. That being said, it will be tasked with an ambitious ground-moving project upon arrival. Specifically, excavating the roughly 2.7 meter deep by 37-meter-wide circular pit in which the habitat modules will be installed. This process, fortunately, is largely automatable, but there are certain considerations that must be made regarding habitat placement and astronaut access. Most importantly, when installed, the habitat modules will need to be rolled into position via the four wheels installed at their base. This means that ramps down into the pit must be cleared and the modules must have enough room to travel down them into the pit before being aligned. Additionally, the four airlocks along the outer perimeter of the habitat must be accessible by those ramps. A small army of RASSOR's will be necessary to meet these goals.

With an idea of what is required of RASSOR, its operation can now be summarized. There are three main components to the system: the chassis, the excavators, and the cameras/automation. The RASSOR system uses a simple chassis with four 17-inch (43.18 cm) diameter wheels. These are used to move RASSOR and are capable of reaching speeds up to 56.5 centimeters per second [160]. In the event of RASSOR getting stuck in loose regolith, the wheels are aided by the excavators, which lower themselves into contact with the ground in order to further distribute the mass of the system. A similar recovery method is used if RASSOR is turned upside-down. The excavators that make this possible are more complex, using a bucket drum system that is designed to counter rotate. Each drum features several individual buckets, which are "clocked" such that only one scoop is in contact with the ground on either drum at a time. Carbon fiber and aluminum make up the structure of these drums, giving them the strength needed to support a full 80

kilograms of regolith. Finally, stereo cameras and automated software work together to control RASSOR and intelligently navigate between the regolith excavation site and the drop off site. This software first maps the route and potential hazards, later using its collected data to traverse the route at higher speeds. Combined, these systems give RASSOR the ability to autonomously travel between the excavation and drop of sites efficiently [160].

A single RASSOR, making tens of trips in its operational period of 16 hours (8 hours to recharge), can collect about 2.7 metric tons of regolith per day/sol. Impressively, this comes at the cost of only about 4 watts per kilogram of regolith extraction rate [160]. For a small army of RASSORs 22 strong, operating in staggered shifts (7 charge, 15 excavate; 7 charge, 15 excavate; 8 charge, 14 excavate), this means that the average power required to recharge them is only about 4.95 kilowatts at any given time. It would also only take about 162 sols of continuous operation to clear the habitat installation site and the ramps. While this does not take into account RASSOR casualties during the campaign, it is a realistic estimate for a project that can be completed before the crew arrives on the surface. Once the crew does arrive, and the habitat has been covered, the regolith collected by the RASSORs can be used for water extraction, as regolith has been found to contain at least 2% water by weight. Eventually, this regolith could also be used for Martian concrete research and other infrastructure.

Figure 45. RASSOR 2.0 Unloading Simulated Regolith

MOXIE:

The third ISRU system selected for this mission is based on the MOXIE experiment that was sent to Mars on the Perseverance Rover. MOXIE utilizes a solid oxide electrolysis unit (SOXE) to extract O_2 from the Martian atmosphere, a critical piece of technology because it not only facilitates the replacement of lost O_2, but it also creates the possibility of performing large-scale propellant production on the surface of Mars [161]. This is a goal that would eventually require the use of both the Redwater extractor (for fuel production) and a scaled-up MOXIE system (for oxidizer production). MOXIE technology currently has a TRL of 5 [161].

While plans for propellant storage have not yet been discussed, it can be revealed that the mission will not budget for propellant production on Mars (during this mission). Rather, propellants brought from Earth will be refrigerated to prevent boil off until ascent from the surface. Because of this, the demands placed on a MOXIE-like system are drastically reduced, relegated mainly to generating O_2 for science experiments and replacing that which is lost within the life support system.

Despite the lowered reliance on the system, an industrial-sized MOXIE will be an important aspect of the ISRU technology suite. As such, its operation is now summarized. An industrial-sized MOXIE will contain several major components: an intake HEPA (high efficiency particulate air) filter, a scroll pump, a preheater, the SOXE, and composition sensors. First, Martian air is drawn through the HEPA filter by the scroll pump. This filter aims to prevent dust and other particulates from damaging the pump and other components. Once filtered, the air is compressed by the scroll pump and sent into the preheater, which brings its temperature up to about 800 °C, MOXIE's operating temperature. From there, it enters the SOXE, and anywhere from 30-50% of the CO_2 in the air is converted to CO and O_2. The mixture is then passed over a set of nickel-catalyzed cathodes, which diverts "CO, unreacted CO_2, and residual atmospheric gases to the cathode exhaust plenum" [161]. The remaining pure O_2 is sent to the oxygen plenum. Outlet gases are characterized before they are vented back into the atmosphere, and the purity of the O_2 is verified by measuring the amount of trace CO_2 it contains [161].

Within the last few years, this technology has been validated during a multitude of tests, and based on the data generated by them, it is possible to estimate the output and size of a scaled-up system. For the purposes of this mission, the system has been defined such that it consists of a mass of about 1000 kg, requires a power input of about 25-30 kW, and is capable of generating 2 kg of oxygen per hour of operation. Similar to the Redwater extraction system, the scaled-up MOXIE system will not need to operate continuously. Rather, it can simply be warmed up and used according to an oxygen need schedule. This is not to say, however, that the system could not be run for significant lengths of time. In fact, generating oxidizer would require that the system be run for many hours on end and would potentially require additional units or an even larger system. For this mission, the needs are met by specifications above, and propellant generation research, oxygen loss replacement, and other science missions can each be catered to.

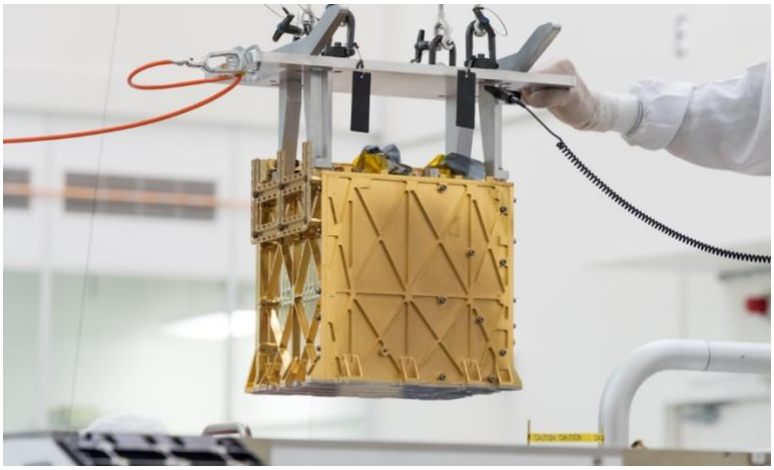

Figure 46. Small-Scale MOXIE Test Unit [157]

KRUSTY:

The technologies detailed in the preceding paragraphs represent innovative and creative methods for addressing complex problems. Each of them, after being sized, have confirmed themselves to be realistic and prudent approaches to meeting the goals outlined for this mission. That being said, these technologies each require a significant amount of a common resource. Namely, power. Combined with the rest of the base, the total draw on the power system averages about 148 kW under normal operation. This amount of power represents a significant challenge for a mission to Mars: the infrastructure required to provide that much power can be massive depending on the method of power generation selected. It is because of this that debates over solar versus nuclear power often arise. In reality, some combination of the two is likely to show long-term promise. For this mission, however, the decision has been made to rely solely on nuclear power. This is due to a recent innovation in the space, which promises impressive specific masses (kg/kW), on-off operation, and significant safety benefits. This system has been termed KRUSTY (Kilopower Reactor Using Stirling TechnologY).

The KRUSTY system is currently a TRL 5 proof of concept that is undergoing development specifically for applications on Lunar and Martian missions, as well as in purely space-based missions [162]. A fission-based reactor, KRUSTY offers several benefits over older technology, and they will be discussed before the operation of the system is described.

The first benefit of this new system comes in the form of its specific mass and power output. The first KRUSTY prototype (1 kW output) had a specific mass of about 134 kg/kW [163]. This figure is largely expected to remain the same once the system is scaled up (10 kW output), hitting about 150 kg/kW. That is significantly higher than the specific mass for common solar power systems (~6-20 kg/kW), but it is in line with existing nuclear alternatives. At the same time, KRUSTY will be capable of producing a much greater power output than those alternatives [162]. This means that KRUSTY successfully maintains its specific mass at higher power outputs, as can be seen in the next figure. Next, KRUSTY offers significant improvements in the realm of safety. This is accomplished in two ways. First, KRUSTY is controlled by a boron carbide control rod that can be dropped to turn the reactor “off” or raised to turn the reactor “on”. Secondly, KRUSTY utilizes

solid cast fuel made primarily from uranium 235. This means that the reactor is less fragile during launch and transportation, effectively ensuring that criticality is never reached unintentionally [163]. The last benefit discussed here returns to the fuel choice. By using highly enriched uranium instead of plutonium, KRUSTY has been designed to operate with fuel that is readily available and well understood.

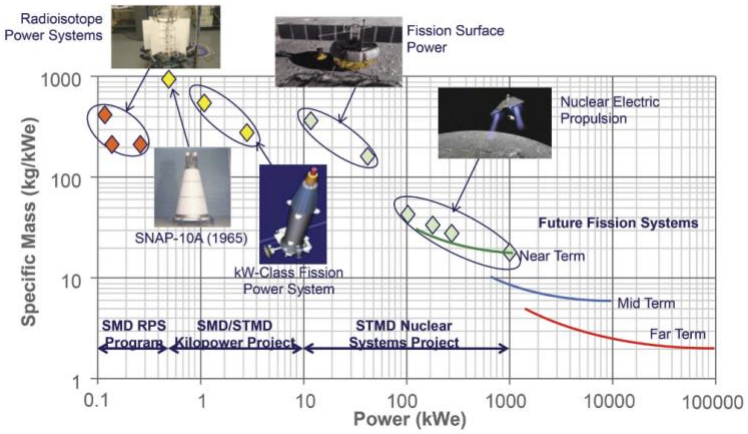

Figure 47. Power Output Performance Map for Nuclear Power Systems [162]

With the benefits of the system covered, the basic operating principle behind KRUSTY can now be detailed. At its core, KRUSTY uses a cast piece of uranium-molybdenum fuel measuring 11 cm in outer diameter and 25 cm in length. A 4 cm inner diameter opening runs the length of the fuel. Eight heat pipes measuring 1.27 cm in outer diameter route the heat from the core to the Stirling engines, which produce power. Various assemblies mate these components and deal with the heat transfer requirements of the reactor. Those details were deemed outside the scope of this report, however, so they are omitted here. Critical to the operation and safety of the reactor are both the neutron reflector and the shielding. The neutron reflector is made of beryllium oxide, and its purpose is to prevent neutrons from leaving the core, scattering them back towards it so as to propagate the reaction and ensure efficient operation. The shielding will be made from solid stainless steel, wrapping all the way around the reactor.

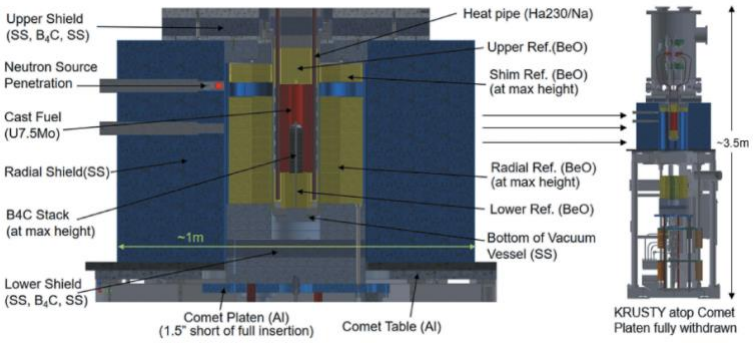

Figure 48. KRUSTY Reactor Configuration [163]

The discussion above lays out the basic principles of the KRUSTY reactor and describes the benefits of using such a system. There is one key detail that remains, however. KRUSTY is not technically classified as an ISRU technology. As alluded to in the goals laid out previously, the power system does not make use of resources found in the Martian environment. Rather, its self-sufficiency and relative autonomy contribute to its honorary acknowledgement as a pseudo-ISRU system. KRUSTY's benefit to the ISRU suite, and indeed the entirety of the base, supports its selection over older nuclear technology or solar power alternatives. A small army of KRUSTY's will be required to support this mission, but they will be well suited to accomplish the goals set for them.

6.5.5 Conclusion and Sizing (Austin Koeblitz)

The technologies discussed in the recent sections can broadly be classified as ambitious, innovative, and effective. Their selection was informed not only by the mission's underlying requirements, but also by an understanding of how they can later benefit future missions. The KRUSTY reactors are expected to have lifetimes of greater than 10 years, allowing them to provide reliable energy for multiple missions. The Redwater extractor can be moved from point to point, extracting water reliably and in quantities that may well enable fuel production on Mars. The sized-up MOXIE will be able to generate O_2 in quantities that enable the production of oxidizer on Mars, and finally, the RASSOR's will enable small-scale terraforming that facilitates base growth and infrastructure build up.

These systems are not expected to be perfectly characterized by the information in the preceding paragraphs. It is understood that their respective performances are likely to change, at least slightly, before the mission takes place. Because of this, the following sizing estimates are noted as being preliminary, and are not intended to be taken as final values. First, sizing the Redwater extractor, which already has a defined size, is a task of estimating the number of hours per sol that the system must be run. Based on estimates of water generation needs (taking reclamation into account) we expect to require extraction of about 11 kg of liquid water per sol. Redwater's extraction rate is estimated to be about 5.97 kg of liquid water per hour, so we expect to operate Redwater for about 1.84 hours per sol. Next, sizing the RASSOR units, which also have a predetermined size, is a task of determining the number of individual RASSOR units to send. This problem is defined by the

amount of mass we are willing to allocate to the RASSOR systems as well as how quickly we would like to be able to excavate the habitat pit and cover the installed habitat in regolith. Additionally, the power draw of the RASSOR systems is something to consider, as anything prohibitively large will limit the number of RASSORs that can be charged at any given time. Iteration led to the decision to take 22 individual RASSOR units and charging infrastructure to support 8 units at a time. This allows for one third of the units to be charged during every 8-hour period, requiring an estimated average power draw of 4.95 kW. Most importantly, this number of RASSORs is estimated to be able to clear the habitat pit (and install ramps) in about 162 sols, assuming continuous operation. This fits within our mission objectives in that it allows for the habitat pit to be cleared, the habitat to be installed, and the habitat to be covered before the first crew shows up. Finally, sizing the scaled-up MOXIE, also having a predetermined size, again becomes a task of determining how many hours per sol to run the system. Based on life support calculations, we expect to require generation of about 5.885 kg of O_2 per sol. Since the scaled-up MOXIE system is expected to have a generation rate of 2 kg of O_2 per hour, we expect to run the system for about 2.94 hours per sol. The power required by these systems is analyzed in the following section, where the sizing of the KRUSTYs is also discussed.

6.6 Habitat Power and Thermal Analysis (Austin Koeblitz and Nathan Berry)

The surface habitat designed for this mission is intended to support each crew continuously for the duration of each of their stays. This necessitates the employment of systems which will not only maintain the survivability of the habitat but will also provide a certain level of comfort to the astronauts. In an attempt to estimate power needs and allocations, major systems have been considered and sized according to the size of the crew, the objectives of the mission, and the expected difficulties associated with living on the surface of Mars. A small excess margin was applied when sizing the power generation system such that later additions to installed systems, and redundancy, can be addressed. The accounting presented in this section is therefore not intended to represent a precise and complete view of habitat infrastructure. Rather, it represents a rough estimate which can be iteratively refined as mission planning continues.

6.6.1 Habitat Power Analysis (Austin Koeblitz)

Power Draw Accounting:

Before discussing the power generation system, it is important to account for all major systems that will draw power on the surface. These details are presented in Table 43.

Table 43. High Level Power Requirements

High-Level Power Requirements		
System	**Description**	**Power Required (kW)**
Habitat Greenhouse	Greenhouse heating, lights, and fluid management systems	100.00
Refrigeration of CH4 and O2	Preventing boil off	31.00
Industrial Size MOXIE	O2 generation at a rate of 2 kg/hr	30.00
Habitat Life Support Systems	Atmospheric and water reclamation/processing	10.00

RASSOR Systems	Staggered charging schedule	4.95
Habitat Thermal Control Systems	Heat pumps and distribution equipment	4.60
Water Production Equipment	Honeybee Redwater	2.94
Communications Equipment	Radios, repeaters, transponders, antennas, dishes, etc.	0.92
Habitat Lights	LED and UV lights	0.15

As can be seen, the four largest power draws (≥10 kW) come from the greenhouse, propellant refrigeration, O_2 generation, and life support systems. These are followed by the RASSORs, the thermal control systems, and the operation of the Redwater extractor (all between 2.5 and 5 kW). Communications and lighting systems make up the remaining power draw (<1 kW each).

Combined, these systems would draw nearly 185 kW of power if run concurrently. Fortunately, applying system operation scheduling can significantly reduce the total power draw, as is detailed in the next section.

System Scheduling:

There are approximately four scenarios when it comes to habitat system operations: the typical operation during the habitat covering phase, the typical operation after the habitat has been covered, emergency operation in the event of a catastrophe, and high-demand operation during consumables replenishment.

The first scenario describes the phase of the mission when the final installation of the habitat is underway. During this phase, all systems but O_2 generation and water extraction are operating, resulting in a power draw of about 151 kW.

The second scenario describes the phase of the mission after the habitat has been fully installed, when the RASSORs are no longer required and the O_2 generation and water extraction equipment are still idle. This results in a power draw of about 146 kW.

The third scenario describes what happens in the event of an emergency. In such a situation, only systems essential to the short-term survival of the crew are in operation. This includes habitat life support, thermal control, communications, and lighting systems. The resulting power draw is about 15 kW.

The final scenario describes times when consumables such as O_2 or liquid water need to be topped off. In such a situation, either the water extraction equipment or the O_2 generation equipment is run in addition to the systems described in the second scenario. This is done to avoid overtaxing the power generation system, and it results in power draws between 150 and 176 kW.

It is important to note here that, due to the use of water and atmosphere reclamation, as well as the plans to bring and refrigerate propellants rather than produce them, periods of consumables replenishment are expected to be rather infrequent. Therefore, durations during which power draw exceeds 150 kW are also expected to be infrequent.

Power Generation Sizing:

Based on the power draws estimated in the previous section, a max draw of about 176 kW is to be budgeted for without significant additional margin. This decision was made for one main reason: 176 kW draws are expected to be very infrequent and short in duration. If needed, certain systems can be scaled back or shut down during these periods to free up power (greenhouse and propellant refrigeration). Because this mission will utilize KRUSTY reactors to supply power, each having a capacity of about 10 kW, 18 KRUSTYs are required to achieve a total power capacity of 180 kW. This capacity is enough to provide redundancy during normal operation, meet requirements during high-draw periods, and allow for the inclusion of additional systems without adding more reactors. With regards to the four scenarios laid out in the previous section, this capacity results in percent utilizations as shown in Table 44.

Table 44. Power Draw and Percent Utilization by Scenario

	Scenario 01 (Typical Operation, Habitat Covering Phase)	**Scenario 02 (Typical Operation, Post Habitat Covering Phase)**	**Scenario 03 (Emergency Operation)**	**Scenario 04 (Typical Operation with Consumables Replenishment)**
Power Draw (kW)	151.62	146.67	15.67	149.61-176.67
Percent Utilization (%)	84.23%	81.48%	8.71%	83.12-98.15%

6.6.2 Habitat Thermal Analysis (Nathan Berry)

The habitat design also underwent a thermal analysis to ensure it met all requirements for sustaining astronauts during the mission. The following figure is the control volume utilized in the analysis.

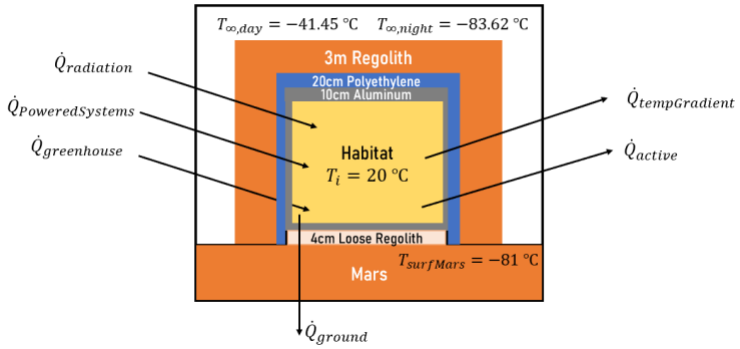

Figure 49: Habitat Thermal Control Volume with Mars Temperatures [164]

The above control volume shows the layers of regolith, polyethylene, and aluminum that were sized in the radiation analysis of the habitat. An additional layer of 4-centimeter-thick bags of loose regolith were added in between the floor of the habitat to help insulate the floor from ground losses. The following table shows the thermal properties of the different materials making up these layers.

Table 45: Thermal Properties of Habitat Materials

Metric	Value	Source of Value
Thermal Conductivity of Regolith, $k_{regolith}$	$0.039 \frac{W}{m*K}$	[165]
Thermal Conductivity of Polyethylene, $k_{polyethylene}$	$0.34 \frac{W}{m*K}$	[166]
Thermal Conductivity of Aluminum, $k_{aluminum}$	$237 \frac{W}{m*K}$	[167]
Absorptivity of Martian Regolith, $\alpha_{regolith}$	0.743	[168]
Emissivity of Martian Regolith, $\varepsilon_{regolith}$	0.927	[168]
Outer Surface Area of Habitat Regolith Cover, A_s	$1228\ m^2$	Design Parameter
Projected Area Facing Space, A_{proj}	$908\ m^2$	Design Parameter
Distance of Mars from Sun	1.52 AU	[48]

The heat transfer to the surrounding air and ground were assumed to be conducted through the surrounding materials of the habitat where the inside wall of the habitat is at room temperature and the outside wall of the habitat structure in any direction is the temperature of the surrounding

environment. These temperatures can all be seen in Figure 49. The following two figures demonstrate the thermal resistor diagrams utilized to calculate the heat lost to the outside environment and the ground.

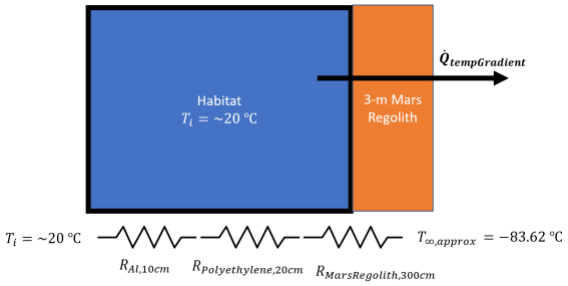

Figure 50: Thermal Resistor Diagram for Heat Transfer to Air

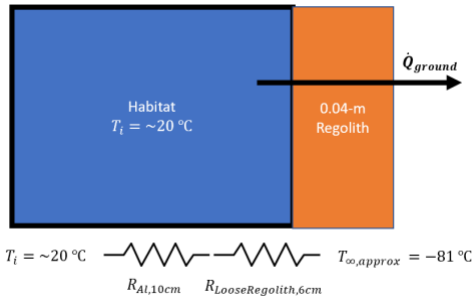

Figure 51: Thermal Resistor Diagram for Heat Transfer to Ground

Utilizing the above resistor diagrams, the desired heat transfers can be computed. The thermal resistance for any "i-th" layer can be computed using the following equation where L is its thickness, k is the thermal conductivity, and A is the area.

Equation 30: Thermal Resistance in Layer [167]

$$R_i = \frac{L_i}{k_i * A}$$

As all of the resistor diagrams in this habitat are in series, the total resistance between the inside wall and outside wall can be found using the following equation.

Equation 31: Total Thermal Resistance [167]

$$R_{total} = \sum_{i=1}^{n} R_i$$

Finally, the rate of thermal heat transfer can be found using the following equation.

Equation 32: Thermal Heat Transfer (Conduction) [167]

$$\dot{Q} = \frac{T_i - T_\infty}{R_{total}}$$

Furthermore, the equations for radiation heat transfer can be seen below.

Equation 33: Absorbed Radiation Equation for Habitat [57]

$$\dot{Q}_{absorbed} = \alpha * A_{proj} * \left(\frac{1}{AU_{mars}}\right)^2 1316 \frac{W}{m^2}$$

Equation 34: Emitted Radiation from Habitat into Space [57]

$$\dot{Q}_{emmitted} = \varepsilon * A_{proj} * \sigma * \left(T_s^4 - T_{space}^4\right)$$

Equation 35: Total Radiation Thermal Transfer Rate

$$\dot{Q}_{radiation} = \dot{Q}_{absorbed} - \dot{Q}_{emmitted}$$

Finally, the heat transfer due to powered systems is found to be the power input of all powered systems assuming all the power gets converted into heat. This is separated into greenhouse and non-greenhouse terms. The following thermal balance can be used to find the active thermal control required to maintain a steady-state temperature within the habitat.

Equation 36: Habitat Steady State Thermal Balance

$$\dot{Q}_{radiation} + \dot{Q}_{poweredSystems} + \dot{Q}_{greenhouse} = \dot{Q}_{ground} + \dot{Q}_{tempGradient} + \dot{Q}_{active}$$

The results can be seen in the following table where all positive values are into the habitat and negative values are out of the habitat.

Table 46: Habitat Thermal Results

Heat Transfer	Description	Magnitude (kW)
$\dot{Q}_{radiation}$	Net Radiation Heat Transfer	+32.54
$\dot{Q}_{poweredSystems}$	Thermal Input Due to Lights and Other Powered Systems	+10.15
$\dot{Q}_{greenhouse}$	Thermal Input Due to Greenhouse	+100.00
$\dot{Q}_{ground}$	Thermal Output to Ground	-127.24
$\dot{Q}_{tempGradient}$	Thermal Output Due to Colder Outside Temperatures	-1.64
$\dot{Q}_{active}$	Active Thermal Control to Maintain Steady State	-13.81

As heat pumps typically have at least 300% efficiency, the power required to maintain this thermal balance is found to be 4.60 kW [168].

6.7 Ascent Operations (Zachary Kessler)

6.7.1 Propellant Storage

For the length of the Martian stay, being a maximum of 3.56 years for any one crew, production of enough propellant for SpaceX Starship to launch from Mars is infeasible. With the needed 198.6 metric tons of propellant to return to LEO from the surface, more than 1 MW of power would be needed to produce and store this fuel in a reasonable timeline of 16 months. This propellant production process would be unlike that used in the science objectives, using electrolysis to form hydrogen and oxygen from water. From these products, as well as gaseous carbon dioxide from the Martian atmosphere, a Sabatier reactor would then be used to create methane. In addition to the high-power costs for the electrolysis and Sabatier reactions, this propellant would then need to be stored at cryogenic temperatures, drastically raising the required power of this propellant production process. This timeline was picked as this would give the astronauts enough time to correct the system of any unexpected errors once arriving on Mars without jeopardizing the launch window from the surface.

Instead of propellant production, the required methane and oxygen will instead be brought from Earth. The crewed missions to Mars will have overfilled propellant tanks with enough capacity to launch from Mars. If needed, resupply missions to Mars can also be used to top up on the propellant if an issue arises with the propellant from a previous mission. Once the propellant arrives on Mars, 31.3 kW of continuous power will be used to keep the propellant below their boiling temperatures, 90.2 K for oxygen and 111.4 K for methane, both at atmospheric pressures of 1.013 bar. Using the convection heat transfer coefficient as calculated for laminar flow, as well as the outer surface area of the propellant tanks, the Convection resistance was calculated using Equation 38. This value was inputted into Equation 37, along with the appropriate temperatures. $T_{propellant}$ is the temperature that the fuel and oxidizer must be kept at to avoid evaporation. $T_{ambient}$ is the average Martian temperature at the proposed landing site. To perform a more accurate analysis, the calculations were run twice each for the fuel and oxidizer, with the average daytime temperature and average nighttime temperature being separated. This analysis gave the rate of heat transfer out of the propellant tanks, which indicated how much heat would need to be added back into the propellant to ensure it always remains a liquid.

As the propellant in the tank boils off, this gaseous propellant will be removed from the storage tanks via hoses. The storage tanks are propellant tanks from pre-supply Starship rockets which will already be on the Martian surface and can be taken apart for a variety of parts. These hoses will be run though a refrigerant, which will condense the gaseous oxygen and methane back into propellant. After condensation, the liquid propellant will be pumped back into the storage tanks containing the remaining liquid propellant. As the propellant will be kept in liquid form, this mitigates the issues of decreasing propellant volume through boil off. This ensures that enough liquid propellant is present at all times to power Starship off the surface of Mars. Having all of the

propellant already liquified will allow for an unexpected launch in case of emergency, where the astronauts are required to evacuate the mission site.

$$\dot{Q}_{conv} = \frac{(T_{propellant} - T_{ambient})}{R_{conv}}$$

Equation 37: Convection Heat Transfer

$$R_{conv} = \frac{1}{h * A_s}$$

Equation 38: Convection Resistance

$$h = Convection\ heat\ transfer\ coefficient,\ A_s = \ Outer\ surface\ area\ of\ tanks$$

6.7.2 Ascent from Martian Surface

As was used as the Martian descent vehicle, SpaceX Starship will be used as the ascent vehicle. For each of the two crews, the ascent propellant is stored in liquid form as discussed in an above section. As calculated from the ideal rocket equation, 174.618 metric tons of propellant will be required to rendezvous with the cycler from the Martian surface. Another 23.982 metric tons will be required to reach LEO from the S1L1. When preparing for launch from the Martian surface, the liquid propellant will be loaded from the cooling tanks into the ascent vehicle. This will be the last process required for ascent from Mars. Once this process is completed and Starship is completely fueled, the astronauts will board into the crew compartment of the ascent vehicle. Once boarded, the astronauts will launch into a low Martian orbit, and from there boost into the path of the inbound S1L1 cycler, rendezvousing with the cycler to return the astronauts back to Earth. Starship will ride the inbound cycler until departing to LEO from the S1L1 cycler. Thus, a total of 198.6 tons of propellant will be required for the entire return journey, as calculated from the ideal rocket equation in appendix 12.3. Due to this and the potential for propellant boiloff during transport, a two times factor will be put onto the propellant needed to bring. Therefore, a total of 400 tons of propellant will be required to be transported to Mars for the ascent of each crew.

6.8 Crew Time (Vishnu Vijay and Zachary Kessler)

The following section will define how the astronauts spend time on the surface of Mars, from personal time to completing science objectives. Table 47 outlines the nominal daily schedule of the crew. It should be noted that the first crew is baselined to follow an Earth-day, with 24 hours of allocated activities. The second crew will follow a Mars sol, with 24.6 hours of allocated activities. The mental health, productivity levels, and sleep quality of each crew can be measured and compared to the other to determine the feasibility of resetting the human circadian rhythm and maintaining a schedule consistent with that of a day on Mars.

Table 47: Daily Crew Schedule

Nominal Daily Activity	Crew 1		Crew 2	
Activity	Weekday (hr/day)	Weekend (hr/day)	Weekday (hr/day)	Weekend (hr/day)
Daily Planning Meetings	0.5	0	0.5	0
Daily Plan Review / Report Preparation	1	0	1	0
Work Preparation	0.5	0	0.5	0
Scheduled Assembly, Systems, and Utilizations	6.5	0.5	6.5	0.5
Meals	3	3	3	3
Housekeeping and Laundry	0	2	0	2
Post Sleep	0.5	0.5	1.1	1.1
Exercise, Hygiene, Setup / Stow	2.5	2.5	2.5	2.5
Recreation	0	6	0	6
Pre-Sleep	1	1	1	1
Sleep	8.5	8.5	8.5	8.5
Total	**24**	**24**	**24.6**	**24.6**

This will be a part of the science objective studying the effect on humans in space. This objective will also require frequent physiological, behavioral, and psychological testing to identify any changes due to a prolonged space mission. These tests will begin once the astronauts first arrive aboard the Cycler and continue until the astronauts arrive back on Earth. Short physical evaluations will take place daily, testing coordination and organ health by completing balance tests, blood pressure tests, heartrate tests and more. Less frequently, the astronauts will complete behavioral and psychological tests, comparing those tests to baselines taken of each astronaut before the start of the mission. These tests collectively will determine how humans react to an extended stay on a planet beyond Earth.

When astronauts land on the surface, the RASSOR rovers would have completed regolith collection, for placement on top of the habitat for radiation protection. This is a part of the first primary objective for the astronauts: setting up the habitat. The remaining regolith will be processed into Martian concrete, using many different formulas. All these samples of concrete will be tested to determine the effectiveness of Martian concrete.

The Space Exploration Vehicles (SEVs), shown inFigure 52: Space Exploration Vehicle delivered in the pre-supply mission will be used to support operations far beyond the habitat. From radiation analysis, astronauts in Crew 1 will be allotted 4560 hours outside of the habitat, while astronauts in Crew 2 will be allotted 5531 hours. As seen in Figure, there are many locations of interest near a potential landing location in Acheron Fossae. The crew will use the SEVs to travel to and investigate these locations of interest. The vehicles are capable of supporting astronauts for up to 14 days, or 336 hours [108].

Figure 52: Space Exploration Vehicle

In the search for water, initial water will be extracted from the collected regolith. This can be accomplished by evaporating the water from the collected regolith. This is a method that will likely come with mixed results, as extracting water from the regolith will be dependent on the ground having moderate water contents, which is assumed but not confirmed at this time. Water will also be collected by astronauts from drilling ice using a Rodriguez Well. This will expand the water collection, as subsurface ice will be turned into water. In addition, many different areas will be tested for regolith water content, as one of the most important objectives of this mission is to determine the water richness of Martian regolith.

The greenhouse, as discussed in an earlier section, will be a designated location within the habitat to grow plants. To sustain healthy plant growth, the crew will need to care for the plants every day.

Searching for life on the Martian surface will be the most dangerous science objective to complete. The potential sites for life will be flagged both by the satellites orbiting Mars and scouting rovers sent out before the humans arrive on the surface. Using the Space Exploration Vehicle, astronauts will travel to these marked locations. This requires long periods of time where the crew is split up, with some crew remaining at the base for daily operations, while the rest of the crew investigates the flagged site. Another part of this objective will be completed in daily activities like regolith extraction, where items with signs of potential life can be found.

The production of 2,3-butanediol will begin once the astronauts arrive and assemble the plant once all other mission critical set up is complete. Using the cyanobacteria and engineered E.coli transported from Earth, the system will run autonomously, with the astronauts only needed to check the system every so often to ensure proper functionality of the propellant. Then, performance tests on the propellant created will occur, having relevant data sent back to Earth. The process will require 0.882 kW of power and 1.047 metric tons of payload to produce 0.5 metric tons of 2,3-butanediol and 3.1705 metric tons of oxygen [109]. This will be more than enough fuel and

oxidizer to test the performance of the fuel, with any excess oxygen created from the process capable of being fed into the life support systems of the astronauts.

7: TELEMETRY, TRACKING, & COMMAND

7.1 Point Design Selection (Nathan Berry)

Through generating a morphological matrix, using first order algorithms, and performing a Pareto Analysis, a basic point design for the mission was created based around three categories. The first category is the frequency band of communication used, the second is the existing communication network to use, and the third is the architecture to be sent to Mars to enable communication.

As combination of frequency bands between Ka-Band and Optical were present in the top three results of the Pareto Analysis, a trade study was performed between the two options. As optical communication systems boast a maximum data rate of 80,000,000 bytes per second and are typically much lighter than typical radio antennas, this form of communication is perfect for the mission as a long-duration human mission requires a large amount of data to be continuously transmitted [110]. However, as optical is a much lower TRL and there is a mission requirement to use Ka-Band for science data return, Ka-Band also has many redeeming qualities. The Ka-Band has a maximum data rate of 3,500,000 bytes per second and has been proven on the Mars Reconnaissance Orbiter [111]. Therefore, it was determined that a dual-band system was the best option as Ka-Band can be used for science data and helps ensure consistent communications while optical communications help boost the data rate and ensure that astronauts can send videos back and forth to both mission control and their families to boost morale and better ensure their safety.

As a dual-band system was implemented, the networks implemented were the combination of the Near Space Network (NSN), Deep Space Network (DSN), and Deep Space Optical Communication (DSOC) capabilities. The NSN is utilized during launch, cycler assembly, and when the cycler enters cislunar space. This is due to the NSN being cheaper and more reliable, 99.3% reliability versus 95%, than the DSN while within cislunar space [112]. The DSN, however, is the most reliable and effective network for deep space radio frequency communications. Additionally, DSOC is NASA's only existing network for optical communications, so it is utilized for all optical transmissions. However, the current DSOC locations only exist in California, USA, so the network will have to be expanded around the globe to always ensure coverage in deep space. Therefore, it is proposed to combine DSOC capabilities with the DSN to create a radio frequency and optical communication network.

Finally, as the existing Mars Relay Network is going to be near or past end-of-life by the mission time, a new set of satellites for the Mars Relay Network will need to be designed and sent to Mars to ensure communications from the surface of Mars to Earth [113].

Considering these results, the following is the resulting point design.

Table 48: Communications Point Design

Communications Point Design			
	Frequency Bands	Communication Network	Mars Architecture
Point Design	Ka-Band + Optical	NSN+DSN/DSOC	New Mars Relay Network

7.2 New Ka-Band/Optical DSN Network (Nathan Berry)

As the mission is operating on both radio frequency and optical communication, the Earth tracking stations must be able to receive and transmit signals in both forms. Currently all Deep Space Optical Communications (DSOC) are downlinked to Palomar Observatory's Hale Telescope in San Diego, California and are uplinked from a transmitter in Wrightwood, California near NASA JPL's Table Mountain facility [1114]. However, for a manned Mars mission, there must be global coverage and one station in California is not sufficient on its own. The DSN has three global stations to enable global coverage and optical communication architecture must follow this design. The DSN has one located in California, U.S.A, one in Madrid, Spain, and one in Canberra, Australia [115]. To adapt to optical communications, the Spain and Australia DSN sites need to add infrastructure like the deep space transmitter that exists at JPL.

Figure 53: JPL Optical Transmitter [116]

Additionally, all sites must add additional novel technology. This technology is a receiving antenna that receives signals for both optical and radio frequency communications. These new hybrid optical-radio frequency antennas would allow for a dedicated antenna for the Mars mission and enable constant communication instead of having to compete with other missions for communication time. NASA's JPL is currently developing this technology and has demonstrated it in small scale tests and plans on developing these 34-m hybrid antennas primarily for Mars missions [117]. This TRL 5 technology is an optimal novel technology for the mission as it is necessary to remain in constant contact with the astronauts while also not adding any additional critical fail points to the mission.

Figure 54: JPL Hybrid Optical/Radio Antenna [118]

This antenna allows for a simplified form of receiving both kinds of signals from Mars and allows for complete, dedicated coverage for the mission. Furthermore, it utilizes existing DSN locations to save cost and maintain worldwide coverage.

7.3 Data Volume & Rates (Andrew Darmody)

Quantifying the rate of data transfer and total data volume of a mission is an important, although tricky, evaluation. With the risks of a crewed mission to Mars being so high, and also due to the fact that astronauts are to be away from their loved ones for multiple years, it is essential that the communication network connecting Mars and the Earth can enable the exchange of information at a high quality very quickly. With the newer development of Ka-band and DSOC technology, the mission to Mars boasts a data rate of 3.5 MBps – 80 MBps (Ka-band and DSOC, respectively). Although it is not possible at this stage of the design of the mission to quantify the amount and type of data that will be sent from all the scientific and robotic equipment on the surface of Mars, a preliminary study can be done from the crew-wellbeing perspective. If each of the four astronauts are to send a video message to the Earth every day at 1080p resolution and at 30 frames per second, the total data volume transmitted is roughly 1.2 GB per day. The same is true for the astronauts' loved ones sending video messages from Earth to Mars. In this mission design, astronauts will either be in transit to or from Mars or on the surface of Mars for 3,164 days, meaning that the total data volume for crew-wellbeing alone is 3,800 GB.

7.4 Satellite Constellation (Andrew Darmody)

The key driving factor of the design of the communications network for the mission is the idea of 100% communication availability. Although having the ability to communicate between Earth and Mars for every single second of a long-duration mission is realistically unfeasible, steps were taken in this design to ensure the maximum possible communication availability. The three main issues that arise in this goal are when the Mars ground base does not have direct line of sight to the Earth, the complications that arise from the loss of a communications satellite in Martian orbit, and the existence of Earth-Sun-Mars conjunction. The first two issues can be mitigated by the satellite constellation around Mars, and the third will be addressed in a future section.

It was determined that the constellation will consist of four identical satellites equally spaced and placed in a circular orbit of altitude 3,500 km, inclined to the Martian ground base. This configuration ensures that at nearly all times a minimum of one satellite is in view of the ground base. When the ground base (and hence the satellite(s) in view of the ground base) do not have a direct line of sight to the Earth, a signal can be relayed to other satellites that can see the Earth. In the case of the complete loss of a satellite, the mission will see a communication blackout of around 4 hours per sol, although not all at once. The most straightforward way to avert this blackout is for two of the three remaining satellites to perform a phasing maneuver to reestablish equidistant positioning in orbit, illustrated below.

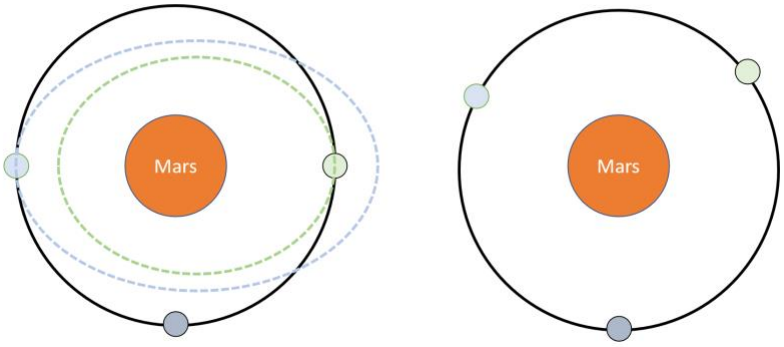

Figure 55: Phasing Maneuver In Case of Satellite Loss

Each satellite will support Ka-band, Deep Space Optical Communications (DSOC), and Ultra-High Frequency (UHF) communication. This will be accomplished with a 3m radio antenna, a DSOC transceiver similar to the one on the Psyche mission launching in October 2023, and a UHF antenna as seen on missions like the Curiosity rover. This communication equipment boasts a data rate of around 80 million bytes per second and includes many redundancies in case of an antenna failure. Such a high rate of data transmission was deemed necessary to support crew wellbeing via high-quality video and audio messages to and from family and loved ones.

7.4.1 Satellite Operational Modes (Vishnu Vijay)

Each satellite of the constellation will operate with the following modes:

Table 49: Satellite Operational Modes

MODE	Explanation
Acquisition	System initialization after launch or on system reset
Orbital Insertion	Large ΔV maneuver to enter the ballistic cycler trajectory
Nominal Communications	Act as relay to communicate with Earth
Nominal Science	Measures Mars weather conditions when not in com mode
Conjunction Communications	Find and use cycler as relay to communicate with Earth
Slew	Reorienting system when required
Safe	Lower power usage in case of fault detection

The modes in Table 49 were inspired by the SMAD, with small additions to account for the constellation's mission. The inclusion of two nominal modes is one such addition. A satellite will be in the *nominal communications* mode if it is being used as a relay for communications from the Mars surface to Earth. The *nominal science* mode is reserved for the satellites not currently being used as a relay, but the science instruments are still run for data collection. The *conjunction*

communications mode is activated when Mars and Earth are in solar conjunction, and thus the nominal relay communication system is not sufficient. In this case, the satellites use the cycler vehicle(s) as a relay for data transmission to Earth.

7.5 Mass and Power Budget (Andrew Darmody)

A preliminary mass and power budget was created for the four communication satellites around Mars by using the Mars Reconnaissance Orbiter (MRO) as a baseline. The reported mass and power of the MRO were taken, and MRO science instruments and subsystems not necessary to the new communications satellites were removed, and hence their masses and power requirements were subtracted from the totals of the MRO. The PMIRR instrument's mass and power requirements were then added. Additionally, a new ADCS had to be sized to account for the more strict pointing requirements of the DSOC system [119], detailed below. It is important to note that the addition of this new ADCS system increased the total power draw of the new communication satellites beyond the 1 kW capabilities of the MRO (and hence the new satellites). This was deemed acceptable, as the new satellites will never be using all its systems at one time. If future work requires that the power system to be sized to support all systems being used all at once, the solar panels of the new satellites can be increased. This process overall ensures that the majority of the mass and power requirements are shared between the MRO and the new communication satellites, and the PMIRR instrument could be added. The resultant mass and power values were determined:

Table 50: Mass and Power for New Communication Satellites [120, 119]

Feature	Purpose	Mass (kg)	Power (W)
3m antenna dish	Ka-band	19.1	216
DSOC transceiver	DSOC	29	76
Pressure Modulated Infrared Radiometer	Atmospheric studies	40.2	34.1
Total (with fuel and all systems)		1,993	1,216.1
Total (4 satellites)		7,972	

7.5.1 New ADCS System (Vishnu Vijay)

Keeping the attitude determination and control system from the Mars Reconnaissance Orbiter for the modified-MRO communication satellites was deemed illogical. The old systems were designed to support the pointing accuracy of the MRO's HGA and LGAs. With the addition of an optical communication system, a significantly more robust and accurate ADCS system is required to handle the increase in pointing accuracy from 2.08 milliradians [121] to 3.36 microradians [119].

The new ADCS system for the MRO-based communication satellites will be based on the attitude determination and control system used on the Psyche mission that tested Deep-Space Optical Communications. The attitude determination equipment includes 2 Jena-Optronik star tracker sensors [43], 2 Honeywell Miniature Inertial Reference Units (MIMUs) [44], and 8 Adcole coarse sun sensors [45]. The number of each instrument was selected with redundancy in mind to mitigate any risks arising from sensor failures. The attitude control system will use four Honeywell HR 16-100 reaction wheel assemblies (RWA) [122] to support 3-axis stabilization of the system. The attitude control thrusters from the MRO will be maintained for RWA momentum unloading and large attitude reorientations [123].

The power and mass of each individual instrument listed above can be found in the table below:

Table 51: Mass and Power for New Communication Satellites ADCS

Instrument	Mass (kg)	Power (W)
Star Tracker	2	5
Inertial Measurement Unit	4.6	25
Coarse Sun Sensor	0.13	~0
Reaction Wheel Assembly	12	195

7.5.2 Preliminary Sizing for New Satellite Solar Panels (Nathan Berry)

As the power required for the improved satellite surpasses the reference vehicle's capabilities, the solar panels were re-sized using simple scaling techniques. As the MRO's 20 m^2 solar panels delivered 1 kW of power, it was determined to meet the 1.216 kW requirement, plus a 30% margin, on the new satellite system, the solar panels would increase in area to 31.62 m^2 [124]. This scaling's purpose was not to create a definite final design, but instead create an introductory value for this architecture as a beginning to satellite sizing iterations in future work.

7.6 Antenna Sizing and Link Budget Results (Nathan Berry)

There were many considerations that were considered while sizing the antennas and satellites mentioned in the above subsections. The analysis was mostly completed through completing a radio frequency link budget under severe, worst-case conditions. These conditions include the maximum separation distance between Earth and Mars, dust storms on Mars, and rain on Earth. The first step of the analysis was to determine an appropriate uplink and downlink signal-to-noise ratio, Eb/No, and bit error rate (BER) for the telemetry system to meet the required link margin. The design was set to have a BER of 10^{-7} which, using quadrature phase shift keying (QPSK) phase modulation, it requires an Eb/No of 11.2 dB [125]. The summary of these values and NASA DSN requirements are provided in the table below.

Table 52: Telemetry Link Budget Goals/Requirements [126]

NASA DSN Eb/No Requirement	3 dB
NASA DSN Eb/No Required Link Margin	3 dB
Eb/No to hit Target BER	11.2 dB
Target Bit Error Rate (BER)	10^{-7}

Utilizing the target Eb/No and the end-to-end Eb/No equation presented in Equation 48 within the appendix, the target uplink and downlink Eb/No values were computed to be 37.58 dB and 11.21 dB, respectively.

Utilizing the above uplink requirement, the Mars ground antenna was sized. This was completed by selecting three possible antennas and iterating the power required to meet the uplink requirement [127, 128, 129]. The result is shown below.

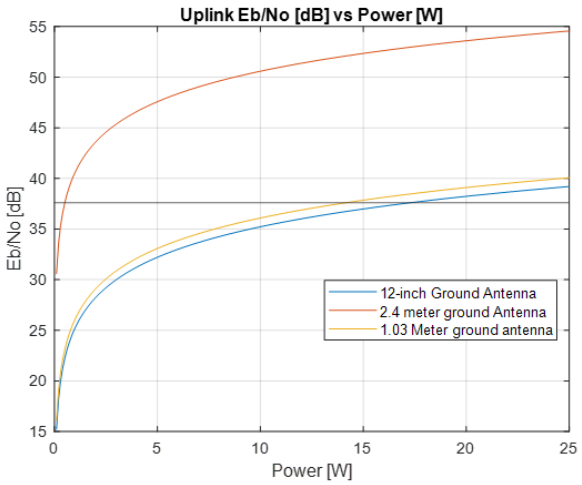

Figure 56: Mars Antenna Sizing

As all antennas require minimal power, the lightest antenna was chosen. This is the 12” ground antenna which requires 17.3 Watts to maintain the target uplink Eb/No. The 12” ground antenna that was chosen is manufactured by Smiths Interconnect and has full 360-degree rotation capabilities to track the satellites in the sky. Furthermore, it weighs 12 kg and is shown in the figure below [127]

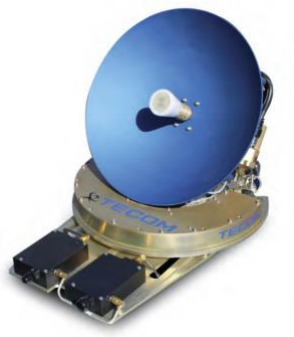

Figure 57: 12" Antenna for Mars Ground Base [127]

The third consideration was determining the power required for the satellites to meet the downlink Eb/No. The plot for the worst-case and average scenario is shown below.

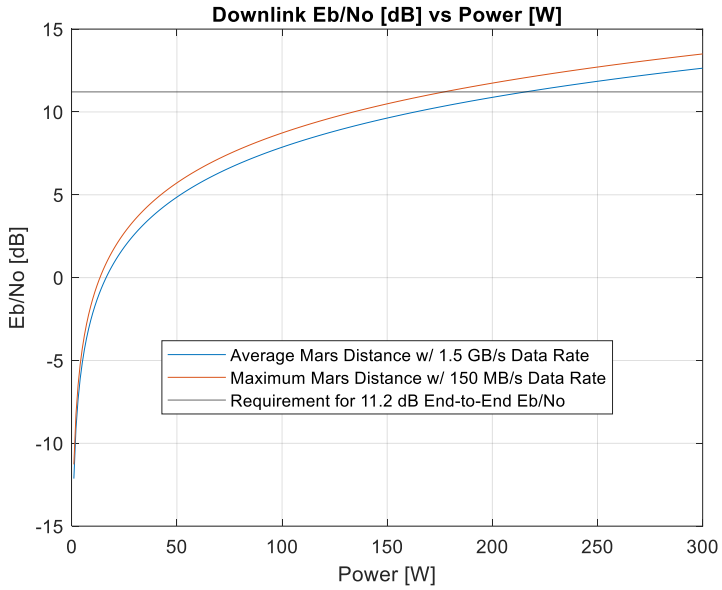

Figure 58: Downlink Link Budget Plot

The sizing shows that there is a requirement of 216 Watts of power input in worst case scenario and 177 Watts on average. The full tables for this analysis can be found in Appendix section 11.1.

7.7 Satellite Deployment Strategy (Andrew Darmody, Chris Manilla)

As a part of the satellite pre-pre-supply mission, the new communication constellation will be inserted into Martian orbit. This will be a dedicated mission to the deployment of this system using a Starship launch vehicle that will return to Earth once the satellites have been deployed. This mission must support the transfer of the satellite constellation from Earth to a Martian orbit inclined to 75°. The delta-V breakdown of that mission is as follows:

Table 53: Delta V Budget for Pre-Pre-Supply Mission

Mission Leg	ΔV (km/s)
Earth Surface – LEO	9.4
LEO – Mars Transfer Orbit	4.3
Mars Transfer Orbit – Mars Capture Orbit	0.9
Mars Capture Orbit – Final Inclined Orbit	2.11

7.8 Conjunction Mitigation Strategy (Andrew Darmody)

The existence of the conjunction of the Earth, the Sun, and Mars (henceforth referred to as "conjunction") poses a challenge to consistent communication between Earth and astronauts on Mars. While direct communication through the Sun is technically possible [193], the rate of data transmission is not sufficient for the needs of a human mission to Mars. The table below depicts the communication blackout that is present between Earth and Mars (of particular note is the outages for Ka-band and Optical communication). It is worth noting that the table shows the effects of conjunction outages that are mostly before the timeline of the mission in this design; the table is only presented to generally show the severity and frequency of conjunction events.

Table 54: Communication Outage Schedule [193]

Date	Optical Outage (days)	X-band Outage (days)	Ka-band Outage (days)
5/25/2030	78.1	23.5	7.7
7/11/2032	66.4	19.0	1.5
8/19/2034	60.9	17.1	0.0
9/23/2036	59.8	17.3	3.1
11/1/2038	63.3	19.0	6.3
12/17/2040	74.0	21.7	5.7

With the reliance on optical communication for crew wellbeing, it was determined that a contingency plan was necessary for always maintaining communication between the Earth and Mars. Again, it is acknowledged that 100% communication availability is realistically not achievable, but the blackout caused by conjunction was deemed too lengthy for this mission.

Many options were considered for avoiding conjunction, with the most notable being the use of Sun-Earth or Sun-Mars Lagrange points and placing an additional satellite in a heliocentric orbit equivalent to Mars but phased ahead or behind Mars. After these options had been considered, it was realized that the Cycler vehicles used to transport crew to and from Mars can be used as a relay during conjunction.

The motivating factors for choosing the Cycler spacecraft for this task was their need for communication technology regardless of their use as a communications relay, and that during every conjunction event during the mission's duration, at least one of the two cycler vehicles will be in a position in their orbit where the spacecraft sees both Earth and Mars clearly. This makes the use of the cycler spacecraft the optimal choice for mitigating the effects of conjunction.

7.9 Satellite Orbit Tracking (Chris Manilla)

The constellation orbit is defined as a circular orbit with semi-major axis of 6890 km and inclination of 75°. The four orbiters are spaced equidistant from one another along the orbit, as seen in Figure 59. The ground tracks in Figure 60 show the location of the sub-satellite point for each of the four orbiters over an average day during mission operations. Figure 61 is a plot showing the times at which each satellite is within line of sight of the ground station at Acheron Fossae. There are two points during a given day of about 15 minutes each where line of sight between the ground station and all four orbiters are broken.

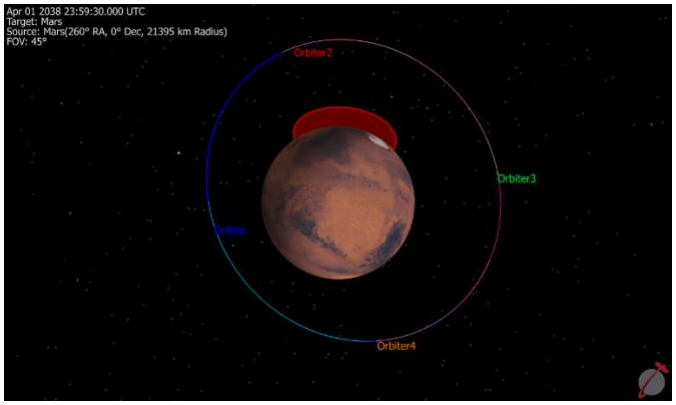

Figure 59: Orbital View of Communications Constellation

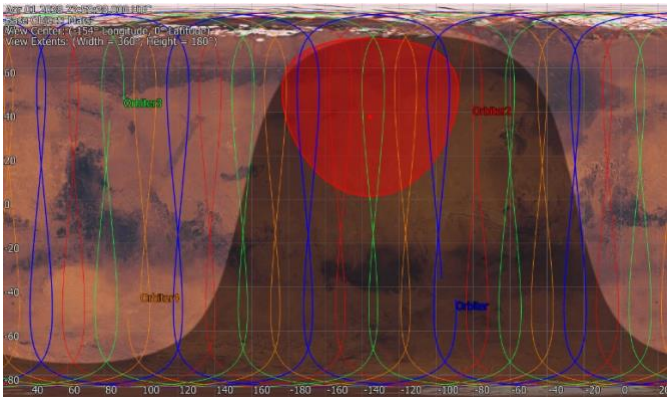

Figure 60: Ground Tracks for Communications Constellation

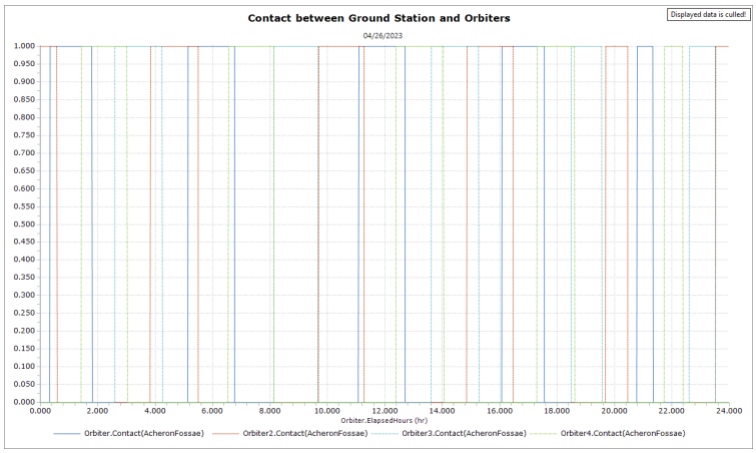

Figure 61: Contact between Ground Station and Orbiter over One Day

7.10 EVA Communication (Andrew Darmody)

During Extravehicular Activities (EVAs), it is critical for astronauts to communicate with each other and with the ground base. While current astronauts use a "snoopy cap" head piece for International Space Station EVAs, the new spacesuit produced by Axiom Space boasts a new design aimed to improve the sound quality of Artemis astronauts. The Axiom Space suit will likely be chosen for a mission to Mars and hence, their communication system will be used. Although little is known about the next generation of spacesuit, it can be inferred that an Ultra-High Frequency system will be used as a sort of space "walkie-talkie." Each astronaut's suit will be equipped with the technology to communicate directly to another astronaut in case an EVA requires the astronauts to venture past the line of sight of the ground base. However, during nominal operations, it can be assumed that EVAs will take place in a range where the UHF system can keep all astronauts and the ground base in the same communications loop.

7.11 Mission Control (Nathan Berry)

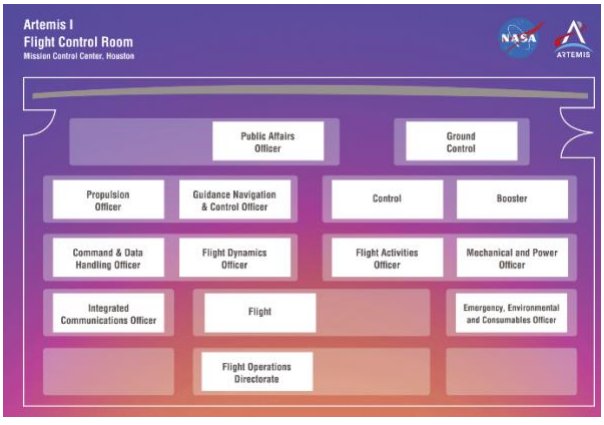

Figure 62: Mission Control Layout [172]

Additionally, the command centers for the mission were chosen. As mission control has been based at NASA's Johnson Space Center for the Apollo and Artemis missions, the same location was deemed to be optimal for the Mars architecture [172]. The mission control would have the same mission control layout for all stages of the mission as the Artemis 1 mission with several engineering support teams in Mission Evaluation rooms 24/7 to provide technical support to the astronauts if needed [172].

8: Cost Estimation (Ryan Horvath)

To begin the process of calculating the final cost estimate for the manned mission to Mars, a Work Breakdown Structure or WBS was drafted. The following is the result:

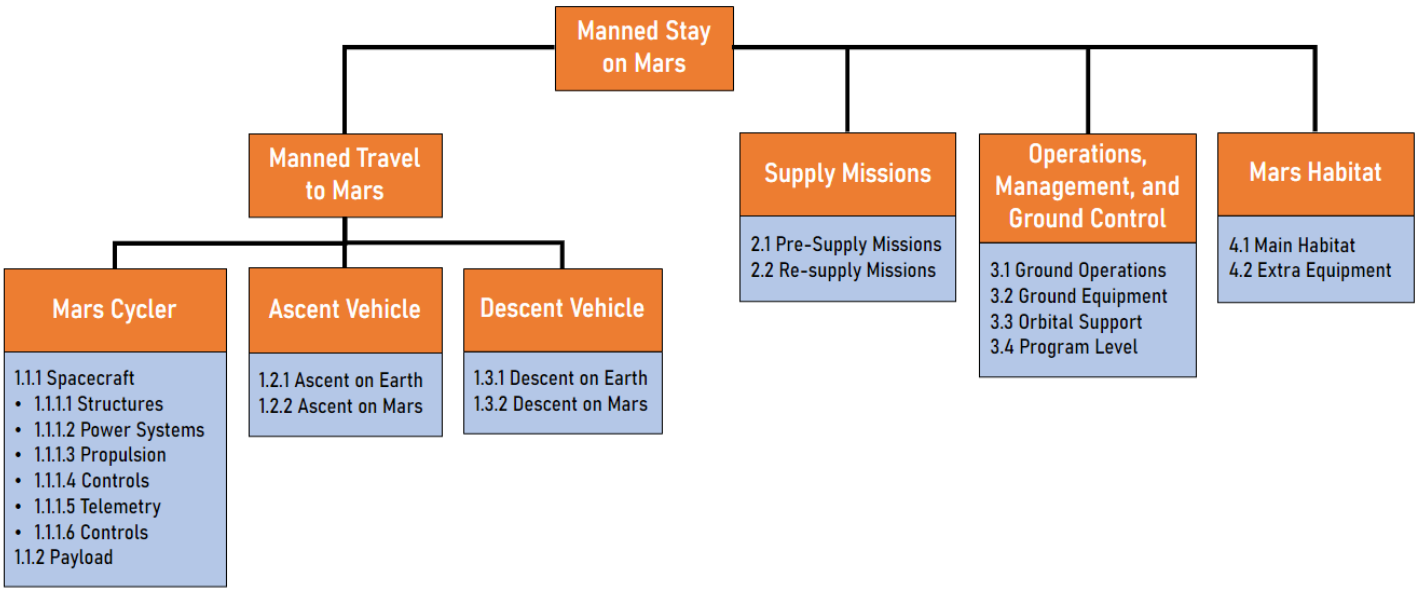

Figure 63: Work Breakdown Structure

To begin the process of calculating the final cost estimate for the manned mission to Mars, a Work Breakdown Structure or WBS was drafted. The following is the result:

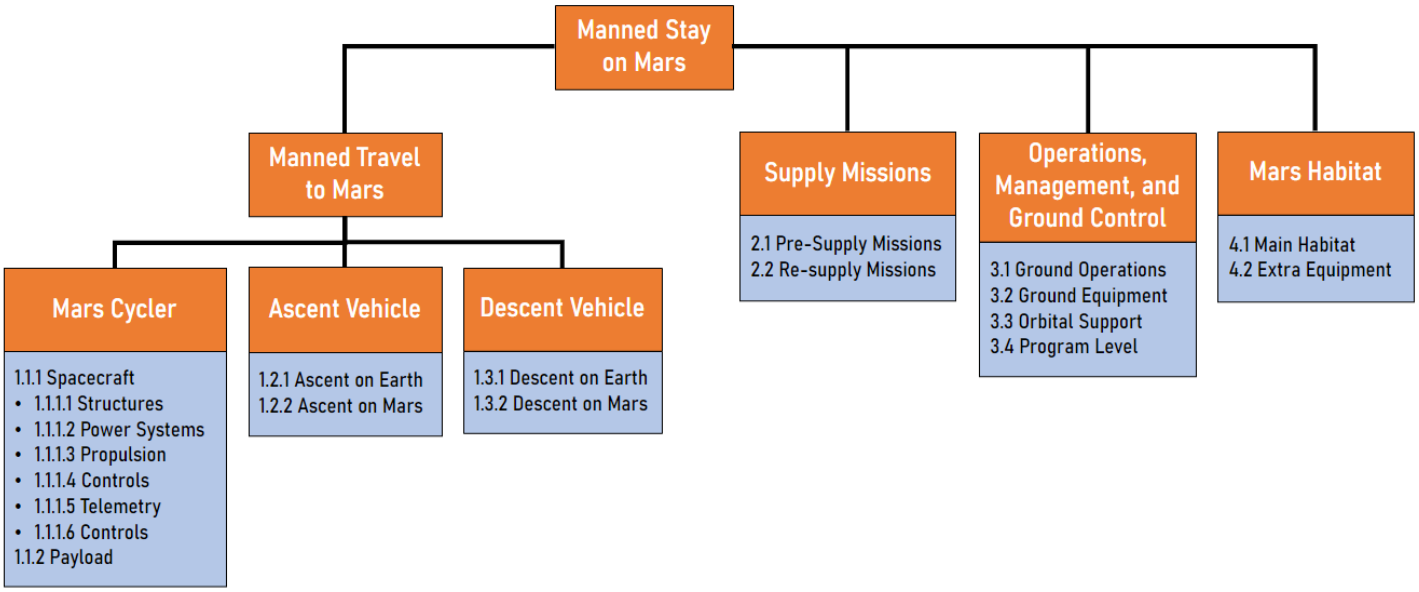

Figure 63 has the budget was broken down into the four following main categories being the manned travel to Mars, the Mars habitat, the supply missions, and the Mars Habitats.

There were various methods used to calculate the final cost for the project, starting with that of the Mars Cycler. For the cost of the Mars Cycler, the Advanced Missions Cost Model developed by Johnson Space Center and written about in more depth in [130]. This is a model based upon over 260 previous programs to get a cost estimation relationship (CER).

The resulting equation for the Advanced Missions Cost Model ends up being the following:

$$\text{Cost} = \alpha Q^{\beta} M^{\Xi} \delta^{S} \varepsilon^{\left[\frac{1}{IOC-1900}\right]} B^{\varphi} \gamma^{D}$$

The variables and constants in this equation are the following and are gained from [130]:

Table 55: Advanced Missions Cost Model Constants

Constant:	Definition:
α	$5.56 * 10^{-4}$
β	0.5941
Ξ	0.6604
δ	80.599
ε	$3.8085 * 10^{-55}$
φ	-0.3553
γ	1.5691

Table 56: Advanced Missions Cost Model Variables

Variable:	Meaning:
Q	Quantity
M	Dry Mass (lbs)
S	Specification
IOC	Initial Operating Capacity
B	Block Number
D	Definition

There were 6 main variables to consider for the model being quantity, mass, specification, initial operating capacity (IOC), block number, and difficulty. Quantity is the number of units being produced. Mass is the dry mass of the system in pounds. Specification is a constant that varies dependent on the mission, for example a human habitat like a cycler has a value of 2.13. IOC is the year at which operation would begin. Block number is design inheritance, with 1 being a completely new design. Difficulty is a subjective opinion on how difficult the system might be. To decrease the subjectivity and base it off previous missions, the team used example mission calculations for space stations done in this cost model. All other values were based on quantities determined earlier within this report for the Cycler. The same method of calculation and quantity

gathering was used for the Mars Habitat. This cost given will account for all cycler development, integration, testing, and subsystems in the Cycler.

The ascent, descent, and supply missions had a similar calculation for how much it would cost, and it was based around how many expendable and reusable starships that are going to be used during the mission. An expendable starship is one that will likely not be reused during the mission, so considerations of how much a starship will cost is the following: referring to Elon's interview with CNN [131], the cost of development for each individual starship should be between $2 billion and $10 billion but should be on the lower end of that range. This isn't a precise estimate so to be safest with the cost estimate, the average value will be used making each expendable starship cost $6 billion but error will always be considered since this was a vague source. Next for the reusable starship, according to another quote of Elon's [132], each reusable starship launch should be about $2 million. So, taking account for all expendable and reusable starships that will be used throughout the duration for the mission, the total cost for starship will be determined.

Moving onto the payloads for all supply missions. This calculation once again relies on the testimony of how much carrying a kg of payload would cost on a starship. According to [133], the cost per kg for starship will be about $10. Through the collection of the weight for each supply part of each mission and then multiplying the total by the estimation provided results in the final payload amount.

Ground equipment, ground operations, program level and orbital support are part of the various costs used to support and secure a successful mission. For ground equipment, program level, and orbital support CERs used from the SMAD resulted in the cost estimations for those individual sections [46]. Ground operations on the other hand relied had its estimate reliant on comparison to previous operational costs for other missions. Referring to NASA report [134], the amount of money spent on the ISS per year, which is the most comparable past mission that can be used here, is about $3 billion. Using that as a reference for the entire operating capacity time in the mission provides the final operational costs.

Returning to payload costs there are various tools that are necessary to budget for throughout the mission. These mainly include the tools necessary to succeed in the science objectives. The estimate would normally just be adding together the cost of all necessary tools to complete the science objectives, but there is one issue that comes. The issue being that not every tool needed does not have a provided price due to it not being currently available. So instead, a budget for all necessary science equipment needed in the mission was made instead. The budget was decided upon by taking the budget used by the ISS initially and adding onto the total of science equipment that has available costs.

Now using these methods of calculation, the following results were obtained for the cost estimation all done in fiscal year (FY) 2023 since that is the most accurate data that can be calculated for the budget currently:

Table 57: Cost Estimation Breakdown

Element:	Cost (in FY 2023 billions):
Mars Cycler:	$236.61 B
Martian Habitat:	$95.23 B
Starships:	$108.02 B
Payload:	$0.05 B
Science and Research Funds:	$10.34 B
Operations:	$21 B
Program Level:	$57.27 B
Ground and Orbital Support:	$31.76 B
Total:	$555.48 B

Now using this, a probabilistic model of the cost estimation can be made. For this simple probabilistic calculation an error of 0.3 was used. This means the standard error would be $172.11 B. With this value and the total, various percentiles for the cost estimation can be made. These are made under the assumption that the distribution will be normalized. Calculations were made specifically for the 70^{th} percentile which will be most likely where the budget will result where z = 0.524 and for the 95^{th} percentile which will be the upper limit of the project budget where z = 1.645. The percentiles were then calculated by multiplying the error times the z value and adding it to the current total. With all this information the following results for cost are gained:

Table 58: Probabilistic Cost Estimate

Element:	Amount (in FY 2023 billions):
Total:	$555.48 B
Error:	$166.64 B
70^{th} Percentile Cost Estimate:	$642.80 B
95^{th} Percentile Cost Estimate:	$829.60 B

These totals are justifiable and worthwhile for devoting funds into for a few reasons. The initial total is similar in cost to a combination of the ISS initial development cost and the Apollo Program cost adjusted to FY 2023. Since the ISS is the closest currently existing structure to the cycler and the Apollo Program was the first manned program to land humans on the moon, these are the most comparable missions to what is being achieved here. Each are both ~250 B, and the extra costs for the mission in comparison are explainable due to Mars being much further away than the moon. This is also an incredibly worthwhile investment since the Mars Cycler will be able to be used in future missions and so will the Martian Habitat, which can heavily reduce costs for any future mission onto the Martian surface.

9: RISKS AND MITIGATION (LUKE HARPRING)

The guiding philosophy of managing risk for the mission is the prioritization of crew health and wellbeing above all else. Crewed spaceflight requires considering human lives as precious and being prepared to sacrifice all mission objectives and obtainable resources to protect the safety of the crew. The safest option is always to not conduct the mission altogether, which of course is not being done. Deciding to embark on a mission of the magnitude and novelty of Martian habitation requires accepting that some level of risk inherent to the endeavor. Therefore, the established NASA risk method of ALARA (As Low as Reasonably Achievable) [135]. For the mission profile needed to meet mission requirements, risk was not capped by a specific numerical success rate, but rather minimized via the ALARA principle and reported at the conclusion of risk analysis, along with recommendations and conclusions for further analysis during future phases of mission design.

In many places, numerical values for risk analysis were unavailable for a multitude of reasons. Novel technologies have limited published literature arrow scopes that do not align directly with this mission's applications. Whenever possible, numerical values were sought after and evaluated. When valid numerical values were either not present or required analysis beyond the scope of this phase of mission design, best efforts were made regarding engineering judgement in determining risk scale placement. NASA standards for likelihood and consequence served as the basis for risk determination. Risks were accordingly managed via avoidance of single points of failure (SPOF), implementing mitigation strategies when SPOFs were unavailable, and determining contingencies for all mission failure modes in which feasible to do so.

To quantify likelihood, the NASA Goddard Space Flight Center (GSFC) standard likelihood matrix was adopted, seen in the figure below [136]. This standard considers three risk types on independent scales: safety, technical, and cost schedule. Safety risks are rightfully the most conservative, followed by technical risks, and finally cost schedule risks are the most lenient in terms of likelihood.

Likelihood	**Safety** Estimated likelihood of Safety event occurrence	**Technical** Estimated likelihood of not meeting performance requirements	**Cost Schedule** Estimated likelihood of not meeting cost or schedule commitment
5 Very High	$(P_{SE} > 10^{-1})$	$(P_T > 50\%)$	$(P_{CS} > 75\%)$
4 High	$(10^{-2} < P_{SE} \leq 10^{-1})$	$(25\% < P_T \leq 50\%)$	$(50\% < P_{CS} \leq 75\%)$
3 Moderate	$(10^{-3} < P_{SE} \leq 10^{-2})$	$(15\% < P_T \leq 25\%)$	$(25\% < P_{CS} \leq 50\%)$
2 Low	$(10^{-5} < P_{SE} \leq 10^{-3})$	$(2\% < P_T \leq 15\%)$	$(10\% < P_{CS} \leq 25\%)$
1 Very Low	$(10^{-6} < P_{SE} \leq 10^{-5})$	$(0.1\% < P_T \leq 2\%)$	$(2\% < P_{CS} \leq 10\%)$

Figure 64: GSFC Likelihood Standards [136]

Consequence scale was similarly borrowed from the GSFC standard risk methodology (Figure 65), which uses a five-point scale with varying qualitative statements describing the consequences constituting each value for safety, technical, schedule, and cost risks independently.

Consequence Categories					
Risk	**1 Very Low**	**2 Low**	**3 Moderate**	**4 High**	**5 Very High**
Safety	Negligible or not impact	Could cause the need for only minor first aid treatment	May cause minor injury or occupational illness or minor property damage	May cause severe injury or occupational illness or major property damage.	May cause death or permanently disabling injury or destruction of property.
Technical	No impact to full mission success criteria	Minor impact to full mission success criteria	Moderate impact to full mission success criteria. Minimum mission success criteria is achievable with margin	Major impact to full mission success criteria. Minimum mission success criteria is achievable	Minimum mission success criteria is not achievable
Schedule	Negligible or no schedule impact	Minor impact to schedule milestones; accommodates within reserves; no impact to critical path	Impact to schedule milestones; accommodates within reserves; moderate impact to critical path	Major impact to schedule milestones; major impact to critical path	Cannot meet schedule and program milestones
Cost	<2% increase over allocated and negligible impact on reserve	Between 2% and 5% increase over allocated and can handle with reserve	Between 5% and 7% increase over allocated and cannot handle with reserve	Between 7% and 10% increase over allocated, and/or exceeds proper reserves	>10% increase over allocated, and/or can't handle with reserves

HIGH RISK
MODERATE RISK
LOW RISK

Figure 65: GSFC Consequence Standards [136]

These likelihood and consequence scores are applied to a risk score standard, which was again taken from NASA risk management documentation shown in the figure above. Risk score is a useful tool for identifying relative criticality but has limitations. Risk matrices, for example, cannot deal with aggregate risks, coupling between failure modes, or uncertainties [137]. Regardless, risk matrices are a valuable tool, especially at the high-level of this system architecture risk assessment.

NASA Baseline Risk Score						
Likelihood	5	7	16	20	23	25
	4	6	13	18	22	24
	3	4	10	15	19	21
	2	2	8	11	14	17
	1	1	3	5	9	12
		1	2	3	4	5
		Consequence				

Figure 66: NASA Baseline Risk Score Matrix [138]

9.1 Mission Segments

It is useful to consider the mission risk as composed of two distinct segments. The first segment encompasses phases of the mission composed of the launch, maneuver, cruise, and atmospheric entry of spacecraft to transport crew and resources. This segment of risk is referred to as "spaceflight risk". The complement of spaceflight risk is risk associated with activities conducted on the Martian surface, such as in-situ resource utilization, habitat construction and sustainment, science objective completion, as well as all day-to-day activities that are conducted on Mars. This risk segment is referred to as "surface risk".

9.2 Spaceflight Risk

The spaceflight risk analysis began informally during the FOA phase of the mission design. During the brainstorming phase, the idea of risk arose naturally when considering mission elements such as the launch vehicle, propulsion system type, inclusion of artificial gravity modules, etc. Reliability was weighed heavily in the FOA algorithm, justified by the fact that the system is to be used for crewed missions. As the point solution began to take hold, the need for a formal risk assessment became clear.

The first step to assessing risk was a group-wide Failure Modes and Effects Analysis (FMEA). This phase occurred in a brainstorming phase with supplemental literature review to consider as many possible failure modes as reasonably practicable. From this list, those with

9.2.1 Risk Assessment and Mitigation Strategies

Table 59: Spaceflight Failure Modes

Potential Failure Mode	Consequence	Likelihood	ID	Risk Score (NASA Baseline)
Structural Failure of Artificial Gravity Module	4	1	1	**9**
Module Joint Failure	4	1	8	**9**
Missed Mars Return Window	3	2	4	**11**
Missed Mars Return Rendezvous	4	2	5	**12**
Missed Earth Departure Rendezvous	4	2	6	**12**
Attitude Control Failure (Tumbling)	4	1	7	**12**
Life Support System Failure	5	1	9	**12**
Power Generation Failure	5	1	10	**12**
Acute/Chronic Radiation Exposure	4	2	2	**14**
Missed Entry Window	3	1	3	**14**

Cycler Risk Matrix						
Likelihood	5					
	4					
	3					
	2			[4]	[2,3,5,6]	
	1				[1,7,8]	[9,10]
		1	2	3	4	5
		Consequence				

Figure 67: Cycler Risk Matrix

[ID-01] Firstly, considering the structural integrity of the cycler vehicle, the Artificial Gravity Module (AGM) poses a structural challenge from a design standpoint. The potential for a structural failure of the AGM spindles or hub must be considered. During the next stages, the system will be physically allocated at the component level and through analysis and testing, designed with industry standard safety margins in place. In addition, testing in LEO prior to deployment on the cycler trajectory with crew will ensure that the structure poses minimal risk to the crew. This risk is therefore given a likelihood score of 1. In the fringe case that such an anomaly was to occur, severe injury could arise. Crew could be thrown about the AGM if a spindle were to fail, with the worst case being a pod disconnecting mechanically from the cycler altogether. A failure could also be milder, however, simply requiring the AGM to be spun down and leaving the crew without artificial gravity. Taking a weighted average of these cases by a preliminary assumption of their plausibility, the consequence score is taken to be a 4, with the possibility of serious bodily harm to crew.

[ID-08] Structural failures within the cycler vehicle also include a module joint failure. This could include fasteners mechanically failing, resulting in deformation or complete separation of a portion of the vehicle. In such an event, pressurization could be lost, crew could be stranded in an isolated portion of the vehicle, and the ability of the vehicle to maintain course could be compromised. Considering such effects, a risk consequence of 4 is assigned due to the potential for serious bodily harm to crew and potentially putting the vehicle on an irrecoverable course if ACS or propulsion equipment were disabled during such an event. However, much like the case of AGM structural failure, the likelihood is deemed low (1) due to large safety factor on structural systems as well as the planned testing in LEO. In addition, the system will not have significant aging or weathering which might accelerate wear.

[ID-04] Missing a Mars return window describes the case of not having the capability for the crew to depart the Martian surface and enter an orbit to approach a rendezvous with the cycler. Such a scenario would arise primarily from a failure within the ascent vehicle (Starship). The ascent vehicle viability is challenged by a long sedentary period on the Martian surface in which lubricants may degrade, regolith particles could enter sensitive components, and weathering effects

could damage the airframe and shielding. Because the mechanical properties of Martian regolith are an area of active research, not a lot is known about what effects the Martian weather could have on the Starship configuration that is ultimately used for the mission. Based on the fineness and abrasiveness of lunar regolith as a surrogate, the effects could prevent the viability of the vehicle if not mitigated. This risk is assigned a consequence of 3 and a likelihood of 2, given the expected crew health risk of missing a return window and remaining on Mars under reduced workload awaiting the next cycler opportunity.

Because this risk is not a well understood phenomenon, it is wise to baseline regular mechanical maintenance and monitoring of the ascent vehicle during crew stay. Engine coverings will be utilized to prevent the entry of foreign objects and debris, and full vehicle covering will be available if weathering is detected during early checks in the crew stay. Prior to crew departure, a more thorough mechanical check-up of the vehicle will be conducted, in which critical fluids will be inspected and/or replaced, with the final list of actions to be determined in collaboration with the contractor of the vehicle. If the mitigation strategies still prove ineffective and a crew return window is missed, the contingency planned is for the crew to remain in the well-protected surface habitat where adequate supplies will be kept on hand to last at minimum until the worst-case emergency direct-transfer resupply mission can arrive. Non-critical crew EVA time can be eliminated to minimize the additional radiation dosage, and a replacement ascent vehicle can be sent from earth.

[ID-05, ID-06] Performing a Mars return rendezvous or an Earth departure rendezvous with a cycler both require the crew vehicle to perform a rendezvous along a hyperbolic trajectory from their launching body, which may initially seem a high-risk maneuver given the consequences of a failure during such a stage of flight. While certainly one of the main aspects of concern the Earth-Mars cycler selection, an analysis conducted by Damon F. Landau and James M. Longuski in 2006 demonstrates not only the feasibility of such a maneuver with existing technologies at the time of publication but estimate that such a maneuver is around 99% reliable [139].

Monte Carlo simulation of Gaussian distributions of thrust errors and navigation uncertainties calculated the taxi encounter locations assuming a 10 cm diameter target and 7 cm/s approach speed [139]. Redundancies in this maneuver include the ability to abort an approach when additional propellant is brought aboard the ascent vehicle, and the ability to make multiple passes for rendezvous attempts (Table 60). The cycler docking system could be designed to tolerate an even larger diameter target, thus further increasing an already industry-standard docking reliability. Furthermore, it is not unreasonable to expect that control and guidance technologies will have improved between the findings of the paper (2006) and the mission timeline (2030s-2040s), granting even higher reliabilities.

Ultimately, while the consequence of a failed rendezvous sequence could lead to an aborted rendezvous or in the worst-case, loss of crew (consequence level 4 taken as average), the analysis of Landau and Longuski (2006) justifies a likelihood rating of 2, placing this risk in the yellow region of criticality. This risk is one that will need to be continuously reevaluated and watched during the development of the system at a deeper technical level to ensure that it continues to be mitigated following the ALARA principle.

Table 60: Failure Modes and Contingency Plans of Hyperbolic Rendezvous [139]

Table 2 Failure modes and contingency plans

Event	Strategy
Random navigation and control errors	Design for 3-σ reliability
Loss of navigation en route to transfer vehicle	Switch to backup system(s) or Track from surface (Earth) or Track from cycler
Loss of navigation while docking	"Eyeball" it[7]
Failure of 1st upper-stage	Retry after one orbit or Abort to surface
Failure of 2nd upper-stage	Abort to surface
2nd upper-stage cuts off prematurely	None
Failure of rendezvous engine	Use remaining engines or Switch to upper-stage engine
Loss of rendezvous propellant	Carry backup propellant in upper-stage engine[a]
Failure of docking engine or loss of propellant	Carry backup system or Use transfer vehicle to dock

[a]May not be feasible without in-situ propellant production.

[ID-07] Attitude control failure of the cycler vehicle describes the event of tumbling or otherwise erratic attitude of the vehicle, as well as the inability to maintain proper heading for a correction burn. The consequences of a total Attitude Control System (ACS) failure would likely be loss of vehicle and any crew who may be aboard, as non-corrected tumbling could render the crew unconscious or immediately injure/kill them depending on severity. Again, there is a band of possible scenarios with varying levels of severity, but a weighted average of 4 will be taken as the value for matrix placement. The likelihood for such an event is justifiably a 1, as the hypergolic ACS engine configuration includes both heavy redundancy (30+ engines in array configurations) and high single-component reliability, as hypergolic systems boast high storability and low failure rates.

[ID-09] A life support system failure would have one of the highest imaginable consequences during a crewed flight. While emergency oxygen masks would be equipped for the cases of fires aboard the craft, simulating prolonged atmospheric pressure and composition would be a great challenge, if not an impossibility without the main life support system. EVA suits could be a last-ditch effort for the crew in such an event but would at most grant the opportunity to fix the life support system, not a solution in and of itself. For this reason, a consequence of 5 is assigned to this failure mode. However, life support systems feature high reliability due to long history of successful usage in space, and redundancies as well as fault detection sensors will be equipped in the systems aboard the cycler. The other benefit of the modular AGM system is the physical

redundancy built into the cycler. If piping or other hardware were to fail in one module, the crew could adapt to using the other two nominal modules without major consequence. This was one of the driving considerations in the determination of the number of AGM pods to begin with. For these reasons, a likelihood score of 1 is assigned.

[ID-10] Power generation failure is always a potential risk on a spacecraft, but solar panel technology is a TRL 9 component with decades of flight-proven reliability. Considering the low relative emergency power draw from the baseline power generation rate and the sizing of the panel arrays to account for degradation and varying distance from the sun, this risk is one of the most understood and managed in the mission. For that reason, while it is a consequence 5, it is also a likelihood 1 event.

[ID-02] Radiation exposure during spaceflight is one of the areas of greatest concern for the crew. For this reason, thorough analysis was conducted during the design phase to understand and mitigate such risk. The inclusion of aluminum and HDPE shielding, as well as a water-lined storm shelter for the case of a forecasted Solar Particle Event (SPE) enable the mission profile to keep dosage below the NASA lifetime radiation effective dosage limit of 600 mSv. Accounting for SPEs is not a NASA spaceflight requirement, but the cycler architecture allows for this accommodation, which was taken advantage of due to the presence of water aboard the spacecraft already. In addition, the cycler orbit is deemed to have a shorter transit time than any feasible direct Starship transfers during the same launch window as the mission flight profile. By both minimizing transit time and having multiple shielding strategies, the risk likelihood is brought down to a 2, missing the mark of 1 simply due to the possibility of non-baseline prolonged cycler flight time during beforementioned contingencies. The consequence of radiation dosage is a 4, as the most plausible dosage cases with the mission's countermeasures in place do not result in levels resulting in immediate loss of crew. For overdosage cases from a long-leg cycler stay, for example, the main consequences would not be relevant except for the long-term, in which cancer is a concern. This is discussed in further depth in the radiation analysis portion of this proposal.

[ID-03] A missed entry window describes the event of crew being unable to depart the cycler to land on the Martian surface. This results in the crew remaining on the outbound cycler during its return leg, or in the case of a missed Earth return, remaining on the inbound cycler during its outbound leg. For both cases, the additional flight time is around 865 days, varying slightly based on planet alignment. Because the two cyclers incorporate two Starships capable of docking at once, one of the Starships can contain solely emergency supplies to sustain the crew during this flight phase. The radiation dosage is of concern, but as discussed earlier and in-depth in the radiation analysis section, it is mostly a long-term effect and not a loss of crew event. This consequence is preferrable to no contingency plan for a missed window, making this strategy the best way to preserve crew safety in such an event. For these reasons, this risk is assigned a consequence of 3 and a likelihood of 1.

9.3 Mars Surface Risk and Mitigation

Mars surface risk includes risks posed to crew and equipment during activities on Mars itself. This includes pre-supply mission objectives, science objectives both during crewed and non-crewed phases of the mission, habitat stay of the crew, and any activities completed by the crew outside

of the habitat, colloquially referred to in this assessment as EVAs, while acknowledging it as a slight misnomer.

Considering the duration of stay, introduction of novel technologies, and the novelty of the mission concept, the Mars surface stay poses some of the greatest risks to the crew of the entire mission. While rover missions have sought to understand as much as possible about the surface of Mars, the limited knowledge of subsurface water ice deposits, regolith properties, and thermal modeling pose challenges to maintaining crew health for such a mission profile. The following risk assessment is meant to address the most prominent risks which impact system design and does not encompass all the failure modes that could be encountered.

9.3.1 Risk Assessment and Mitigation Strategies

Table 61: Mars Surface Failure Modes

Mission Hazard	Consequence	Likelihood	ID	Risk Score (NASA Baseline)
Meteorite Impact on HAB	1	1	13	**1**
HAB Airlock Failure	2	1	17	**3**
Acute Radiation Dosage during EVA	3	1	5	**5**
Acute Radiation Dosage in HAB	3	1	6	**5**
Electrical Distribution Failure	3	1	10	**5**
HAB Deployment Failure	3	1	15	**5**
Communication Failure	3	1	3	**5**
Structural Failure of Habitat	3	1	1	**5**
Food Production Failure	2	2	9	**8**
Extreme Weather Event	2	2	14	**8**
Life Support System Failure	4	1	2	**9**
EVA Suit Failure	4	1	4	**9**
Ox Generation Failure	4	1	7	**9**
Power Generation Failure	4	1	8	**9**
Crew Physiological Deterioration	3	2	11	**11**
Regolith Extraction Failure	3	2	16	**11**
Crew Psychological Health Decline	3	2	19	**11**

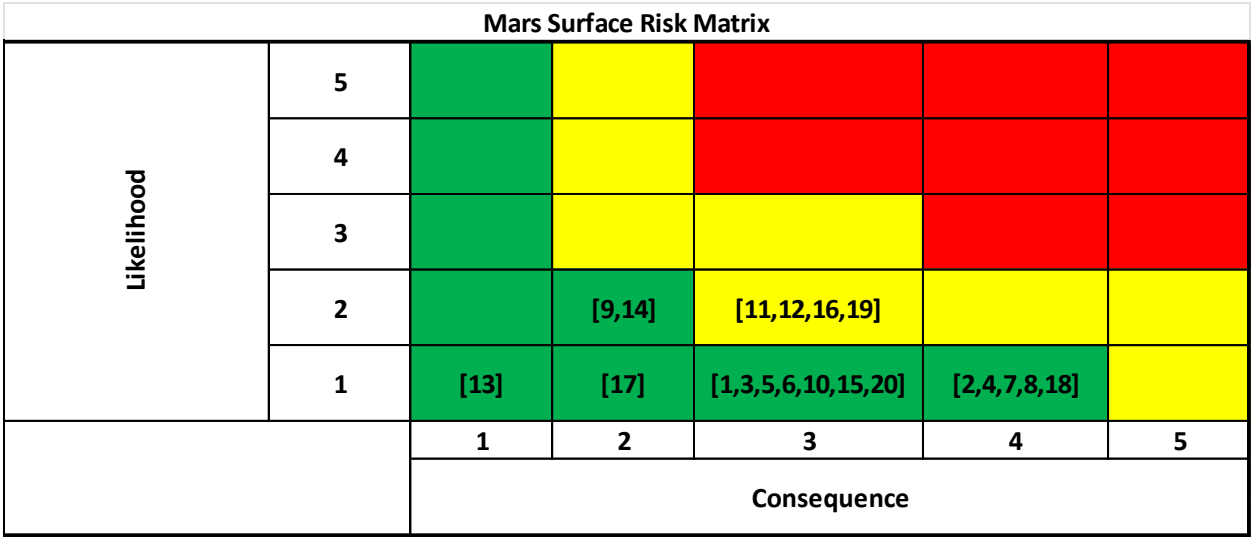

Figure 68: Mars Surface Risk Matrix

[ID-13] Meteorite impact events are exceedingly rare given the small area that the habitat will occupy. The likelihood of this risk is a 1. Consequences could vary based on the size of the meteorite and the impact point, but the 3-meter regolith habitat shielding combined with aluminum structural components makes it unlikely that such an event would harm the crew. A consequence of 2 is assigned to include very rare cases in which a larger impact object could disable a module and potentially injure a crew member.

[ID-17] Habitat airlock failure describes the event of an airlock losing the ability to function as designed. Such an event could occur in a multitude of ways, not all of which result in any serious impact on the mission. In fact, due to the double wall configuration and safeguards of existing systems, most failures would only prevent the airlock from being used any further. In such an event, the other usable airlocks would be utilized, and the habitat module vacated if the airlock is deemed not to be safe. This risk is given a likelihood score of 1 and a consequence score of 2 due to the reliability of existing systems and redundancies built into the habitat system.

[ID-05] Acute radiation dosage during EVA describes the event of crew receiving an event such as a Solar Particle Event (SPE) which delivers significant dosage in a short period of time. During EVA, suit protection is limited, however a single event exposure has only minor health ramifications if future dosage is managed accordingly. The total mSv budget for an astronaut can still be met by managing future EVA activities. Radiation dosage budgeting accounts for single-event dosage. This risk therefore has a consequence of 3 and a likelihood of 1.

[ID-06] In the habitat, the crew has exceptional shielding for a space environment. Three meters of regolith combined with the Martian atmosphere greatly mitigates the risk of an acute radiation event on the crew, which is in itself an already rare event at the scale needed to be a factor. In recorded history there has not been a solar event that would induce a greater than 250 mSv dosage. This risk has a consequence of 3 and a likelihood of 1.

[ID-10] A failure of the power systems to distribute electricity to the habitat and other critical systems poses a risk to daily operations on the Martian surface. Cables will need to be run from the KRUSTY reactors to the systems drawing power, which introduces the risks of cables fraying, weathering, or corroding. Further regolith abrasion studies will help to ensure that cables are well

protected, and independence of KRUSTY reactors will help to eliminate single-point-failures in the power distribution system. This risk receives a consequence score of 3 and a likelihood score of 1 due to the countermeasures which will be in place.

[ID-15] If the habitat were to fail in deployment during the pre-arrival phase of the mission, attempts could be made to firstly troubleshoot the issue and rely on redundant mechanisms in place for automatic deployment. However, if the worst-case scenario occurred in which the module is unable to be deployed, a replacement would need to be sent from Earth, which would either dig into schedule margin or push back crew arrival time. However, there would be no safety risk to the crew, hence why this risk receives a consequence score of 3 for schedule criteria of nearing a critical path slip. The likelihood is deemed to be a 1, as again, redundant, and well-tested deployment mechanisms will be utilized once the habitat is designed to the component-level.

[ID-03] Failure of communication systems would leave the crew without the ability to seek guidance from mission control on performing science objectives or solving issues with equipment. Prolonged communication outage would begin to pose a safety risk, as any emergencies which arise in this period are internalized to the crew to solve. The benefit of the chosen telemetry system architecture is that multiple satellites would have to fail to not have at least partial communication channels with Earth. In addition, the EVA antenna on the habitat is capable of emergency direct transmission to Earth, albeit at a reduced bit rate. For these reasons, this risk is allocated a consequence rating of 3 and a likelihood rating of 1.

[ID-01] The habitat structure will be designed and built with a minimum of a 1.4 factor of safety. The thickness for radiation shielding utility already brings the thickness beyond this, however. Structures are static systems that experience stable environments. Martian wind, for example, does not carry significant momentum to load the habitat structurally. This risk is a likelihood score of 1 and a consequence score of 3, as the redundancy of the habitat modules means that if there were to be a failure in one place, that module can be decommissioned. The oversizing of the habitat allows for this to occur without loss of quality of life for crew or loss of science objectives.

[ID-09] Due to resupply mass constraints imposed from mission objectives, it is not possible to sustain the crew via food shipments from Earth. As such, growing food is a necessary component to maintaining crew health. The greenhouse will be supplied with hydroponic systems and supplemental nutrients, which along with proven technology aboard the Veggie system of the ISS give assurance that such a system is feasible [140]. Contingencies for production failures include the ability to send resupply missions from Earth with either replacement nutrients and equipment or packaged food as a last resort. Note that while it would violate the 5,000 kg resupply requirement, the safety of the crew would supersede such an artificially imposed limit and the mission could be salvaged apart from this mission objective. Considering these consequences and the existing technologies proven aboard the ISS, food production risk is placed at a consequence of 2 and a likelihood of 2, as scaling issues could arise from the modest operation of the Veggie system.

[ID-14] Extreme weather events include dust and electrical storms which are observed phenomena on Mars. Dust storms carry insignificant momentum due to the thin Martian atmosphere, although airborne regolith can potentially be an abrasion concern [141]. Structures and outdoor equipment will need to be designed with consideration for this weathering. Lightning can be grounded using lightning rods, and electronic shielding along with circuit breakers can be used to prevent overloading circuits. Considering the minimal effects after mitigation, extreme weather is given a

consequence of 2, most a result of potential science return losses due to visibility concerns during a long-duration storm. The risk is given a likelihood of 2 based on the observed frequency of dust storms from rover missions.

[ID-02] Life support system failures are among the worst-case scenarios for any crewed space mission. As such, decades of refinement and safety considerations have led to robust designs which demonstrate strong reliability. However, the distance from Earth in the application of the life support architecture on Mars poses additional risk, as the current systems aboard the ISS rely on regular missions from Earth to maintain such systems [142]. However, built-in redundancies, the modularity of habitat design, and regular preventative measures such as maintenance and part replacement should adequately manage these additional risks, especially considering that new, deep-space capable systems are currently being improved upon in their development stages. Therefore, this risk is assigned a consequence score of 4 and a likelihood of 1.

[ID-04] When crews are performing EVAs, their suit is an essential piece of equipment to protect them from debris, an inhospitable atmosphere, and micrometeorite events. Failure modes of this equipment include depressurization, lack of oxygen flow, lack of heat regulation, among countless other fringe events. Ultimately, this suit would be contracted out with a list of specifications derived via a detailed study of intended activities and expected environmental parameters, and testing would take place to validate the design. Given the reliability of past EVA suits and the continual improvements over time, this risk is allocated the lowest likelihood score of 1, with a consequence score of 4, which rides on a pessimistic assumption that failures occur far from the habitat or vehicle. For incidents close to a pressurized environment, the astronaut will have a period (albeit short) to seek shelter, as the first fatal condition they would likely encounter would be asphyxiation.

[ID-07] Oxygen generation is a crucial capability to sustain a crew on Mars. Fortunately, technology demonstrations such as the MOXIE module aboard the Perseverance rover have proven the processes needed to produce pure oxygen from CO_2. The mission architecture will use a scaled version of this same technology. When the system is designed on the component level, modularity will need to be a feature to prevent a single-point failure of oxygen production. Storage of liquid or condensed oxygen will allow for a buffer in the event of a production issue. The consequence of oxygen production failure would be severe (4) but is unlikely (1) for these reasons.

[ID-08] Along with oxygen production and life support, power generation poses one of the major backbones of sustaining a presence on the Martian surface. The use of 18 KRUSTY units gives a high level of redundancy, and RTG technology has been used successfully on many deep space missions lasting much longer than the mission profile of this application (the Voyager probes are still operational from the 1970s). Power generation is therefore deemed to be a very unlikely event (1). The consequence of a large-scale outage would of course be grave (4) but considering that the low emergency utilization is 25.2 percent of maximum and severe emergency utilization is only 7.8% of maximum, the crew could theoretically remain alive with as little as two operational KRUSTYs.

[ID-11] The Martian gravity environment poses a risk via long-term effects to crew physiology. Notably, muscle mass and bone density are known to be affected in lower gravity environments, although no human has ever lived in such an environment, so knowing exactly how the body will respond is difficult to say. Testing aboard the cycler AGM in LEO is a potential option to preliminarily investigate and/or validate assumptions on these effects. In addition, there is ongoing

research in potential drug and supplement countermeasures, including the use of the supplement resveratrol [143]. In combination with supplemental loading on the astronauts' person while on Mars (weights added to clothing/suits) it is reasonable to expect that effects will be minimized to a tolerable amount. The AGM gives the best possible transition from Spaceflight to the Martian environment, so there should not be any immediate concerns about when the crew arrives on Mars. Mild to moderate health consequences (3) are deemed unlikely to occur (2) due to the mitigation strategies mentioned.

[ID-16] Regolith extraction via the 15 RASSORs allocated is a critical step during the pre-supply phase of the mission to prepare for crew arrival. Failure to extract regolith leaves the crew without radiation shielding and without level terrain to land and deploy the habitat on. Fortunately, because this phase is conducted remotely before the crew departs Earth, any issues which arise can be managed without posing risk to crew health. Redundant RASSORs enable the mission to proceed if a few units run into issues. In addition, if a large-scale issue is identified early, replacement units can be sent, or a secondary landing location can be identified. Ultimately, the mission could be delayed if the problem is severe enough. Therefore, consequences are almost entirely cost and schedule (3) and are deemed unlikely to occur (2) due to redundancies and intelligence gathered from landing sight rover missions.

[ID-19] Crew psychological health is an important consideration when designing a mission architecture of the scope covered in this proposal. Every crewed space mission places a stress load on astronauts, although the duration and nature of this mission make risks and therefore mitigation considerations unique. The mission architecture prioritizes crew safety above all else, whether that be science objectives or cost/schedule. Investments in comfortably sized habitats and spacecraft, as well as a manageable workload allocated each day mitigate the stresses of interplanetary travel as best as feasibly possible. However, regular baseline comparison screenings will be utilized to identify when crew are being pushed too far, and workloads can be tuned back in these cases to allow for crew adaptation to the new environment. The first crew will serve in part as a data-collecting phase that the second crew can benefit from. Considering the measures taken to make the mission as achievable as possible from a crew psychological level, the risk is assigned a consequence level of 3 and a likelihood of 2.

9.4 Limitations of Analyses

This risk analysis is intended to serve as a preliminary high-level overview of the driving risks that must be considered in the viability of the system architecture. As the engineering development process advances to the component level, additional failure modes would need to be appropriately identified, analyzed, and mitigated through similar strategies. At the mission architecture level, certain risks were difficult to quantify, and required the use of engineering judgement in their assessment and mitigation. While best efforts were made to be as rigorous as possible within the confines of the scope of this project, it is worth noting that ideally all of these risk placements would be quantified via component testing, analysis, or Monte Carlo simulation when application environments are infeasible to simulate. These limitations are further explored in Section 9.2 of Further Work.

10: METHODOLOGY (LUKE HARPRING AND BRIAN WODETZKI)

A three-stage process was used to make design decisions. First is the initial system definition. This takes the form of a Pareto Analysis that defines the major components of the design. The following step in the process is design refinement. This step filled any unknowns in the point design by completing trade studies and other methods of design determination. The final step in this process is design validation, this is to conduct analysis like power and thermal analysis to determine whether the chosen design delivers on the requirements. If the design does not satisfy the requirements, then the second step in the process is repeated and a new design is selected using trade studies and other methods.

10.1 Initial Design Definition (Luke Harpring)

Initial design definition began as a team-wide brainstorming session to first identify the key mission parameters. This breaks down the decision-making process into a set of smaller elements. These elements give rise to brainstorming alternatives such as different available launch systems, propellant types, among others shown in Table 62.

Table 62: Crewed Mission Parameters

Crewed Mission Parameters	Element
Propulsion	Launch System
	Orbit
	Kind of Propulsion
Structures	Landing System
	Propellant Source
	Structures Source
Telemetry	Ground Control
	Data Return Frequencies
	Types of Communication
	Communications Architectures - Mars
	Communications Architectures - In Space
Spaceflight Environment	Cruise Vehicle
General	Power Generation
	Landing Locations
	Science Missions
	Mission Operations
	Payload
	Crew

Upon determining the driving elements of the mission architecture, the team had multiple brainstorming sessions spaced apart to maintain an environment conducive to nurturing creative thought. Concept generation requires that no ideas be criticized at this stage, so many fringe and potentially infeasible ideas arose.

To analyze the solution space, a three-dimensional Pareto analysis was conducted to optimize cost, reliability, and science value. Values for each of these three dimensions were arrived at by team consensus and entered into a table for import into a MATLAB script. The values were originally chosen on varying scales but ultimately normalized to a +/- 10 scale from a datum reference of 0. In addition to the values for each of the three categories, weights were assigned to each of three optimized criteria independently for each option, shown in Table 63. This decision was made since each system element had disproportional impact on mission cost, reliability, and science value. For example, the launch vehicle has much greater impact on mission cost and reliability than it does science value. It also has higher cost and reliability weight to the mission architecture as a whole relative to a mission element such as the landing location.

Table 63: Pareto Inputs Excerpt

Sub Team	Topic	Option	Cost	Reliability	Sci_Val	C_Gain	R_Gain	S_Gain
MD	ORBIT	CYCLER	-1	6	9	9	8	4
MD	ORBIT	EM_TRANS	0	8	-10	9	8	4
MD	ORBIT	EM_TRANSSLING	2	-6	3	9	8	4
PROP	LV	SLS	0	0	0	10	10	4
PROP	LV	STARSHIP	10	-1	10	10	10	4
PROP	LV	FALCONHEAVY	9.787286	10	-5.40741	10	10	4
PROP	LV	ARIANEV	9.530587	1.304348	-7.25185	10	10	4
PROP	LV	DELTAIVHEAVY	9.168704	-4.285714	-7.03704	10	10	4
PROP	LV	FALCON9	9.860636	9	-7.77778	10	10	4
PROP	LV	ARIANE6	9.718826	-2	-7.59259	10	10	4
PROP	LV	ATLASV	9.650367	10	-8.32407	10	10	4
PROP	IP	SOLIDS	0	-5	-2	8	8	4
PROP	IP	LIQBIPROP	0	-3	0	8	8	4

Following the Pareto algorithm execution, an immense number of possible solutions emerged due to the factorial nature of permutations. Over 300 billion possible solutions emerged, which made readability difficult and computation expensive. Therefore, aspects were combined to reduce the number of element choices from 720 to 85. Elements were reduced by taking certain decisions out of Pareto analysis and instead conducting a trade study or informal white paper argument on the merit of landing locations and science objectives. Partitioning the frontier by sub-team also aided in readability. In addition, certain architectures were identified as being incompatible, such as certain propulsion systems requiring a specific orbit type, etc. These incompatibilities were removed from the solution space which aided in the readability further.

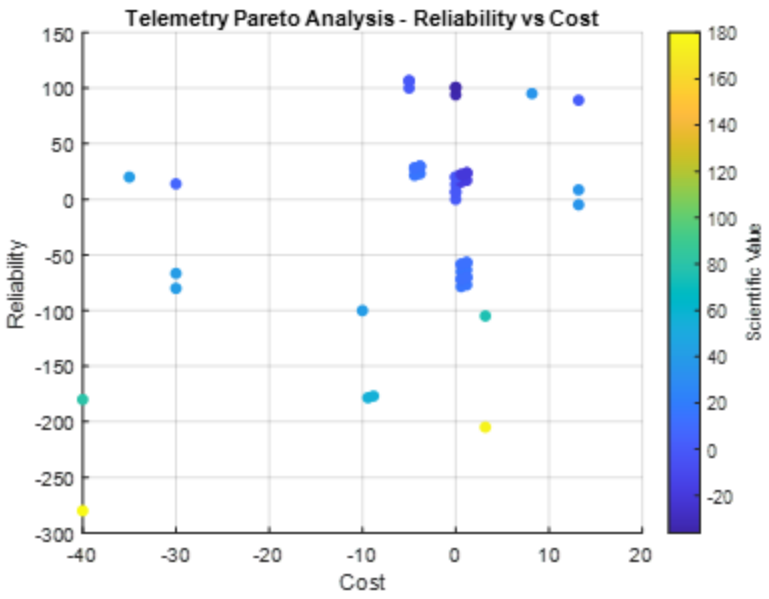

Figure 69:Pareto Graph Example (Telemetry Subsystem)

Upon analyzing the solution space via the developed Python script, a Pareto frontier arose, which describes the ideal frontier of the generated surface which optimizes cost, reliability, and science value. For readability, the frontier was decomposed to the sub-team level, with two variables represented on the x and y axes with the third represented as a color gradient. Three graphs are necessary, therefore, to view the frontier in its entirety for each sub-team. **Error! Reference source not found.** shows an example of this for the telemetry sub-team with cost and reliability on the axes and scientific value as the color gradient dimension. The graphs used the notation of a higher value being the best case for all three dimensions, so a higher cost score correlates to a less expensive architecture. The three independent scores were aggregated into a single solution score which the team calculated by determining relative weights of cost, reliability, and scientific value. The team ultimately determined that cost and scientific value should be weighted equally, so both were given a weight of 1. Reliability was deemed to be more important due to the nature of this mission being crewed. Therefore, reliability was given a relative weight of 1.2. From this point, candidate solution architecture emerged, and the team was able to move onto the next phase of design refinement.

10.2 Design Refinement (Brian Wodetzki)

10.2.1 Trade Study

There are two primary methods used to refine the designs. The first method is using the trade study outlined in Table 64.

Table 64: Trade Study Template

Trade Study Template	Selections:		Option 1	Option 2
FOAs:	Weights:	Scale:		
Weighted Totals:			0	0

All trade studies were completed by first determining FOA's that will be used to gauge the performance of a given design. Often these FOA's took the form of quantifying cost, mass, volume, power requirements, and so on. These categories made by the FOA's are then weighted against each other, and scaling is determined for the results of each category. If one category has a much different upper or lower bound for its values than another, then this scaling must be considered when selecting the weights. Next a list of options is chosen and compared using these categories. The conglomerated score for each design is then output and the design with the highest score will be chosen. This method was used for choosing the landing location, the habitat design, and other features of the design.

10.2.2 Science Mission Selection

The second method of selecting a design was used when selecting the scientific missions. This method involved the use of detailed research into each science mission, culminating in a one-page report written on the efficacy of each science mission. This method was employed for this to ensure each possible science mission is fully explored. The possible science missions that had been reviewed are shown in Table 65.

Table 65: Possible Science Missions

Science Missions
Astronomy
Flyby of Martian Moons
Fuel Production on Mars
Growth of Plants in Space
Growth of Plants on Mars
Search for Life on Mars
Search for Water on Mars

The 5 science missions that are being pursued in this mission were chosen, thus completing the requirement of pursuing 5 science objectives.

The Astronomy science objective was not chosen primarily due to the payload mass required to accomplish this mission. To adequately conduct astronomy either in space or on the surface a sizeable telescope is needed. If a telescope was needed in space, it was deemed that this should be a standalone mission as there would be no need to have it be a part of the mission. If a telescope were to be put on the surface of mars it was deemed that it would not be economical because of the high mass of such a system.

Performing Moon Flyby's was another option that was not chosen. As a result of the use of the cycler space station there are simply no opportunities to do a moon flyby in any other mission phase aside from mars EDL and mars ascent. However, these are risky parts of the mission and to add one other optional mission objective during these phases was deemed to be careless. This is without stating that the increased fuel needed to perform a moon flyby during EDL or ascent would be an unnecessarily large expense.

Finally studying the growth of plants in space was also deemed to be a mission that would not be pursued or covered in this proposal. This is mainly since much study on this has been done on the ISS. This goes along with the fact that since the crew will not be relying on plants for food when transiting on the cycler this would be a superfluous science objective that has limited benefit. Although small scale experiments surrounding plant growth in space is likely to occur if a mission like this were to happen, the details of such a mission were not an objective for this proposal.

10.3 Design Validation (Brian Wodetzki)

Throughout the development of the design there were three core analyses that prompted iteration to a more efficient design. The first analysis is power analysis on both the cycler and the surface operations. The second analysis was thermal analysis on both the cycler and the surface operations. The third analysis was total payload mass of the mission. If a component of the design did not lend itself well to this analysis due to it causing the overall design to become more complex, that component was redesigned, often out of necessity. For example, producing fuel on the surface of mars for use on the ascent starship was deemed to power intensive of a process. As a result, a fuel refrigeration system was chosen that would store the fuel for the duration of the mission.

11: FUTURE WORK (BRIAN WODETZKI AND EVERYONE)

11.1 Habitat Downsizing (Luke Miller)

A major advantage of the presented architecture is the relatively large size of the habitat. The current habitat design has 890m^3 of livable volume. Approximately 100m^3 of livable volume will be dedicated to the greenhouse. This represents one module being used for the greenhouse, where some of the planting units will be stacked vertically. The proposed mission has no crew overlap, so there will never be more than 4 crew members in the habitat at once. This translates to nearly 200m^3 of livable volume per astronaut for the current design. Previous studies have suggested that for a long-term mission to Mars the required livable volume is only 37m^3 per crew member [144]. Clearly the size of the habitat is this architecture is much larger than it needs to be. A key driver for the extra size is that the team found it desirable to have an architecture that can support future growth of human presence on the Martian surface beyond the first two crews. The larger size opens flexibility and opportunities for the proposed mission and future crewed missions to Mars. Additionally, the larger habitat will potentially lessen psychological stressors on the astronauts. The team evaluated such a large habitat size as feasible based on the lack of budgetary constraints on the mission. However, it is not lost on the team that this large habitat is a major cost driver in the mission. For this reason, it should be noted that the habitat design is easily adaptable due to its modular design. Therefore, it is still within the trade space to decrease the number of modules used in the habitat to reduce mission costs. One proposed solution is to reduce the number of modules by five, which would leave four modules. In this configuration there would be approximately 390m^3 of livable volume, 100 m^3 of which would be used by the greenhouse. This leaves 72 m^3 of livable volume per crew member, which is still nearly double the requirement. Not only would this reduce the cost of materials sent to Mars, but it would also reduce power and regolith extraction requirements. Another potential path to reduce the cost of the habitat is to reduce the thickness of aluminum and polyethylene used. This can be done by:

1. Using more regolith to shield from radiation.
2. Using in-situ water instead of polyethylene for habitat radiation shielding. This adds complexity and risk as previously mentioned.
3. Accept a lower scientific return by reducing the dosage allowance for activities outside of the habitat so that more radiation can be accepted in the habitat.
4. Accept a greater total radiation exposure at the cost of astronaut safety. For this option a radiation dose limit of 1 Sv could be set, which is beyond NASA's current standard of 600 mSv, but is still in line with some of NASA's international partners.

With these options in mind, preliminary analysis with NASA OLTARIS suggests that the polyethylene and aluminum thicknesses could be reduced by a factor of two. Between fewer modules and half the thickness, the team sees a path to reduce the habitat mass that needs to be ferried to Mars from 790 metric tons to 190 metric tons (75% mass reduction). This would ultimately reduce the number of starships needed to transport the habitat from 8 to 2 on a mass basis. This reduction in size and launches represents a large cost saving. However, ultimately the

final habitat configuration will depend on economic and political factors as is common to all space missions. For this reason, further studies into reducing the habitat size are left as future work.

11.2 Detailed Risk Analysis (Luke Harpring)

To stay relevant to the scope of this proposal, risk analysis was largely qualitative, and multiple failure modes were consolidated for ease of assessment. As the engineering design cycle progresses to physical allocation at the component level, the risk assessment will need to be maintained, tracked, and updated to reflect any changes or increased depth of knowledge available of mission failure modes and risks. Eventually, a true analytical risk analysis should be conducted using testing data in accurate environmental conditions or simulation results if such conditions cannot be emulated. A fault tree analysis was not attempted at this level of mission development, as the main benefit of such an analysis is only achieved when event probabilities (and therefore logic gate probability contributions) are readily and accurately available, which is simply not the case at this stage of design. As those probabilities become available, a fault tree should be constructed, and analysis should take place to identify minimal cut sets. These cut sets describe the shortest possible set of failures which could lead to a mission-level event such as loss of mission objective, loss of equipment, or loss of crew. Minimal cut sets should be identified and appropriately managed via key risk mitigation or planning contingencies for the most likely events along the cut set. ALARA guiding principles should always be upheld to place crew safety and wellbeing above all else while still seeking to accomplish science objectives in an economically feasible manner.

It is likely the case that the risk analysis of a mission of this scale will need to be iterated upon as more information is available. As the current architecture relies on emerging technologies whose reliability and TRL at the mission timeline are speculative, it is possible that systems will evolve during the development stages as more promising options emerge. With these evolutions comes the need to track changes to mission risk. As bids are awarded to contractors and many entities become stakeholders in the mission, it will be important for a unification of risk assessment resources. Cloud-based databases can enable systems engineers at the mission level to maintain continual communication channels with sub-contractors to track reliability and performance data at the component level and integrate this data into mission-level assessments of risk.

For a mission of this magnitude and nature, it will become a mission-defining decision in determining where to draw the line on what an acceptable level of risk looks like for such a profile. Gone are the days of the politically charged Mercury/Gemini/Apollo risk philosophies which value delivering results over all else. Today's industry as well as global political climate expects a higher standard, and that standard of safety will need to be met by utilizing all available risk management tools and upholding the highest standards of ethics from start to end of the mission design process.

11.3 Combined Fuel Production and Fuel Storage Systems (Brian Wodetzki)

Currently this mission baselines the use of fuel refrigeration equipment to refrigerate Methane and LOX on the surface of mars throughout the mission to be used for the ascent starship. This decision was made from necessity, as the power consumption to produce the fuel fully measured in the megawatt range, a number that is prohibitively expensive.

This decision, however, has the downside of needing to send fuel beforehand and rely on the safe storage of the fuel throughout the 7-year mission. If a leak were to spring in the system, the astronauts would not be in a good place to get home. Although there is an allocation of 1,000 kg of resupply payload mass to restock any lost fuel in the event of a leak, there are still many risks associated with this design.

The option that needs to be explored is a hybrid system that both produces fuel and refrigerates fuel. This system would be robust if a leak were to happen. This would also have the added benefit of theoretically adding to the autonomy that the astronauts have from the Earth, overall increasing the robustness of the mission design.

11.4 Future Work on Cycler ADCS (Vishnu Vijay)

With a finalized design for a cycler, with component-level masses and moments of inertia, a concrete plan for a cycler vehicle ADCS can be determined. This includes placement of reaction control thrusters and determining whether control moment gyroscopes are feasible for a long-term mission to Mars. This in turn would determine the sizing of the ADCS tanks.

With recent research into automated fault detection, identification, and reconfiguration of control systems, using some form of this would greatly improve the robustness of the system. Robust algorithms for the control system are vital for the autonomous operation of such a large space vehicle.

12: APPENDIX

12.1 System Requirements

Table 66: Requirements Nomenclature

Sub Team	Abbreviation
Systems	SYS
Telemetry	TEL
Structures	STR
Mission Design	DES
Cost/Schedule	COST
Attitude Dynamics & Control	ADC
Space Environment	ENV
Propulsion	PROP
Architecture Levels	
1	Mars Mission System
2	Sub-System
3	Element
4	Component
5	Part
Naming Convention (ID)	
Req. ID: SUB-Parent.Child…	
SUB:	Sub Team Abbreviation
Parent:	High Level Mission Req.
Child:	Lower Level Supporting Req. of Parent

Table 67: Requirement Traceability Architecture

Req. ID	Level	Short Text	Long Text	Criticality	Req. Type	Traceability
ADC-1.0	**2**	**3-Axis Stabilization**	The control system shall enable three-axis stabilization.	**N**	**Functional**	**Derived, Crew Safety**
ADC-2.0	**2**	**Pointing**	The control system shall maintain constant pointing of signal sources to Earth-based receivers.	**N**	**Functional**	**TEL-4.0**
ADC-2.1	**3**	**High-Gain Pointing Accuracy**	The high-gain antenna shall point within 2.08 mRad of the Earth-based receiver.	**N**	**Specification**	**TEL-4.0**
ADC-2.2	**3**	**Optical System Pointing Accuracy**	The optical system shall point within 3.36 microRad of the Earth-based receiver.	**N**	**Specification**	**TEL-4.0**
ADC-3.0	**3**	**AGM Spin-Up**	The control system shall enable spin-up and spin-down of the artificial gravity module (AGM).	**N**	**Functional**	**Derived, Crew Health**
ADC-4.0	**3**	**Antenna Scan Rate**	Antennas shall be able to gimbal at a required scan rate to remain pointing at receivers.	**N**	**Performance**	**TEL-4.0**
COST-01.0	**1**	**Cost Estimate Deliverable**	A cost estimate of all program costs shall be completed and delivered upon the completion of the project.	**Y**	**Assigned**	**Mission Requirement**
DES-01.0	**2**	**Mars Cycler**	The system shall include a Mars Cycler intermediate vehicle for crew cruise flight.	**Y**	**Functional**	**DES-4.0**
DES-02.0	**2**	**Crewed Mission Launch Window**	The system shall be able to launch within the time frame of 2035-2040.	**Y**	**Assigned**	**Mission Requirement**
DES-03.0	**2**	**Rendezvous with Cycler on Earth**	The system shall enable rendezvous with the Mars Cycler Orbit from Earth.	**N**	**Functional**	**DES-1.0**
DES-03.1	**3**	**Rendezvous at Earth Speed**	The cycler shall maintain a velocity of less than 8 km/s during rendezvous at Earth.	**N**	**Specification**	**DES-3.0**
DES-04.0	**2**	**Length of Travel to Mars**	The system shall minimize transit time for crew and resupply.	**N**	**Performance**	**ENV-01.0**
DES-05.0	**2**	**Arrival on Mars**	The system shall safely descend the crew from the Mars Cycler onto the Martian surface.	**N**	**Functional**	**SYS-8.0**

DES-06.0	**2**	**Pre-supply Launch**	The system shall have pre-supply launched at least 1-2 years before the crewed launch.	**Y**	**Functional**	**SYS-8.0**
DES-06.1	**3**	**Pre-supply Trajectory**	The pre-supply system shall have the most cost-effective trajectory.	**N**	**Performance**	**DES-6.0**
DES-06.2	**3**	**Pre-supply Landing**	The Pre-supply system shall land safely on the Martian surface	**Y**	**Functional**	**DES-6.0**

Req. ID	Level	Short Text	Long Text	Criticality	Req. Type	Traceability
DES-07.0	**2**	**Crewed Mission Return Window**	The system shall be able to launch within the time frame of 2042-2047 from Mars for return.	**Y**	**Functional**	**SYS-10.0**
DES-08.0	**2**	**Rendezvous with Cycler on Mars**	The system shall be able to rendezvous with the Mars Cycler Orbit from Mars.	**N**	**Functional**	**DES-1.0**
DES-08.1	**3**	**Flyby Velocity**	The system shall have a flyby velocity of less than 8 km/s at both Earth and Mars.	**N**	**Performance**	**DES-8.0**
DES-08.2	**3**	**Rendezvous at Mars Altitude**	The system shall rendezvous at an altitude range of [TBD] above Mars.	**N**	**Performance**	**DES-8.0**
DES-09.0	**2**	**Length of Travel to Earth**	The travel time of crewed transit shall be minimized.	**N**	**Performance**	**DES-10.0**
DES-10.0	**2**	**Arrival on Earth**	The system shall safely descend the crew from the Mars Cycler onto the Earth's surface.	**Y**	**Functional**	**SYS-8.0**
ENV-01.0	**2**	**Crew Effective Radiation Dosage**	The crew radiation exposure shall not exceed 600 millisieverts (mSv) over the course of the mission.	**Y**	**Performance**	**Derived, NASA Standard**
HF-01.0	**1**	**Crew Psychological Health**	The crew's psychological health shall be cared for and monitored throughout the mission.	**Y**	**Functional**	**Derived, Crew Health**
PROP-01.0	**2**	**Crew Launch Vehicle Propulsion System**	The propulsion system shall enable the crew launch vehicle to perform necessary propulsive maneuvers.	**Y**	**Functional**	**SYS-8.0**
PROP-01.1	**3**	**Crew Launch Minimum DeltaV**	The propulsion subsystem shall provide the necessary deltaV to enter target orbits and perform necessary orbital maneuvers.	**N**	**Functional**	**PROP-1.0**
PROP-02.0	**2**	**Cycler Propulsion System**	The propulsion system shall enable the crew launch vehicle to perform necessary propulsive maneuvers.	**Y**	**Functional**	**DES-1.0**
PROP-02.1	**3**	**Cycler Minimum DeltaV**	The propulsion subsystem shall provide 250 m/s of deltaV to maintain the cycler orbit.	**N**	**Performance**	**PROP-2.0**

SO-FUE-1.0	**1**	**ISRU for Fuel Production**	The system shall enable demonstration production of 2,3-butanediol through photosynthesis of cyanobacteria, breakdown of bacteria into sugars by enzymes, and breakdown of sugars by E. coli to produce rocket propellant.	**N**	**Functional**	**SYS-4.0**
SO-HUM-01.0	**1**	**Analyze Psychological Impacts of Space Isolation**	The system shall have the capability to send psychological results from back to Earth for a psychologist to analyze.	**Y**	**Functional**	**SYS-4.0**
Req. ID	**Level**	**Short Text**	**Long Text**	**Criticality**	**Req. Type**	**Traceability**
SO-HUM-02.0	**1**	**Analyze Effects of Prolonged Habitation on Mars**	The system shall be capable of analyzing the physiological effects on the crew from prolonged habitation on the Martian surface.	**Y**	**Functional**	**SYS-4.0**
SO-LIF-01.0	**1**	**Martian Soil and Gas Samples**	The system shall collect Martian soil and gas samples from diverse locations on the surface of Mars.	**Y**	**Functional**	**SYS-4.0**
SO-LIF-02.0	**1**	**Sample Analysis**	The system shall be able to analyze samples on the Martian surface or otherwise be able to return select samples back to Earth.	**Y**	**Functional**	**SYS-4.0**
SO-MAT-1.0	**1**	**ISRU for Materials**	The system shall enable the collection of regolith, processing of concrete, and testing of numerous concrete samples.	**N**	**Functional**	**SYS-4.0**
SO-WAT-01.0	**1**	**Landing Site Selection Water Criterion**	The system shall be at a landing site chosen within areas previously noted to potentially have water within from satellite information.	**Y**	**Functional**	**SYS-4.0**
SO-WAT-02.0	**1**	**Martian Water Analysis**	The system shall include the ability to analyze Martian water composition and potability.	**Y**	**Functional**	**SYS-4.0**
STR-01.0	**2**	**Cruise Habitat**	The system shall include a habitat which provides a livable space for crew during the flight to Mars.	**N**	**Functional**	**SYS-8.0**
STR-02.0	**2**	**Mars Habitat**	The system shall include a habitat which provides a livable space for crew during the ground stay on Mars.	**N**	**Functional**	**SYS-8.0**
SYS-01.0	**1**	**Crew Size**	The system shall support a continuous crew of at least 4 throughout the entire mission.	**Y**	**Functional**	**Mission Requirement**
SYS-02.0	**1**	**Mission Duration**	The system shall support a mission duration of 7 years.	**Y**	**Functional**	**Mission Requirement**
SYS-03.0	**1**	**Novel Technologies**	The mission shall include the usage of at least 3 novel technologies.	**Y**	**Functional**	**Mission Requirement**

SYS-04.0	**1**	**Science Objectives**	The system shall accomplish at least 5 scientific objectives during its mission.	**Y**	**Functional**	**Mission Requirement**
SYS-05.0	**1**	**Minimum TRL**	A TRL of 6+ shall be the baseline for all system components unless a citation is provided on the prospect of the lower TRL technology.	**Y**	**Functional**	**Mission Requirement**

Req. ID	Level	Short Text	Long Text	Criticality	Req. Type	Traceability
SYS-06.0	**1**	**Maximum Pre-Supply Logistics**	The system shall deploy no more than 2 years' worth of logistics and spares prior to the start of the crewed mission.	**Y**	**Functional**	**Mission Requirement**
SYS-07.0	**1**	**Maximum Cargo**	The system shall require no more than 5,000 kg of consumable cargo from Earth every two years after the crewed mission begins.	**Y**	**Functional**	**Mission Requirement**
SYS-08.0	**1**	**System Architecture**	The system architecture shall include launch, in-space transportation, Mars entry-descent-landing, surface habitation and operations, and any other additional logistics support required from Earth to sustain the crew and their systems.	**Y**	**Functional**	**Mission Architecture**
SYS-09.0	**1**	**Mass, Power, Volume, and Costs**	The mass, power, volume, and costs for all elements, as well as the total lifecycle cost for the whole mission should be provided.	**Y**	**Functional**	**Mission Requirement**
SYS-10.0	**1**	**Crew Arrival and Departure**	The first crew shall land between 2035 and 2040, and the last crew shall return between 2040 and 2050.	**Y**	**Functional**	**Mission Requirement**
SYS-11.0	**1**	**Assumption Statements**	All assumptions made for the design of the architecture shall be clearly brought out and justified.	**Y**	**Deliverable**	**Mission Requirement**
SYS-12.0	**1**	**Risk Mitigation and Contingency**	Risks shall be mitigated, and contingency plans shall be provided for all aspects of the mission. The principle of ALARA (As Low As Reasonably Achievable) shall always govern risk management philosophy.	**Y**	**Deliverable**	**Derived, Best Practices**
TEL-01.0	**2**	**Science Data Return**	The system shall return science data within two weeks of acquisition.	**Y**	**Performance**	**Mission Requirement**
TEL-02.0	**2**	**Baseline Band**	The system shall baseline Ka-band for science data return.	**Y**	**Functional**	**Mission Requirement**

TEL-02.1	**3**	**Ground Network Range**	Ground network must have operational range that extend to the trajectories furthest point.	**N**	**Performance**	**TEL-2.0**
TEL-03.0	**2**	**34-m Antenna**	The system shall baseline the use of only one 34-m antenna at a time.	**N**	**Performance**	**Mission Requirement**
TEL-04.0	**2**	**Telemetry/Tracking Coverage**	The system shall return telemetry/tracking coverage during all critical events.	**N**	**Performance**	**Mission Requirement**

Req. ID	Level	Short Text	Long Text	Criticality	Req. Type	Traceability
TEL-04.1	**3**	**Antenna Coverage**	Earth-based ground system network must be able to have worldwide coverage.	**N**	**Functional**	**TEL-4.0**
TEL-05.0	**2**	**Minimum Decibel and Margin**	The Earth-based ground system shall receive data with the network's minimum dB level plus a 3 dB margin.	**N**	**Performance**	**TEL-4.0**
TEL-06.0	**2**	**EVA Direct Transmission**	The habitat EVA antenna shall be capable of emergency direct transmission to Earth for contingency.	**N**	**Functional**	**TEL-4.0**
TEL-08.0	**2**	**Ground Network**	The telemetry subsystem shall include an Earth-based ground station to receive and send signals.	**N**	**Functional**	**TEL-4.0**
TEL-09.0	**2**	**Relay Satellites**	The telemetry subsystem shall include Mars-based orbiting relay satellites.	**N**	**Functional**	**TEL-4.0**
TEL-09.1	**3**	**Relay Sat. Safe Mode**	All Mars relay satellites shall have a safe mode to redetermine attitude in the case of sensor malfunction.	**N**	**Functional**	**TEL-9.0**
TEL-10.0	**3**	**Solar Conjunction Relay**	The telemetry subsystem shall utilize a cycler as a relay node during solar conjunction.	**N**	**Functional**	**TEL-4.0, TEL-1.0**
TEL-11.0	**2**	**Blackout Periods**	The telemetry subsystem shall keep blackout periods to no more than 30 minutes per sol.	**N**	**Performance**	**TEL-4.0**

12.2 Link Budget Equations & Results (Nathan Berry)

The following are the link budget equations for the radio frequency communication system all found in Ref. [46].

Equation 39: Ground Antenna Gain Equation

$$G_t = 20.4 + 20\log_{10}(f) + 20\log_{10}(D) + 10\log_{10}(\eta_t)$$

Equation 40: Satellite Gain Equation

$$G_r = 10\log_{10}\left(\frac{41253}{A_\theta}\right) + 10\log_{10}(\eta_r)$$

Equation 41: Path Loss Equation

$$L_s = 92.45 + 20\log_{10}(r) + 20\log_{10}(f)$$

Equation 42: Equivalent Isotropic Radiated Power (EIRP) Equation

$$EIRP = 10\log_{10}\left(\frac{P}{1\ W}\right) + G_t - L_{line} - L_{backoff}$$

Equation 43: Received Signal Equation

$$C = EIRP + G_r - L_s - L_{atm,dust} - L_{line,r}$$

Equation 44: Receiver Gain to Noise Temperature Ratio Equation

$$\frac{G}{T} = G_r - 10\log_{10}\left(\frac{T_s}{1\ K}\right)$$

Equation 45: Received Signal Power to Noise Ratio

$$\frac{C}{N_o} = EIRP - L_s - L_{atm,dust} - L_{line,r} + \frac{G}{T} + 228.6$$

Equation 46: Data Rate Equation

$$R_b = 10\log_{10}\left(\frac{Data\ Rate}{1\ bps}\right)$$

Equation 47: Eb/No Equation

$$\frac{E_b}{N_o} = \frac{C}{N_o} - R_b$$

The following is the uplink budget from Mars to the orbiting relay satellites.

Table 68: Uplink Budget Ka-Band

Uplink to Satellite Link Budget			
Link Budget Cases	Data	Units	Source
Uplink Frequency	32	GHz	Ka-Band Frequency
Data Rate	1.5e5	bps	Design Choice
Transmitter Specifications	Data	Units	
Transmit Antenna Diameter	0.3048	m	Design
Transmit Antenna Efficiency	75	%	[145]
Transmit Power	17.3	W	Optimal Power
Transmit Gain	38.93	dBi	Equation 39
Transmit Backoff & Line Loss	-7	dB	[46]
EIRP	44.31	dBW	Equation
Path Losses	Data	Units	
Propagation Distance	5998.33	km	Furthest Point in Sight from Base
Space Loss	-198.11	dB	Equation 41
Atmospheric Losses	-0.35	dB	[146]
Dust Storm Losses	-3	dB	[146]
Net Path Loss	-201.46	dB	Sum of Above Losses
Receiver Specifications	Data	Units	
Coverage Area	0.0842	deg^2	High Gain Antenna Design Parameter
Antenna Efficiency	70	%	[147]
Receiver Gain	38.934	dBi	Equation 40
Receiver Line Loss	2	dB	[46]
System Noise Temperature	25.441	dBK	[46]
System Performance	Data	Units	
Received Carrier Power, C	-103.80	dBW	Equation 43
G/T	29.91	dB/K	Equation 44
Receiver C/No	99.36	dB-Hz	Equation 45
Data Rate	61.76	dB-Hz	Equation 46
Available Eb/No Uplink	37.60	dB	Equation 47

Similarly, the downlink Link Budget table can be found below.

Table 69: Downlink Budget Ka-Band

Downlink to Earth Link Budget			
Link Budget Cases	Data	Units	Source
Downlink Frequency	32	GHz	Ka-Band Frequency
Transmitter Specifications	Data	Units	
Coverage Area	0.0842	deg^2	Design
Transmit Antenna Diameter	3	m	[148]
Transmit Antenna Efficiency	42	%	[147]
Transmit Power	216	W	Optimal Design
Transmit Gain	53.134	dBi	Equation 40Equation 40
Transmit Backoff & Line Loss	-4.5	dB	[46]
EIRP	71.98	dBW	Equation 42
Path Losses	Data	Units	
Propagation Distance	401000000	km	Furthest Mars Distance from Earth
Space Loss	-294.62	dB	Equation 41
Atmospheric Losses	-7	dB	[149]
Dust Storm Losses	0	dB	*Included in Atmospheric Value
Net Path Loss	-301.62	dB	Sum of Above Losses
Receiver Specifications	Data	Units	
Antenna Efficiency	75	%	[150]
Receiver Gain	79.88	dBi	Equation 39
Receiver Line Loss	-2	dB	[46]
System Noise Temperature	13.01	dBK	[150]
System Performance	Data	Units	
Received Carrier Power, C	-151.75	dBW	Equation 43
G/T	66.87	dB/K	Equation 44
Receiver C/No	63.84	dB-Hz	Equation 45
Data Rate	51.76	dB-Hz	Equation 46
Available Eb/No Uplink	12.07	dB	Equation 47

The following equation was utilized to compute an end-to-end Eb/No from the above uplink and downlink link budgets.

Equation 48: End-to-End Eb/No

$$\left(\frac{E_b}{N_o}\right)_{composite} = 10\log_{10}\left(10^{-\frac{\left(\frac{E_b}{N_o}\right)_{uplink}}{10}} + 10^{-\frac{\left(\frac{E_b}{N_o}\right)_{downlink}}{10}}\right)$$

12.3 Starship Accounting (Mark Paral)

The following section demonstrates propellant mass calculations and refueling costs using the Starship launch vehicle.

Consider the following specifications of Starship detailed in Table.

Table 70: Starship Specifications [24, 171]

Specification	Symbol	Value
Specific Impulse of Superheavy Booster	ISP_1	330s
Specific Impulse of Starship	ISP_2	375s
Propellant Mass Fraction of Superheavy Booster	λ_1	0.95
Propellant Mass Fraction of Starship	λ_2	0.91
Payload Mass	m_{pay}	100-150 metric tons (LEO reusable)
Maximum Propellant of Superheavy Booster	M_{prop1}	3400 metric tons
Maximum Propellant of Starship	M_{prop2}	1200 metric tons

To calculate the required propellant mass for given ΔV maneuvers, the team employed the following formulas:

$$MR = e^{\frac{\Delta V}{g * I_{sp}}}$$

$$m_{prop} = m_{pay} \frac{MR - 1}{MR - \frac{MR - 1}{\lambda}}$$

Additionally, the team will use the reusable LEO payload mass number provided by SpaceX to size the number of refueling starships required for each maneuver. LEO is defined as 200 km altitude and LMO is defined as 1000 km above the surface.

There were several mission profiles that required sizing. These included launch to LEO, LEO to Mars surface via the cycler rendezvous, LEO to Mars surface direct transfer, Mars surface to LEO, and cycler boost.

Launching to LEO is a topic extensively covered by SpaceX, and the appropriate payload masses have been specified above.

The following covers calculating the propellant mass necessary for maneuvers taking astronauts from LEO to the Martian surface via the cycler assuming a full payload mass of 150 metric tons.

Table 71: Maneuvers from Earth to Mars (Astronauts)

Mission Leg	$\Delta V\ (km/s)$
LEO to S1L1 Rendezvous	3.796
S1L1 to Martian Surface	2.68

The following equations outline the calculation methodology to determine the total required propellant for this mission leg.

$$MR_{MS} = e^{\frac{\Delta V_{MS}}{g * I_{sp}}}$$

$$m_{prop_{MS}} = m_{pay} \frac{MR_{MS} - 1}{MR_{MS} - \frac{MR_{MS} - 1}{\lambda}}$$

$$MR_{S1L1} = e^{\frac{\Delta V_{S1L1}}{g * I_{sp}}}$$

$$m_{prop_{S1L1}} = \left(m_{pay} + m_{prop_{MS}}\right) \frac{MR_{S1L1} - 1}{MR_{S1L1} - \frac{MR_{S1L1} - 1}{\lambda}}$$

This results in a propellant mass of 905.3110 metric tons to get humans from LEO to the surface of Mars. To determine a worst-case scenario, assume that the Starship arrives in LEO with no remaining propellant. As Starship can deliver 150 metric tons reusable, it is estimated that getting the necessary 905.3110 metric tons of propellant will require 7 Starship propellant launches.

The following covers calculating the propellant mass necessary for maneuvers taking astronauts from the Martian surface back to LEO via the cycler assuming a semi-empty payload mass of 20 metric tons.

Table 72: Maneuvers from Mars to Earth (Astronauts)

Mission Leg	$\Delta V\ (km/s)$
Martian Surface to LMO	4.1
LMO to S1L1	1.18
S1L1 to LEO	2.68

The following equations outline the calculation methodology to determine the total required propellant for this mission leg.

$$MR_{LEO} = e^{\frac{\Delta V_{LEO}}{g * I_{sp}}}$$

$$m_{prop_{LEO}} = m_{pay} \frac{MR_{LEO} - 1}{MR_{LEO} - \frac{MR_{LEO} - 1}{\lambda}}$$

$$MR_{S1L1} = e^{\frac{\Delta V_{S1L1}}{g*I_{sp}}}$$

$$m_{prop_{S1L1}} = \left(m_{pay} + m_{prop_{LEO}}\right)\frac{MR_{S1L1} - 1}{MR_{S1L1} - \frac{MR_{S1L1} - 1}{\lambda}}$$

$$MR_{LMO} = e^{\frac{\Delta V_{LMO}}{g*I_{sp}}}$$

$$m_{prop_{LMO}} = \left(m_{pay} + m_{prop_{MS}} + m_{prop_{S1L1}}\right)\frac{MR_{LMO} - 1}{MR_{LMO} - \frac{MR_{LMO} - 1}{\lambda}}$$

This results in a required propellant mass of 198.6001 metric tons to get humans from the surface of Mars to LEO.

The following covers calculating the propellant mass necessary for maneuvers taking cargo from LEO to the Martian surface via a direct transfer assuming full payload mass of 150 metric tons.

Table 73: Direct Transfer Maneuver

Mission Leg	$\Delta V\ (km/s)$
LEO to Mars Surface	4.33

$$MR_{MS} = e^{\frac{\Delta V_{MS}}{g*I_{sp}}}$$

$$m_{prop_{MS}} = m_{pay}\frac{MR_{MS} - 1}{MR_{MS} - \frac{MR_{MS} - 1}{\lambda}}$$

This reports a necessary propellant mass of 432.791 metric tons. Performing another worst case analysis, it would require 3 Starships to transport the required propellant to an orbital tanker.

The following covers calculating the propellant mass necessary for boosting the cycler into the S1L1 orbit. The cycler mass during boost will be approximately 880 $\pm$ 10 metric tons.

Table 74: Maneuver for Boosting Cycler

Mission Leg	$\Delta V\ (km/s)$
LEO to S1L1	3.796

$$MR_{S1L1} = e^{\frac{\Delta V_{S1L1}}{g*I_{sp}}}$$

$$m_{prop_{S1L1}} = \left(m_{pay}\right)\frac{MR_{S1L1} - 1}{MR_{S1L1} - \frac{MR_{S1L1} - 1}{\lambda}}$$

The total propellant mass required to boost the cycler is therefore 1935.3 metric tons. This can be effectively divided between two starships, each filled with 967.65 metric tons of propellant. Performing a similar analysis as before (assuming worst case two empty starships in orbit requiring the full amount of propellant), this would require 13 Starships bringing 150 metric tons of propellant to refueling tanks in orbit.

12.4 Linear Acceleration (Tim Osifchin)

Production of a force field with linear acceleration is quite indistinguishable from a true gravity force. This was postulated by Einstein in the Equivalence Principle in General Relativity [151]. This form of artificial gravity simply involves firing thrusters on the spacecraft continuously at a thrust level that is suitable for human comfort such as 1.0 g (9.81 m/s^2). The basic profile of a mission to mars starting from Low Earth Orbit (LEO) would involve accelerating continuously toward Mars at 1.0 g until just beyond the halfway point, where the engines would cut out and the spacecraft would flip. Once in a retrograde orientation, the engines would fire up again producing a 1.0 g acceleration away from Mars. This flip ensures that the spacecraft is going slow enough on approach to Mars so that it can be captured into an orbit.

As mentioned earlier, the production of artificial gravity with linear acceleration is indistinguishable from true gravity in the sense that objects moving within the accelerating frame will behave identically in both cases. An on-Earth comparison to this phenomenon would be the acceleration of an elevator. Before the elevator moves, the occupants are in a standard Earth environment with 1.0 g experienced gravity force. The occupants could toss a ball between each other in a very predictable fashion and catch the ball with ease. Once the elevator begins to accelerate upward, the occupants feel an increased gravity force. The behavior of the ball being tossed between the occupants is identical to the stationary case, as it is still very predictable moves exactly how an internal observer would predict. The increased gravity makes the ball fall faster, but its trajectory is exactly proportional to the stationary case.

Being indistinguishable from true gravity is a major benefit to linear acceleration as a method of producing artificial gravity. However, there are other aspects to consider before ruling out rotational artificial gravity. The primary consideration for building a linearly accelerated spacecraft is going to be the propulsion system. To judge the general requirements of this propulsion, consider the Starship spacecraft with a dry mass of 120 mt and a payload mass of 100 mt. Starship can hold about 1200 mt of propellant. Assume that Martian gravity is an acceptable lower limit on the gravity force that the human body can easily adapt to. To accelerate this mass at 0.38 g (Mars gravity) the engines would need to be outputting on average 3.06 MN of thrust. Standard missions to Mars typically last around 6 months. Assuming a trajectory of constant linear acceleration cuts this trip down to 2 month(s), the absolute minimum impulse the engines would need to output is 1.585e13 Ns. To completely use the 1200 mt of propellant, the specific impulse required would be on the order of 1.3e6 seconds. The most efficient electric propulsion systems barely approach specific impulse on the order of 10,000 seconds [152]. These engines produce thrust on the order of one newton, which is six orders of magnitude less than the required average thrust. Looking at a chemical propulsion system, that might be able to approach the 3.06 MN thrust, the specific impulse will be on the order of 400 seconds [152], which again is not even close to the required performance parameter of 1.3e6 seconds specific impulse.

Even with all the simplifying assumptions made through this process – operating at Martian gravity instead of Earth gravity, taking an average thrust value, and cutting mission length to a third of typical missions – the required engine performance is completely unrealistic. The engine needs to output thrust similar to a small launch vehicle, while having two orders of magnitude greater

efficiency than the most efficient electric propulsion systems. Therefore, despite having the advantage of producing a gravity field indistinguishable from true gravity, current propulsion system technology prohibits the use of this method to produce artificial gravity by requiring completely unrealistic performance parameters.

REFERENCES

[1] Vorobets, M., "Imagery from NASA's Ames Research Center," *NASA* Available: https://www.nasa.gov/centers/ames/images/.

[2] Young, L. R., and Sutton, J. P., "Part IV Physiological Effects of Spaceflight," *Handbook of bioastronautics*, Cham, Switzerland: Springer, 2021, pp. 91–239.

[3] Byrnes, D., McConaghy, T. T., & Longuski, J. (2002, August). Analysis of various two synodic period Earth-Mars cycler trajectories. In AIAA/AAS Astrodynamics Specialist Conference and Exhibit (p. 4423).

[4] McConaghy, T. T., Landau, D. F., Yam, C. H., and Longuski, J. M., "Notable Two-Synodic-Periodic Earth-Mars Cycler," Journal of Spacecraft and Rockets, Vol. 43, 2006, pp. 456-465.

[5] "SPICE Toolkit," NASA Available: https://naif.jpl.nasa.gov/naif/toolkit.html.

[6] Annex, A., Pearson, B. Seignovert, B., Carcich, B., Eichhorn, H., Mapel, J., von Forstner, J., McAuliffe, J., del Rio, J., Berry, K., Aye, K.-M., Stefko, M., de Val-Borro, M., Kulumani, S., and Murakami, S.-ya, "SpiceyPy: A Pythonic Wrapper for the SPICE Toolkit," Journal of Open Source Software, Vol. 5, Feb. 2020, p. 2050.

[7] Hu, S. (2017, March 31). *Solar Particle Events and Radiation Exposure in Space.* https://three.jsc.nasa.gov/articles/hu-spes.pdf

[8] *NASA-STD-3001 Technical Brief: Design for Ionizing Radiation Protection*. (2022, February 4). https://www.nasa.gov/sites/default/files/atoms/files/radiation_protection_technical_brief_ochmo_021420.pdf

[9] National Research Council. 2008. Managing Space Radiation Risk in the New Era of Space Exploration. Washington, DC: The National Academies Press. https://doi.org/10.17226/12045

[10] Solar Proton Events Affecting the Earth Environment. (n.d.). NOAA Space EnvironmentServices Center; NASA Goddard Space Flight Center. Retrieved March 29, 2023, from https://umbra.nascom.nasa.gov/SEP/

[11] Radiation risk from medical imaging. (2021, September 30). Harvard Health; Harvard Health Publishing. https://www.health.harvard.edu/cancer/radiation-risk-from-medical-imaging

[12] NASA SPACE FLIGHT HUMAN-SYSTEM STANDARD: VOLUME 1: CREW HEALTH. (2022, January 5). https://standards.nasa.gov/sites/default/files/standards/NASA/B/2022-01-05-NASA-STD-3001-Vol1-Rev-B-Final-Draft-Signature-010522.pdf

[13] National Aeronautics and Space Administration. (n.d.). OLTARIS User Guide.

https://oltaris.nasa.gov/static_pages/OLTARIS_USER_GUIDE/sendfile

[14] Dobynde, M. I., Shprits, Y. Y., Drozdov, A. Y., Hoffman, J., & Li, J. (2021). Beating 1 sievert: Optimal radiation shielding of astronauts on a mission to Mars. Space Weather, 19, e2021SW002749. https://doi.org/10.1029/2021SW002749

[15] Klamm, B. (n.d.). *Passive Space Radiation Shielding: Mass and Volume Optimization of Tungsten-Doped PolyPhenolic and Polyethylene Resins*. https://digitalcommons.usu.edu/cgi/viewcontent.cgi?referer=&httpsredir=1&article=3188&context=smallsat

[16] Cao, D., Yang, G., Bourham, M., & Mondeghan, D. (2020). Gamma radiation shielding properties of poly (methyl methacrylate) / Bi2O3 composites. *Nuclear Engineering and Technology*, *52*(11), 2613-2619. https://www.sciencedirect.com/science/article/pii/S1738573319310940

[17] Frazier, S. (2015, September 30). Real Martians: How to Protect Astronauts from Space Radiation on Mars. NASA.gov. https://www.nasa.gov/feature/goddard/real-martians-how-to-protect-astronauts-from-space-radiation-on-mars

[18] Dunbar, B., "Human needs: Sustaining life during exploration," *NASA* .Available: https://www.nasa.gov/vision/earth/everydaylife/jamestown-needs-fs.html.

[19] "Pancopia Water Recycling," *NASA*. Available: https://www.ars.usda.gov/ARSUserFiles/ott/New%20Website/Partnerships/SBIR%20-%20TT/Pancopia%20NASA%20Success%20Story.pdf.

[20] Carter, L., "Status of the regenerative ecls water recovery system - NASA" Available: https://ntrs.nasa.gov/api/citations/20100033089/downloads/20100033089.pdf.

[21] Marshall Space Flight Center, "International Space Station Environmental Control and Life Support System," *NASA*. Available: https://www.nasa.gov/centers/marshall/pdf/174687main_eclss_facts.pdf.

[22] "Survival! Exploration: Then and Now," *NASA*. Available: https://www.nasa.gov/pdf/166504main_Survival.pdf.

[23] Larson, W., and Pranke, L., Human Spaceflight: Mission Analysis and Design, McGraw–Hill, New York, 2000

[24] Mars, K., ed., "What happens to the human body in space?", *NASA*. Available: https://www.nasa.gov/hrp/bodyinspace.

[25] Sutton, J., and Cintrn, N., "How does spending prolonged time in microgravity affect the bodies of astronauts?", *Scientific American* Available: https://www.scientificamerican.com/article/how-does-spending-prolong/.

[26] Kruesi, L., "Six Months in Space Leads to a Decade's Worth of Bone Loss", *Science News*, published online 30 Jun. 2022. Available: https://www.sciencenews.org/article/space-bone-loss-density-astronaut-recovery-gravity

[27] O'Neill, G. K., "The Colonization of Space," *Physics Today*, Sep. 1974, pp. 32–40. Available: https://space.nss.org/o-neill-cylinder-space-settlement/

[28] Johnson, R. D., and Holbrow, C., eds., "Space Settlements: A Design Study," *stanford.edu*, 1977. Available: http://large.stanford.edu/courses/2016/ph240/martelaro2/docs/nasa-sp-413.pdf

[29] Williams, D.R., "Planetary Fact Sheet - Metric", *NASA Goddard Spaceflight Center*. Available: https://nssdc.gsfc.nasa.gov/planetary/factsheet/index.html

[30] Harris, L. R., Herpers, R., Hofhammer, T., and Jenkin, M., "How much gravity is needed to establish the perceptual upright?", *PloS one*. Available: https://www.ncbi.nlm.nih.gov/pmc/articles/PMC4153541/.

[31] Nesti, A., Barnett-Cowan, M., MacNeilage, P. R., and Bülthoff, H. H., "Human sensitivity to vertical self-motion," *Experimental brain research* Available: https://www.ncbi.nlm.nih.gov/pmc/articles/PMC3898153/.

[32] Cohen, M. M., Hargens, A. R., Yates, B. J., and Bowley, S. M., "Effects of prolonged centrifugation on orthostasis - NASA technical reports server (NTRS)," *NASA* Available: https://ntrs.nasa.gov/citations/20010106394.

[33] "Wheelchair Ramp Slope: Your Own ADA Compliance Ramps," *BarunAbility*.Available: https://www.braunability.com/us/en/blog/disability-rights/wheelchair-ramp-slope.html#:~:text=In%20truth%2C%20there%20is%20not,12%20or%20almost%2015%20degrees.

[34] Globus, A., and Hall, T., "Space Settlement Population Rotation Tolerance," *NSS Space Settlement,* Jun. 2017.

[35] Dunbar, B., "International Space Station Facts and Figures", *NASA,* Jan. 2023. Available: https://www.nasa.gov/feature/facts-and-figures

[36] "Human Integration Design Handbook," *NASA,* SP-2010-3407/REV1. 2014.

[37] Osifchin, T.R., "Cycler Spacecraft V4", *GrabCAD*, published online 27 Apr. 2023. Available: https://grabcad.com/library/cycler-spacecraft-v4-1

[38] *Centrifuge* Available: https://iss.jaxa.jp/iss/contribution/issjpdoc3_2_e.html.

[39] Poplawski, J. V., Loewenthal, S. H., Oswald, F. B., Zaretsky, E. V., Morales, W., and Street, K. W., "Analysis of Space Station Centrifuge Rotor Bearing Systems: A Case Study," *NASA*, 2014.

[40] "Products," *Kitanihon Seiki Co., Ltd.,* Available: https://www.ezo-brg.co.jp/english/product/document-detail11.html.

[41] "Electric motors - torque vs. Power and Speed," *Engineering ToolBox* Available: https://www.engineeringtoolbox.com/electrical-motors-hp-torque-rpm-d_1503.html.

[42] "In-Space Propulsion Data Sheets," *Aerojet Rocketdyne* Available: https://www.rocket.com/sites/default/files/documents/In-Space%20Data%20Sheets%204.8.20.pdf.

[43] "Star Sensors," *Astro APS - Star Sensors - Jena Optronik* Available: https://www.jena-optronik.de/products/star-sensors/astro-aps.html.

[44] "Miniature Inertial Measurement Unit," *Honeywell* Available: https://aerospace.honeywell.com/us/en/products-and-services/product/hardware-and-systems/space/miniature-inertial-measurement-unit-mimu.

[45] "Coarse Sun Sensor Pyramid Fact Sheet," *Redwire Space* Available: file:///C:/Users/19rya/Downloads/MIS21-001-Redwire-Brand-Fact-Sheet_SunSensorPyramid_R3_28_APRIL_2021.pdf.

[46] Wertz, J., Everett, D., and Puschell, J., Space Mission Engineering: The New SMAD, Microcosm Press, Hawthorn, CA, 2015.

[47] Burt, R. R., and Loffi, R. W., "Failure Analysis of International Space Station Control Moment Gyro," *Boeing and NASA Johnson Space Center*. Available: https://articles.adsabs.harvard.edu/pdf/2003ESASP.524...13B.

[48] Wilde, M., Patel, B., & Kish, B. (2022). Design considerations for an Earth–mars cycler spacecraft using the S1L1 cycler. Journal of Spacecraft and Rockets, 59(3), 916–928. https://doi.org/10.2514/1.a35160

[49] *LR87-11* Available: http://www.astronautix.com/l/lr87-11.html.

[50] *N2O4/aerozine-50* Available: http://www.astronautix.com/n/n2o4aerozine-50.html.

[51] *Titan I first stage engines (LR-87)* Available: http://heroicrelics.org/info/titan-i/titan-i-stage 1-engines.html.

[52] Rogers, B., Hughes, K., Longuski, J. M., and Aldrin, B., "Preliminary Analysis of Establishing Cycler Trajectories Between Earth and Mars via V∞ Leveraging," AIAA/AAS Astrodynamics Specialist Conference, AIAA Paper 2012-4746, 2012

[53] "Mobile Servicing System Data Sheet," MDRobotics, MacDonald Dettwiler Company, http://www.spacenet.on.ca/data/pdf/canada-inspace/mss-ds.pdf [retrieved 20 Nov. 2019].

[54] Fortson, K., "Ba 500BC / CF500 F (beta cloth, beta fabric)," *Bron Aerotech* Available: https://bronaerotech.com/product/ba-500bc-cf500f-beta-cloth/.

[55] Kamenetzky, R. R., and Finckenor, M. M., "Comparison of Observed Beta Cloth Interactions ," *NASA*, Sep. 1999.

[56] Kauder, L., "Spacecraft Thermal Control," *AC*.

[57] Cunningham, Thomas. "AAE450 Lecture 16 - Thermal Control". *Purdue University*.

[58] US Department of Commerce, N. O. A. A., "The planet Mars," *National Weather Service* Available: https://www.weather.gov/fsd/mars#:~:text=Temperatures%20on%20Mars%20average%20about,lower%20latitudes%20in%20the%20summer.

[59] Phillips, T., "The coldest spot in the known universe," *NASA* Available: https://science.nasa.gov/science-news/science-at-nasa/2014/30jan_coldspot.

[60] "Staying cool on the ISS," *NASA* Available: https://science.nasa.gov/science-news/science-at-nasa/2001/ast21mar_1/.

[61] Leonard, C., "Challenges for electronic circuits in space applications," *Challenges for Electronic Circuits in Space Applications | Analog Devices* Available: https://www.analog.com/en/thought-leadership/challenges-for-electronic-circuits-in-space-applications.html.

[62] “Starship Users Guide V1”, *SpaceX*, published online March 2020.Available: https://www.spacex.com/media/starship_users_guide_v1.pdf

[63] “About Canadarm,” *Government of Canada*, Mar. 2021. Available: https://www.asc-csa.gc.ca/eng/canadarm/about.asp

[64] Hirata, C. M. (2007). The division of physics, mathematics and astronomy. The Division of Physics, Mathematics and Astronomy. Retrieved April 23, 2023, from https://pma.caltech.edu/

[65] Genta, G. (2017). Interplanetary journey to Mars. In: Next Stop Mars. Springer Praxis Books(). Springer, Cham. https://doi.org/10.1007/978-3-319-44311-9_6

[66] Palmer, C. (2021). SpaceX starship lands on Earth, but manned missions to Mars will require more.

[67] Foster, C. (2013). Trajectory Browser: An online tool for interplanetary trajectory analysis and visualization. 2013 IEEE Aerospace Conference, 1-6.

[68] “Learn about the Rover,” NASA Available: https://mars.nasa.gov/mars2020/spacecraft/rover/.

[69] Osifchin, T.R., “Martian Habitat V4”, *GrabCAD*, published online 24 Apr. 2023.Available: https://grabcad.com/library/martian-habitat-v4-1

[70] “Topographic map of Mars: USGS I map 2782,” Topographic Map of Mars | USGS I Map 2782 Available: https://pubs.usgs.gov/imap/i2782/.

[71] Koren, M., “What makes a good landing site on Mars?,” *The Atlantic* Available: https://www.theatlantic.com/science/archive/2017/04/mars-landing-site/521715/.

[72] “The devils of Mars,” *NASA* Available: https://science.nasa.gov/science-news/science-at-nasa/2005/14jul_dustdevils/.

[73] Koktas, E., and Basar, E., “Communications for the planet Mars: Past, present, and future,” *arXiv.org* Available: https://arxiv.org/abs/2211.14245.

[74] Wilson, J., “How on Earth does NASA choose a landing site on Mars?,” *NASA* Available: https://www.nasa.gov/feature/how-on-earth-does-nasa-choose-a-landing-site-on-mars.

[75] “Resource library,” *Tomatosphere* Available: http://tomatosphere.letstalkscience.ca/Resources/library/ArticleId/5302/soil-on-mars.aspx.

[76] Good, A., “Insight is meeting the challenge of winter on Dusty Mars,” *Phys.org* Available: https://phys.org/news/2021-02-insight-winter-dusty-mars.html.

[77] “Insight's landing site: Elysium Planitia,” NASA Available: https://solarsystem.nasa.gov/resources/861/insights-landing-site-elysium-planitia/#:~:text=Elysium%20is%20from%20the%20ancient,and%20135.9%20degrees%20east%20longitude.

[78] “Water ice is buried near Mars equator in small areas,” Red Planet Report Available: http://redplanet.asu.edu/?p=25376.

[79] Mellon, M. T., and Sizemore, H. G., “The history of ground ice at Jezero crater Mars and other past, present, and future landing sites,” Icarus Available: https://www.sciencedirect.com/science/article/pii/S0019103521003249.

[80] Vincendon, M., Mustard, J., Forget, F., Kreslavsky, M., Spiga, A., Murchie, S., and Bibring, J.-P., “Near-tropical subsurface ice on Mars,” *Geophysical Research Letters*, vol. 37, 2010.

[81] Grant, J., Irwin, R., and Milliken, R., “2020 landing site for Mars rover mission - dev,” *JPL* Available: https://marsnext.jpl.nasa.gov/documents/LandingSiteWorksheet_Holden_final.pdf.

[82] Golombek, M., Grant, J., Kipp, D., Vasavada, A., Kirk, R., Fergason, R., Bellutta, P., Calef, F., Larsen, K., Katayama, Y., Huertas, A., Beyer, R., Chen, A., Parker, T., Pollard, B., Lee, S., Sun, Y., Hoover, R., Sladek, H., Grotzinger, J., Welch, R., Noe Dobrea, E., Michalski, J., and Watkins, M., “Selection of the mars science laboratory landing site,” *Space Science Reviews*, vol. 170, 2012, pp. 641–737.

[83] Rice, M. S., Bell, J. F., Gupta, S., Warner, N. H., Goddard, K., and Anderson, R. B., “A detailed geologic characterization of Eberswalde crater, Mars,” *The International Journal of Mars Science and Exploration*, May 2013, pp. 15–57.

[84] “Olympus Mons,” *Encyclopædia Britannica* Available: https://www.britannica.com/place/Olympus-Mons.

[85] “Mysteries in nili fossae,” *ESA* Available: https://www.esa.int/Science_Exploration/Space_Science/Mars_Express/Mysteries_in_Nili_Fossae.

[86] Markle, L. J., “Nili Fossae Workshop Abstract #1010,” *NASA* Available: https://www.nasa.gov/sites/default/files/atoms/files/nili_fossae_landing_site_and_eztagged.pdf.

[87] Longo, A. Z., "First Landing Site /Exploration Zone Workshop for human missions ... - USRA," *First Landing Site/Exploration Zone Workshop for Human Missions to the Surface of Mars* Available: https://www.hou.usra.edu/meetings/explorationzone2015/pdf/1008.pdf.

[88] Milam, K. A., Stockstill, K. R., Moersch, J. E., McSween, H. Y., Tornabene, L. L., Ghosh, A., Wyatt, M. B., and Christensen, P. R., "Themis characterization of the Mer Gusev Crater Landing Site," *Journal of Geophysical Research: Planets*, vol. 108, 2003.

[89] Golombek, M., Williams, N., Wooster, P., McEwen, A., Putzig, N., Bramson, A., Head, J., Heldmann, J., Marinova, M., and Beaty, D., "SPACEX STARSHIP LANDING SITES ON MARS," *52nd lunar and planetary science conference* Available: https://www.hou.usra.edu/meetings/lpsc2021/.

[90] "Weather and geology short introduction on hellas - marspolar" Available: https://www.marspolar.space/files/hellas-basin-preliminary.pdf.

[91] "Navigation," *ESA Science & Technology - Craters within the Hellas Basin* Available: https://sci.esa.int/web/mars-express/-/55575-craters-within-the-hellas-basin.

[92] Stucky de Quay, G., and Grindrod, P. M., "A COMPLETE CATALOGUE OF LANDSLIDES IN VALLES MARINERIS, MARS," *45th Lunar and Planetary Science Conference* Available: https://www.hou.usra.edu/meetings/lpsc2014/pdf/1601.pdf.

[93] "Exomars discovers hidden water in Mars' grand canyon," *ESA* Available: https://www.esa.int/Science_Exploration/Human_and_Robotic_Exploration/Exploration/ExoMars/ExoMars_discovers_hidden_water_in_Mars_Grand_Canyon.

[94] "Elevations within the floor of the Valles Marineris," *NASA* Available: https://www.jpl.nasa.gov/images/pia02039-elevations-within-the-floor-of-the-valles-marineris.

[95] *Planetary names* Available: https://planetarynames.wr.usgs.gov/Feature/6288.

[96] McEwen, A., Chojnacki, M., Miyamoto, H., Hemmi, R., Weitz, C., Williams, R., Quantin, C., Flahaut, J., Wray, J., Turner, S., Bridges, J., Grebby, S., Leung, C., and Rafkin, S., "East Melas Chasm Exploration Zone," *NASA* Available: https://www.nasa.gov/sites/default/files/atoms/files/e-melas-ez.pdf.

[97] Smith, M. D., Siili, T., Savijärvi, H., Möhlmann, D., Grassi, D., Hess, S. I., and Jakosky, B. M., "Fog phenomena on Mars," *Planetary and Space Science* Available: https://www.sciencedirect.com/science/article/abs/pii/S0032063309002323.

[98] Davila, A., Rodriguez, A. G., Schulze-Makuch, D., Rask, J., and Zavaleta, J., "The Hebrus Valles Exploration Zone: Access to the martian surface," *First Landing Site/Exploration Zone Workshop for Human Missions to the Surface of Mars* Available:

[99] Yadav, S. K., "The elevation (a) and slope (b) map of a part of the Hebrus Valles ...," *The elevation (a) and slope (b) map of a part of the Hebrus Valles region* Available: https://www.researchgate.net/figure/The-elevation-a-and-slope-b-map-of-a-part-of-the-Hebrus-Valles-region-prepared-using_fig2_335342371.

[100] Grant, J., "A milestone for curiosity: 10 years of exploration in Gale Crater on Mars," *Air and Space Museum* Available: https://airandspace.si.edu/stories/editorial/10-years-curiosity-mars.

[101] Rayne, E., "Curiosity rover discovers Opal Gems on Mars with clues to watery past," *Space.com* Available: https://www.space.com/mars-opals-water-habitable.

[102] "Gale crater," *NASA* Available: https://mars.nasa.gov/msl/timeline/prelaunch/gale-crater/.

[103] Viola, D., McEwen, A. S., and Dundas, C. M., "Arcadia Planitia: Acheron Fossae and Erebus Montes Workshop Abstract #1011," *1st EZ Workshop for Human Missions to Mars* Available:

[104] Viola, D., McEwen, A. S., and Dundas, C. M., "MID-LATITUDE MARTIAN ICE AS A TARGET FOR HUMAN EXPLORATION, ASTROBIOLOGY, AND IN-SITU RESOURCE UTILIZATION," *First Landing Site/Exploration Zone Workshop for Human Missions to the Surface of Mars* Available: https://www.hou.usra.edu/meetings/explorationzone2015/pdf/1011.pdf.

[105] Kronberg, P., Hauber, E., Grott, M., Werner, S. C., Schäfer, T., Gwinner, K., Giese, B., Masson, P., and Neukum, G., "Acheron Fossae, Mars: Tectonic rifting, volcanism, and implications for lithospheric thickness," *Journal of Geophysical Research*, vol. 112, 2007.

[106] Webster, G., "MRO shows that recurring martian streaks are flowing sand, not water," *SciTechDaily* Available: https://scitechdaily.com/mro-shows-that-recurring-martian-streaks-are-flowing-sand-not-water/.

[107] Hassler, D. M., Zeitlin, C., Ehresmann, B., Wimmer-Schweingruber, R. F., Guo, J., Matthiä, D., et al (2018). Space weather on the surface of Mars: Impact of the September 2017 events. Space Weather, 16, 1702– 1708. https://doi.org/10.1029/2018SW001959

[108] *Space Exploration Vehicle Concept*. (n.d.). NASA.gov. https://www.nasa.gov/pdf/464826main_SEV_FactSheet_508.pdf

[109] Kruyer, N. S., Realff, M. J., Sun, W., Genzale, C. L., and Peralta-Yahya, P., "Designing the bioproduction of martian rocket propellant via a biotechnology-enabled in situ Resource Utilization Strategy," *Nature Communications*, vol. 12, 2021.

[110] Monaghan, H., "Optical communications," *NASA* Available: https://www.nasa.gov/directorates/heo/scan/opticalcommunications.

[111] "Ka-Band Communications," *NASA* Available: https://mars.nasa.gov/mro/mission/communications/commkaband/.

[112] "Near Space Network User Manual" Available: https://esc.gsfc.nasa.gov/static-files/ESC-LCRNS-REQ-0090-Rev-10-18-2022.pdf.

[113] "Volume 1. The Future Mars Communications Architecture" Available: https://www.ioag.org/Public%20Documents/MBC%20architecture%20report%20final%20version%20PDF.pdf.

[114] Harbaugh, J., "Deep Space Optical Communications (DSOC)," *NASA* Available: https://www.nasa.gov/mission_pages/tdm/dsoc/index.html.

[115] Monaghan, H., "About the Deep Space Network," *NASA* Available: https://www.nasa.gov/directorates/heo/scan/services/networks/deep_space_network/about.

[116] Harbaugh, J., "Deep Space Optical Communications (DSOC)," *NASA* Available: https://www.nasa.gov/mission_pages/tdm/dsoc/index.html.

[117] Torrez, T., "RF/Optical Hybrid Antenna" Available: https://tmo.jpl.nasa.gov/progress_report/42-201/201B.pdf.

[118] "NASA prepares for Moon and Mars with new addition to its Deep Space Network," *NASA* Available: https://www.jpl.nasa.gov/news/nasa-prepares-for-moon-and-mars-with-new-addition-to-its-deep-space-network.

[119] Ventura, M. C. *STUDY: AN ASSESSMENT ON THE REQUIREMENTS FOR DEEP SPACE OPTICAL COMMUNICATIONS*. NASA. Retrieved April 30, 2023, from https://upcommons.upc.edu/bitstream/handle/2117/361519/Casanovas_Ventura_Marc_TFM_2021.pdf?sequence=3&isAllowed=y

[120] Taylor, J., Lee, D. K., & Shambayati, S. (n.d.). *Mars Reconnaissance Orbiter*. NASA. Retrieved April 30, 2023, from https://descanso.jpl.nasa.gov/monograph/mono.html

[121] Taylor, J., Lee, D. K., and Shambayati, S., “Mars Reconnaissance Orbiter,” 2016, pp. 201–262.

[122] SatCatalog, “HR16-100,” *SatCatalog* Available: https://www.satcatalog.com/component/hr16-100/.

[123] Oh, D. Y., Collins, S., Hart, B., Lantoine, G., Snyder, S., and Whiffen, G., “Development of the Psyche Mission for NASA’s Discovery Program,” Oct. 2017.

[124] “Electrical power,” *NASA* Available: https://mars.nasa.gov/mro/mission/spacecraft/parts/electricalpower/.

[125] Cunningham, Thomas. “AAE450 Telecommunications Slides.” *Purdue University*.

[126] “Telecommunications Link Design Handbook (810-005) - deep space network,” *NASA* Available: https://deepspace.jpl.nasa.gov/dsndocs/810-005/.

[127] “Connectors, components, subsystems, and RF microwave products,” *Smiths Interconnect* Available: https://www.smithsinterconnect.com/.

[128] “CPI SAT series 3122 1.2m Tx/rx ka-band antenna,” *Digisat* Available: https://www.digisat.org/satcom-technologies-3122-1-2m-ka-band-antenna-1.

[129] “CPI Sat Prodelin 3244 Ka-band 2.4m Antenna,” *Digisat* Available: https://www.digisat.org/cpi-3244-ka-band-2-4m-antenna.

[130] Owens, A., & de Weck, O. (2016, July). Sensitivity Analysis of the Advanced Missions Cost Model. 46th International Conference on Environmental Systems.https://ttu-ir.tdl.org/handle/2346/67725

[131] Wattles, J., “Elon Musk says SpaceX's Mars rocket will be cheaper than he once thought. here's why | CNN business,” *CNN* Available: https://www.cnn.com/2019/09/29/business/elon-musk-spacex-mars-starship-cost/index.html.

[132] Wall, M., “SpaceX's starship may fly for just $2 million per mission, Elon Musk says,” *Space.com* Available: https://www.space.com/spacex-starship-flight-passenger-cost-elon-musk.html?utm_source=twitter&utm_medium=social&utm_campaign=dlvr.it.

[133] Scoles, S., “Are space scientists ready for starship—the biggest rocket ever?,” *Science.org* Available: https://www.science.org/content/article/space-scientists-ready-starship-biggest-rocket-ever.

[134] Office of Audits, and NASA Office of Attorney General, “NASA’S MANAGEMENT AND UTILIZATION OF THE INTERNATIONAL SPACE STATION,” Jul. 2018.

[135] “Acceptable risk Walter Schimmerling, ph.D.. what is acceptable? - NASA” Available: https://three.jsc.nasa.gov/articles/AcceptableRiskWS.pdf.

[136] “Goddard Procedural Requirements (GPR) - NASA” Available: https://lws.larc.nasa.gov/pdf_files/GPR%207120.4D%20Adm%20Ext_07282020.pdf.

[137] “NASA Risk Management Handbook” Available: https://ntrs.nasa.gov/api/citations/20120000033/downloads/20120000033.pdf.

[138] “S3001: Guidelines for Risk Management - NASA,” *S3001: Guidelines for Risk Management* Available: https://www.nasa.gov/sites/default/files/atoms/files/s3001_guidelines_for_risk_management_-_ver_g_-_10-25-2017.pdf.

[139] Longuski, J. M., and Landau, D. F., “Guidance strategy for hyperbolic rendezvous,” purdue.edu Available: https://engineering.purdue.edu/people/james.m.longuski.1/ConferencePapersPresentation s/2006GuidanceStrategyforHyperbolicRendezvous.pdf.

[140] “Veggie fact sheet” Available: https://www.nasa.gov/sites/default/files/atoms/files/veggie_fact_sheet_508.pdf?vase.

[141] Hille, K., “The fact and fiction of martian dust storms,” *NASA* Available: https://www.nasa.gov/feature/goddard/the-fact-and-fiction-of-martian-dust-storms.

[142] Jackson, S., “Life Support Systems,” *NASA* Available: https://www.nasa.gov/content/life-support-systems/.

[143] Mortreux, M., Riveros, D., Bouxsein, M. L., and Rutkove, S. B., “A moderate daily dose of resveratrol mitigates muscle deconditioning in a martian gravity analog,” Frontiers in physiology Available: https://www.ncbi.nlm.nih.gov/pmc/articles/PMC6656861/.

[144] Chel Stromgren, Callie Burke, Jason Cho, Michelle A. Rucker and Maria Garcia-Robles. "Defining the Required Net Habitable Volume for Long-Duration Exploration Missions," AIAA 2020-4032. ASCEND 2020. November 2020.

[145] “KaStream® 5000 MK II,” *Smiths Interconnect* Available: https://www.smithsinterconnect.com/.

[146] Ho, C., Golshan, N., and Kliore, A., “Radio Wave Propogation Handbook,” *NASA* Available: https://descanso.jpl.nasa.gov/propagation/propagation.html.

[147] Morabito, D. D., Lee, D., and Franco, M. M., “Measurement of Mars Reconnaissance Orbiter equivalent isotropic ...” Available: https://ipnpr.jpl.nasa.gov/progress_report/42-168/168F.pdf.

[148] “MRO Antennas,” *NASA* Available: https://mars.nasa.gov/mro/mission/spacecraft/parts/antennas/.

[149] Drazic, P., “The propagation of ka-band signals through the atmosphere” Available: https://ieeexplore.ieee.org/document/8124434.

[150] “Telecommunications Link Design Handbook (810-005) - deep space network,” *NASA* Available: https://deepspace.jpl.nasa.gov/dsndocs/810-005/.

[151] "Equivalence Principle". *Encyclopedia Britannica*, May. 2022, Available: https://www.britannica.com/science/equivalence-principle.

[152] Camilleri, V, “Electric Propulsion and Electric Satellites”, *University of Colorado Boulder*, May. 2017, Available: https://www.colorado.edu/faculty/kantha/sites/default/files/attached-files/172038-172568_-_vincent_camilleri_-_may_11_2017_208_am_-_final_rp.pdf

[153] Donald M. Hassler et al., Mars’ Surface Radiation Environment Measured with the Mars Science Laboratory’s Curiosity Rover. Science 343,1244797(2014). DOI:10.1126/science.1244797

[154] Machine Learning for Planetary and Space Physics. (2021, July). *How Well Can We Forecast Solar Radiation Storms?* [Video]. YouTube. https://www.youtube.com/watch?v=Nnw6gSwTEck

[155] Finger, B. W., Lantz, G. A., and Theno, T. W., “Mars One Habitat ECLSS,” 2013.

[156] “Mars oxygen in-situ resource utilization experiment (moxie),” *NASA* Available: https://mars.nasa.gov/mars2020/spacecraft/instruments/moxie/.

[157] Babakhanova, S., Baber, S., Zazzera, F. B., Hinterman, E., Hoffman, J., Kusters, J., Lordos, G., Lukic, J., Maffia, F., Maggiore, P., Mainini, L., Moccia, A., Nowak, H., Schneiderman, T., Sciarretta, S., Seager, S., Seaman, S., Smith, T., Stamler, N., Sumini, V. M., and Zhan, Z., “AIAA Propulsion and Energy 2019 Forum,” *Mars Garden An Engineered Greenhouse for a Sustainable Residence on Mars*, 2019, pp. 1–17.

[158] Palmowski, J., Zacny, K., Mellerowicz, B., Vogel, B., Bocklund, A., Stolov, L., Yen, B., Sabahi, D., Ware, L., Faris, D., Ridilla, A., Nguyen, H., van Susante, P., Johnson, G., Putzig, N. E., Hecht, M., and Nayar, H., "Redwater: Extraction of water from Mars' ice deposits," *Earth and Space 2022*, 2023.

[159] Bramson, A. M., Byrne, S., Putzig, N. E., Sutton, S., Plaut, J. J., Brothers, T. C., and Holt, J. W., "Widespread excess ice in Arcadia Planitia, Mars," *Geophysical Research Letters*, vol. 42, 2015, pp. 6566–6574.

[160] Mueller, R. P., Smith, J. D., Schuler, J. M., Nick, A. J., Gelino, N. J., Leucht, K. W., Townsend, I. I., and Dokos, A. G., "Design of an excavation robot: Regolith Advanced Surface Systems Operations Robot (RASSOR) 2.0," *Earth and Space 2016*, 2016.

[161] Hoffman, J. A., Hecht, M. H., Rapp, D., Hartvigsen, J. J., SooHoo, J. G., Aboobaker, A. M., McClean, J. B., Liu, A. M., Hinterman, E. D., Nasr, M., Hariharan, S., Horn, K. J., Meyen, F. E., Okkels, H., Steen, P., Elangovan, S., Graves, C. R., Khopkar, P., Madsen, M. B., Voecks, G. E., Smith, P. H., Skafte, T. L., Araghi, K. R., and Eisenman, D. J., "Mars Oxygen ISRU experiment (moxie)—preparing for human mars exploration," *Science Advances*, vol. 8, 2022.

[162] McClure, P. R., Poston, D. I., Gibson, M. A., Mason, L. S., and Robinson, R. C., "Kilopower project: The Krusty Fission Power Experiment and potential missions," *Nuclear Technology*, vol. 206, 2020.

[163] Poston, D. I., Gibson, M. A., Godfroy, T., and McClure, P. R., "Krusty Reactor Design," *Nuclear Technology*, vol. 206, 2020.

[164] Broccia, G., "Energy Production in Martian Environment," *SciVerse ScienceDirect*, 2014.

[165] Grott, M., Spohn, T., Knollenberg, J., Krause, C., Nagihara, S., Morgan, P., Piqueux, S., Miller, N., Golombek, M., Murphy, J., Siegler, M., King, S., Hudson, T. L., Vrettos, C., Smrekar, S. E., and Banerdt, W. B., "THERMAL CONDUCTIVITY OF THE MARTIAN REGOLITH AT THE INSIGHT LANDING SITE FROM HP3 ACTIVE HEATING EXPERIMENTS," *LPI*.

[166] exsource, "THERMAL AND ELECTRICAL PROPERTIES OF PE," *exsource* Available: https://www.qenos.com/internet/home.nsf/(LUImages)/Tech%20Guide:%20Thermal%20and%20electrical%20properties%20of%20PE/$File/144%20QEN%20eX%20TN%20Thermal%20&%20Electrical%20properties%20of%20PE.pdf.

[167] Wang, H., "AAE338 Thermal Sciences". *Purdue University*.

[168] “Heat Pump Systems,” *Energy.gov* Available: https://www.energy.gov/energysaver/heat-pump-systems.

[169] Hargitai, H., *Mars climate zone map based on TES data* Available: http://planetologia.elte.hu/mcdd/climatemaps.html.

[170] “Planet mars wallpaper,” Planet Mars Wallpaper Available: https://getwallpapers.com/collection/planet-mars-wallpaper.

[171] Clark, J. R., “On-Orbit Cryogenic Refueling: Potential Mission Benefits, Associated Orbital Mechanics, and Fuel Transfer Thermodynamic Modeling Efforts,” NASA Available: https://ntrs.nasa.gov/api/citations/20210014171/downloads/Masters_Thesis_Final_Reformatted.pdf.

[172] Kraft, R., “Artemis I Mission Control at a glance,” *NASA* Available: https://www.nasa.gov/feature/artemis-i-mission-control-at-a-glance.

[173] Hu, S. (2017, March 31). *Solar Particle Events and Radiation Exposure in Space.* https://three.jsc.nasa.gov/articles/hu-spes.pdf

[174] *NASA-STD-3001 Technical Brief: Design for Ionizing Radiation Protection*. (2022, February 4). https://www.nasa.gov/sites/default/files/atoms/files/radiation_protection_technical_brief_ochmo_021420.pdf

[175] National Research Council. 2008. Managing Space Radiation Risk in the New Era of Space Exploration. Washington, DC: The National Academies Press. https://doi.org/10.17226/12045

[176] Solar Proton Events Affecting the Earth Environment. (n.d.). NOAA Space EnvironmentServices Center; NASA Goddard Space Flight Center. Retrieved March 29, 2023, from https://umbra.nascom.nasa.gov/SEP/

[177] Radiation risk from medical imaging. (2021, September 30). Harvard Health; Harvard Health Publishing. https://www.health.harvard.edu/cancer/radiation-risk-from-medical-imaging

[178] NASA SPACE FLIGHT HUMAN-SYSTEM STANDARD: VOLUME 1: CREW HEALTH. (2022, January 5). https://standards.nasa.gov/sites/default/files/standards/NASA/B/2022-01-05-NASA-STD-3001-Vol1-Rev-B-Final-Draft-Signature-010522.pdf

[179] National Aeronautics and Space Administration. (n.d.). OLTARIS User Guide. https://oltaris.nasa.gov/static_pages/OLTARIS_USER_GUIDE/sendfile

[180] Dobynde, M. I., Shprits, Y. Y., Drozdov, A. Y., Hoffman, J., & Li, J. (2021). Beating 1 sievert: Optimal radiation shielding of astronauts on a mission to Mars. Space Weather, 19, e2021SW002749. https://doi.org/10.1029/2021SW002749

[181] Klamm, B. (n.d.). *Passive Space Radiation Shielding: Mass and Volume Optimization of Tungsten-Doped PolyPhenolic and Polyethylene Resins*. https://digitalcommons.usu.edu/cgi/viewcontent.cgi?referer=&httpsredir=1&article=3188&context=smallsat

[182] Cao, D., Yang, G., Bourham, M., & Mondeghan, D. (2020). Gamma radiation shielding properties of poly (methyl methacrylate) / Bi2O3 composites. *Nuclear Engineering and Technology*, *52*(11), 2613-2619. https://www.sciencedirect.com/science/article/pii/S1738573319310940

[183] Frazier, S. (2015, September 30). Real Martians: How to Protect Astronauts from Space Radiation on Mars. NASA.gov. https://www.nasa.gov/feature/goddard/real-martians-how-to-protect-astronauts-from-space-radiation-on-mars

[184] "Kilopower reactor using Stirling Technology (p) nuclear ... - NASA" Available: https://ntrs.nasa.gov/api/citations/20180007389/downloads/20180007389.pdf?attachment=true.

[185] Owens, A., & de Weck, O. (2016, July). Sensitivity Analysis of the Advanced Missions Cost Model. 46th International Conference on Environmental Systems. https://ttu-ir.tdl.org/handle/2346/67725

[186] Wattles, J., "Elon Musk says SpaceX's Mars rocket will be cheaper than he once thought. here's why | CNN business," *CNN* Available: https://www.cnn.com/2019/09/29/business/elon-musk-spacex-mars-starship-cost/index.html.

[187] Larson, W., and Pranke, L., Human Spaceflight: Mission Analysis and Design, McGraw–Hill, New York, 2000

[188] Byrnes, D., McConaghy, T. T., & Longuski, J. (2002, August). Analysis of various two synodic period Earth-Mars cycler trajectories. In AIAA/AAS Astrodynamics Specialist Conference and Exhibit (p. 4423).

[189] McConaghy, T. T., Landau, D. F., Yam, C. H., and Longuski, J. M., "Notable Two-Synodic-Periodic Earth-Mars Cycler," Journal of Spacecraft and Rockets, Vol. 43, 2006, pp. 456-465.

[190] "SPICE Toolkit," NASA Available: https://naif.jpl.nasa.gov/naif/toolkit.html.

[191] Annex, A., Pearson, B. Seignovert, B., Carcich, B., Eichhorn, H., Mapel, J., von Forstner, J., McAuliffe, J., del Rio, J., Berry, K., Aye, K.-M., Stefko, M., de Val-Borro, M., Kulumani, S., and Murakami, S.-ya, "SpiceyPy: A Pythonic Wrapper for the SPICE Toolkit," Journal of Open Source Software, Vol. 5, Feb. 2020, p. 2050.

[192] Dorminey, B., "5 top landing sites for a manned mission to Mars," *Forbes* Available: https://www.forbes.com/sites/brucedorminey/2014/12/09/5-top-landing-sites-for-a-manned-mission-to-mars/?sh=dfc0663c185d. https://www.nasa.gov/sites/default/files/atoms/files/viola_arcadiaplanitia_final_tagged.pdf.

[193] Howard, R. L., & Seibert, M. (n.d.). *Lagrange-based options for relay satellites to eliminate Earth-Mars Communications outages during solar superior conjunctions*. NASA. Retrieved April 30, 2023, from https://ntrs.nasa.gov/citations/20205007788

[194] Quattrocchi, G., Pittari, A., dalla Vedova, M. D. L., and Maggiore, P., "The thermal control system of NASA's Curiosity rover: a case study," *IOP Conference Series: Materials Science and Engineering*, 2022.

[195] Cunningham, Thomas. "AAE450 Telecommunications Slides." *Purdue University*.

[196] "Connectors, components, subsystems, and RF microwave products," *Smiths Interconnect* Available: https://www.smithsinterconnect.com/.

[197] "CPI SAT series 3122 1.2m Tx/rx ka-band antenna," *Digisat* Available: https://www.digisat.org/satcom-technologies-3122-1-2m-ka-band-antenna-1.

[198] "CPI Sat Prodelin 3244 Ka-band 2.4m Antenna," *Digisat* Available: https://www.digisat.org/cpi-3244-ka-band-2-4m-antenna.

[199] "Telecommunications Link Design Handbook (810-005) - deep space network," *NASA* Available: https://deepspace.jpl.nasa.gov/dsndocs/810-005/.

[200] "Electrical power," *NASA* Available: https://mars.nasa.gov/mro/mission/spacecraft/parts/electricalpower/.